UNITED STATES DISTRICT COURT
EASTERN DISTRICT OF TEXAS
MARSHALL DIVISION

Omni MedSci, Inc., *Plaintiff/Counter-Defendant,* **v.** **Apple Inc.,** *Defendant/Counter-Plaintiff.*	**Case No. 2:18-cv-429-RWS**

AMENDED COMPLAINT FOR PATENT INFRINGEMENT AND DEMAND FOR JURY TRIAL

Plaintiff, Omni MedSci, Inc. ("Omni MedSci"), alleges as follows:

The Parties

1. Plaintiff Omni MedSci is a Michigan corporation having its principal place of business at 1718 Newport Creek Drive, Ann Arbor, Michigan 48103. Dr. Mohammed N. Islam is the principal of Omni MedSci. Dr. Islam is a tenured Professor of Optics and Photonics in the Electrical and Computer Engineering Department, and a Professor of Biomedical Engineering, at the University of Michigan's College of Engineering. Omni MedSci is part of the Omni family of companies, which create, develop, and commercialize Dr. Islam's optical technology in various fields. The Omni companies also develop and provide unique optical products to the U.S. Department of Defense and intelligence community.

2. Defendant Apple Inc. ("Apple") is a California corporation, having a regular and established place of business at 1 Infinite Loop, Cupertino, California 95014. Apple may be

served with process through its registered agent for service of process C T Corporation System (C0168406).

Jurisdiction and Venue

3. This is a complaint for patent infringement under 35 U.S.C. §§ 101, *et seq*. The Court has subject matter jurisdiction under 28 U.S.C. §§ 1331 and 1338.

4. The court has personal jurisdiction over Apple, and venue under 28 U.S.C. §§1391(a)(1) and 1400(b) is proper in this district, because Apple has two regular and established places of business in this district and because Apple offers for sale and sells infringing Apple Watches in this district at those locations.

5. A lawsuit, Case No. 2:18-cv-134-RWS, is currently pending in this district between Omni MedSci and Apple involving several of the same patents and much of the same Apple Watch technology as is at issue in the present lawsuit.

The Patents-in-Suit

6. On October 16, 2018, the U.S. Patent and Trademark Office issued U.S. Patent No. 10,098,546 ("the '546 patent") (Exhibit A) to Dr. Mohammed N. Islam.

7. On January 9, 2018, the U.S. Patent and Trademark Office issued U.S. Patent No. 9,861,286 ("the '286 patent") (Exhibit B) to Dr. Mohammed N. Islam. This patent is also asserted against Apple in Case No. 2:18-cv-134-RWS. In the present lawsuit, the '286 patent is asserted only against the Series 4 Apple Watch, a watch that did not exist at the time of the complaint in Case No. 2:18-cv-134-RWS and was not accused in that Case.

8. On February 6, 2018, the U.S. Patent and Trademark Office issued U.S. Patent No. 9,885,698 ("the '698 patent") (Exhibit C) to Dr. Mohammed N. Islam. This patent is also asserted against Apple in Case No. 2:18-cv-134-RWS. In the present lawsuit, the '698 patent is

asserted only against the Series 4 Apple Watch, a watch that did not exist at the time of the complaint in Case No. 2:18-cv-134-RWS and was not accused in that Case.

9. On February 29, 2018, the U.S. Patent and Trademark Office issued U.S. Patent No. 10,188,299 ("the '299 patent") (Issue Notification attached as Exhibit D) to Dr. Mohammed N. Islam.

10. The '546 patent, the '286 patent, the '698 patent, and the '299 patent are, collectively, the "Patents-in-Suit."

11. Omni MedSci has been, and remains, the owner by assignment of the Patents-in-Suit.

Background Facts

12. By 2012, Omni MedSci had invented technology for using lasers in medical and other applications, including wearable measurement devices incorporating lasers and other components that can detect and monitor physiological parameters such as glucose, ketones, heart rate, blood constituents, and dental carries.

13. On December 31, 2012, Omni MedSci filed a set of patent applications covering its developments using lasers for medical and other applications.

14. Between June 2014 and July 2016, Dr. Islam had a series of meetings and email exchanges with Apple personnel regarding the technology underlying his then-pending patent applications, including some of the now-issued Patents-in-Suit. In those exchanges, Apple was offered the opportunity to license or acquire Omni MedSci's patented and patent-pending technology, but Apple declined.

15. On June 11-12, 2014, Dr. Islam met with Apple employees Drs. Michael O'Reilly and Michael Hillman at Apple's headquarters in Cupertino, California to discuss Omni MedSci's then patent-pending technology.

16. Dr. Hillman then arranged for a meeting with Dr. Islam and approximately ten Apple employees at Apple's headquarters in Cupertino, California to discuss technical details of Omni MedSci's then patent-pending technology. The meeting took place at Apple on February 5, 2015.

17. On July 14, 2016, Apple employee Greg Joswiak emailed Dr. Islam inviting him to provide additional information about his technology. Mr. Joswiak indicated that he would share the information with his team at Apple.

18. Four days later, Apple employees Drs. Ed Hull and Shonn Hendee arranged a meeting with Dr. Islam and approximately ten Apple employees at Apple's headquarters in Cupertino, California to discuss technical details of Omni MedSci's then patent-pending technology. The meeting took place at Apple on July 18, 2016. At the meeting, Dr. Islam shared the published patent application for the '546 patent and the published parent patent applications for the '698 and '286 patents.

19. Dr. Islam continued to correspond with Apple employees regarding the status of his pending patent applications and technological development. On December 21, 2017, Dr. Islam emailed Drs. O'Reilly, Hull, and Hendee enclosing copies of the allowed claims for the '268 and '698 patents. In response, Dr. O'Reilly emailed Dr. Islam stating, "We [Apple] don't wish to receive any information about any of your IP [Intellectual Property]."

<u>Apple's Infringing Apple Watch Products</u>

20. On information and belief,[1] Apple has made and sold several models of its Apple Watch product, including, for example, "Series 1," "Series 2," "Series 3 GPS," "Series 3 GPS + Cellular," and "Series 4" watches. Omni MedSci asserts infringement by all models, including the models sold to date and models sold in the future, which are covered by the claims of the Patents-in-Suit (collectively, "Watches"). Exemplary Watches advertised on Apple's web site (https://www.apple.com/watch/compare/, captured on March 8, 2018 and October 10, 2018) as shown below:

21. The Watches are wearable devices that measure a physiological parameter, namely, heart rate.

---

[1] For allegations based on information and belief, Omni MedSci believes that the allegations will have evidentiary support after a reasonable opportunity for investigation and discovery.

22. The Watches measure heart rate non-invasively using light emitting diodes ("LEDs").

23. The light emitted from the LEDs in the Watches includes near-infrared wavelengths.

24. The Watches can modulate the light emitted from the LEDs.

25. The Watches can use a lock-in technique, such as synchronous demodulation, which is used to detect the modulation frequency.

26. The Watches can improve the signal-to-noise ratio of the LED light reflected from the skin by increasing the intensity of the light emitted from the LEDs.

27. The Watches can also improve the signal-to-noise ratio of the LED light reflected from the skin by increasing the pulse rate of the LEDs.

28. The Watches have one or more lenses that deliver the light from the LEDs to a Watch wearer's skin.

29. The one or more lenses in the Watches include a spectral filter.

30. The Watches have at least two detectors that receive LED light reflected from the skin.

31. The detectors in the Watches capture light while the LEDs are off.

32. The Watches have one or more analog to digital converters that process the reflected light received by the detectors.

33. A receiver in the Watches can be synchronized to the LED light sources.

34. The Watches can capture light while the LEDs are off to improve the signal-to-noise ratio of the light captured from the LED light reflected from the skin by differencing

between the light captured while the LEDs are off and the light captured from the LED light reflected from the skin.

35. The Watches can communicate with an Apple smart phone or tablet.

Count 1 – Infringement of the '546 Patent

36. Omni MedSci reasserts and incorporates the allegations contained in the paragraphs above.

37. Apple has directly infringed and is directly infringing the '546 patent by making using, offering for sale, and selling the Watches, and importing the Watches into the United States.

38. Based on publicly available information, the Watches infringe at least claims 1, 2, 4, 5, 7-13, and 15-18 of the '546 patent. Omni MedSci may assert additional claims of the '546 patent after a reasonable opportunity for investigation and discovery.

39. Apple's infringement is described further below with respect to exemplary claim 1. The analysis below is based on publicly available information.

40. Claim 1 recites: "A wearable device, comprising: a measurement device including a light source comprising a plurality of light emitting diodes (LEDs) for measuring one or more physiological parameters." Apple sells Watches, which are wearable, and that include a measurement device that can measure heart rate, which is a physiological parameter. The measurement device in the Watches uses multiple light emitting diodes for measuring the heart rate. *See, e.g.*, Apple's website at support.apple.com/en-us/HT204666 and www.ifixit.com/Teardown/Apple+Watch+Series+3+Teardown/97521.

41. Claim 1 further recites: "the measurement device configured to generate, by modulating at least one of the LEDs having an initial light intensity, an optical beam having a

plurality of optical wavelengths, wherein at least a portion of the optical beam includes a near-infrared wavelength between 700 nanometers and 2500 nanometers." The Watches include infrared LEDs, which emit an optical beam with more than one wavelength. At least a portion of the wavelengths emitted are between 700 nanometers and 2500 nanometers. The LEDs are modulated and have an initial light intensity. *See, e.g.*, Apple website at support.apple.com/en-us/HT204666; www.ifixit.com/Teardown/Apple+Watch+Series+3+Teardown/97521; U.S. Patent Publication No. 2017/0281024.

42. Claim 1 further recites: "the measurement device comprising one or more lenses configured to receive and to deliver at least a portion of the optical beam to tissue." The Watches include one or more lenses that receive the optical beam from the LEDs and deliver a portion of that beam to a wearer's tissue.

43. Claim 1 further recites: "wherein the tissue reflects at least a portion of the optical beam delivered to the tissue." The wearer's tissue reflects at least part of the optical beam delivered to the tissue. *See, e.g.*, U.S. Patent Publication No. 2016/0058367.

44. Claim 1 further recites: "the measurement device further comprising a receiver, the receiver having a plurality of spatially separated detectors." The Watches include a receiver, with multiple photodiode detectors, each detector being separated from the others in space. *See,*

e.g., www.ifixit.com/Teardown/Apple+Watch+Series+3+Teardown/97521; support.apple.com/en-us/HT204666; U.S. Patent Publication No. 2016/0058367.

45. Claim 1 further recites that the receiver includes "one or more analog to digital converters coupled to the spatially separated detectors, the one or more analog to digital converters configured to generate at least two receiver outputs." The receiver in the Watches uses analog to digital converters, coupled to the detectors, which generate at least two output signals. *See, e.g.*, www.ifixit.com/Teardown/Apple+Watch+Series+3+Teardown/97521; support.apple.com/en-us/HT204666; U.S. Pub. No. 2016/0058312; U.S. Pub. No. 2016/0038045.

46. Claim 1 further recites: "the receiver configured to: capture light while the LEDs are off and convert the captured light into a first signal and capture light while at least one of the LEDs is on and to convert the captured light into a second signal, the captured light including at least a portion of the optical beam reflected from the tissue." The receiver in the Watches can capture light while the LEDs are off and convert that light into a first signal. It also captures light from the LEDs, which light includes light reflected from the tissue, and converts that light into a second signal. *See, e.g.*, U.S. Pub. No. 2016/0058367.

47. Claim 1 further recites: "the measurement device configured to improve a signal-to-noise ratio of the optical beam reflected from the tissue by differencing the first signal and the second signal and by differencing the two receiver outputs." The measurement device in the Watches improves the signal-to-noise ratio of the light reflected from the tissue by differencing the first signal and the second signal. It also improves the signal-to-noise ratio of the light reflected from the tissue by differencing the two receiver outputs. *See, e.g.*, U.S. Pub. No. 2016/0058367; U.S. Pub. No. 2016/0058312; U.S. Pub. No. 2016/0038045; U.S. Pub. No. 2016/0296173.

48. Claim 1 further recites: "the measurement device configured to further improve the signal-to-noise ratio of the optical beam reflected from the tissue by increasing the light intensity relative to the initial light intensity from at least one of the LEDs." The measurement device in the Watches improves the signal-to-noise ratio of the light reflected from the tissue by increasing LED brightness. *See, e.g.*, Apple website at http://support.apple.com/en-us/HT204666.

49. Claim 1 further recites: "the measurement device further configured to generate an output signal representing at least in part a non-invasive measurement on blood contained within the tissue." The measurement device in the Watches generates a signal that represents the heart rate of the blood in the tissue. *See*, *e.g.*, Apple website at http://support.apple.com/en-us/HT204666; U.S. Pub. No. 2016/0058367.

50. Claim 1 further recites: "wherein the output signal is generated at least in part by using a Fourier transform of signals from the receiver including at least one of the first and second signals and signals from the at least two receiver outputs." The Watches apply a Fourier transform to at least one of the signals from the receiver to, in part, generate the output signal. *See*, *e.g.*, U.S. Pub. No. 2016/0051201.

51. Claim 1 further recites: "wherein the receiver further comprises one or more spectral filters positioned in front of at least some of the plurality of spatially separated detectors." The Watches include spectral filters in front of one or more of the Watch lenses. *See, e.g.*, www.ifixit.com/Teardown/Apple+Watch+Series+3+Teardown/97521; support.apple.com/en-us/HT204666.

Count 2 – Infringement of the ‘286 Patent

52. Omni MedSci reasserts and incorporates the allegations contained in the paragraphs above.

53. Apple has directly infringed and is directly infringing the ‘286 patent by making using, offering for sale, and selling the Series 4 Watch, and importing the Series 4 Watch into the United States.

54. Based on publicly available information, the Series 4 Watch infringes at least claims 16 and 19 of the ‘286 patent. Omni MedSci may assert additional claims of the ‘286 patent after a reasonable opportunity for investigation and discovery.

55. Apple’s infringement is described further below with respect to exemplary claim 16. The analysis below is based on publicly available information.

56. Claim 16 recites: “A wearable device for use with a smart phone or tablet, the wearable device comprising: a measurement device including a light source comprising a plurality of light emitting diodes (LEDs) for measuring one or more physiological parameters.” Apple sells Series 4 Watches, which are wearable devices that use multiple light emitting diodes. *See, e.g.*, Apple’s website at http://support.apple.com/en-us/HT204666.

57. Claim 16 further recites: “the measurement device configured to generate, by modulating at least one of the LEDs having an initial light intensity.” The Series 4 Watch modulates at least one of the LEDs, which fluctuate in brightness (intensity). *See, e.g.*, Apple’s website at http://support.apple.com/en-us/HT204666.

58. Claim 16 further recites: “an optical beam having a plurality of optical wavelengths, wherein at least a portion of the plurality of optical wavelengths is a near-infrared wavelength between 700 nanometers and 2500 nanometers.” The Series 4 Watch includes infrared LEDs, which emit wavelengths between 700 nanometers and 2500 nanometers. *See,*

e.g., Apple website at http://support.apple.com/en-us/HT204666; U.S. Patent Publication No. 2017/0281024.

59. Claim 16 further recites: "the measurement device comprising one or more lenses configured to receive and to deliver a portion of the optical beam to tissue." The Series 4 Watch includes one or more lenses capable of receiving and delivering a portion of an optical beam to skin.

60. Claim 16 further recites: "wherein the tissue reflects at least a portion of the optical beam delivered to the tissue." When the Series 4 Watch delivers the optical beam to the skin, the skin reflects at least a portion of that optical beam. *See, e.g.,* U.S. Patent Publication Nos. 2016/0058309 and 2016/0058367.

61. Claim 16 further recites: "wherein the measurement device is adapted to be placed on a wrist or an ear of a user." The Series 4 Watch is adapted to be placed on the user's wrist.

62. Claim 16 further recites: "the measurement device further comprising a receiver configured to: capture light while the LEDs are off and convert the captured light into a first signal and capture light while at least one of the LEDs is on and convert the captured light into a second signal, the captured light including at least a portion of the optical beam reflected from the tissue." The Series 4 Watch includes a receiver with sensors, which capture light while the

LEDs are off and convert the captured light into a first signal and capture light while at least one of the LEDs is on and convert the captured light into a second signal, the captured light including at least a portion of the input optical beam reflected from the skin. *See, e.g.*, Apple website at http://support.apple.com/en-us/HT204666; U.S. Patent Publication No. 2016/0058367.

63. Claim 16 further recites: "the measurement device configured to improve a signal-to-noise ratio of the optical beam reflected from the tissue by differencing the first signal and the second signal." The Series 4 Watch reduces the signal-to-noise ratio of the optical beam received from the skin by differencing the first signal and the second signal. *See, e.g.*, U.S. Patent Publication No. 2016/0058367.

64. Claim 16 further recites: "the light source configured to further improve the signal-to-noise ratio of the optical beam reflected from the tissue by increasing the light intensity relative to the initial light intensity from at least one of the LEDs." The Series 4 Watch improves the signal-to-noise ratio of the optical beam reflected from the skin by increasing the brightness (intensity) of the Series 4 Watch LEDs. *See, e.g.*, Apple website at http://support.apple.com/en-us/HT204666.

65. Claim 16 further recites: "the measurement device further configured to generate an output signal representing at least in part a non-invasive measurement on blood contained within the tissue." The Series 4 Watch can generate an output signal, which represents the user's heart rate. *See, e.g.*, Apple website at http://support.apple.com/en-us/HT204666; U.S. Patent Publication No. 2016/0058367.

66. Claim 16 further recites: "wherein the receiver includes a plurality of spatially separated detectors." The Series 4 Watch includes a receiver with multiple photodiode sensors,

which are spatially separated. *See, e.g.*, Apple website at http://support.apple.com/en-us/HT204666.

67. Claim 16 further recites: "wherein at least one analog to digital converter is coupled to the spatially separated detectors." The Series 4 Watch includes at least one analog to digital converter, which is coupled to the spatially separated photodiode sensors. *See, e.g.*, U.S. Patent Publication No. 2019/0038045.

Count 3 – Infringement of the '698 Patent

68. Omni MedSci reasserts and incorporates the allegations contained in the paragraphs above.

69. Apple has directly infringed and is directly infringing the '698 patent by making using, offering for sale, and selling the Series 4 Watch, and importing the Series 4 Watch into the United States.

70. Based on publicly available information, the Series 4 Watch infringes at least claims 1, 2, 3 and 5 of the '698 patent. Omni MedSci may assert additional claims of the '698 patent after a reasonable opportunity for investigation and discovery.

71. Apple's infringement is described further below with respect to exemplary claim 1. The analysis below is based on publicly available information.

72. Claim 1 recites: "A wearable device, comprising: a measurement device including a light source comprising a plurality of light emitting diodes (LEDs) for measuring one or more physiological parameters." Apple sells Series 4 Watches, which are wearable devices that use multiple light emitting diodes. *See, e.g.*, Apple's website at http://support.apple.com/en-us/HT204666.

73. Claim 1 further recites: "the measurement device configured to generate, by modulating at least one of the LEDs having an initial light intensity." The Series 4 Watch modulates at least one of the LEDs by fluctuating the LEDs' brightness (intensity). *See, e.g.*, Apple's website at http://support.apple.com/en-us/HT204666.

74. Claim 1 further recites: "an input optical beam having one or more optical wavelengths, wherein at least a portion of the one or more optical wavelengths is a near-infrared wavelength between 700 nanometers and 2500 nanometers." The Series 4 Watch includes infrared LEDs, which emit wavelengths between 700 nanometers and 2500 nanometers. *See, e.g.*, Apple website at http://support.apple.com/en-us/HT204666; U.S. Patent Publication No. 2017/0281024.

75. Claim 1 further recites: "the measurement device comprising one or more lenses configured to receive and to deliver a portion of the input optical beam to tissue." The Series 4 Watch includes one or more lenses capable of receiving and delivering a portion of an optical beam to skin.

76. Claim 1 further recites: "wherein the tissue reflects at least a portion of the input optical beam delivered to the tissue." When the Series 4 Watch delivers the optical beam to the

skin, the skin reflects at least a portion of that optical beam. *See, e.g.,* U.S. Patent Publication Nos. 2016/0058309 and 2016/0058367.

77. Claim 1 further recites: "the measurement device further comprising a receiver, wherein the receiver includes a plurality of spatially separated detectors." The Series 4 Watch includes a receiver with multiple photodiode sensors that are spatially separated. *See, e.g.*, Apple website at http://support.apple.com/en-us/HT204666; U.S. Patent Publication No. 2016/0058367.

78. Claim 1 further recites: "the detectors configured to: capture light while the LEDs are off and convert the captured light into a first signal; and capture light while at least one of the LEDs is on and convert the captured light into a second signal, the captured light including at least a portion of the input optical beam reflected from the tissue." The Series 4 Watch includes sensors, which capture light while the LEDs are off and convert the captured light into a first signal; and capture light while at least one of the LEDs is on and convert the captured light into a second signal, the captured light including at least a portion of the input optical beam reflected from the skin. *See, e.g.,* Apple website at http://support.apple.com/en-us/HT204666; U.S. Patent Publication No. 2016/0058367.

79. Claim 1 further recites: "wherein at least one analog to digital converter is coupled to the spatially separated detectors and is configured to generate at least a first data signal from the first signal and at least a second data signal from the second signal." The Series 4 Watch includes at least one analog to digital converter, which is coupled to the spatially separated photodiode sensors, and is configured to generate at least a first data signal from the first signal and at least a second data signal from the second signal. *See, e.g.*, U.S. Patent Publication No. 2019/0038045.

80. Claim 1 further recites: "the measurement device configured to improve a signal-to-noise ratio of the input optical beam reflected from the tissue by differencing the first data signal and the second data signal." The Series 4 Watch reduces the signal-to-noise ratio of the optical beam received from the skin by differencing the first signal and the second signal. *See, e.g.*, U.S. Patent Publication No. 2016/0058367.

81. Claim 1 further recites: "to generate an output signal representing at least in part a non-invasive measurement on blood contained within the tissue." The Series 4 Watch can generate an output signal, which represents the user's heart rate. *See, e.g.*, Apple website at http://support.apple.com/en-us/HT204666; U.S. Patent Publication No. 2016/0058367.

82. Claim 1 further recites: "wherein the modulating at least one of the LEDs has a modulation frequency and wherein the receiver is configured to use a lock-in technique that detects the modulation frequency." The Series 4 Watch LEDs have a modulation frequency of hundreds of times per second. Further, on information and belief, the Series 4 Watch receiver uses a lock-in technique that detects the modulation frequency. *See, e.g.*, Apple website at http://support.apple.com/en-us/HT204666; U.S. Patent Publication No. 2008/0297487.

Count 5 – Infringement of the '299 Patent

83. Omni MedSci reasserts and incorporates the allegations contained in the paragraphs above.

84. Apple has directly infringed and is directly infringing the '299 patent by making using, offering for sale, and selling the Watches, and importing the Watches into the United States.

85. Based on publicly available information, the Watches infringe at least claims 1-9 and 14-20 of the '299 patent. Omni MedSci may assert additional claims of the '299 patent after a reasonable opportunity for investigation and discovery.

86. Apple's infringement is described further below with respect to exemplary claim 1. The analysis below is based on publicly available information.

87. Claim 1 recites: "A system comprising: a light source comprising a plurality of light emitting diodes." Apple sells Watches that include multiple light emitting diodes used for measuring the heart rate. *See, e.g.*, Apple's website at support.apple.com/en-us/HT204666 and www.ifixit.com/Teardown/Apple+Watch+Series+3+Teardown/97521.

88. Claim 1 further recites: "each of the light emitting diodes configured to generate an output optical beam having one or more optical wavelengths, wherein at least a portion of the one or more optical wavelengths is a near-infrared wavelength between 700 nanometers and 2500 nanometers." The Watches include infrared LEDs, which emit an optical beam with one or more wavelengths. At least a portion of the wavelengths emitted are between 700 nanometers and 2500 nanometers. The LEDs are modulated and have an initial light intensity. *See, e.g.*, Apple website at support.apple.com/en-us/HT204666; www.ifixit.com/Teardown/Apple+Watch+Series+3+Teardown/97521; U.S. Patent Publication No. 2017/0281024.

89. Claim 1 further recites: "a lens positioned to receive at least a portion of at least one of the output optical beams and to deliver a lens output beam to tissue." The Watches include lenses that receive the optical beam from the LEDs and deliver a portion of that beam to a wearer's tissue.

90. Claim 1 further recites: "a detection system located to receive at least a portion of the lens output beam reflected from the tissue." The Watches include a receiver, with multiple photodiode detectors. Each detector can receive at least a portion of the beam output by the lens that is reflected from the wearer's skin. *See, e.g.*, www.ifixit.com/Teardown/Apple+Watch+Series+3+Teardown/97521; support.apple.com/en-us/HT204666; U.S. Pub. No. 2016/0058367.

91. Claim 1 further recites that the detection system is "configured to generate an output signal based on the received portion of the lens output beam reflected from the tissue, the output signal having a signal-to-noise ratio." The detection system in the Watches generates at least one output signal, which signal has a signal-to-noise ratio. *See, e.g.*, www.ifixit.com/Teardown/Apple+Watch+Series+3+Teardown/97521; support.apple.com/en-us/HT204666; U.S. Pub. No. 2016/0058367.

92. Claim 1 further recites: "wherein the detection system is further configured to be synchronized to the light source." The detection system in the Watches works by synchronizing with the light source. *See, e.g.*, U.S. Pub. No. 2016/0058367.

93. Claim 1 further recites: "a personal device comprising a wireless receiver, a wireless transmitter, a display, a microphone, a speaker, one or more buttons or knobs, a

microprocessor, and a touch screen, the personal device configured to receive and process at least a portion of the output signal, wherein the personal device is configured to store and display the processed output signal." Apple sells a system, which includes personal devices (*e.g.*, iPhone) that have a wireless receiver, a wireless transmitter, a display, a microphone, a speaker, one or more buttons or knobs, a microprocessor and a touch screen. The personal devices can receive and process data (*e.g.*, heart rate information) from the Apple watch and store and display the processed data. *See, e.g.*, Apple website at http://support.apple.com/en-us/HT204666; U.S. Pub. No. 2016/0058312.

94. Claim 1 further recites: "wherein at least a portion of the processed output signal is configured to be transmitted over a wireless transmission link." Apple sells a system, with a personal device (*e.g.*, iPhone), which can transmit the data it receives (*e.g.*, heart rate information) and processes from Watches over a wireless transmission link to Apple's iCloud. *See, e.g.*, Apple website at support.apple.com/en-us/HT204666; www.imore.com/how-sync-your-health-data-ios-11-and-how-it-works; U.S. Pub. No. 2016/0058312.

95. Claim 1 further recites: "a remote device configured to receive over the wireless transmission link an output status comprising the at least a portion of the processed output signal, to process the received output status to generate processed data, and to store the processed data." Apple sells a system, which includes the Apple iCloud that can receive over a wireless transmission link an output status comprising at least a portion of the processed data transmitted from Apple personal devices (*e.g.*, iPhones). The Apple iCloud can then process the transmitted output status to generate and store data such as heart rate information. *See, e.g.*, Apple website at support.apple.com/en-us/HT204666; www.imore.com/how-sync-your-health-data-ios-11-and-how-it-works.

96. Claim 1 further recites: "wherein the output signal is indicative of one or more physiological parameters." The output signal from the Watches represents, *inter alia*, the wearer's heart rate. *See, e.g.*, U.S. Pub. No. 2016/0058367.

97. Claim 1 further recites: "the remote device is configured to store a history of at least a portion of the one or more physiological parameters over a specified period of time." Apple's iCloud stores historical user data, including health data. The stored health data includes historical heart rate information. *See, e.g.*, Apple website at support.apple.com/en-us/HT204666; www.imore.com/how-sync-your-health-data-ios-11-and-how-it-works.

98. Claim 1 further recites: "the light source configured to improve the signal-to-noise ratio of the output signal by increasing light intensity relative to an initial light intensity from at least one of the plurality of light emitting diodes and by increasing pulse rate relative to an initial pulse rate of at least one of the plurality of light emitting diodes." The Watches have the ability to improve the signal-to-noise ratio of the output signal "by increasing both LED brightness [light intensity] and sampling rate [pulse rate]." *See, e.g.*, Apple website at support.apple.com/en-us/HT204666.

99. Claim 1 further recites: "wherein the detection system includes a plurality of spatially separated detectors." The detection system in the Watches includes multiple photodiode detectors, each detector being separated from the others in space. *See, e.g.*, www.ifixit.com/Teardown/Apple+Watch+Series+3+Teardown/97521; support.apple.com/en-us/HT204666; U.S. Pub. No. 2016/0058367.

100. Claim 1 further recites: "wherein at least one analog to digital converter is coupled to at least one of the spatially separated detectors and is configured to generate at least two data signals." The Watches include at least one analog to digital converter, which is coupled

to the spatially separated photodiode sensors. The A-to-D converter generates at least two signals, a first signal and a second signal. *See*, *e.g.*, www.ifixit.com/Teardown/Apple+Watch+Series+3+Teardown/97521; support.apple.com/en-us/HT204666; U.S. Pub. No. 2016/0058312; U.S. Pub. No. 2016/0038045.

101. Claim 1 further recites: "the system is configured to further improve the signal-to-noise ratio by differencing two of the at least two data signals." The Watches improve the signal-to-noise ratio of the light reflected from the tissue by differencing the first signal and the second signal. *See, e.g.*, U.S. Pub. No. 2016/0058367; U.S. Pub. No. 2016/0058312; U.S. Pub. No. 2016/0038045; U.S. Pub. No. 2016/0296173.

102. Claim 1 further recites: "wherein the detection system further comprises one or more spectral filters positioned in front of at least some of the plurality of spatially separated detectors." The Watches include spectral filters on one or more of the Watch lenses. *See, e.g.*, www.ifixit.com/Teardown/Apple+Watch+Series+3+Teardown/97521; support.apple.com/en-us/HT204666.

Count 6 – Willful Infringement

103. Omni MedSci reasserts and incorporates the allegations contained in the paragraphs above.

104. Based on the communications and meetings between Dr. Islam and Apple personnel, Apple knew of its infringement of the Patents-in-Suit or was willfully blind to its infringement.

105. Apple's infringement of the Patents-in-Suit has been willful.

Demand for Relief

WHEREFORE, Omni MedSci requests entry of judgment against Apple as follows:

A. Finding Apple liable for infringement of the Patents-in-Suit and that the infringement has been willful;

B. Awarding Omni MedSci damages under 35 U.S.C. § 271 adequate to compensate for Apple's infringement;

C. Permanently enjoining Apple, together with any officers, agents, servants, employees, and attorneys, and such other persons in active concert of participation with them, who receive actual notice of the Order, from further infringement of the Patents-in-Suit;

D. A declaration this case is exceptional within the meaning of 35 U.S.C. § 285 and awarding Omni MedSci its reasonable attorney fees, costs, and disbursements;

E. Awarding Omni MedSci interest in all damages awarded; and

F. Granting Omni MedSci all other relief to which it is entitled.

Demand for Jury Trial

Omni MedSci demands trial by jury for all issues so triable.

Date: January 29, 2019

Respectfully submitted,

/s/ John S. LeRoy

Thomas A. Lewry LEAD COUNSEL (MI Bar No. P36399)
John S. LeRoy (MI Bar No. P61964)
Robert C. J. Tuttle (MI Bar No. P25222)
John M. Halan (MI Bar No. P37616)
Christopher C. Smith (MI Bar No. P73936)
Brooks Kushman P.C.
1000 Town Center, Twenty-Second Floor
Southfield, Michigan 48075
Telephone: (248) 358-4400
Facsimile: (248) 358-3351
Email: tlewry@brookskushman.com
jleroy@brookskushman.com
rtuttle@brookskushman.com
jhalan@brookskushman.com
csmith@brookskushman.com

T. John Ward, Jr.
Texas State Bar No. 00794818
E-mail: jw@wsfirm.com
Claire Abernathy Henry
Texas State Bar No. 24053063
E-mail: claire@wsfirm.com
WARD, SMITH & HILL, PLLC
PO Box 1231
Longview, Texas 75606
Telephone: (903) 757-6400
Facsimile: (903) 757-2323

Attorneys for Plaintiff

CERTIFICATE OF SERVICE

I hereby certify that a copy of the foregoing document was filed electronically in compliance with Local Rule CV-5(a). Therefore, this document was served on all counsel who are deemed to have consented to electronic service. Local Rule CV-5(a)(3)(A). Pursuant to Fed. R. Civ. P. 5(d) and Local Rule CV-5(d) and (e), all other counsel of record not deemed to have consented to electronic service were served with a true and correct copy of the foregoing by email on January 29, 2019.

/s/ John S. LeRoy

EXHIBIT A

US010098546B2

(12) **United States Patent**
Islam

(10) **Patent No.: US 10,098,546 B2**
(45) **Date of Patent: *Oct. 16, 2018**

(54) **WEARABLE DEVICES USING NEAR-INFRARED LIGHT SOURCES**

(71) Applicant: **OMNI MEDSCI, INC.**, Ann Arbor, MI (US)

(72) Inventor: **Mohammed N. Islam**, Ann Arbor, MI (US)

(73) Assignee: **OMNI MEDSCI, INC.**, Ann Arbor, MI (US)

(*) Notice: Subject to any disclaimer, the term of this patent is extended or adjusted under 35 U.S.C. 154(b) by 0 days.

This patent is subject to a terminal disclaimer.

(21) Appl. No.: **15/860,065**

(22) Filed: **Jan. 2, 2018**

(65) **Prior Publication Data**

US 2018/0140198 A1 May 24, 2018

Related U.S. Application Data

(63) Continuation of application No. 15/686,198, filed on Aug. 25, 2017, now Pat. No. 9,861,286, which is a
(Continued)

(51) **Int. Cl.**
G01J 3/00 (2006.01)
A61B 5/00 (2006.01)
(Continued)

(52) **U.S. Cl.**
CPC ***A61B 5/0088*** (2013.01); ***A61B 5/0013*** (2013.01); ***A61B 5/0022*** (2013.01);
(Continued)

(58) **Field of Classification Search**
CPC G01J 3/02; G01J 3/28; G01J 3/42; G01N 21/31; G01N 21/552
(Continued)

(56) **References Cited**

U.S. PATENT DOCUMENTS

4,063,106 A	12/1977	Ashkin et al.
4,158,750 A	6/1979	Sakoe et al.

(Continued)

FOREIGN PATENT DOCUMENTS

DE	102010012987 A1	10/2010
EP	1148666	10/2001

(Continued)

OTHER PUBLICATIONS

Lee, Ju Han, et al., "Continuous-wave supercontinuum laser based on an erbium-doped fiber ring cavity incorporating a highly nonlinear optical fiber", Optics Letters, vol. 30, No. 19, Oct. 1, 2005, pp. 2599-2601.

(Continued)

Primary Examiner — Md M Rahman
(74) *Attorney, Agent, or Firm* — Brooks Kushman P.C.

(57) **ABSTRACT**

A wearable device includes a measurement device having light emitting diodes (LEDs) measuring a physiological parameter. The measurement device modulates the LEDs to generate an optical beam having a near-infrared wavelength between 700-2500 nanometers. Lenses receive and deliver the optical beam to tissue, which reflects the optical beam to a receiver having spatially separated detectors coupled to analog-to-digital converters configured to generate receiver outputs. The receiver captures light while the LEDs are off, and reflected light from the tissue while the LEDs are on, to generate first and second signals, respectively. Signal-to-noise ratio is improved by differencing the first and second signals and by differencing the receiver outputs. The measurement device further improves signal-to-noise ratio of the reflected optical beam by increasing light intensity of the LEDs relative to an initial light intensity. The measurement device generates an output signal representing a non-invasive measurement on blood contained within the tissue.

19 Claims, 19 Drawing Sheets

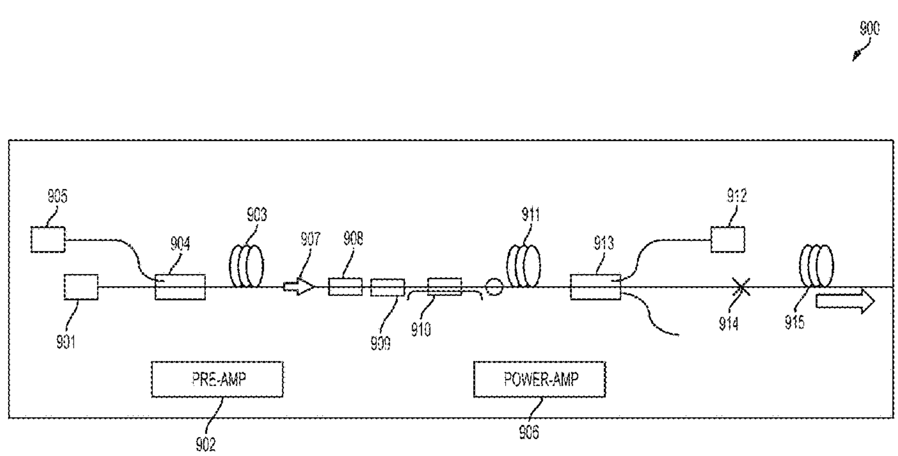

Related U.S. Application Data

continuation of application No. 15/357,136, filed on Nov. 21, 2016, now Pat. No. 9,757,040, which is a continuation of application No. 14/651,367, filed as application No. PCT/US2013/075736 on Dec. 17, 2013, now Pat. No. 9,500,635.

(60) Provisional application No. 61/754,698, filed on Jan. 21, 2013.

(51) **Int. Cl.**

G01N 33/49	(2006.01)
G01N 33/44	(2006.01)
G01N 33/15	(2006.01)
G01N 33/02	(2006.01)
G01N 21/88	(2006.01)
G01N 21/3563	(2014.01)
G01N 21/359	(2014.01)
G01J 3/453	(2006.01)
A61B 5/145	(2006.01)
A61B 5/1455	(2006.01)
G01N 21/39	(2006.01)
G01M 3/38	(2006.01)
G01J 3/28	(2006.01)
G01J 3/10	(2006.01)
G01J 3/18	(2006.01)
G01J 3/14	(2006.01)
H01S 3/30	(2006.01)

(52) **U.S. Cl.**

CPC ***A61B 5/0075*** (2013.01); ***A61B 5/0086*** (2013.01); ***A61B 5/1455*** (2013.01); ***A61B 5/14532*** (2013.01); ***A61B 5/14546*** (2013.01); ***A61B 5/4547*** (2013.01); ***G01J 3/108*** (2013.01); ***G01J 3/28*** (2013.01); ***G01J 3/2823*** (2013.01); ***G01J 3/453*** (2013.01); ***G01N 21/359*** (2013.01); ***G01N 21/3563*** (2013.01); ***G01N 21/39*** (2013.01); ***G01N 21/88*** (2013.01); ***G01N 33/02*** (2013.01); ***G01N 33/15*** (2013.01); ***G01N 33/442*** (2013.01); ***G01N 33/49*** (2013.01); *A61B 2562/0233* (2013.01); *A61B 2562/0238* (2013.01); *A61B 2562/146* (2013.01); *A61B 2576/02* (2013.01); *G01J 3/14* (2013.01); *G01J 3/1838* (2013.01); *G01J 2003/104* (2013.01); *G01J 2003/2826* (2013.01); *G01M 3/38* (2013.01); *G01N 2021/399* (2013.01); *G01N 2201/061* (2013.01); *G01N 2201/062* (2013.01); *G01N 2201/08* (2013.01); *G01N 2201/12* (2013.01); *H01S 3/302* (2013.01)

(58) **Field of Classification Search**

USPC 356/300

See application file for complete search history.

(56) **References Cited**

U.S. PATENT DOCUMENTS

4,221,997	A	9/1980	Flemming
4,275,266	A	6/1981	Lasar
4,374,618	A	2/1983	Howard
4,403,605	A	9/1983	Tanikawa
4,462,080	A	7/1984	Johnstone et al.
4,516,207	A	5/1985	Moriyama et al.
4,523,884	A	6/1985	Clement et al.
4,605,080	A	8/1986	Lemelson
4,641,292	A	2/1987	Tunnell et al.
4,704,696	A	11/1987	Reimer et al.
4,728,974	A	3/1988	Nio et al.
4,762,455	A	8/1988	Coughlan et al.
4,776,016	A	10/1988	Hansen
4,958,910	A	9/1990	Taylor et al.
4,989,253	A	1/1991	Liang et al.
5,078,140	A	1/1992	Kwoh
5,084,880	A	1/1992	Esterowitz et al.
5,086,401	A	2/1992	Glassman et al.
5,134,620	A	7/1992	Huber
5,142,930	A	9/1992	Allen et al.
5,180,378	A	1/1993	Kung et al.
5,191,628	A	3/1993	Byron
5,218,655	A	6/1993	Mizrahi
5,230,023	A	7/1993	Nakano
5,246,004	A	9/1993	Clarke et al.
5,267,152	A	11/1993	Yang et al.
5,267,256	A	11/1993	Saruwatari et al.
5,267,323	A	11/1993	Kimura
5,300,097	A	4/1994	Lerner et al.
5,303,148	A	4/1994	Mattson et al.
5,305,427	A	4/1994	Nagata
5,313,306	A	5/1994	Kuban et al.
5,323,404	A	6/1994	Grubb
5,345,538	A	9/1994	Narayannan et al.
5,368,224	A	11/1994	Richardson et al.
5,400,165	A	3/1995	Gnauck et al.
5,408,409	A	4/1995	Glassman et al.
5,458,122	A	10/1995	Hethuin
5,544,654	A	8/1996	Murphy et al.
5,572,999	A	11/1996	Funda et al.
5,617,871	A	4/1997	Burrows
5,631,758	A	5/1997	Knox et al.
5,687,734	A	11/1997	Dempsey et al.
5,695,493	A	12/1997	Nakajima et al.
5,696,778	A	12/1997	MacPherson
5,704,351	A	1/1998	Mortara et al.
5,718,234	A	2/1998	Warden et al.
5,746,206	A	5/1998	Mannheimer
5,747,806	A	5/1998	Khalil
5,748,103	A	5/1998	Flach et al.
5,792,204	A	8/1998	Snell
5,795,300	A	8/1998	Bryars
5,812,978	A	9/1998	Nolan
5,855,550	A	1/1999	Lai et al.
5,862,803	A	1/1999	Besson et al.
5,867,305	A	2/1999	Waarts et al.
5,912,749	A	6/1999	Harstead et al.
5,919,134	A	7/1999	Diab
5,944,659	A	8/1999	Flach et al.
5,950,629	A	9/1999	Taylor et al.
5,957,854	A	9/1999	Besson et al.
5,970,457	A	10/1999	Brant et al.
6,014,249	A	1/2000	Fermann et al.
6,031,603	A	2/2000	Fine et al.
6,043,927	A	3/2000	Islam
6,115,673	A	9/2000	Malin
6,185,535	B1	2/2001	Hedin et al.
6,200,309	B1	3/2001	Rice et al.
6,224,542	B1	5/2001	Chang et al.
6,246,707	B1	6/2001	Yin et al.
6,246,896	B1	6/2001	Dumoulin
6,273,858	B1	8/2001	Fox et al.
6,278,975	B1	8/2001	Brant et al.
6,281,471	B1	8/2001	Smart
6,285,897	B1	9/2001	Kilcoyne
6,289,238	B1	9/2001	Besson et al.
6,301,271	B1	10/2001	Sanders et al.
6,301,273	B1	10/2001	Sanders et al.
6,325,978	B1	12/2001	Labuda et al.
6,333,803	B1	12/2001	Kurotori et al.
6,337,462	B1	1/2002	Smart
6,340,806	B1	1/2002	Smart et al.
6,350,261	B1	2/2002	Domankevitz et al.
6,364,834	B1	4/2002	Reuss et al.
6,374,006	B1	4/2002	Islam et al.
6,381,391	B1	4/2002	Islam et al.
6,402,691	B1	6/2002	Peddicord et al.
6,407,853	B1	6/2002	Samson et al.
6,436,107	B1	8/2002	Wang et al.
6,441,747	B1	8/2002	Khair et al.

(56) **References Cited**

U.S. PATENT DOCUMENTS

6,442,430	B1	8/2002	Ferek-Petric
6,443,890	B1	9/2002	Schulze et al.
6,450,172	B1	9/2002	Hartlaub et al.
6,453,201	B1	9/2002	Daum et al.
6,454,705	B1	9/2002	Cosentino et al.
6,458,120	B1	10/2002	Shen et al.
6,462,500	B1	10/2002	L'Hegarat et al.
6,463,361	B1	10/2002	Wang et al.
6,480,656	B1	11/2002	Islam et al.
6,512,936	B1	1/2003	Monfre
6,534,012	B1	3/2003	Hazen et al.
6,549,702	B2	4/2003	Islam et al.
6,567,431	B2	5/2003	Tabirian et al.
6,587,702	B1	7/2003	Ruchti
6,603,910	B2	8/2003	Islam et al.
6,605,080	B1	8/2003	Altshuler et al.
6,611,643	B2	8/2003	Birk
6,625,180	B2	9/2003	Bufetov et al.
6,631,025	B2	10/2003	Islam et al.
6,640,117	B2	10/2003	Makarewicz
6,659,947	B1	12/2003	Carter et al.
6,659,999	B1	12/2003	Anderson et al.
6,701,170	B2	3/2004	Stetson
6,708,048	B1	3/2004	Chance
6,731,967	B1	5/2004	Turcott
6,738,652	B2	5/2004	Mattu
6,760,148	B2	7/2004	Islam
6,773,922	B2	8/2004	Jeng
6,788,965	B2	9/2004	Ruchti
6,802,811	B1	10/2004	Slepian
6,816,241	B2	11/2004	Grubisic
6,847,336	B1	1/2005	Lemelson
6,864,978	B1	3/2005	Hazen
6,885,498	B2	4/2005	Islam
6,885,683	B1	4/2005	Fermann et al.
6,916,096	B2	7/2005	Eberl et al.
6,943,936	B2	9/2005	Islam et al.
6,990,364	B2	1/2006	Ruchti
7,010,336	B2	3/2006	Lorenz
7,027,467	B2	4/2006	Baev et al.
7,060,061	B2	6/2006	Altshuler et al.
7,133,710	B2	11/2006	Acosta
7,167,300	B2	1/2007	Fermann et al.
7,184,148	B2	2/2007	Alphonse
7,209,657	B1	4/2007	Islam
7,233,816	B2	6/2007	Blank
7,259,906	B1	8/2007	Islam
7,263,288	B1	8/2007	Islam
7,294,105	B1	11/2007	Islam
7,299,080	B2	11/2007	Acosta
7,317,938	B2	1/2008	Lorenz
7,318,909	B2	1/2008	Lehmann et al.
7,332,784	B2	2/2008	Mills et al.
7,356,364	B1	4/2008	Bullock et al.
7,395,158	B2	7/2008	Monfre
7,433,116	B1	10/2008	Islam
7,468,036	B1	12/2008	Rulkov et al.
7,519,253	B2	4/2009	Islam
7,519,406	B2	4/2009	Blank
7,620,674	B2	11/2009	Ruchti
7,648,463	B1	1/2010	Elhag et al.
7,697,966	B2	4/2010	Monfre
7,787,503	B2	8/2010	Wadsworth
7,787,924	B2	8/2010	Acosta
7,800,818	B2	9/2010	Mattsson
7,807,718	B2	10/2010	Hashim
8,000,574	B2	8/2011	Buchter
8,145,286	B2	3/2012	Arai
8,172,761	B1	5/2012	Rulkov et al.
8,180,422	B2	5/2012	Rebec
8,180,591	B2	5/2012	Yuen et al.
8,310,336	B2	11/2012	Muhsin et al.
8,315,682	B2	11/2012	Such et al.
8,463,576	B2	6/2013	Yuen et al.
8,472,108	B2	6/2013	Islam
8,475,367	B1	7/2013	Yuen et al.
RE44,875	E	4/2014	Kiani et al.
8,755,871	B2	6/2014	Weng et al.
8,945,017	B2	2/2015	Venkatraman et al.
8,954,135	B2	2/2015	Yuen et al.
9,142,117	B2	9/2015	Muhsin et al.
9,179,876	B2	11/2015	Ochs et al.
9,192,329	B2	11/2015	Al-Ali
9,207,121	B2	12/2015	Adler
9,241,676	B2	1/2016	Lisogurski et al.
9,596,990	B2	3/2017	Park et al.
9,651,533	B2	5/2017	Islam
9,675,250	B2	6/2017	Tverskoy
9,757,040	B2	9/2017	Islam
9,820,658	B2	11/2017	Tran
9,861,286	B1	1/2018	Islam
9,885,698	B2	2/2018	Islam
2002/0013518	A1	1/2002	West et al.
2002/0019584	A1	2/2002	Schulze et al.
2002/0032468	A1	3/2002	Hill et al.
2002/0082612	A1	6/2002	Moll et al.
2002/0109621	A1	8/2002	Khair et al.
2002/0115914	A1	8/2002	Russ
2002/0128846	A1	9/2002	Miller
2002/0178003	A1	11/2002	Gehrke et al.
2003/0022126	A1	1/2003	Buchalla
2003/0107739	A1	6/2003	Lehmann et al.
2003/0109055	A1	6/2003	Lehmann et al.
2003/0152307	A1	8/2003	Drasek et al.
2004/0174914	A1	9/2004	Fukatsu
2004/0240037	A1	12/2004	Harter
2005/0049468	A1	3/2005	Carlson et al.
2005/0111500	A1	5/2005	Harter et al.
2005/0133691	A1	6/2005	Doppke et al.
2005/0209516	A1	9/2005	Fraden
2006/0223032	A1	10/2006	Fried
2006/0245461	A1	11/2006	Islam
2006/0268393	A1	11/2006	Islam
2006/0283931	A1	12/2006	Polli et al.
2007/0021670	A1	1/2007	Mandelis et al.
2007/0078348	A1	4/2007	Holman
2008/0105665	A1	5/2008	Kondo
2009/0028193	A1	1/2009	Islam
2009/0204110	A1	8/2009	Islam
2010/0046067	A1	2/2010	Fermann et al.
2010/0322490	A1	12/2010	Pan
2010/0331637	A1	12/2010	Ting
2011/0143364	A1	6/2011	Kim
2011/0237911	A1	9/2011	Lamego et al.
2011/0267688	A1	11/2011	Kleppe et al.
2011/0282167	A1	11/2011	Ridder et al.
2012/0013722	A1	1/2012	Wong
2012/0203077	A1	8/2012	He et al.
2012/0239013	A1	9/2012	Islam
2012/0310062	A1	12/2012	Li et al.
2013/0274569	A1	10/2013	Islam
2013/0303921	A1	11/2013	Chu et al.
2013/0327966	A1	12/2013	Fidler et al.
2014/0078510	A1	3/2014	Rubio Guivernau et al.

FOREIGN PATENT DOCUMENTS

JP	2005270544	A	10/2005
WO	09715240		5/1997
WO	97049340		12/1997
WO	200189362		11/2001
WO	200227640		4/2002
WO	200228123		4/2002
WO	2005013843	A2	2/2005
WO	2007061772	A2	5/2007
WO	2009130464	A1	10/2009
WO	01150959		7/2011
WO	2013012938		1/2013

OTHER PUBLICATIONS

Genty, G., et al., "Supercontinuum generation in large mode-area microstructured fibers", Optics Express, vol. 13, No. 21, Oct. 17, 2005, pp. 8625-8633.

(56) **References Cited**

OTHER PUBLICATIONS

Schreiber, T., et al., "Supercontinuum generation by femtosecond single and dual wavelength pumping in photonic crystal fibers with two zero dispersion wavelengths", Optics Express, vol. 13, No. 23, Nov. 14, 2005, pp. 9556-9569.
Travers, J. C., et al., "Extended blue supercontinuum generation in cascaded holey fibers", Optics Letters, vol. 30, No. 23, Dec. 1, 2005, pp. 3132-3134.
Hagen, C. L., et al., "Generation of a Continuum Extending to the Midinfrared by Pumping ZBLAN Fiber With an Ultrafast 1550-nm Source", IEEE Photonics Technology Letters, vol. 18, No. 1, Jan. 1, 2006, pp. 91-93.
Moon, Sucbei, et al., "Generation of octave-spanning supercontinuum with I550-nm amplified diode-laser pulses and a dispersion-shifted fiber", Optics Express, vol. 14, No. 1, Jan. 9, 2006, pp. 270-278.
Fedotova, O., et al., "Supercontinuum generation in planar rib waveguides enabled by anomalous dispersion", Optics Express, vol. 14, No. 4, Feb. 20, 2006, pp. 1512-1517.
Harrington, James A., "Infrared Fiber Optics", OSA Handbook, vol. III, white paper, to be published by McGraw Hill, Undated, 13 pages.
Aaviksoo, J., et al., "Observation of optical precursors at pulse propagation in GaAs", Physical Review A, vol. 44, No. 9, Nov. 1, 1991, pp. R5353-R5356.
Boppart, Stephen A., et al., "Imaging developing neural morphology using optical coherence tomography", Journal of Neuroscience Methods 70, 1996, pp. 65-72.
Boppart, Stephen A., et al., "Noninvasive assessment of the developing Xenopus cardiovascular system using optical coherence tomography", Prec. Natl. Acad. Sci. USA, vol. 94, Apr. 1997, pp. 4256-4261.
Tearney, Guillermo J., et al., "In vivo Endoscopic Optical Biopsy with Optical Coherence Tomography", Science, New Series, vol. 276, Jun. 27, 1997, pp. 2037-2039.
De Boer, Johannes F., et al., "Imaging thermally damaged tissue by polarization sensitive optical coherence tomography", Optics Express 212, vol. 3, No. 6, Sep. 14, 1998, pp. 212-218.
Roggan, Andre, et al., "Optical Properties of Circulating Human Blood in the Wavelength Range 400-2500 NM", Journal of Biomedical Optics, vol. 4, No. 1, Jan. 1999, pp. 36-46.
De Boer, Johannes R, et al., "Determination of the depth-resolved Stokes parameters of light backscattered from turbid media by use of polarization-sensitive optical coherence tomography", Optics Letters, vol. 24, No. 5; Mar. 1, 1999, pp. 300-302.
Rollins, Andrew M., et al., "Real-time in vivo imaging of human gastrointestinal ultrastructure by use of endoscopic optical coherence tomography with a novel efficient interferometer design", Optics Letters, vol. 24, No. 19, Oct. 1, 1999, pp. 1358-1360.
D'Amico, Anthony V., et al., "Optical Coherence Tomography as a Method for Identifying Benign and Malignant Microscopic Structures in the Prostate Gland", Basic Science, Urology 55 (5), 2000, pp. 783-787.
Li, Xingde, et al., "Imaging needle for optical coherence tomography", Optics Letters, vol. 25, No. 20, Oct. 15, 2000, pp. 1520-1522.
Oughstun, Kurt E., "Influence of precursor fields on ultrashort pulse autocorrelation measurements and pulse width evolution", Optics Express, vol. 8, No. 8, Apr. 9, 2001, pp. 481-491.
Kowalevicz, Andrew M., et al., "Ultrahigh resolution optical coherence tomography using a superluminescent light source" Optics Express 349, vol. 10, No. 7, Apr. 8, 2002, pp. 349-353.
Povazay, B., et al., "Submicrometer axial resolution optical coherence tomography", Optics Letters, vol. 27, No. 20, Oct. 15, 2002, pp. 1800-1802.
Xie, T.-Q., et al., "Detection of tumorigenesis in urinary bladder with optical coherence tomography: optical characterization of morphological changes", Optics Express, vol. 10, No. 24, Dec. 2, 2002, 2003, pp. 1431-1443.
Seefeldt, Michael, et al., "Compact white-light source with an average output power of 2.4 Wand 900 nm spectral bandwidth", Optics Communications 216, pp. 199-202.
Wang, Yimin, et al., "Ultrahigh-resolution optical coherence tomography by broadband continuum generation from a photonic crystal fiber", Optics Letters, vol. 28, No. 3, Feb. 1, 2003, pp. 182-184.
Bizheva, K, et al., "Compact, broad-bandwidth fiberlaserforsub-2-pm axial resolution optical coherence tomography in the 1300-nm wavelength region", Optics Letters, vol. 28, No. 9, May 1, 2003, pp. 707-709.
Pan, Yingtian, et al., "Hand-held arthroscopic optical coherence tomography for in vivo high-resolution imaging of articular cartilage", Journal of Biomedical Optics 8(4), Oct. 2003, pp. 648-654.
Xie, Tuqiang, et al., "Endoscopic optical coherence tomography with a modified microelectromechanical systems mirror for detection of bladder cancers", Applied Optics, vol. 42, No. 31, Nov. 1, 2003, pp. 6422-6426.
Dubois, A., et al., "Three-dimensional cellular-level imaging using full-field optical coherence tomography", Physics in Medicine and Biology, Phys. Med. Biol. 49, 2004, pp. 1227-1234.
Park, Jesung, et al., "Analysis of birefringent image in the retinal nerve fiber layer by polarization sensitive optical coherence tomography", Ophthalmic Technologies XIV, Proceedings of SPIE, vol. 5314, 2004, pp. 188-194.
Unterhuber, A., et al., "Advances in broad bandwidth light sources for ultrahigh resolution optical coherence tomography", Physics in Medicine and Biology, Phys. Med. Biol. 49, 2004, pp. 1235-1246.
Drexler, Wolfgang, "Ultrahigh-resolution optical coherence tomography", Journal of Biomedical Optics, vol. 9, No. 1, Jan./Feb. 2004, pp. 47-74.
Schmitt, Joseph, et al., "Intravascular Optical Coherence Tomography Opens a Window Onto Coronary Artery Disease", Optics & Photonics News, Feb. 2004, pp. 20-25.
Nassif, N.A., et al., "In vivo high-resolution video-rate spectral-domain optical coherence tomography of the human retina and optic nerve", Optics Express, vol. 12, No. 3, Feb. 9, 2004, pp. 367-376.
Choi, Seung-Ho, et al., "Observation of Optical Precursors in Water", Physical Review Letters, vol. 92, No. 19, May 14, 2004, pp. 193903-1-193903-.3.
Pierce, Mark C., et al., "Advances in Optical Coherence Tomography imaging for Dermatology", Optical Coherence Tomography Advances, The Journal of Investigative Dermatology, Sep. 3, 2004, pp. 458-463.
"State-Specific Trends in Chronic Kidney Failure—United States, 1990-2001", Morbidity and Mortality Weekly Report, Department of Health and Human Services Centers for Disease Control and Prevention, vol. 53, No. 39, copied from internet: file://C:\Documents and Settings\eturlo\Desktop\State-Specific Trends in Chronic Kidney . . . Feb. 12, 2010, Oct. 8, 2004, pp. 918-920.
I.B. Ads, A.A.E. Wagie, N.B. Mariun, A.B.E. Jammal, "An Internet-based blood pressure monitoring system for patients," Journal of Telemedicine and Telecare, 2001, pp. 51-53.
R.H. Istepanian, B. Woodward, P.A. Bales, S. Chen, B. Luk, "The comparative performance of mobile telemediCal systems based on the IS-54 and GSM cellular telephone standards," Journal of Telemedicine and Telecare, 1999, pp. 97-104.
Shaw, et al, IR Supercontinuum Generation in As—Se Photonic Crystal Fiber, Optical Society of America, Copyright 2005, 3 pages.
PCT/US06/44451, Notification of Transmittal of the International Search Report and the Written Opinion of the International Searching Authority, or the Declaration, Nov. 29, 2007, 12 pages.
G.S. Edwards et al., "Free-electron-laser-based biophysical and biomedical instrumentation," American Institute of Physics, vol. 74, No. 7, Jul. 2003, pp. 3207-3245.
Computer Motion, Inc., "501(k) Summary—ZEUS® MicroWrist™ Surgical System and Accessories," Sep. 24, 2002, 6 pages.
Computer Motion, Inc. "HERMES™ O.R. Control Center—510(k) Summary of Safety and Effectiveness," Oct. 11, 2002, 5 pages.
K.M. Joos, et al. "Optic Nerve Sheath Fenestration with a Novel Wavelength Produced by the Free Electron Laser (FEL)," Lasers in Surgery and Medicine, 27: 2000,191-205.
J. Sanghera, I. Aggarwal, "IR Fiber Optics at NRL," undated, 10 pages.
J. Sanghera, L.B. Shaw, I.D. Aggarwal, "Applications of chalcogenide glass optical fibers," Academic of Science, 2003, pp. 1-11.

(56) **References Cited**

OTHER PUBLICATIONS

B. Rigas, P.T.T. Wong, "Human Colon Adenocarcinoma Cell Lines Display Infrared Spectroscopic Features," Cancer Research, Jan. 1, 1992, pp. 84-88.
G. Edwards, et al., "Comparison of OPA and Mark-III FEL for Tissue Ablation at 6.45 Microns," Department of Physics and Free Electron Laser Laboratory, Duke University, 2002, 7 pages.
Glenn Edwards, "Biomedical and potential clinical applications for pulsed lasers operating near 6.45 um," Society of Photo-Optical Instrumentation Engineers, 1995, 2 pages.
Passat, "Solid-State Lasers and Optical Components," Jul. 14, 2003, 5 pages.
P.A. Thielen and L.B. Shaw, et al., "Small-core As—Se fiber for Raman amplification," Optics Leti-ers, vol. 28, No. 16, Aug. 15, 2003, 3 pages.
R.Rox Anderson, et al., "Selective Photothermolysis: Precise Microsurgery by Selective Absorption of Pulsed Radiation," Department of Dermatology, Harvard Medical School, Science, vol. 220, Apr. 29, 1983, 4 pages.
U.S. Appl. No. 10/652,276, "System and Method for Voice Control of Medical devices," by Mohammed N. Islam, abandoned (074036.0129) Date filed: Aug. 29, 2003.
U.S. Appl. No. 10/757,341, "System and Method for Voice Control of Medical devices," by Mohammed N. Islam, issued (074036.0132) Date filed: Jan. 13, 2004.
U.S. Appl. No. 12/206,432, "System and Method for Voice Control of Medical Devices," by Mohammed N. Islam, pending (074036.0154) Date filed: Sep. 8, 2008.
U.S. Patent and Trademark Office, Office Action for U.S. Appl. No. 12/206,432, filed Sep. 8, 2008, Mohammed N, Islam, Date filed: Mar. 12, 2009.
U.S. Patent and Trademark Office, Notice of Allowance and Fee(s) Due for U.S. Appl. No. 12/206,432, filed Sep. 8, 2008, Mohammed N. Islam, Date filed: Aug. 28, 2009.
International Search Report and Written Opinion for International Application No. PCT/US2013/075736 dated Apr. 7, 2014.
International Preliminary Report on Patentability for International Application No. PCT/US2013/075736 dated Jul. 9, 2015.
Hori, Takashi, et al., "Flatly broadened, wideband and low noise supercontinuum generation in highly nonlinear hybrid fiber", Optics Express, vol. 12, No. 2, Jan. 26, 2004, pp. 317-324.
Wadsworth, W. J., et al., "Supercontinuum and four-wave mixing with Q-switched pulses in endlessly single-mode photonic crystal fibres", Optics Express, vol. 12, No. 2, Jan. 26, 2004, pp. 299-309.
Hilligsoe, Karen Marie, et al., "Supercontinuum generation in a photonic crystal fiber with two zero dispersion wavelengths", Optics Express, vol. 12, No. 6, Mar. 22, 2004, pp. 1045-1054.
Venugopalan, V., "Optical Society of America BIOMED Topical Meeting Tutorial on Tissue Optics", Apr. 27, 2004, pp. 1-32.
Slusher, Richart E., et al., "Large Raman gain and nonlinear phase shifts in high-purity As2So3 chalcogenide fibers", J. Opt. Soc. Am. B, vol. 21, No. 6, Jun. 2004, pp. 1146-1155.
Leon-Saval, S. G., et al., "Supercontinuum generation in submicron fibre waveguides", Optics Express, vol. 12, No. 13, Jun. 28, 2004, pp. 2864-2869.
Nicholson, J. W., et al., "High power, single mode, all-fiber source of femtosecond pulses at 1550 nm and its use in supercontinuum generation", Optics Express, vol. 12, No. 13, Jun. 28, 2004, pp. 3025-3034.
Genty, G., et al., "Enhanced bandwidth of supercontinuum generated m microstructured fibers", Optics Express, vol. 12, No. 15, Jul. 26, 2004, pp. 3471-3480.
Champert, Pierre-Alain, et al., "White-light supercontinuum generation in normally dispersive optical fiber using original multi-wavelength pumping system", Optics Express, vol. 12, No. 19, Sep. 20, 2004, pp. 4366-4371.
Nicholson, J. W., "Supercontinuum generation in ultraviolet-irradiated fibers", Optics Letters, vol. 29, No. 20, Oct. 15, 2004, pp. 2363-2365.
Hori, Takashi, et al., "Experimental and numerical analysis of widely broadened supercontinuum generation in highly nonlinear dispersion-shifted fiber with a femtosecond pulse", J. Opt. Soc. Am. B, vol. 21, No. 11, Nov. 2004, pp. 1969-1980.
Demircan, Ayhan, et al., "Supercontinuum generation by the modulation instability", Optics Communications 244, 2005, pp. 181-185.
Papemyi, S. B., et al., "Sixth-Order Cascaded Raman Amplification", OFC/NFOEC, 2005, 3 pages.
Tanaka, Keiji, "Optical nonlinearity in photonic glasses", Journal of Materials Science: Materials in Electronics 16, 2005, pp. 633-643.
Westbrook, Paul S., "Improved Supercontinuum Generation Through UV Processing of Highly Nonlinear Fibers", Journal of Lightwave Technology, vol. 23, No. 1, Jan. 2005, pp. 13-18.
Abeeluck, Akheelesh K., et al., "Continuous-wave pumping in the anomalous- and normal dispersion regimes of nonlinear fibers for supercontinuum generation", Optics Letters, vol. 30, No. 1, Jan. 1, 2005, pp. 61-63.
Kutz, J. Nathan, et al., "Enhanced Supercontinuum Generation through Dispersion-Management", Optics Express, vol. 13, No. 11, May 30, 2005, pp. 3989-3998.
Lee, Ju Han, et al., "Experimental performance comparison for various continuous-wave supercontinuum schemes: ring cavity and single pass structures", Optics Express, vol. 13, No. 13, Jun. 27, 2005, pp. 4848-4853.
Saliminia, A., et al., "Ultra-broad and coherent white light generation in silica glass by focused femtosecond pulses at 1.5pm", Optics Express, vol. 13, No. 15, Jul. 25, 2005, pp. 5731-5738.
Takushima, Yuichi, High average power, depolarized supercontinuum generation using a 1.55-um ASE noise source, Optics Express, vol. 13, No. 15, Jul. 25, 2005, pp. 5871.-5877.
Travers, J. C., et al., "Extended continuous-wave supercontinuum generation in a low-water-loss holey fiber", Optics Letters, vol. 30, No. 15, Aug. 1, 2005, pp. 1938-1940.
Kobtsev, Serguei M., et al., "Modelling of high-power supercontinuum generation in highly nonlinear, dispersion shifted fibers at CW pump", Optics Express, vol. 13, No. 18, Sep. 5, 2005, pp. 6912-6918.
Falk, Peter, et al., "Supercontinuum generation in a photonic crystal fiber with two zero-dispersion wavelengths tapered to normal dispersion at all wavelengths", Optics Express, vol. 13, No. 19, Sep. 19, 2005, pp. 7535-7540.
Tombelaine, Vincent, et al., "Ultra wide band supercontinuum generation in air-silica holey fibers by SHG-induced modulation instabilities", Optics Express, vol. 13, No. 19, Sep. 19, 2005, pp. 7399-7404.
Hazen, K.H., M.A. Arnold, G.W. Small, "Measurement of glucose and other analytes in undiluted human serum with near-infrared transmission spectroscopy," Analytica Chimica Acta, vol. 371, pp. 255-267 (1998).
Malin, S.F., T.L. Ruchti, T.B. Blank, S.N. Thennadil, S.L. Monfre, "Noninvasive prediction of glucose by near-infrared diffuse reflectance spectroscopy," Clinical Chemistry, vol. 45, No. 9, pp. 1651-1658 (1999).
Thennadil, S.N., J.L. Rennert, B.J. Wenzel, K.H. Hazen, T.L. Ruchti, M.B. Block, "Comparison of glucose concentration in interstitial fluid, and capillary and venous blood during rapid changes in blood glucose levels," Diabetes Technology & Therapeutics, vol. 3, No. 3, pp. 357-365 (2001).
Troy, T.L., S.N. Thennadil, "Optical properties of human skin in the near infrared wavelength range of 1000 to 2200nm," Journal of Biomedical Optics, vol. 6, No. 2, pp. 167-176, (2001).
Blank, T.B., T.L. Ruchti, A.D. Lorenz, S.L. Monfre, M.R. Makarewicz, M. Mattu, K.H. Hazen, "Clinical results from a non-invasive blood glucose monitor," Optical Diagnostics and Sensing of Biological Fluids and Glucose and Cholesterol Monitoring II, A.V. Priezzhev and G.L. Cote, Editors, Proceedings of SPIE, vol. 4624, pp. 1019 (2002).
Yeh, S-J, C.F. Hanna, O.S. Khalil, "Monitoring blood glucose changes in cutaneous tissue by temperature-modulated localized reflectance measurements," Clinical Chemistry, vol. 49, No. 6, pp. 924-934 (2003).

(56) **References Cited**

OTHER PUBLICATIONS

Marbach, R., T. Koschinsky, F.A. Gries, H.M. Heise, "Noninvasive blood glucose assay by near-infrared diffuse reflectance spectroscopy of the human inner lip," Applied Spectroscopy, vol. 47, No. 7, pp. 875-881 (1993).

Enejder, A.M.K., T.G. Scecina, J. Oh, M. Hunter, W.C. Shih, S. Sasic, G.L. Horowitz, M.S. Feld, "Raman spectroscopy for noninvasive glucose measurements," Journal of Biomedical Optics, vol. 10, No. 3, 031114 (2005).

Olesberg, J.T., L. Liu, V.V. Zee, M.A. Arnold, "In vivo near-infrared spectroscopy of rat skin tissue with varying blood glucose levels," Analytic Chemistry, vol. 78, No. 1, pp. 215-223 (2006).

Olesberg, J.T., M.A. Arnold, C. Mermelstein, J. Schmitz, J. Wagner, "Tunable laser diode system for noninvasive blood glucose measurements," Applied Spectroscopy, vol. 59, No. 12, pp. 1480-1484 (2005).

Harman-Boehm, I. A. Gal, A.M. Raykhman, J.D. Zahn, E. Naidis, Y. Mayzel, "Noninvasive glucose monitoring: a novel approach," Journal of Diabetes Science and Technology, vol. 3, No. 2 pp. 253-260 (2009).

Kim-K.D., G.S. Son, S.S. Lim, S.S. Lee, "Measurement of glucose level exploiting a relative optical absorption at discrete probe wavelengths," Japanese Journal of Applied Physics, vol. 48, 077001 (2009).

Smith, J.L., "The Pursuit of Noninvasive Glucose: Hunting the Deceitful Turkey," 2nd Edition, pp. 1-141 (2011).

Pezzaniti, J.L., T.W. Jeng, L. McDowell, G.M. Oosta, "Preliminary investigation of near-infrared spectroscopic measurements of urea, creatinine, glucose, protein and ketone in urine," Clinical Biochemistry, vol. 34, pp. 239-246 (2001).

Lussi, A., R. Hibst, R. Paulus, "Diagnodent: An optical method for caries detection," Journal of Dental Research, vol. 83, special issue C, pp. C80-C83 (2004).

Reese, E.L, E.E. Fisher, D.A. Horowitz, "Photoelectric densitometry of the circulation of the human dental pulp," The Journal of the Baltimore College of Dental Surgery, vol. 26, No. 1, pp. 6-18 (1971).

Zakian, C., I. Pretty, R. Ellwood, "Near-infrared hyperspectral imaging of teeth for dental caries detection," Journal of Biomedical Optics, vol. 16, No. 6, 064047 (2009).

Belikov, A.V., A.V. Skripnik, K.V. Shatilova, "Study of the dynamics of the absorption spectra of human tooth enamel and dentine under heating and ablation by submillisecond pulse radiation of an erbium laser with a generation wavelength of 2.79 um," Optics and Spectroscopy, vol. 109, No. 2, pp. 211-216 (2010).

Karlsson, L. "Caries detection methods based on changes in optical properties between healthy and carious tissue," International Journal of Dentistry, vol. 2010, Article ID 270729, 9 pages (2010).

Fried, D. M. Staninec, C.L. Darling, "Near-infrared imaging of dental decay at 1310nm," Journal of Laser Dentistry, vol. 18, No. 1, pp. 8-16 (2010).

Burmen, M. P. Usenik, A. Fidler, F. Pernus, B. Likar, "A construction of standardized near infrared hyper-spectral teeth database—a first step in the development of reliable diagnostic tool for quantification and early detection of caries," Lasers in Dentistry XVII, edited by P. Rechmann, D. Fried, Proceedings of SPIE, vol. 7884, Paper 78840E (2011).

Maia, A., L. Karlsson, W. Margulis, A. Gomes, "Evaluation of two imaging techniques: near-infrared transillumination and dental radiographs for the detection of early approximal enamel caries," Dentomaxillofacial Radiology, vol. 40, pp. 429-433 (2011).

Chung, S., D. Fried, M. Staninec, C.L. Darling, "Multispectral near-IR reflectance and transillumination imaging of teeth," Biomedical Optics Express, vol. 2, No. 10, pp. 2804-2814 (2011).

Chung, S., D. Fried, M. Staninec, C.L. Darling, "Near infrared imaging of teeth at wavelengths between 1200 and 1600nm," Proceedings of the Society of Photo Optical Instrument Engineering, paper 7884 (2011).

Staninec, M., S.M. Douglas, C.L. Darling, K. Chan, H. Kang, R. C. Lee, D. Fried, "Nondestructive clinical assessment of occlusal caries lesions using near-IR imaging methods," Lasers in Surgery and Medicine, vol. 43, No. 10, pp. 951-959 (2011).

Nishizawa, N., "Generation and application of high-quality supercontinuum sources," Optical Fiber Technology, vol. 18, pp. 394-402 (2012).

Robert S. Jones et al.; Near-Infrared Transillumination at 1310-nm for the Imaging of Early Dental Decay; vol. 11, No. 18; Optics Express 2259; Sep. 8, 2003.

Extended European Search Report for European Application No. 13867892.5 dated Jul. 22, 2016.

Extended European Search Report for European Application No. 13867874.3 dated Jul. 15, 2016.

Vinay V. Alexander et al.; Modulation Instability High Power All-Fiber Supercontinuum Lasers and Their Applications; Optical Fiber Technology 18; 2012; pp. 349-374.

Final Office Action dated Oct. 21, 2016 for U.S. Appl. No. 14/875,709.

Islam, M. N., et al., "Broad bandwidths from frequency-shifting solitons in fibers", Optics Letters, vol. 14, No. 7, Apr. 1, 1989, pp. 370-372.

Islam, M. N., et al., "Femtosecond distributed soliton spectrum in fibers", J. Opt. Soc. Am. B, vol. 6, No. 6, Jun. 1989, pp. 1149-1158.

Busse, Lynda E., et al., "Design Parameters for Fluoride Multimode Fibers", Journal of Lightwave Technology, vol. 9, No. 7, Jul. 1991, pp. 828-831.

Wuthrich, Stefan, et al., "Optical damage thresholds at 2.94 urn in fluoride glass fibers", Applied Optics, vol. 31, No. 27, Sep. 20, 1992, pp. 5833-5837.

Inoue, H., et al., "Computer simulation of the vibrational spectra and properties of fluoride glasses based on ZrF4", Journal of Non-Crystalline Solids, vol. 161, 1993, pp. 118-122.

Mizunami, Toru, et al., "Gain saturation characteristics of Raman amplification in silica and fluoride glass optical fibers", Optics Communications 97, 1993, pp. 74-78.

Desthieux, B., et al., "111 kW (0. 5 mJ) pulse amplification at 1.5 um using a gated cascade of three erbium-doped fiber amplifiers," Appl. Phys. Lett. vol. 63, Aug. 2, 1993, pp. 586-588.

Edwards, Glenn, et al., Tissue ablation by a free-electron laser tuned to the amide II band, Nature, vol. 371, Sep. 29, 1994, pp. 416-419.

Borrelli, N. F., et al., "Resonant and non-resonant effects in photonic glasses", Journal of Non-Crystalline Solids 185, 1995, pp. 109-122.

Asobe, Masaki, et al., "Third-order nonlinear spectroscopy in As2S3 chalcogenide glass fibers", J. Appl. Phys. 77 (11), Jun. 1, 1995, pp. 5518-5523.

Jarman, Richard H., "Novel optical fiber lasers", Current Opinion in Solid State and Materials Science, 1996, pp. 199-203.

Iatridis, James C., et al., "Is the Nucleus Pulposus a Solid or a Fluid? Mechanical Behaviors of the Nucleus Pulposus of the Human Intervertebral Disc", Spine, vol. 21(10), May 15, 1996, pp. 1174-1184.

Asobe, Masaki, "Nonlinear Optical Properties of Chalcogenide Glass Fibers and Their Application to All-Optical Switching", Optical Fiber Technology, vol. 3, Article No. OF970214, 1997, pp. 142-148.

Smektala, F., et al., "Chalcogenide glasses with large non-linear refractive indices", Journal of Non-Crystalline Solids 239, 1998, pp. 139-142.

Hamilton, James D., et al., "High Frequency Ultrasound Imaging with Optical Arrays", IEEE Transactions on Ultrasonics, Ferroelectrics, and Frequency Control, vol. 45, No. 1, Jan. 1998, pp. 216-235.

Hamilton, James D., et al., "High Frequency Ultrasound Imaging Using an Active Optical Detector", IEEE Transactions on Ultrasonics, Ferroelectrics, and Frequency Control, vol. 45, No. 3, May 1998, pp. 719-727.

Nowak, G. A., et al., "Low-power high-efficiency wavelength conversion based on modulational instability in high-nonlinearity fiber," Optics Letters, vol. 23, No. 12, Jun. 15, 1998, pp. 936-938.

Cardinal, T., et al., "Non-linear optical properties of chalcogenide glasses in the system As—S—Se", Journal of Non-Crystalline Solids 256 & 257, 1999, pp. 353-360.

Lucas, Jacques, "Infrared glasses", Current Opinion in Solid State & Materials Science 4, 1999. pp. 181-187.

(56) **References Cited**

OTHER PUBLICATIONS

Sanghera, J. S., et al., Active and passive chalcogenide glass optical fibers for IR applications: a review, Journal of Non-Crystalline Solids 256 & 257, 1999, pp. 6-16.
Nishida, Yoshiki, et al., "Reliability of Fluoride Fiber Module for Optical Amplifier Use", IEEE Photonics Technology Letters, vol. 11, No. 12, Dec. 1999, pp. 1596-1598.
Nowak, George A., et al., "Stable supercontinuum generation in short lengths of conventional dispersion-shifted fiber", Applied Optics, vol. 38, No. 36, Dec. 20, 1999, pp. 7364-7369.
Urban, J. P. G., et al., "The Nucleus of the Intervertebral Disc from Development to Degeneration" Amer. Zool., vol. 40, 2000, pp. 53-61.
Hamilton, James D., et al., "High Frequency Optoacoustic Arrays Using Etalon Detection", IEEE Transactions on Ultrasonics, Ferroelectrics, and Frequency Control, vol. 47, No. 1, Jan. 2000, pp. 160-169.
Ranka, Jinendra K., et al., "Visible continuum generation in air-silica microstructure optical fibers with anomalous dispersion at 800 nm", Optics Letters, vol. 25, No. 1, Jan. 1, 2000, pp. 25-27.
Boult, Maggi, et al., "Systematic Review of Percutaneous Endoscopic Laser Discectomy: Update and Re-appraisal", Australian Safety and Efficacy Register of New Interventional Procedures—Surgical Report No. 5, Feb. 2000, 49 pages.
Boult, Maggi, et aL, "Percutaneous Endoscopic Laser Discectomy", Systematic Review, Aust. N.Z.J. Surg., vol. 70, Apr. 7, 2000, pp. 475-479.
Camacho, Nancy P., et al., "FTIR Microscopic Imaging of Collagen and Proteoglycan in Bovine Cartilage," Biopolymers (Biospectroscopy), vol. 62, 2001, pp. 1-8.
Choi, Joon Y., et al, "Thermal, Mechanical, Optical, and Morphologic Changes in Bovine Nucleus Pulposus Induced by Nd:YAG ((λ =1.32 um) Laser Irradiation", Lasers in Surgery and Medicine, vol. 28, 2001, pp. 248-254.
Hafez, M. I., et al., "The Effect of Irrigation on Peak Temperatures in Nerve Root, Dura, and Intervertebral Disc During Laser-Assisted Foraminoplasty", Lasers in Surgery and Medicine, vol. 29, 2001, pp. 33-37.
Jackson, Stuart D., et al., "Theory and numerical simulation of nth-order cascaded Raman fiber lasers", J. Opt. Soc. Am. B, vol. 18, No. 9, Sep. 2001, pp. 1297-1306.
Werle, Peter, et a!., "Near- and mid-infrared laser-optical sensors for gas analysis", Optics and Lasers in Engineering 37, 2002, pp. 101-114.
Beck, Mattias, et al., "Continuous Wave Operation of a Mid-Infrared Semiconductor Laser at Room Temperature," Science vol. 295, www.sciencemag.org, Jan. 11, 2002, pp. 301-305.
Harbold, J. M., et al., "Highly nonlinear As—S—Se glasses for all-optical switching", Optics Letters, vol. 27, No. 2, Jan. 15, 2002, pp. 119-121.
Coen, Stephane, et al., "Supercontinuum generation by stimulated Raman scattering and parametric four-wave mixing in photonic crystal fibers", J. Opt. Soc. Am. B, vol. 19, No. 4, Apr. 2002, pp. 753-764.
Dudley, John M., et al., "Supercontinuum generation in air-silica microstructured fibers with nanosecond and femtosecond pulse pumping", J. Opt. Soc. Am. B, vol. 19, No. 4, Apr. 2002, pp. 765-771.
Harbold, Jeffrey M., et al., "Highly Nonlinear Ge—As—Se and. Ge—As—S—Se Glasses for All-Optical Switching", IEEE Photonics Technology Letters, vol. 14, No. 6, Jun. 2002, pp. 822-824.
Husakou, Anton V., et al, "Supercontinuum generation, four-wave mixing, and fission of higher-order solitons in photonic-crystal fibers", J. Opt. Soc. Am. B, vol. 19, No. 9, Sep. 2002, pp. 2171-2182.
Wadsworth, William J., et al., "Supercontinuum generation in photonic crystal fibers and optical fiber tapers: a novel light source", J. Opt. Soc. Am. B, vol. 19, No. 9, Sep. 2002, pp. 2148-2155.
Kumar, V.V. Ravi Kanth, et al, "Extruded soft glass photonic crystal fiber for ultrabroad supercontinuum generation", Optics Express, vol. 10, No. 25, Dec. 16, 2002, pp. 1520-1525.
Edwards, Glenn S., et al., "Advantage of the Mark-III FEL for biophysical research and biomedical applications", J. Synchrotron Rad. vol. 10, 2003, pp. 354-357.
Nicholson, J. W., et al., "Pulsed and continuous-wave supercontinuum generation in highly nonlinear, dispersion-shifted fibers", Applied Physics B 77, 2003, pp. 211-218.
Sobol, Emil, et al., "Time-resolved, light scattering measurements of cartilage and cornea denaturation due to free electron laser radiation", Journal of Biomedical Optics, vol. 8, No. 2, Apr. 2003, pp. 216-222.
Nicholson, J. W., et al., "All-fiber, octave-spanning supercontinuum", Optics Letters, vol. 28, No. 8, Apr. 15, 2003, pp. 643-645.
Faralli, S., et al., "Impact of Double Rayleigh Scattering Noise in Distributed Higher Order Raman Pumping Schemes", IEEE Photonics Technology Letters, vol. 15, No. 6, Jun. 2003, pp. 804-806.
"New and Emerging Techniques—Surgical, Rapid Review, Laser Discectomy", Australian Safety and Efficacy Register of New Interventional Procedures—Surgical, Jun. 2003, 12 pages.
Avdokhin, A. V., et al, "Continuous-wave, high-power, Raman continuum generation in holey fibers", Optics Letters, vol. 28, No. 15, Aug. 1, 2003, pp. 1353-1355.
Mussot, Arnaud, et al., "Generation of a broadband single-mode supercontinuum in a conventional dispersion-shifted fiber by use of a subnanosecond microchip laster", Optics Letters, vol. 28, No. 19, Oct. 1, 2003, pp. 1820-1822.
Slusher, Richard, et al., "Highly nonlinear composite chalcogenide/polymer fibers", OSA 2004, 1 page.
Thongtrangan, Issada, et al., "Minimally invasive spinal surgery: a historical perspective", Neurosurg. Focus, vol. 16, Article 13, Jan. 2004, pp. 1-10.
Istepanian, Robert H., "The Comparative Performance of Mobile Telemedical Systems based on the IS-54 and GSM Cellular Telephone Standards"; Journal of Telemedicine and Telecare 1999; pp. 97-104.
Aris, Ishak Bin, "An Internet-Based Blood Pressure Monitoring System for Patients"; Journal of Telemedicine and Telecare 2001; pp. 51-53.
Sun, Y., C.F. Booker, S. Kumari, R.N. Day, M. Davidson, A. Periasamy, "Characterization of an orange acceptor fluorescent protein for sensitized spectral fluorescence resonant energy transfer microscopy using a white-light laser," Journal of Biomedical Optics, vol. 14, No. 5, paper 054009 (2009).
Borlinghaus, R., "Colours Count: how the challenge of fluorescence was solved in confocal microscopy," in Modern Research and Educational Topics in Microscopy, A. Mendez-Vilas and J. Diaz, eds, pp. 890-899, Formatex (2007).
Borlinghaus, R., "The White Confocal: Continuous Spectral Tuning in Excitation and Emission," in Optical Fluorescence Microscopy, A. Diaspro (Ed), Chapter 2, pp. 37-54, ISBN 978-3-642-15174-3, Springer-Verlag, Berlin (2011).
Borlinghaus, R.T., L. Kuschel, "White Light Laser: The Ultimate Source for Confocal Microscopy," http://www.leica-microsystems.com/science-lab/white-light-laser (Jun. 27, 2012).
Ziegler, U., A.G. Bittermann, M. Hoechli, "Introduction to Confocal Laser Scanning Microscopy (LEICA)," www.zmb.unizh.ch, May 29, 2013.
Ooi ET, Zhang XQ, Chen JH, Soh PH, Ng K, Yea JH, "Non-invasive glucose measurement using multiple laser diodes," Optical Diagnostic and Sensing VII, edited by Gerard L. Cote, Alexander V. Priezzhev, Proc. of SPIE vol. 6445, 64450K , (2007).
Schulz, I., J. Putzger, A. Niklas, M. Brandt, A. Jager, A. Hardt, S. Knorzer, K.A. Hiller, S. Loffler, G. Schmalz, S.N. Danilov, S. Giglberger, M. Hirmer, S.D. Ganichev, G. Monkman, "PPG signal acquisition and analysis on in vitro tooth model for dental pulp vitality assessment," ARC Submission 16, (2012).
Drexler, C., Hirmer, M., Danilov, S., Giglberger, S., Putzger, J., Niklas, A., Jager, A., Hiller, K., Loffler, S., Schmalz, G., Redlich, B., Schulz, I., Monkman, G., Ganichev, S. "Infrared spectroscopy for

(56) **References Cited**

OTHER PUBLICATIONS

clinical diagnosis of dental pulp vitality." Infrared, Millimeter, and Terahertz Waves (IRMMW-THz), 2012 37th International Conference on. IEEE (2012).
Hirmer, Marion, Danilov, Sergey, Giglberger, Stephan, Putzger, Jurgen, Niklas, Andreas, Jager, Andreas, Hiller, Karl-Anton, Loffler, Susanne, Schmalz, Gottfried, Redlich, Britta, Schulz, Irene, Monkman, Gareth, Ganichev, Sergey. "Spectroscopic Study of Human Teeth and Blood from Visible to Terahertz Frequencies for Clinical Diagnosis of Dental Pulp Vitality." Journal of Infrared, Millimeter, and Terahertz Waves 33.3 (2012): 366-375.
Na, J, J.H. Baek, S.Y. Ryu, C. Lee, B.H. Lee, "Tomographic imaging of incipient dental-caries using optical coherence tomography and comparison with various modalities," Optical Review, vol. 16, No. 4, pp. 426-431 (2009).
J.G. Webster; Design of Pulse Oximeters; Medical Science Series; Taylor & Francis Group; CRC Press; Oct. 23, 1997; 260 pps.
H. Harry Asada et al.; Mobile Monitoring With Wearable Photoplethysmographic Biosensors; IEEE Engineering in Medicine and Biology Magazine, Jun. 2003; 13 pps.
United States District Court Eastern District of Texas Marshall Division; Defendant and Counter Claimant Apple Inc.'s Amended Answer, Affirmative Defenses, and Counterclaims to Complaint of Plaintiff and Counter Defendant Omni Medsci, Inc.; Document 38; Jul. 19, 2018; 32 pps.
Omni Medsci, Inc. v. *Apple Inc.*; Case No. 2:18-cv-134-RWS (E.D. Tex.); Defendant's Invalidity Contentions, Aug. 28, 2018 (Exhibit A), 66 pps.
Omni Medsci, Inc. v. *Apple Inc.*; Case No. 2:18-cv-134-RWS (E.D. Tex.); Defendant's Invalidity Contentions, Aug. 28, 2018 (Exhibit B), 73 pps.
Omni Medsci, Inc. v. *Apple Inc.*; Case No. 2:18-cv-134-RWS (E.D. Tex.); Defendant's Invalidity Contentions, Aug. 28, 2018 (Exhibit C), 85 pps.
Omni Medsci, Inc. v. *Apple Inc.*; Case No. 2:18-cv-134-RWS (E.D. Tex.); Defendant's Invalidity Contentions, Aug. 28, 2018 (Exhibit D), 38 pps.
Omni Medsci, Inc. v. *Apple Inc.*; Case No. 2:18-cv-134-RWS (E.D. Tex.); Defendant's Invalidity Contentions, Aug. 28, 2018 (Exhibit E), 120 pps.
Omni Medsci, Inc. v. *Apple Inc.*; Case No. 2:18-cv-134-RWS (E.D. Tex.); Defendant's Invalidity Contentions, Aug. 28, 2018 (Exhibit F), 40 pps.
Omni Medsci, Inc. v. *Apple Inc.*; Case No. 2:18-cv-134-RWS (E.D. Tex.); Defendant's Invalidity Contentions, Aug. 28, 2018 (Exhibit G), 66 pps.
Omni Medsci, Inc. v. *Apple Inc.*; Case No. 2:18-cv-134-RWS (E.D. Tex.); Defendant's Invalidity Contentions, Aug. 28, 2018 (Exhibit H), 74 pps.
Omni Medsci, Inc. v. *Apple Inc.*; Case No. 2:18-cv-134-RWS (E.D. Tex.); Defendant's Invalidity Contentions, Aug. 28, 2018 (Exhibit I), 102 pps.
Omni Medsci, Inc. v. *Apple Inc.*; Case No. 2:18-cv-134-RWS (E.D. Tex.); Defendant's Invalidity Contentions, Aug. 28, 2018 (Exhibit J), 64 pps.
Omni Medsci, Inc. v. *Apple Inc.*; Case No. 2:18-cv-134-RWS (E.D. Tex.); Defendant's Invalidity Contentions, Aug. 28, 2018 (Exhibit K), 77 pps.
Omni Medsci, Inc. v. *Apple Inc.*; Case No. 2:18-cv-134-RWS (E.D. Tex.); Defendant's Invalidity Contentions, Aug. 28, 2018 (Exhibit L), 64 pps.
Omni Medsci, Inc. v. *Apple Inc.*; Case No. 2:18-cv-134-RWS (E.D. Tex.); Defendant's Invalidity Contentions, Aug. 28, 2018 (Exhibit M), 119 pps.
Omni Medsci, Inc. v. *Apple Inc.*; Case No. 2:18-cv-134-RWS (E.D. Tex.); Defendant's Invalidity Contentions, Aug. 28, 2018 (Exhibit N), 50 pps.
Omni Medsci, Inc. v. *Apple Inc.*; Case No. 2:18-cv-134-RWS (E.D. Tex.); Defendant's Invalidity Contentions, Aug. 28, 2018 (Exhibit O), 63 pps.
Omni Medsci, Inc. v. *Apple Inc.*; Case No. 2:18-cv-134-RWS (E.D. Tex.); Defendant's Invalidity Contentions, Aug. 28, 2018 (Exhibit P), 78 pps.
Omni Medsci, Inc. v. *Apple Inc.*; Case No. 2:18-cv-134-RWS (E.D. Tex.); Defendant's Invalidity Contentions, Aug. 28, 2018 (Exhibit Q), 69 pps.
Omni Medsci, Inc. v. *Apple Inc.*; Case No. 2:18-cv-134-RWS (E.D. Tex.); Defendant's Invalidity Contentions, Aug. 28, 2018 (Exhibit R), 61 pps.
Omni Medsci, Inc. v. *Apple Inc.*; Case No. 2:18-cv-134-RWS (E.D. Tex.); Defendant's Invalidity Contentions, Aug. 28, 2018 (Exhibit S), 50 pps.
Omni Medsci, Inc. v. *Apple Inc.*; Case No. 2:18-cv-134-RWS (E.D. Tex.); Defendant's Invalidity Contentions, Aug. 28, 2018 (Exhibit T), 174 pps.
Omni Medsci, Inc. v. *Apple Inc.*; Case No. 2:18-cv-134-RWS (E.D. Tex.); Defendant's Invalidity Contentions, Aug. 28, 2018 (Exhibit U), 334 pps.
Omni Medsci, Inc. v. *Apple Inc.*; Case No. 2:18-cv-134-RWS (E.D. Tex.); Defendant's Invalidity Contentions, Aug. 28, 2018 (Exhibit V), 137 pps.
Omni Medsci, Inc. v. *Apple Inc.*; Case No. 2:18-cv-134-RWS (E.D. Tex.); Defendant's Invalidity Contentions, Aug. 28, 2018 (Exhibit W), 384 pps.
Omni Medsci, Inc. v. *Apple Inc.*; Case No. 2:18-cv-134-RWS (E.D. Tex.); Defendant's Invalidity Contentions, Aug. 28, 2018 (Exhibit X), 291 pps.
Omni Medsci, Inc. v. *Apple Inc.*; Case No. 2:18-cv-134-RWS (E.D. Tex.); Defendant's Invalidity Contentions, Aug. 28, 2018 (Exhibit Y), 120 pps.
Omni Medsci, Inc. v. *Apple Inc.*; Case No. 2:18-cv-134-RWS (E.D. Tex.); Defendant's Invalidity Contentions, Aug. 28, 2018 (Exhibit Z), 53 pps.
Omni Medsci, Inc. v. *Apple Inc.*; Case No. 2:18-cv-134-RWS (E.D. Tex.); Defendant's Invalidity Contentions, Aug. 28, 2018 (Exhibit AA), 75 pps.
Omni Medsci, Inc. v. *Apple Inc.*; Case No. 2:18-cv-134-RWS (E.D. Tex.); Defendant's Invalidity Contentions, Aug. 28, 2018 (Exhibit BB), 65 pps.
Omni Medsci, Inc. v. *Apple Inc.*; Case No. 2:18-cv-134-RWS (E.D. Tex.); Defendant's Invalidity Contentions, Aug. 28, 2018 (Exhibit CC), 320 pps.
Omni Medsci, Inc. v. *Apple Inc.*; Case No. 2:18-cv-134-RWS (E.D. Tex.); Defendant's Invalidity Contentions, Aug. 28, 2018 (Exhibit DD), 240 pps.
Rhee et al., Artifact-Resistant Power-Efficient Design of Finger-Ring Plethysmographic Sensors, IEEE Transactions on Biomedical Engineering (Jul. 2001), vol. 48, No. 7, Cambridge, MA, 11 pages.
Branche et al., Signal Quality and Power Consumption of a New Prototype Reflectance Pulse Oximeter Sensor, Proceedings of the IEEE 31st Annual Northeast Bioengineering Conference (2005), Hoboken, NJ, 2 pages.
Peláez, LED Power Reduction Trade-Offs for Ambulatory Pulse Oximetry, Conference Proceedings of the 29th Annual International Conference of the IEEE EMBS (Aug. 2007) Lyon, France, 4 pages.
Luo et al., A Non-Invasive Dual-Channel Oximeter Based on Near-Infrared Spectroscopy (NIRS), Biophotonics Lab, Center of Advanced Research in Photonics (2007), The Chinese University of Hong Kong, China, 2 pages.
Asada et al., The MIT Ring: History, Technology, and Challenges of Wearable Health Monitoring, MIT Industrial Liaison Program (2010) R&D Conference, MA, 72 pages.
Asada et al., Mobile Monitoring with Wearable Photoplethysmographic Biosensors, Technical and Clinical Aspects of a Ring Sensor for Ambulatory, Telemetric, Continuous Health Monitoring in the Field, in the Hospital, and in the Home, IEEE Engineering in Medicine and Biology Magazine, (May/Jun. 2003) 13 pages.
Schreiner et al., Blood Oxygen Level Measurement with a Chest-Based Pulse Oximetry Prototype System, Computing in Cardiology (2010) NIBEC, University of Ulster, Newtownabbey, Northern Ireland, 4 pages.

(56) **References Cited**

OTHER PUBLICATIONS

GE Healthcare, TuffSat User's Guide and Service Manual Electromagnetic Compatibility (EMC), (Mar. 2005) Helsinki, Finland, 43 pages.
Kurylyak et al., Smartphone-Based Photoplethysmogram Measurement, Department of Electronics, Computer and System Sciences, (2012) River Publishers, University of Calabria, Italy, 30 pages.
Patterson et al., Ratiometric Artifact Reduction in Low Power Reflective Photoplethysmography, (Aug. 2011) IEEE Transactions on Biomedical Circuits and Systems, vol. 5, No. 4, 9 pages.
Cai et al., Implementation of a Wireless Pulse Oximeter Based on Wrist Band Sensor, College of Biological Science and Medical Engineering Southeast University, (2010) 3rd International Conference on Biomedical Engineering and Informatics, Nanjing, China, 4 pages.
Yamaha, BODiBEAT, Body, Music, In Sync., BF-1 Quick Guide, Player/Heart Rate Monitor: Quick Manual, 120 pages.
GE Healthcare, GE Ohmeda TufSat Oximeter for Clinicians on the go, (2012), A General Electric Co., www.gehealthcare.com, GE, Finland, 4 pages.
Wang et al., Multichannel Reflective PPG Earpiece Sensor with Passive Motion Cancellation, (Dec. 2007) IEEE Transactions on Biomedical Circuits and Systems, vol. 1, No. 4, 7 pages.
Webster, Design of Pulse Oximeters, Medical Science Series (1997), Department of Electrical and Computer Engineering, University of Wisconsin—Madison, Institute of Physics Publishing, Bristol and Philadelphia, 267 pages.
Taos, Inc., Infrared Light-to-Voltage Optical Sensors, (2006) Texas Advanced Optoelectronic Solutions Inc., The Lumenology Company, TX, 14 pages.
Jung et al., Design of A Low-Power Consumption Wearable Reflectance Pulse Oximetry for Ubiquitous Healthcare System, International Conference on Control, Automation and Systems (Oct. 2008), in COEX, Seoul, Korea, 4 pages.
Embedded-Lab, Introducing Easy Pulse: A DIY Photoplethysmographic Sensor for Measuring Hearth Rate, posted on www.Embedded-Lab.com Sep. 12, 2012, by R-B, 10 pages.
Asare et al., Analysis of Multi-Spectral Photoplethysmograph Biosensors, Proc. SPIE 8801, Novel Biophotonic Techniques and Applications II, 880106 (Jun. 2013), European Conferences on Biomedical Optics, Munich, Germany, 7 pages.
Morón et al, A Wireless Monitoring System for Pulse-Oximetry Sensors, (2005) Electronic Technology Department, University of Málaga, Spain, 6 pages.
Li et al, A Wireless Reflective Pulse Oximeter with Digital Baseline Control for Unfiltered Photoplethysmograms, (Jun. 2012) IEEE Transactions on Biomedical Circuits and Systems, vol. 6, No. 3, 10 pages.
Humphreys et al., Noncontact Simultaneous Dual Wavelength Photoplethysmography: A Further Step Toward Noncontact Pulse Oximetry, (2007) Review of Scientific Instruments 78, 044304, American Institute of Physics, 6 pages.
Mendelson et al., A Wearable Reflectance Pulse Oximeter for Remote Physiological Monitoring, (Aug./Sep. 2006) Proceedings of the 28th IEEE EMBS Annual International Conference New York City, NY, 4 pages.
United States District Court Eastern District of Texas Marshall Division; *Omni Medsci, Inc.* vs. *Apple Inc.*; Civil Action No. 2:18-cv-00134 Jury Trial Demanded; Defendant's Invalidity Contentions; Aug. 28, 2018; 33 pps.

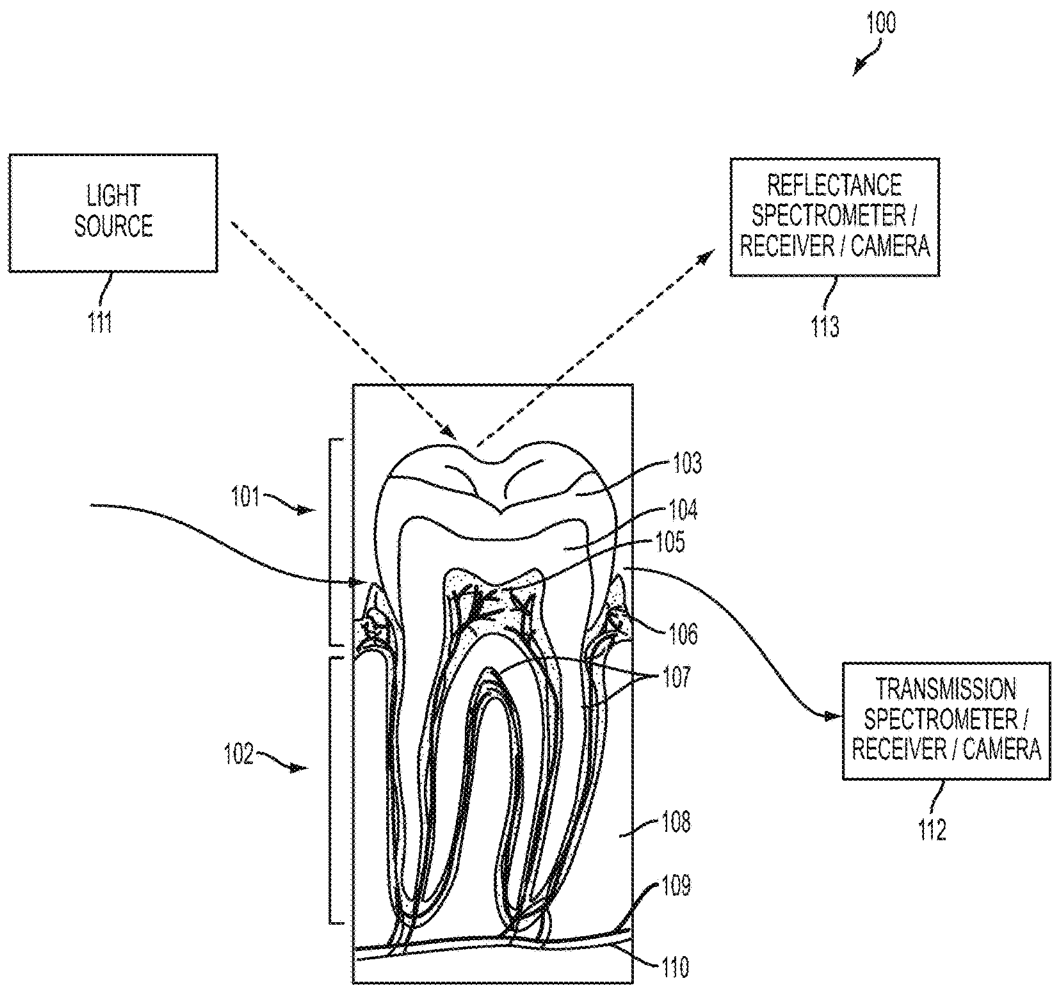
100
LIGHT SOURCE
111
REFLECTANCE SPECTROMETER / RECEIVER / CAMERA
113
101
102
103
104
105
106
107
108
109
110
TRANSMISSION SPECTROMETER / RECEIVER / CAMERA
112

FIG. 1

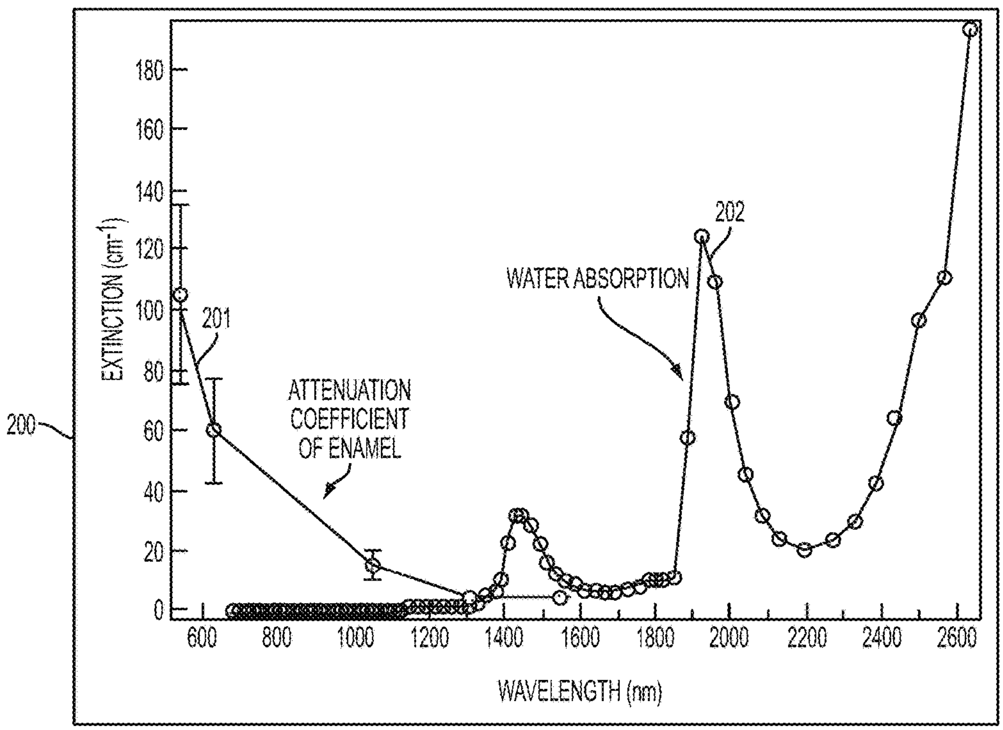

200
180
160
140
120
100
80
60
40
20
0
EXTINCTION (cm^{-1})
600
800
1000
1200
1400
1600
1800
2000
2200
2400
2600
WAVELENGTH (nm)
201
202
ATTENUATION COEFFICIENT OF ENAMEL
WATER ABSORPTION

FIG. 2A

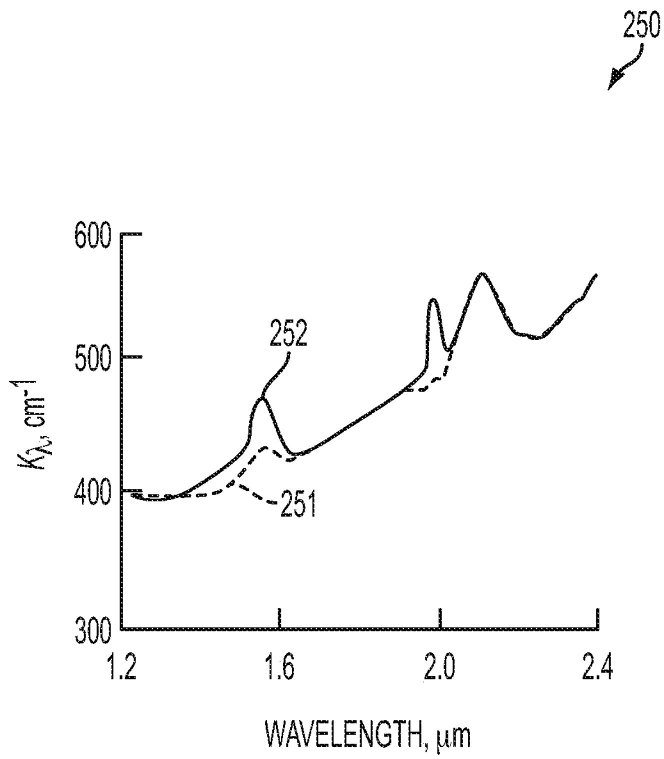
250
600
500
400
300
252
251
K_λ, cm^{-1}
1.2
1.6
2.0
2.4
WAVELENGTH, μm

FIG. 2B

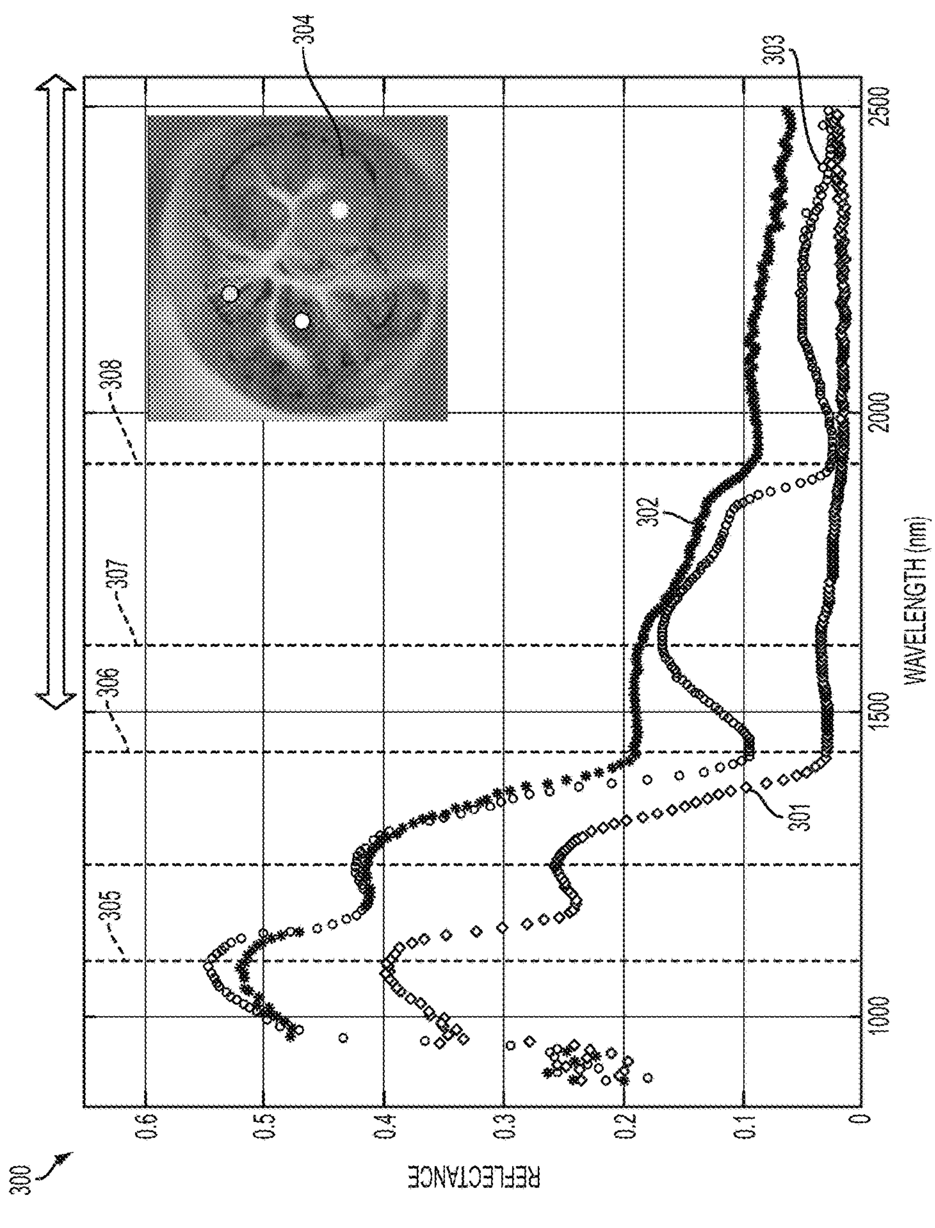
300
REFLECTANCE
WAVELENGTH (nm)
0
0.1
0.2
0.3
0.4
0.5
0.6
1000
1500
2000
2500
301
302
303
304
305
306
307
308

FIG. 3

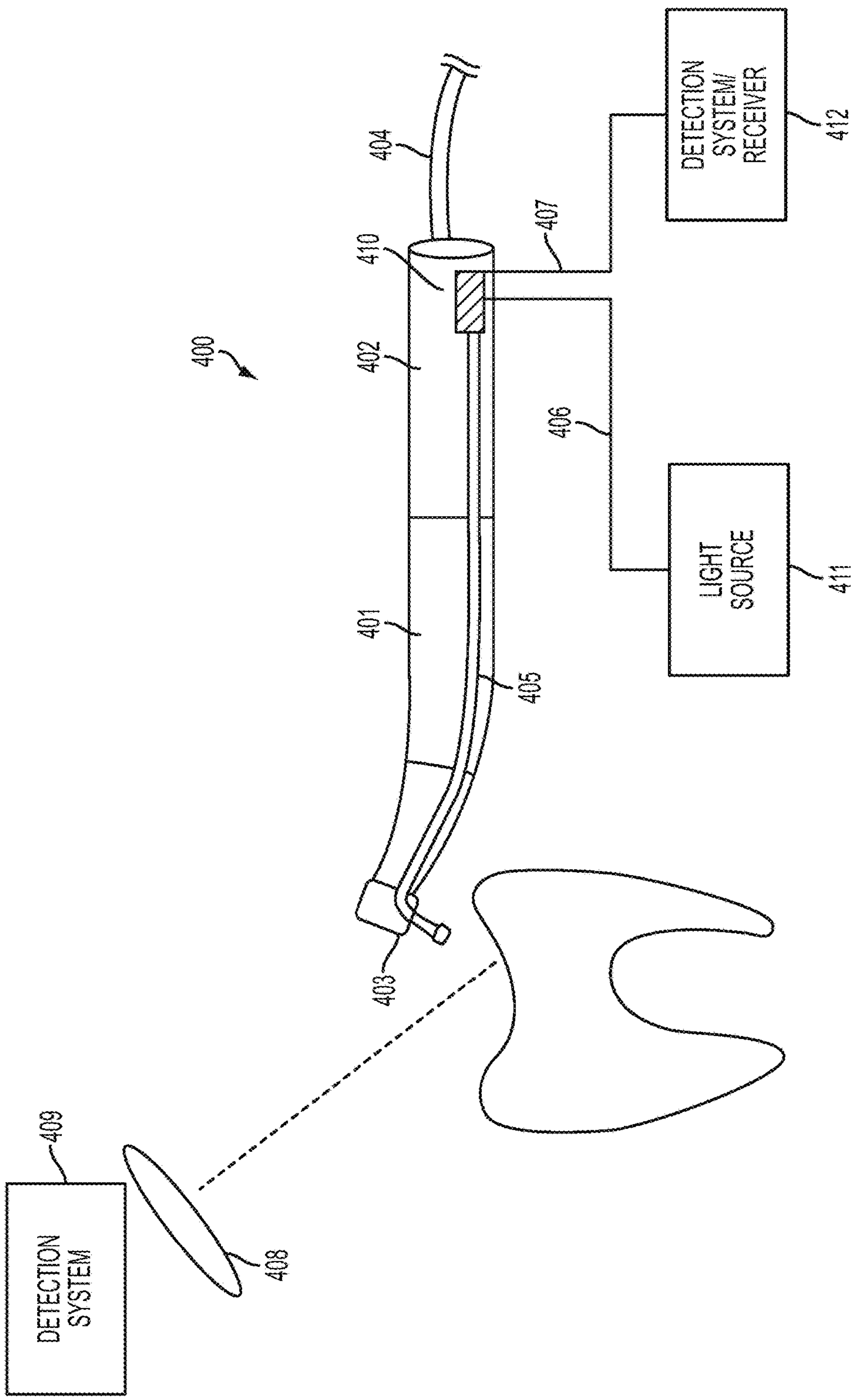
400
404
410
402
407
DETECTION SYSTEM/ RECEIVER
412
406
LIGHT SOURCE
411
401
405
403
409
DETECTION SYSTEM
408

FIG. 4

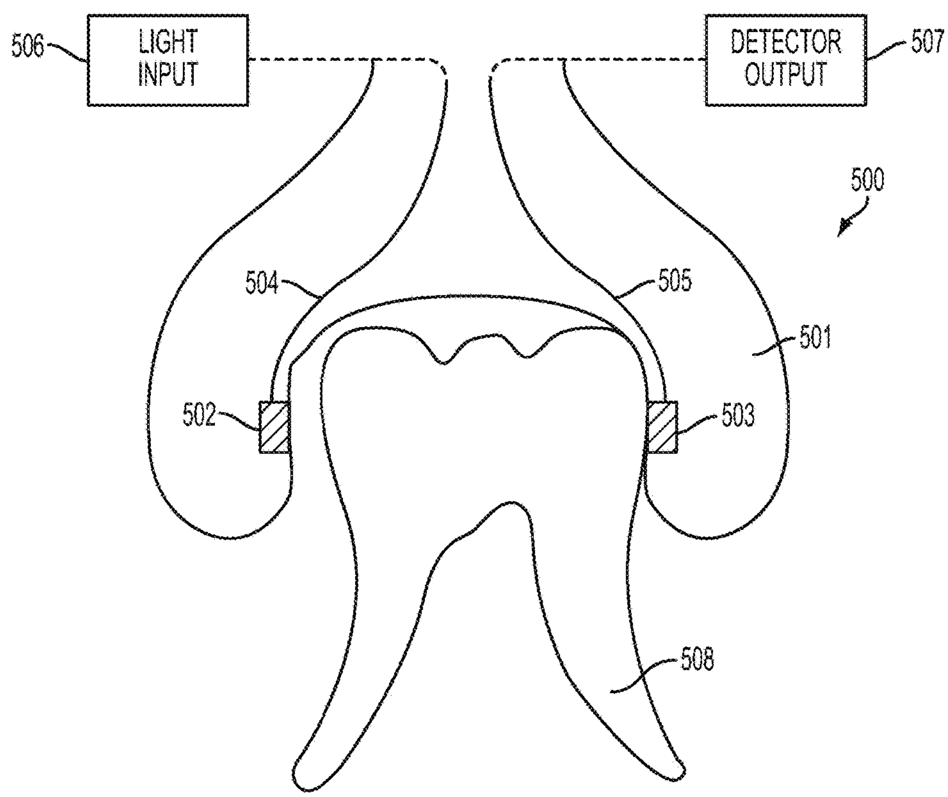

LIGHT INPUT
506
DETECTOR OUTPUT
507
500
504
505
501
502
503
508

FIG. 5A

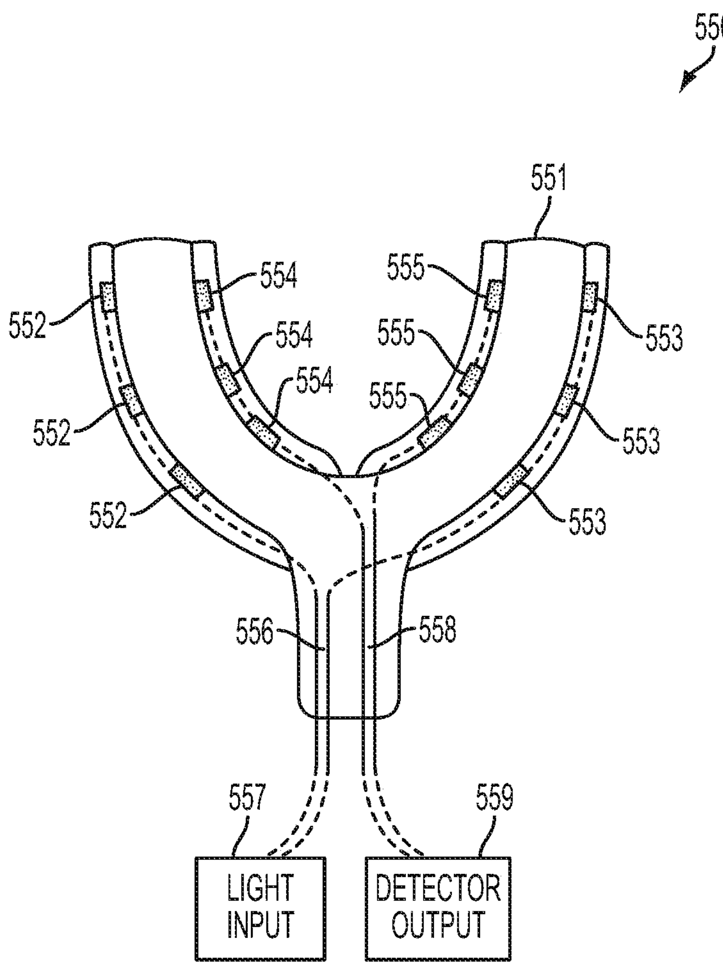
550
551
552
552
552
554
554
554
555
555
555
553
553
553
556
558
557
559
LIGHT INPUT
DETECTOR OUTPUT

FIG. 5B

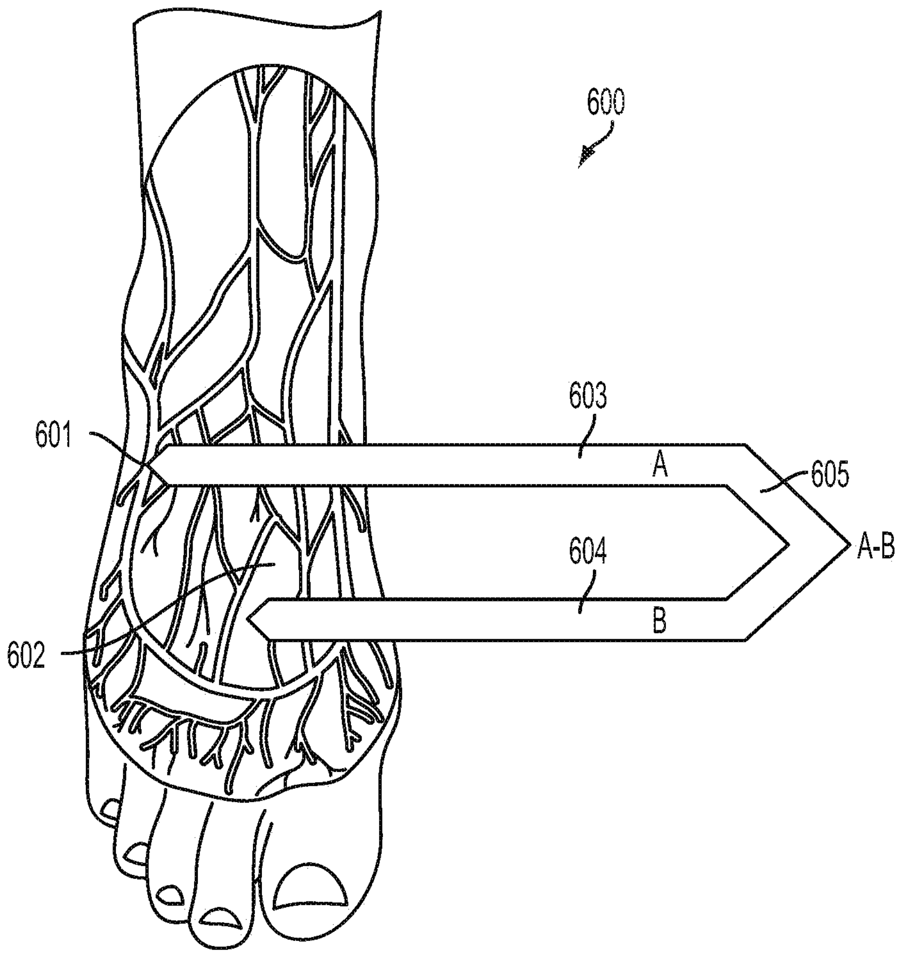

FIG. 6A

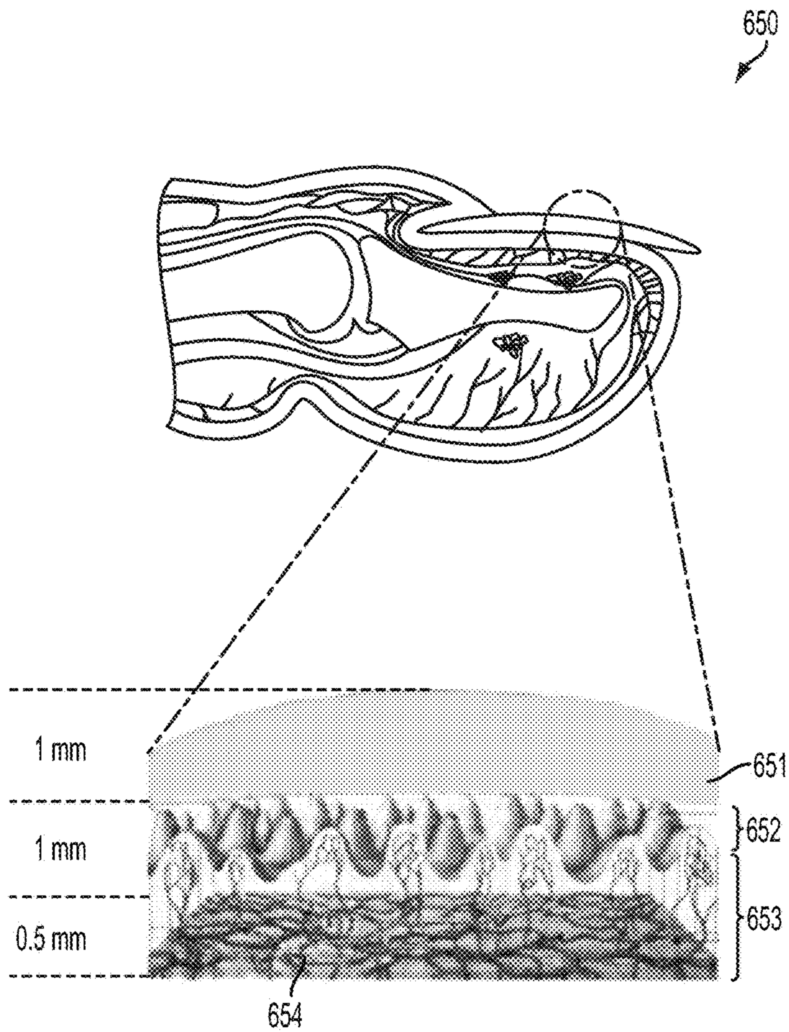

FIG. 6B

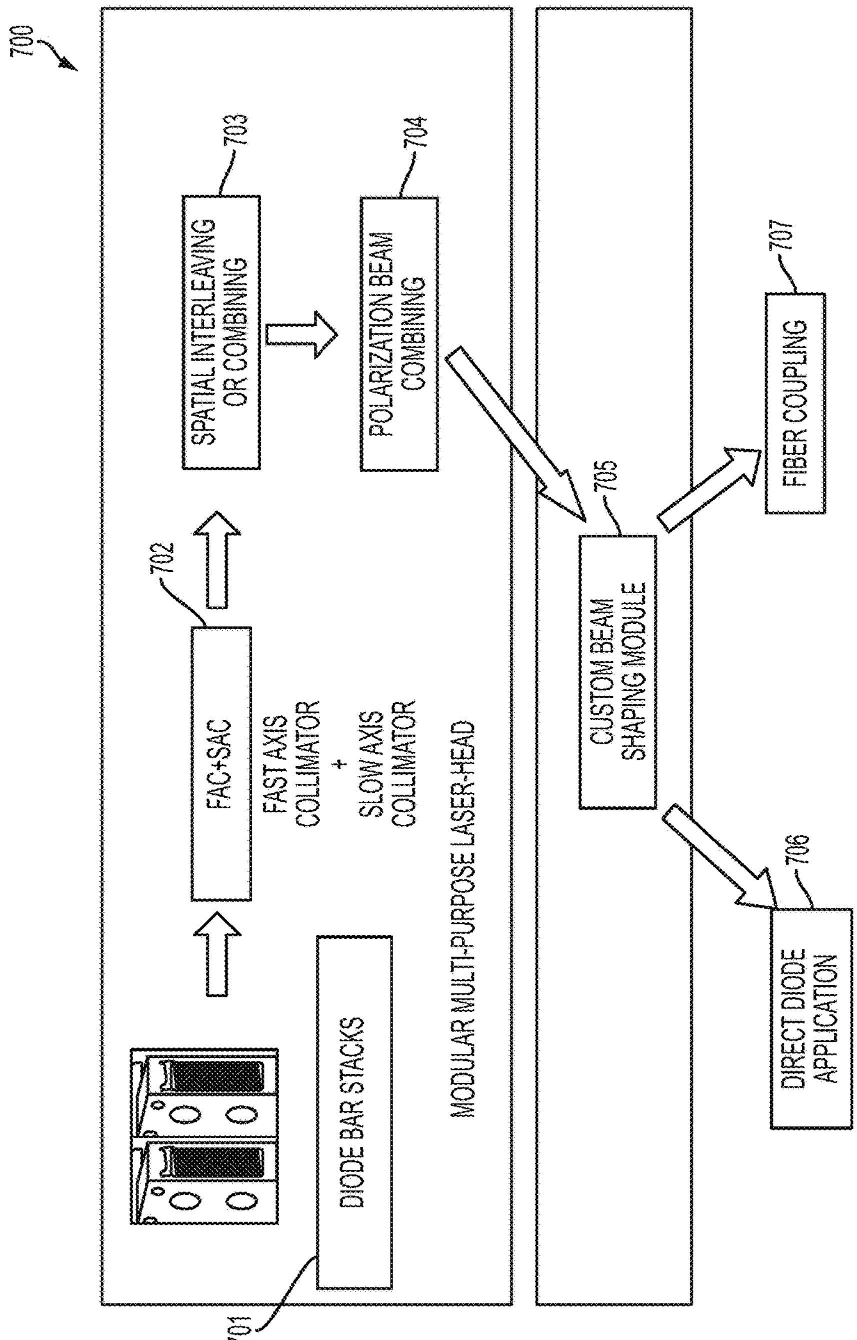
700
701
DIODE BAR STACKS
702
FAC+SAC
FAST AXIS COLLIMATOR + SLOW AXIS COLLIMATOR
703
SPATIAL INTERLEAVING OR COMBINING
704
POLARIZATION BEAM COMBINING
MODULAR MULTI-PURPOSE LASER-HEAD
705
CUSTOM BEAM SHAPING MODULE
706
DIRECT DIODE APPLICATION
707
FIBER COUPLING

FIG. 7

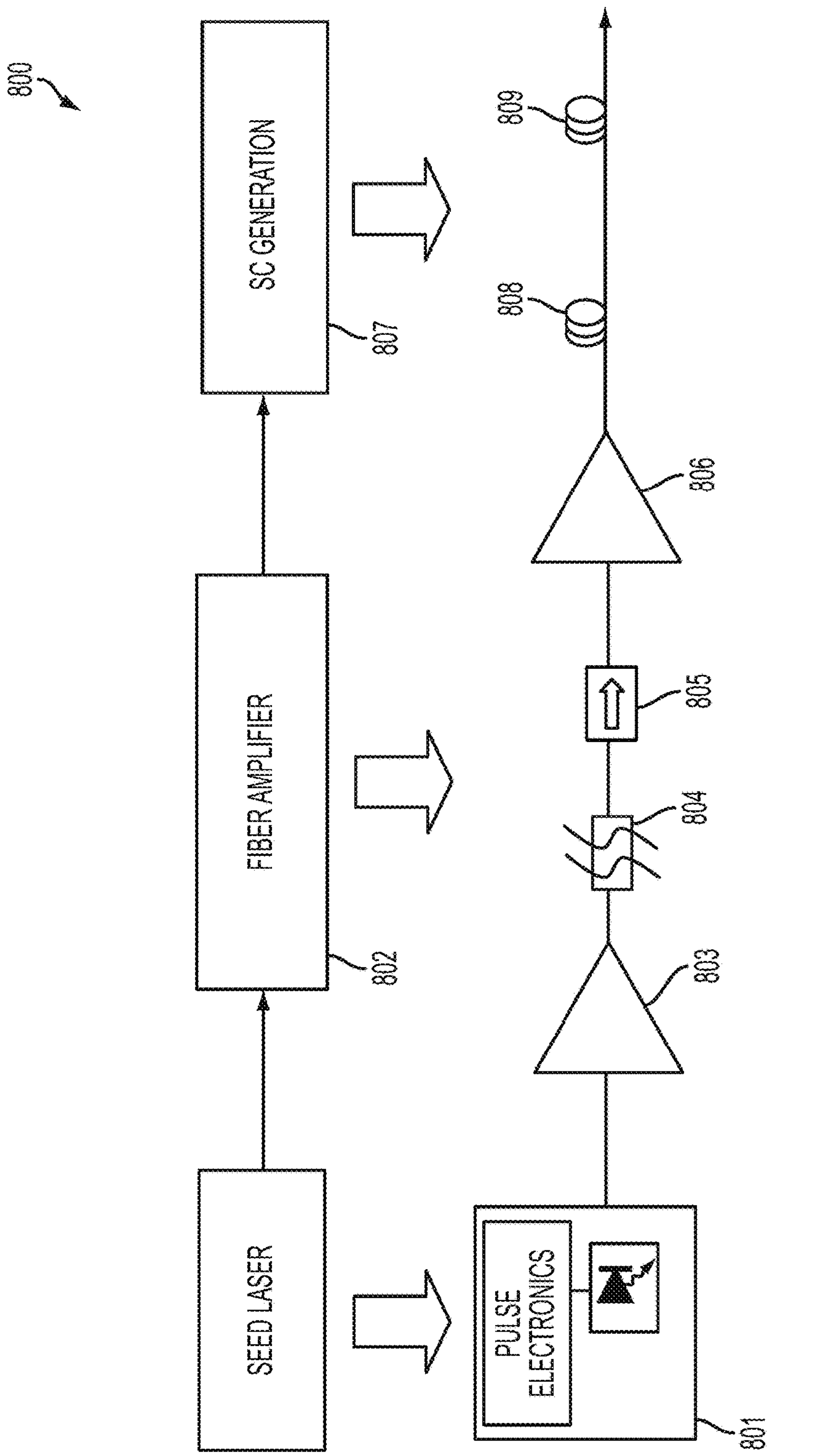
800
SEED LASER
FIBER AMPLIFIER
SC GENERATION
PULSE ELECTRONICS
801
802
803
804
805
806
807
808
809

FIG. 8

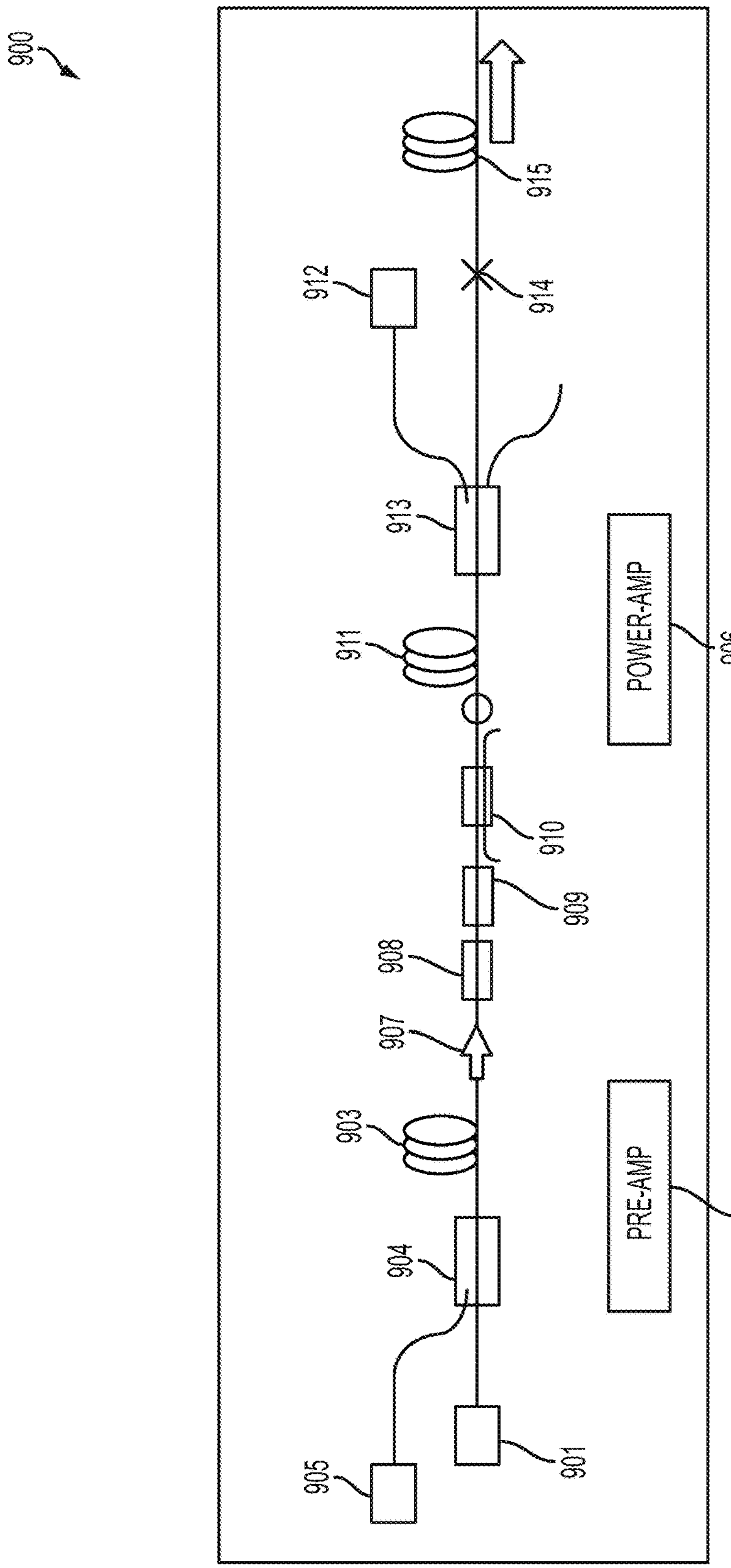
900
901
902
PRE-AMP
903
904
905
906
POWER-AMP
907
908
909
910
911
912
913
914
915

FIG. 9

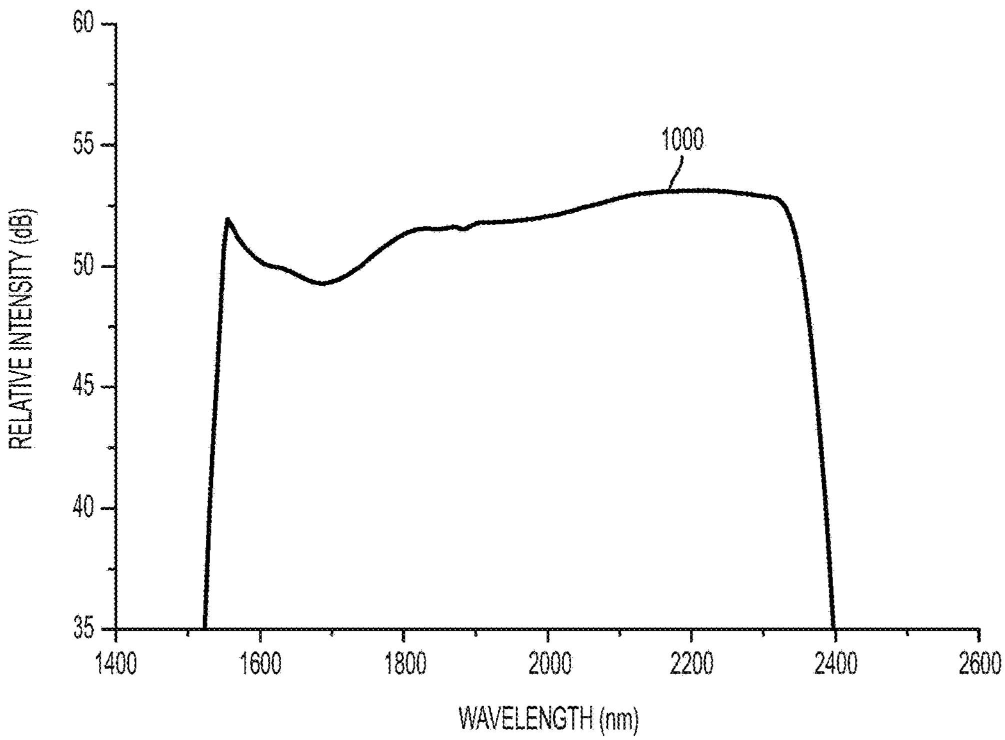
60
55
50
45
40
35
RELATIVE INTENSITY (dB)
1000
1400
1600
1800
2000
2200
2400
2600
WAVELENGTH (nm)

FIG. 10

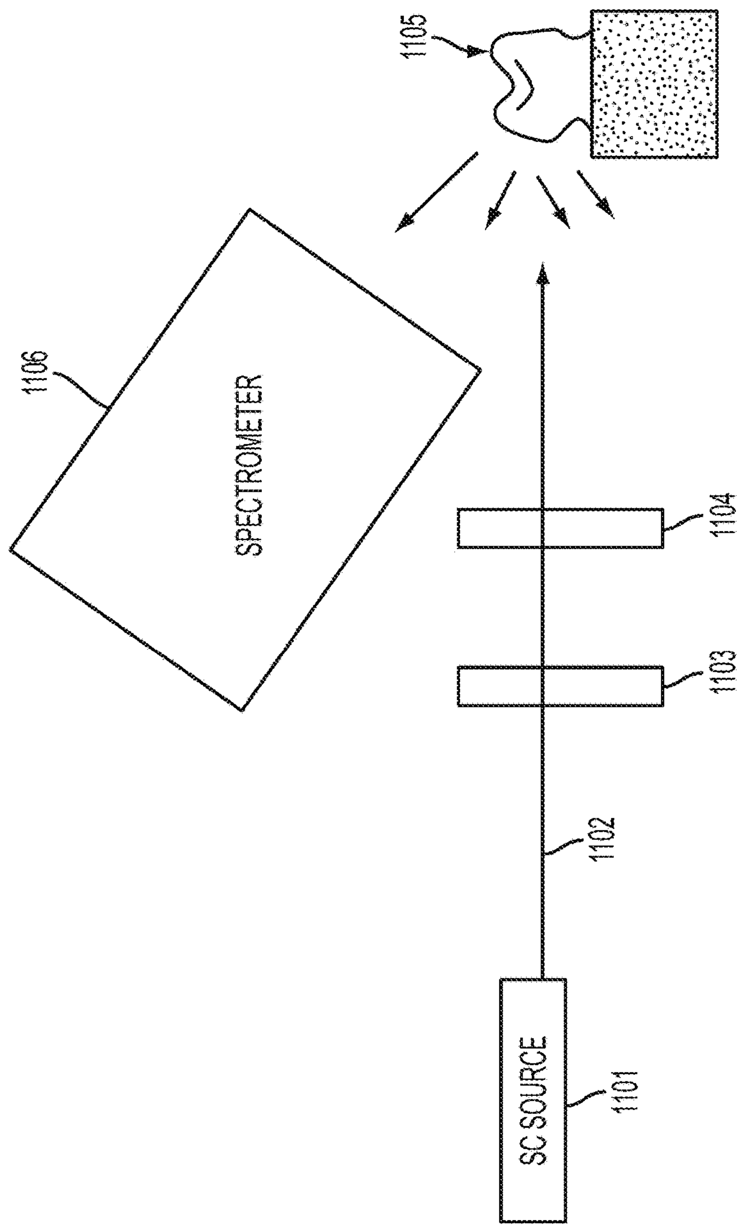

FIG. 11A

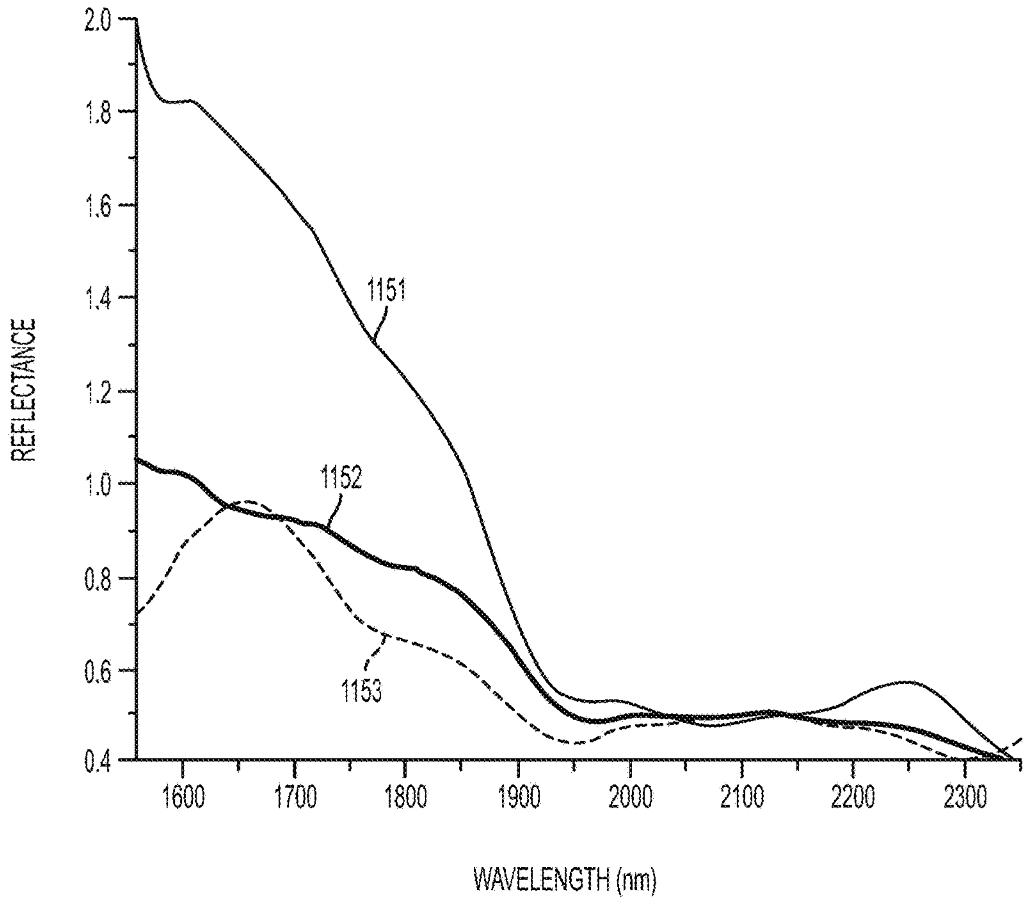
2.0
1.8
1.6
1.4
1.2
1.0
0.8
0.6
0.4
REFLECTANCE
1151
1152
1153
1600
1700
1800
1900
2000
2100
2200
2300
WAVELENGTH (nm)

FIG. 11B

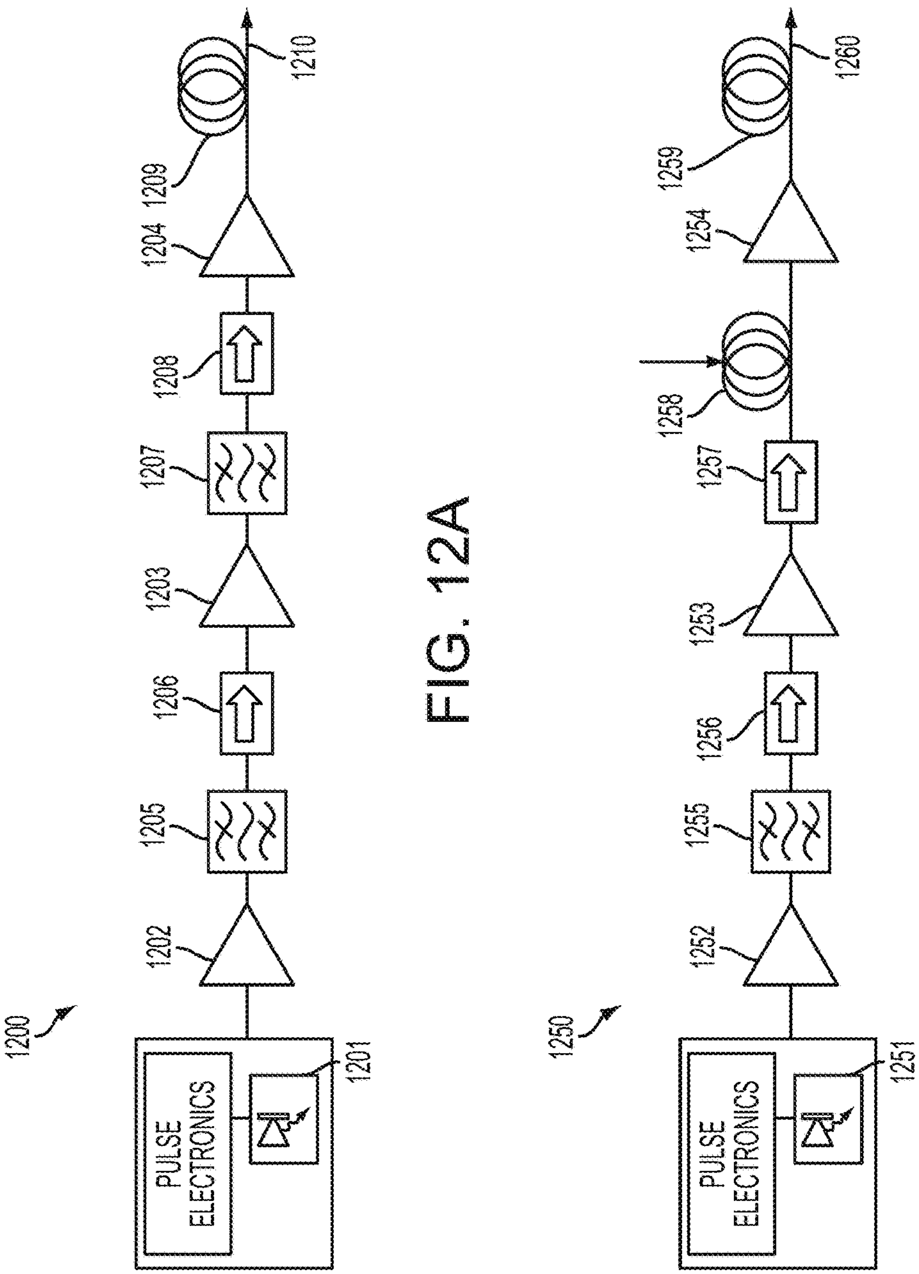

FIG. 12A

FIG. 12B

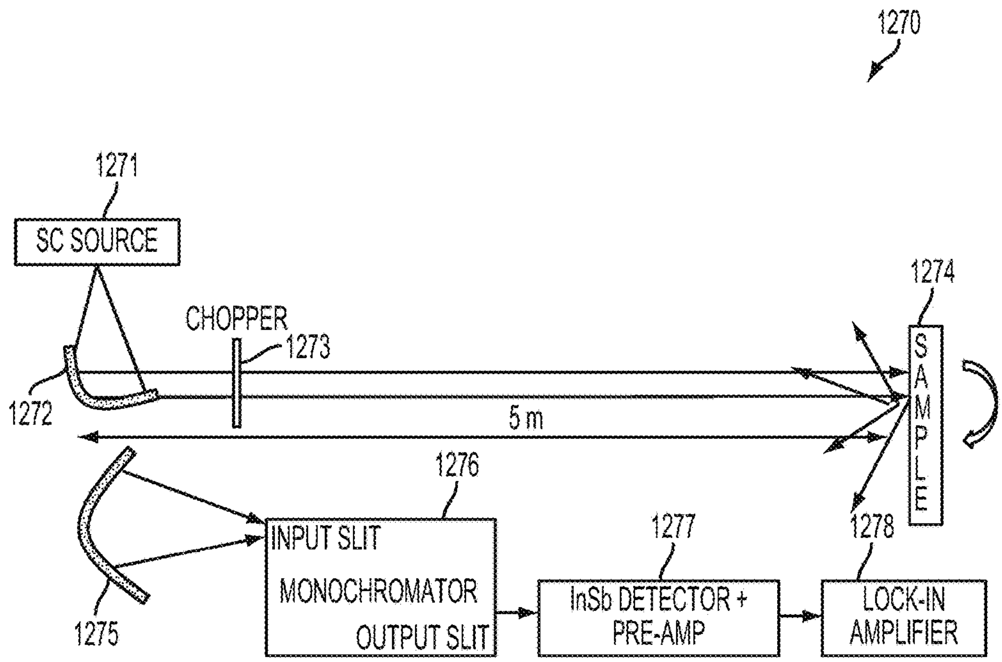
1270
1271
SC SOURCE
CHOPPER
1273
1272
1274
S A M P L E
5 m
1276
INPUT SLIT
MONOCHROMATOR
OUTPUT SLIT
1277
InSb DETECTOR + PRE-AMP
1278
LOCK-IN AMPLIFIER
1275

FIG. 12C

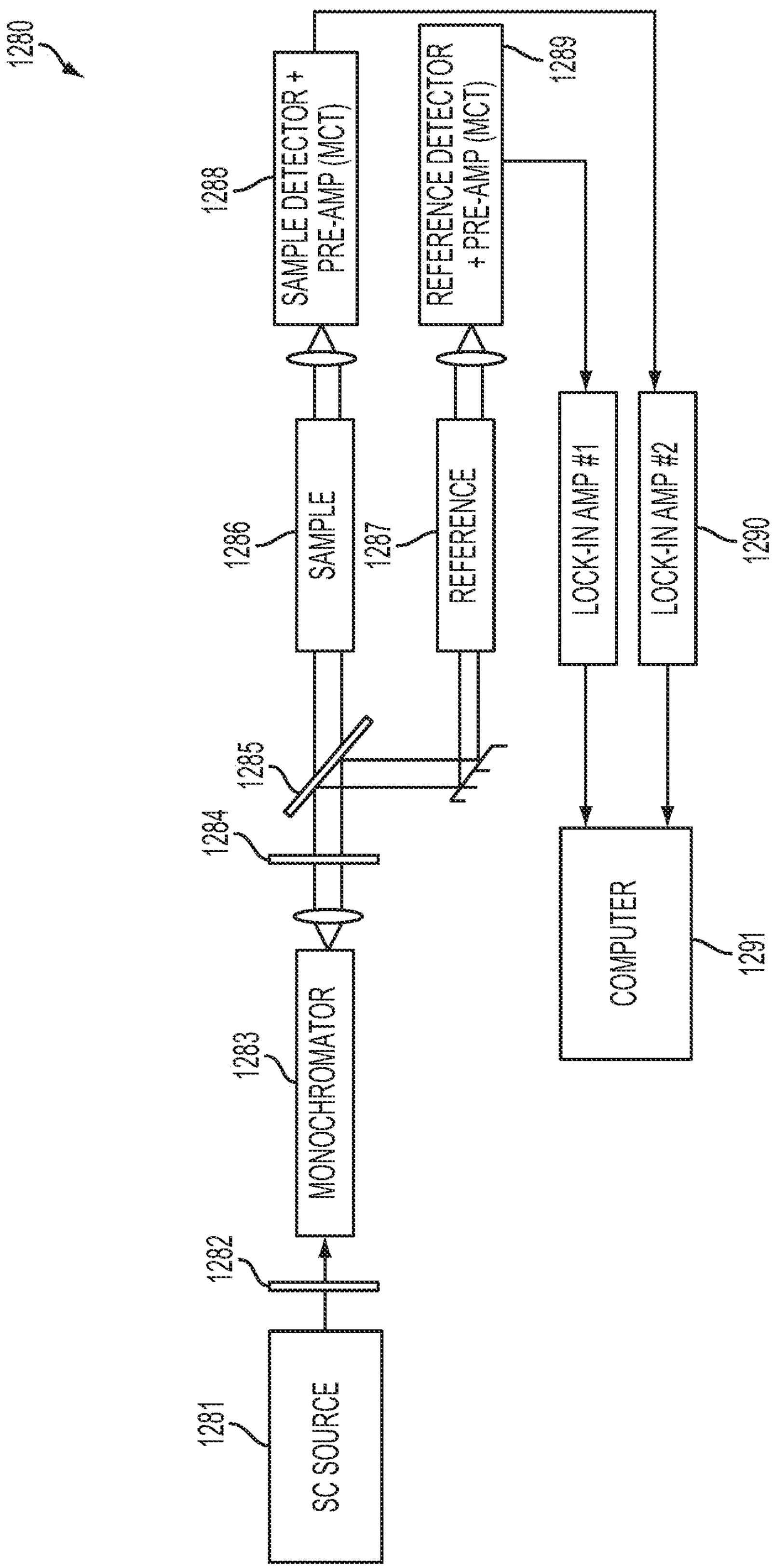
1280
SAMPLE DETECTOR + PRE-AMP (MCT)
1288
REFERENCE DETECTOR + PRE-AMP (MCT)
1289
SAMPLE
1286
REFERENCE
1287
LOCK-IN AMP #1
LOCK-IN AMP #2
1290
1285
1284
COMPUTER
1291
MONOCHROMATOR
1283
1282
SC SOURCE
1281

FIG. 12D

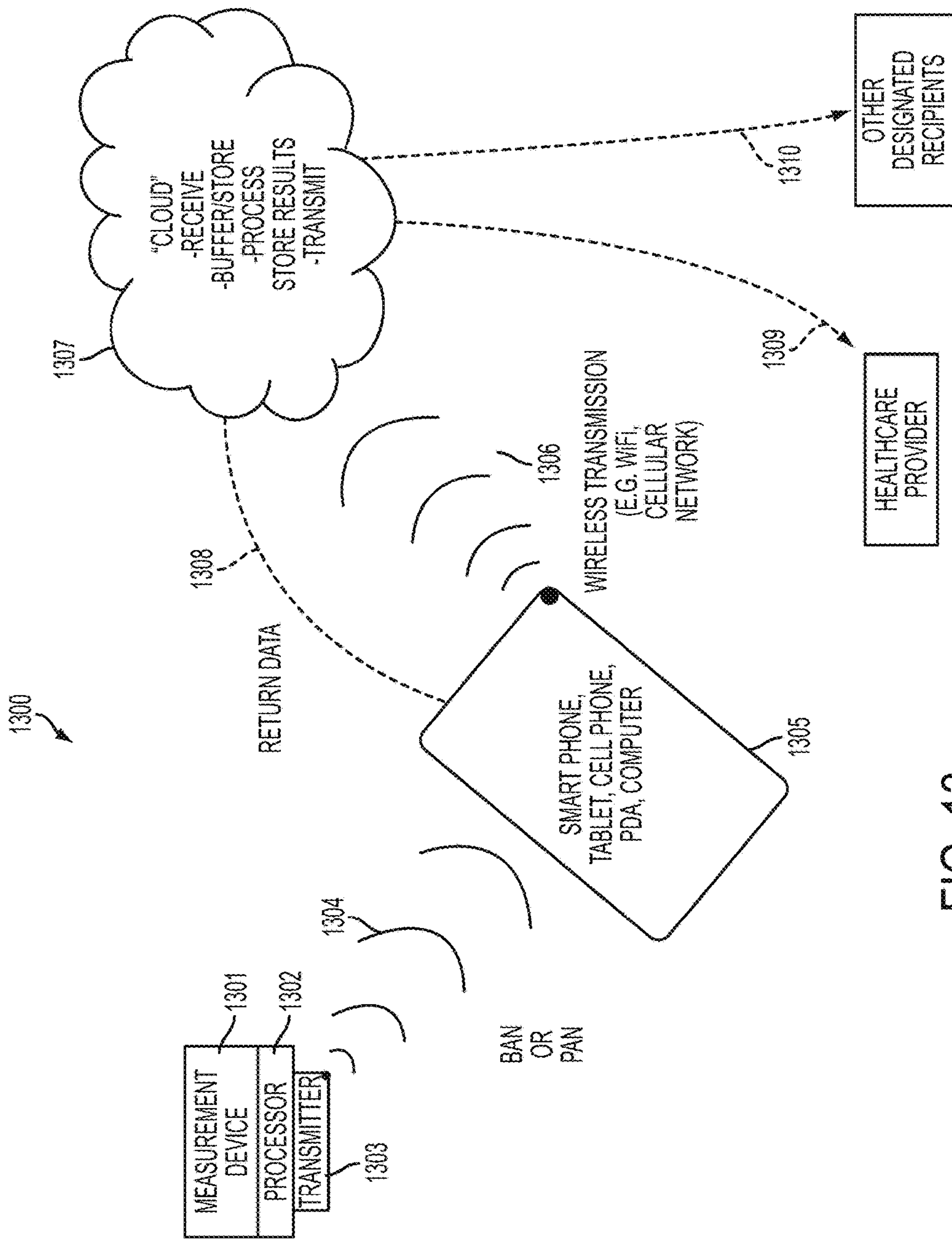
1300
"CLOUD"
-RECEIVE
-BUFFER/STORE
-PROCESS
STORE RESULTS
-TRANSMIT
1307
1310
OTHER DESIGNATED RECIPIENTS
1309
HEALTHCARE PROVIDER
WIRELESS TRANSMISSION (E.G. WIFI, CELLULAR NETWORK)
1306
1308
RETURN DATA
SMART PHONE, TABLET, CELL PHONE, PDA, COMPUTER
1305
1304
BAN OR PAN
MEASUREMENT DEVICE
1301
PROCESSOR
1302
TRANSMITTER
1303

FIG. 13

WEARABLE DEVICES USING NEAR-INFRARED LIGHT SOURCES

CROSS-REFERENCE TO RELATED APPLICATIONS

This application is a Continuation of U.S. application Ser. No. 15/686,198 filed Aug. 25, 2017, which is a Continuation of U.S. application Ser. No. 15/357,136 filed Nov. 21, 2016 (now U.S. Pat. No. 9,757,040), which is a Continuation of U.S. application Ser. No. 14/651,367 filed Jun. 11, 2015 (now U.S. Pat. No. 9,500,635), which is the U.S. national phase of PCT Application No. PCT/US2013/075736 filed Dec. 17, 2013, which claims the benefit of U.S. provisional application Ser. No. 61/747,477 filed Dec. 31, 2012 and U.S. provisional application Ser. No. 61/754,698 filed Jan. 21, 2013, the disclosures of which are hereby incorporated by reference in their entirety.

This application is related to U.S. provisional application Ser. No. 61/747,472 filed Dec. 31, 2012; Ser. No. 61/747,481 filed Dec. 31, 2012; Ser. No. 61/747,485 filed Dec. 31, 2012; Ser. No. 61/747,487 filed Dec. 31, 2012; Ser. No. 61/747,492 filed Dec. 31, 2012; and Ser. No. 61/747,553 filed Dec. 31, 2012, the disclosures of which are hereby incorporated in their entirety in their entirety by reference herein.

This application has a common priority date with commonly owned U.S. application Ser. No. 14/650,897 filed Jun. 10, 2015 (now U.S. Pat. No. 9,494,567), which is the U.S. national phase of International Application PCT/US2013/075700 entitled Near-Infrared Lasers For Non-Invasive Monitoring Of Glucose, Ketones, HBA1C, And Other Blood Constituents; U.S. application Ser. No. 14/108,995 filed Dec. 17, 2013 (published as US 2014/0188092) entitled Focused Near-Infrared Lasers For Non-Invasive Vasectomy And Other Thermal Coagulation Or Occlusion Procedures; U.S. application Ser. No. 14/650,981 filed Jun. 10, 2015 (now U.S. Pat. No. 9,500,634), which is the U.S. national phase of International Application PCT/US2013/075767 entitled Short-Wave Infrared Super-Continuum Lasers For Natural Gas Leak Detection, Exploration, And Other Active Remote Sensing Applications; U.S. application Ser. No. 14/108,986 filed Dec. 17, 2013 (now U.S. Pat. No. 9,164,032) entitled Short-Wave Infrared Super-Continuum Lasers For Detecting Counterfeit Or Illicit Drugs And Pharmaceutical Process Control; U.S. application Ser. No. 14/108,974 filed Dec. 17, 2013 (Published as US2014/0188094) entitled Non-Invasive Treatment Of Varicose Veins; and U.S. application Ser. No. 14/109,007 filed Dec. 17, 2013 (Published as US2014/0236021) entitled Near-Infrared Super-Continuum Lasers For Early Detection Of Breast And Other Cancers, the disclosures of which are hereby incorporated in their entirety by reference herein.

TECHNICAL FIELD

This disclosure relates to lasers and light sources for healthcare, medical, dental, or bio-technology applications, including systems and methods for using near-infrared or short-wave infrared light sources for early detection of dental caries, often called cavities.

BACKGROUND AND SUMMARY

Dental care and the prevention of dental decay or dental caries has changed in the United States over the past several decades, due to the introduction of fluoride to drinking

water, the use of fluoride dentifrices and rinses, application of topical fluoride in the dental office, and improved dental hygiene. Despite these advances, dental decay continues to be the leading cause of tooth loss. With the improvements over the past several decades, the majority of newly discovered carious lesions tend to be localized to the occlusal pits and fissures of the posterior dentition and the proximal contact sites. These early carious lesions may be often obscured in the complex and convoluted topography of the pits and fissures or may be concealed by debris that frequently accumulates in those regions of the posterior teeth. Moreover, such lesions are difficult to detect in the early stages of development.

Dental caries may be a dynamic disease that is characterized by tooth demineralization leading to an increase in the porosity of the enamel surface. Leaving these lesions untreated may potentially lead to cavities reaching the dentine and pulp and perhaps eventually causing tooth loss. Occlusal surfaces (bite surfaces) and approximal surfaces (between the teeth) are among the most susceptible sites of demineralization due to acid attack from bacterial by-products in the biofilm. Therefore, there is a need for detection of lesions at an early stage, so that preventive agents may be used to inhibit or reverse the demineralization.

Traditional methods for caries detection include visual examination and tactile probing with a sharp dental exploration tool, often assisted by radiographic (x-ray) imaging. However, detection using these methods may be somewhat subjective; and, by the time that caries are evident under visual and tactile examination, the disease may have already progressed to an advanced stage. Also, because of the ionizing nature of x-rays, they are dangerous to use (limited use with adults, and even less used with children). Although x-ray methods are suitable for approximal surface lesion detection, they offer reduced utility for screening early caries in occlusal surfaces due to their lack of sensitivity at very early stages of the disease.

Some of the current imaging methods are based on the observation of the changes of the light transport within the tooth, namely absorption, scattering, transmission, reflection and/or fluorescence of light. Porous media may scatter light more than uniform media. Taking advantage of this effect, the Fiber-optic trans-illumination is a qualitative method used to highlight the lesions within teeth by observing the patterns formed when white light, pumped from one side of the tooth, is scattered away and/or absorbed by the lesion. This technique may be difficult to quantify due to an uneven light distribution inside the tooth.

Another method called quantitative light-induced fluorescence—QLF—relies on different fluorescence from solid teeth and caries regions when excited with bright light in the visible. For example, when excited by relatively high intensity blue light, healthy tooth enamel yields a higher intensity of fluorescence than does demineralized enamel that has been damaged by caries infection or any other cause. On the other hand, for excitation by relatively high intensity of red light, the opposite magnitude change occurs, since this is the region of the spectrum for which bacteria and bacterial by-products in carious regions absorb and fluoresce more pronouncedly than do healthy areas. However, the image provided by QLF may be difficult to assess due to relatively poor contrast between healthy and infected areas. Moreover, QLF may have difficulty discriminating between white spots and stains because both produce similar effects. Stains on teeth are commonly observed in the occlusal sites of teeth, and this obscures the detection of caries using visible light.

As described in this disclosure, the near-infrared region of the spectrum offers a novel approach to imaging carious regions because scattering is reduced and absorption by stains is low. For example, it has been demonstrated that the scattering by enamel tissues reduces in the form of 1/(wavelength)^3, e.g., inversely as the cube of wavelength. By using a broadband light source in the short-wave infrared (SWIR) part of the spectrum, which corresponds approximately to 1400 nm to 2500 nm, lesions in the enamel and dentine may be observed. In one embodiment, intact teeth have low reflection over the SWIR wavelength range. In the presence of caries, the scattering increases, and the scattering is a function of wavelength; hence, the reflected signal decreases with increasing wavelength. Moreover, particularly when caries exist in the dentine region, water build up may occur, and dips in the SWIR spectrum corresponding to the water absorption lines may be observed. The scattering and water absorption as a function of wavelength may thus be used for early detection of caries and for quantifying the degree of demineralization.

SWIR light may be generated by light sources such as lamps, light emitting diodes, one or more laser diodes, super-luminescent laser diodes, and fiber-based super-continuum sources. The SWIR super-continuum light sources advantageously may produce high intensity and power, as well as being a nearly transform-limited beam that may also be modulated. Also, apparatuses for caries detection may include C-clamps over teeth, a handheld device with light input and light detection, which may also be attached to other dental equipment such as drills. Alternatively, a mouth-guard type apparatus may be used to simultaneously illuminate one or more teeth. Fiber optics may be conveniently used to guide the light to the patient as well as to transport the signal back to one or more detectors and receivers.

In one or more embodiments, a wearable device includes a measurement device having a light source comprising a plurality of light emitting diodes (LEDs) for measuring one or more physiological parameters. The measurement device is configured to generate, by modulating at least one of the LEDs having an initial light intensity, an optical beam having a plurality of optical wavelengths, wherein at least a portion of the optical beam includes a near-infrared wavelength between 700 nanometers and 2500 nanometers. The measurement device comprises one or more lenses configured to receive and to deliver at least a portion of the optical beam to tissue, wherein the tissue reflects at least a portion of the optical beam delivered to the tissue. The measurement device further comprises a receiver having a plurality of spatially separated detectors and one or more analog to digital converters coupled to the spatially separated detectors, the one or more analog to digital converters being configured to generate at least two receiver outputs. The receiver is configured to capture light while the LEDs are off and convert the captured light into a first signal, and to capture light while at least one of the LEDs is on and to convert the captured light into a second signal, the captured light including at least a portion of the optical beam reflected from the tissue. The measurement device is configured to improve a signal-to-noise ratio of the optical beam reflected from the tissue by differencing the first signal and the second signal and by differencing the two receiver outputs. The measurement device is configured to further improve the signal-to-noise ratio of the optical beam reflected from the tissue by increasing the light intensity relative to the initial light intensity from at least one of the LEDs. The measurement device is further configured to generate an output signal representing at least in part a non-invasive measurement on blood contained within the tissue.

Embodiments may include a wearable device comprising a measurement device including a light source comprising a plurality of light emitting diodes (LEDs) for measuring one or more physiological parameters. The measurement device is configured to generate, by modulating at least one of the LEDs having an initial light intensity, an optical beam having a plurality of optical wavelengths, wherein at least a portion of the plurality of optical wavelengths is a near-infrared wavelength between 700 nanometers and 2500 nanometers. The measurement device comprises one or more lenses configured to receive and to deliver a portion of the optical beam to tissue, wherein the tissue reflects at least a portion of the optical beam delivered to the tissue, and wherein the measurement device is adapted to be placed on a wrist or an ear of a user. The measurement device further comprises a receiver having a plurality of spatially separated detectors and one or more analog to digital converters coupled to the spatially separated detectors. The one or more analog to digital converters is configured to generate at least two receiver outputs. The receiver is configured to capture light while the LEDs are off and convert the captured light into a first signal, and to capture light while at least one of the LEDs is on and convert the captured light into a second signal, the captured light including at least a portion of the optical beam reflected from the tissue. The measurement device is configured to improve a signal-to-noise ratio of the optical beam reflected from the tissue by differencing the first signal and the second signal and by differencing the two receiver outputs. The measurement device is also configured to further improve the signal-to-noise ratio of the optical beam reflected from the tissue by increasing the light intensity relative to the initial light intensity from at least one of the LEDs. The measurement device is further configured to generate an output signal representing at least in part a non-invasive measurement on blood contained within the tissue.

In one or more embodiments, a wearable device comprises a measurement device including a light source comprising a plurality of light emitting diodes (LEDs) for measuring one or more physiological parameters. The measurement device is configured to generate, by modulating at least one of the LEDs having an initial light intensity, an optical beam having a plurality of optical wavelengths, wherein at least a portion of the plurality of optical wavelengths is a near-infrared wavelength between 700 nanometers and 2500 nanometers. The measurement device comprises one or more lenses configured to receive and to deliver a portion of the optical beam to tissue, wherein the tissue reflects at least a portion of the optical beam delivered to the tissue, and wherein the measurement device is adapted to be placed on a wrist or an ear of a user. The measurement device further comprises a receiver having a plurality of spatially separated detectors and one or more analog to digital converters coupled to the spatially separated detectors, the one or more analog to digital converters configured to generate at least two receiver outputs. The receiver is configured to capture light while the LEDs are off and convert the captured light into a first signal, and to capture light while at least one of the LEDs is on and convert the captured light into a second signal, the captured light including at least a portion of the optical beam reflected from the tissue. The measurement device is configured to improve a signal-to-noise ratio of the optical beam reflected from the tissue by differencing the first signal and the second signal and by differencing the two receiver outputs. The measurement device is configured to further improve the signal-to-noise ratio of the optical beam reflected from the tissue by increasing the light intensity relative to the initial light intensity from at least one of the LEDs. The measurement device is further configured to generate an output signal representing at least in part a non-invasive measurement on blood contained within the tissue, wherein the output signal is generated at least in part by using a Fourier transform and mathematical manipulation of a signal resulting from the captured light. The receiver further comprises one or more spectral filters positioned in front of at least some of the plurality of spatially separated detectors.

BRIEF DESCRIPTION OF THE DRAWINGS

For a more complete understanding of the present disclosure, and for further features and advantages thereof, reference is now made to the following description taken in conjunction with the accompanying drawings, in which:

FIG. **1** illustrates the structure of a tooth.

FIG. **2**A shows the attenuation coefficient for dental enamel and water versus wavelength from approximately 600 nm to 2600 nm.

FIG. **2**B illustrates the absorption spectrum of intact enamel and dentine in the wavelength range of approximately 1.2 to 2.4 microns.

FIG. **3** shows the near infrared spectral reflectance over the wavelength range of approximately 800 nm to 2500 nm from an occlusal tooth surface. The black diamonds correspond to the reflectance from a sound, intact tooth section. The asterisks correspond to a tooth section with an enamel lesion. The circles correspond to a tooth section with a dentine lesion.

FIG. **4** illustrates a hand-held dental tool design of a human interface that may also be coupled with other dental tools.

FIG. **5**A illustrates a clamp design of a human interface to cap over one or more teeth and perform a non-invasive measurement for dental caries.

FIG. **5**B shows a mouth guard design of a human interface to perform a non-invasive measurement for dental caries.

FIG. **6**A illustrates the dorsal of a hand for performing a differential measurement for measuring blood constituents or analytes.

FIG. **6**B illustrates the dorsal of a foot for performing a differential measurement for measuring blood constituents or analytes.

FIG. **7** illustrates a block diagram or building blocks for constructing high power laser diode assemblies.

FIG. **8** shows a platform architecture for different wavelength ranges for an all-fiber-integrated, high powered, super-continuum light source.

FIG. **9** illustrates one embodiment for a short-wave infrared super-continuum light source.

FIG. **10** shows the output spectrum from the SWIR SC laser of FIG. **9** when about 10 m length of fiber for SC generation is used. This fiber is a single-mode, non-dispersion shifted fiber that is optimized for operation near 1550 nm.

FIG. **11**A illustrates a schematic of the experimental set-up for measuring the diffuse reflectance spectroscopy using the SWIR-SC light source of FIGS. **9** and **10**.

FIG. **11**B shows exemplary reflectance from a sound enamel region, an enamel lesion region, and a dentine lesion region. The spectra are normalized to have equal value near 2050 nm.

FIGS. **12**A-B illustrate high power SWIR-SC lasers that may generate light between approximately 1.4-1.8 microns (FIG. **12**A) or approximately 2-2.5 microns (FIG. **12**B).

FIG. **12**C shows a reflection-spectroscopy based stand-off detection system having an SC laser source.

FIG. **12**D shows one example of a dual-beam experimental set-up that may be used to subtract out (or at least minimize the adverse effects of) light source fluctuations.

FIG. **13** schematically shows that the medical measurement device can be part of a personal or body area network that communicates with another device (e.g., smart phone or tablet) that communicates with the cloud. The cloud may in turn communicate information with the user, dental or healthcare providers, or other designated recipients.

DETAILED DESCRIPTION OF EXAMPLE EMBODIMENTS

As required, detailed embodiments of the present disclosure are disclosed herein; however, it is to be understood that the disclosed embodiments are merely exemplary of the disclosure that may be embodied in various and alternative forms. The figures are not necessarily to scale; some features may be exaggerated or minimized to show details of particular components. Therefore, specific structural and functional details disclosed herein are not to be interpreted as limiting, but merely as a representative basis for teaching one skilled in the art to variously employ the present disclosure.

Near-infrared (NIR) and SWIR light may be preferred for caries detection compared to visible light imaging because the NIR/SWIR wavelengths generally have lower absorption by stains and deeper penetration into teeth. Hence, NIR/SWIR light may provide a caries detection method that can be non-invasive, non-contact and relatively stain insensitive. Broadband light may provide further advantages because carious regions may demonstrate spectral signatures from water absorption and the wavelength dependence of porosity in the scattering of light.

The wavelength of light should be selected appropriately to achieve a non-invasive procedure. For example, the light should be able to penetrate deep enough to reach through the dermis and subcutaneous fat layers to reach varicose veins. For example, the penetration depth may be defined as the inverse of the absorption coefficient, although it may also be necessary to include the scattering for the calculation. To achieve penetration deep enough to reach the varicose veins, wavelengths may correspond to local minima in water **501** and adipose **502** absorption, as well as potentially local minima in collagen **503** and elastin **504** absorption. For example, wavelengths near approximately 1100 nm, 1310 nm, or 1650 nm may be advantageous for non-invasive procedures. More generally, wavelength ranges of approximately 900 nm to 1150 nm, 1280 nm to 1340 nm, or 1550 nm to 1680 nm may be advantageous for non-invasive procedures.

In general, the near-infrared region of the electromagnetic spectrum covers between approximately 0.7 microns (700 nm) to about 2.5 microns (2500 nm). However, it may also be advantageous to use just the short-wave infrared between approximately 1.4 microns (1400 nm) and about 2.5 microns (2500 nm). One reason for preferring the SWIR over the entire NIR may be to operate in the so-called "eye safe" window, which corresponds to wavelengths longer than about 1400 nm. Therefore, for the remainder of the disclosure the SWIR will be used for illustrative purposes. However, it should be clear that the discussion that follows could also apply to using the NIR wavelength range, or other wavelength bands.

In particular, wavelengths in the eye safe window may not transmit down to the retina of the eye, and therefore, these wavelengths may be less likely to create permanent eye damage from inadvertent exposure. The near-infrared wavelengths have the potential to be dangerous, because the eye cannot see the wavelengths (as it can in the visible), yet they can penetrate and cause damage to the eye. Even if a practitioner is not looking directly at the laser beam, the practitioner's eyes may receive stray light from a reflection or scattering from some surface. Hence, it can always be a good practice to use eye protection when working around lasers. Since wavelengths longer than about 1400 nm are substantially not transmitted to the retina or substantially absorbed in the retina, this wavelength range is known as the eye safe window. For wavelengths longer than 1400 nm, in general only the cornea of the eye may receive or absorb the light radiation.

FIG. **1** illustrates the structure of an exemplary cross-section of a tooth **100**. The tooth **100** has a top layer called the crown **101** and below that a root **102** that reaches well into the gum **106** and bone **108** of the mouth. The exterior of the crown **101** is an enamel layer **103**, and below the enamel is a layer of dentine **104** that sits atop a layer of cementum **107**. Below the dentine **104** is a pulp region **105**, which comprises within it blood vessels **109** and nerves **110**. If the light can penetrate the enamel **103** and dentine **104**, then the blood flow and blood constituents may be measured through the blood vessels in the dental pulp **105**. While the amount of blood flow in the capillaries of the dental pulp **105** may be less than an artery or vein, the smaller blood flow could still be advantageous for detecting or measuring blood constituents as compared to detection through the skin if there is less interfering spectral features from the tooth. Although the structure of a molar tooth is illustrated in FIG. **1**, other types of teeth also have similar structure. For example, different types of teeth include molars, pre-molars, canine and incisor teeth.

As used throughout this document, the term "couple" and or "coupled" refers to any direct or indirect communication between two or more elements, whether or not those elements are physically connected to one another. As used throughout this disclosure, the term "spectroscopy" means that a tissue or sample is inspected by comparing different features, such as wavelength (or frequency), spatial location, transmission, absorption, reflectivity, scattering, refractive index, or opacity. In one embodiment, "spectroscopy" may mean that the wavelength of the light source is varied, and the transmission, absorption, or reflectivity of the tissue or sample is measured as a function of wavelength. In another embodiment, "spectroscopy" may mean that the wavelength dependence of the transmission, absorption or reflectivity is compared between different spatial locations on a tissue or sample. As an illustration, the "spectroscopy" may be performed by varying the wavelength of the light source, or by using a broadband light source and analyzing the signal using a spectrometer, wavemeter, or optical spectrum analyzer.

As used throughout this disclosure, the term "fiber laser" refers to a laser or oscillator that has as an output light or an optical beam, wherein at least a part of the laser comprises an optical fiber. For instance, the fiber in the "fiber laser" may comprise one of or a combination of a single mode fiber, a multi-mode fiber, a mid-infrared fiber, a photonic crystal fiber, a doped fiber, a gain fiber, or, more generally,

an approximately cylindrically shaped waveguide or light-pipe. In one embodiment, the gain fiber may be doped with rare earth material, such as ytterbium, erbium, and/or thulium, for example. In another embodiment, the mid-infrared fiber may comprise one or a combination of fluoride fiber, ZBLAN fiber, chalcogenide fiber, tellurite fiber, or germanium doped fiber. In yet another embodiment, the single mode fiber may include standard single-mode fiber, dispersion shifted fiber, non-zero dispersion shifted fiber, high-nonlinearity fiber, and small core size fibers.

As used throughout this disclosure, the term "pump laser" refers to a laser or oscillator that has as an output light or an optical beam, wherein the output light or optical beam is coupled to a gain medium to excite the gain medium, which in turn may amplify another input optical signal or beam. In one particular example, the gain medium may be a doped fiber, such as a fiber doped with ytterbium, erbium, and/or thulium. In one embodiment, the "pump laser" may be a fiber laser, a solid state laser, a laser involving a nonlinear crystal, an optical parametric oscillator, a semiconductor laser, or a plurality of semiconductor lasers that may be multiplexed together. In another embodiment, the "pump laser" may be coupled to the gain medium by using a fiber coupler, a dichroic mirror, a multiplexer, a wavelength division multiplexer, a grating, or a fused fiber coupler.

As used throughout this document, the term "super-continuum" and or "supercontinuum" and or "SC" refers to a broadband light beam or output that comprises a plurality of wavelengths. In a particular example, the plurality of wavelengths may be adjacent to one-another, so that the spectrum of the light beam or output appears as a continuous band when measured with a spectrometer. In one embodiment, the broadband light beam may have a bandwidth or at least 10 nm. In another embodiment, the "super-continuum" may be generated through nonlinear optical interactions in a medium, such as an optical fiber or nonlinear crystal. For example, the "super-continuum" may be generated through one or a combination of nonlinear activities such as four-wave mixing, the Raman effect, modulational instability, and self-phase modulation.

As used throughout this disclosure, the terms "optical light" and or "optical beam" and or "light beam" refer to photons or light transmitted to a particular location in space. The "optical light" and or "optical beam" and or "light beam" may be modulated or unmodulated, which also means that they may or may not contain information. In one embodiment, the "optical light" and or "optical beam" and or "light beam" may originate from a fiber, a fiber laser, a laser, a light emitting diode, a lamp, a pump laser, or a light source.

Transmission or Reflection Through Teeth

The transmission, absorption and reflection from teeth has been studied in the near infrared, and, although there are some features, the enamel and dentine appear to be fairly transparent in the near infrared (particularly SWIR wavelengths between about 1400 and 2500 nm). For example, the absorption or extinction ratio for light transmission has been studied. FIG. **2**A illustrates the attenuation coefficient **200** for dental enamel **201** (filled circles) and the absorption coefficient of water **202** (open circles) versus wavelength. Near-infrared light may penetrate much further without scattering through all the tooth enamel, due to the reduced scattering coefficient in normal enamel. Scattering in enamel may be fairly strong in the visible, but decreases as approximately $1/(\text{wavelength})^3$ [i.e., inverse of the cube of the wavelength] with increasing wavelength to a value of only 2-3 cm−1 at 1310 nm and 1550 nm in the near infrared. Therefore, enamel may be virtually transparent in the near infrared with optical attenuation 1-2 orders of magnitude less than in the visible range.

As another example, FIG. **2**B illustrates the absorption spectrum **250** of intact enamel **251** (dashed line) and dentine **252** (solid line) in the wavelength range of approximately 1.2 to 2.4 microns. In the near infrared there are two absorption bands in the areas of about 1.5 and 2 microns. The band with a peak around 1.57 microns may be attributed to the overtone of valent vibration of water present in both enamel and dentine. In this band, the absorption is greater for dentine than for enamel, which may be related to the large water content in this tissue. In the region of 2 microns, dentine may have two absorption bands, and enamel one. The band with a maximum near 2.1 microns may belong to the overtone of vibration of PO hydroxyapatite groups, which is the main substance of both enamel and dentine. Moreover, the band with a peak near 1.96 microns in dentine may correspond to water absorption (dentine may contain substantially higher water than enamel).

In addition to the absorption coefficient, the reflectance from intact teeth and teeth with dental caries (e.g., cavities) has been studied. In one embodiment, FIG. **3** shows the near infrared spectral reflectance **300** over the wavelength range of approximately 800 nm to 2500 nm from an occlusal (e.g., top) tooth surface **304**. The curve with black diamonds **301** corresponds to the reflectance from a sound, intact tooth section. The curve with asterisks (*) **302** corresponds to a tooth section with an enamel lesion. The curve with circles **303** corresponds to a tooth section with a dentine lesion. Thus, when there is a lesion, more scattering occurs and there may be an increase in the reflected light.

For wavelengths shorter than approximately 1400 nm, the shapes of the spectra remain similar, but the amplitude of the reflection changes with lesions. Between approximately 1400 nm and 2500 nm, an intact tooth **301** has low reflectance (e.g., high transmission), and the reflectance appears to be more or less independent of wavelength. On the other hand, in the presence of lesions **302** and **303**, there is increased scattering, and the scattering loss may be wavelength dependent. For example, the scattering loss may decrease as the inverse of some power of wavelength, such as $1/(\text{wavelength})^3$—so, the scattering loss decreases with longer wavelengths. When there is a lesion in the dentine **303**, more water can accumulate in the area, so there is also increased water absorption. For example, the dips near 1450 nm and 1900 nm may correspond to water absorption, and the reflectance dips are particularly pronounced in the dentine lesion **303**.

FIG. **3** may point to several novel techniques for early detection and quantification of carious regions. One method may be to use a relatively narrow wavelength range (for example, from a laser diode or super-luminescent laser diode) in the wavelength window below 1400 nm. In one embodiment, wavelengths in the vicinity of 1310 nm may be used, which is a standard telecommunications wavelength where appropriate light sources are available. Also, it may be advantageous to use a super-luminescent laser diode rather than a laser diode, because the broader bandwidth may avoid the production of laser speckle that can produce interference patterns due to light's scattering after striking irregular surfaces. As FIG. **3** shows, the amplitude of the reflected light (which may also be proportional to the inverse of the transmission) may increase with dental caries. Hence, comparing the reflected light from a known intact region with a suspect region may help identify carious regions. However, one difficulty with using a relatively narrow wavelength range and relying on amplitude changes may be the calibration of the measurement. For example, the amplitude of the reflected light may depend on many factors, such as irregularities in the dental surface, placement of the light source and detector, distance of the measurement instrument from the tooth, etc.

In one embodiment, use of a plurality of wavelengths can help to better calibrate the dental caries measurement. For example, a plurality of laser diodes or super-luminescent laser diodes may be used at different center wavelengths. Alternately, a lamp or alternate broadband light source may be used followed by appropriate filters, which may be placed after the light source or before the detectors. In one example, wavelengths near 1090 nm, 1440 nm and 1610 nm may be employed. The reflection from the tooth **305** appears to reach a local maximum near 1090 nm in the representative embodiment illustrated. Also, the reflectance near 1440 nm **306** is higher for dental caries, with a distinct dip particularly for dentine caries **303**. Near 1610 nm **307**, the reflection is also higher for carious regions. By using a plurality of wavelengths, the values at different wavelengths may help quantify a caries score. In one embodiment, the degree of enamel lesions may be proportional to the ratio of the reflectance near 1610 nm divided by the reflectance near 1090 nm. Also, the degree of dentine lesion may be proportional to the difference between the reflectance near 1610 nm and 1440 nm, with the difference then divided by the reflectance near 1090 nm. Although one set of wavelengths has been described, other wavelengths may also be used and are intended to be covered by this disclosure.

In yet another embodiment, it may be further advantageous to use all of some fraction of the SWIR between approximately 1400 and 2500 nm. For example, a SWIR super-continuum light source could be used, or a lamp source could be used. On the receiver side, a spectrometer and/or dispersive element could be used to discriminate the various wavelengths. As FIG. **3** shows, an intact tooth **301** has a relatively low and featureless reflectance over the SWIR. On the other hand, with a carious region there is more scattering, so the reflectance **302**,**303** increases in amplitude. Since the scattering is inversely proportional to wavelength or some power of wavelength, the carious region reflectance **302**, **303** also decreases with increasing wavelength. Moreover, the carious region may contain more water, so there are dips in the reflectance near the water absorption lines **306** and **308**. The degree of caries or caries score may be quantified by the shape of the spectrum over the SWIR, taking ratios of different parts of the spectrum, or some combination of this and other spectral processing methods.

Although several methods of early caries detection using spectral reflectance have been described, other techniques could also be used and are intended to be covered by this disclosure. For example, transmittance may be used rather than reflectance, or a combination of the two could be used. Moreover, the transmittance, reflectance and/or absorbance could also be combined with other techniques, such as quantitative light-induced fluorescence or fiber-optic trans-illumination. Also, the SWIR could be advantageous, but other parts of the infrared, near-infrared or visible wavelengths may also be used consistent with this disclosure.

One other benefit of the absorption, transmission or reflectance in the near infrared and SWIR may be that stains and non-calcified plaque are not visible in this wavelength range, enabling better discrimination of defects, cracks, and demineralized areas. For example, dental calculus, accumulated plaque, and organic stains and debris may interfere significantly with visual diagnosis and fluorescence-based caries detection schemes in occlusal surfaces. In the case of using quantitative light-induced fluorescence, such confounding factors typically may need to be removed by prophylaxis (abrasive cleaning) before reliable measurements can be taken. Surface staining at visible wavelengths may further complicate the problem, and it may be difficult to determine whether pits and fissures are simply stained or demineralized. On the other hand, staining and pigmentation generally interfere less with NIR or SWIR imaging. For example, NIR and SWIR light may not be absorbed by melanin and porphyrins produced by bacteria and those found in food dyes that accumulate in dental plaque and are responsible for the pigmentation.

Human Interface for Measurement System

A number of different types of measurements may be used to image for dental caries, particularly early detection of dental caries. A basic feature of the measurements may be that the optical properties are measured as a function of wavelength at a plurality of wavelengths. As further described below, the light source may output a plurality of wavelengths, or a continuous spectrum over a range of wavelengths. In one embodiment, the light source may cover some or all of the wavelength range between approximately 1400 nm and 2500 nm. The signal may be received at a receiver, which may also comprise a spectrometer or filters to discriminate between different wavelengths. The signal may also be received at a camera, which may also comprise filters or a spectrometer. In one embodiment, the spectral discrimination using filters or a spectrometer may be placed after the light source rather than at the receiver. The receiver usually comprises one or more detectors (optical-to-electrical conversion element) and electrical circuitry. The receiver may also be coupled to analog to digital converters, particularly if the signal is to be fed to a digital device.

Referring to FIG. **1**, one or more light sources **111** may be used for illumination. In one embodiment, a transmission measurement may be performed by directing the light source output **111** to the region near the interface between the gum **106** and dentine **104**. In one embodiment, the light may be directed using a light guide or a fiber optic. The light may then propagate through the dental pulp **105** to the other side, where the light may be incident on one or more detectors or another light guide to transport the signal to **112** a spectrometer, receiver, and/or camera, for example. In one embodiment, the light source may be directed to one or more locations near the interface between the gum **106** and dentine **104** (in one example, could be from the two sides of the tooth). The transmitted light may then be detected in the occlusal surface above the tooth using a **112** spectrometer, receiver, or camera, for example. In another embodiment, a reflectance measurement may be conducted by directing the light source output **111** to, for example, the occlusal surface of the tooth, and then detecting the reflectance at a **113** spectrometer, receiver or camera. Although a few embodiments for imaging the tooth are described, other embodiments and techniques may also be used and are intended to be covered by this disclosure. These optical techniques may measure optical properties such as reflectance, transmittance, absorption, or luminescence.

In one embodiment, FIG. **4** shows that the light source and/or detection system may be integrated with a dental hand-piece **400**. The hand-piece **400** may also include other

dental equipment, such as a drill, pick, air spray or water cooling stream. The dental hand-piece **400** may include a housing **401** and a motor housing **402** (in some embodiments such as with a drill, a motor may be placed in this section). The end of hand-piece **403** that interfaces with the tooth may be detachable, and it may also have the light input and output end. The dental hand-piece **400** may also have an umbilical cord **404** for connecting to power supplies, diagnostics, or other equipment, for example.

A light guide **405** may be integrated with the hand-piece **400**, either inside the housing **401**, **402** or adjacent to the housing. In one embodiment, a light source **410** may be contained within the housing **401**, **402**. In an alternative embodiment, the hand-piece **400** may have a coupler **410** to couple to an external light source **411** and/or detection system or receiver **412**. The light source **411** may be coupled to the hand-piece **400** using a light guide or fiber optic cable **406**. In addition, the detection system or receiver **412** may be coupled to the hand-piece **400** using one or more light guides, fiber optic cable or a bundle of fibers **407**.

The light incident on the tooth may exit the hand-piece **400** through the end **403**. The end **403** may also have a lens system or curved mirror system to collimate or focus the light. In one embodiment, if the light source is integrated with a tool such as a drill, then the light may reach the tooth at the same point as the tip of the drill. The reflected or transmitted light from the tooth may then be observed externally and/or guided back through the light guide **405** in the hand-piece **400**. If observed externally, there may be a lens system **408** for collecting the light and a detection system **409** that may have one or more detectors and electronics. If the light is to be guided back through the hand-piece **400**, then the reflected light may transmit through the light guide **405** back to the detection system or receiver **412**. In one embodiment, the incident light may be guided by a fiber optic through the light guide **405**, and the reflected light may be captured by a series of fibers forming a bundle adjacent to or surrounding the incident light fiber.

In another embodiment, a "clamp" design **500** may be used as a cap over one or more teeth, as illustrated in FIG. **5**A. The clamp design may be different for different types of teeth, or it may be flexible enough to fit over different types of teeth. For example, different types of teeth include the molars (toward the back of the mouth), the premolars, the canine, and the incisors (toward the front of the mouth). One embodiment of the clamp-type design is illustrated in FIG. **5**A for a molar tooth **508**. The C-clamp **501** may be made of a plastic or rubber material, and it may comprise a light source input **502** and a detector output **503** on the front or back of the tooth, for example.

The light source input **502** may comprise a light source directly, or it may have light guided to it from an external light source. Also, the light source input **502** may comprise a lens system to collimate or focus the light across the tooth. The detector output **503** may comprise a detector directly, or it may have a light guide to transport the signal to an external detector element. The light source input **502** may be coupled electrically or optically through **504** to a light input **506**. For example, if the light source is external in **506**, then the coupling element **504** may be a light guide, such as a fiber optic. Alternately, if the light source is contained in **502**, then the coupling element **504** may be electrical wires connecting to a power supply in **506**. Similarly, the detector output **503** may be coupled to a detector output unit **507** with a coupling element **505**, which may be one or more electrical wires or a light guide, such as a fiber optic. This is just one example of a clamp over one or more teeth, but other embodiments may also be used and are intended to be covered by this disclosure. For example, if reflectance from the teeth is to be used in the measurement, then the light input **502** and detected light input **503** may be on the same side of the tooth.

In yet another embodiment, one or more light source ports and sensor ports may be used in a mouth-guard type design. For example, one embodiment of a dental mouth guard **550** is illustrated in FIG. **5**B. The structure of the mouth guard **551** may be similar to mouth guards used in sports (e.g., when playing football or boxing) or in dental trays used for applying fluoride treatment, and the mouth guard may be made from plastic, rubber, or any other suitable materials. As an example, the mouth guard may have one or more light source input ports **552**, **553** and one or more detector output ports **554**, **555**. Although six input and output ports are illustrated, any number of ports may be used.

Similar to the clamp design described above, the light source inputs **552**, **553** may comprise one or more light sources directly, or they may have light guided to them from an external light source. Also, the light source inputs **552**, **553** may comprise lens systems to collimate or focus the light across the teeth. The detector outputs **554**, **555** may comprise one or more detectors directly, or they may have one or more light guides to transport the signals to an external detector element. The light source inputs **552**, **553** may be coupled electrically or optically through **556** to a light input **557**. For example, if the light source is external in **557**, then the one or more coupling elements **556** may be one or more light guides, such as a fiber optic. Alternately, if the light sources are contained in **552**, **553**, then the coupling element **556** may be one or more electrical wires connecting to a power supply in **557**. Similarly, the detector outputs **554**, **555** may be coupled to a detector output unit **559** with one or more coupling elements **558**, which may be one or more electrical wires or one or more light guides, such as a fiber optic. This is just one example of a mouth guard design covering a plurality of teeth, but other embodiments may also be used and are intended to be covered by this disclosure. For instance, the position of the light source inputs and detector output ports could be exchanged, or some mixture of locations of light source inputs and detector output ports could be used. Also, if reflectance from the teeth is to be measured, then the light sources and detectors may be on the same side of the tooth. Moreover, it may be advantageous to pulse the light source with a particular pulse width and pulse repetition rate, and then the detection system can measure the pulsed light returned from or transmitted through the tooth. Using a lock-in type technique (e.g., detecting at the same frequency as the pulsed light source and also possibly phase locked to the same signal), the detection system may be able to reject background or spurious signals and increase the signal-to-noise ratio of the measurement.

Other elements may be added to the human interface designs of FIGS. **4-6** and are also intended to be covered by this disclosure. For instance, in one embodiment it may be desirable to have replaceable inserts that may be disposable. Particularly in a dentist's or doctor's office or hospital setting, the same instrument may be used with a plurality of patients. Rather than disinfecting the human interface after each use, it may be preferable to have disposable inserts that can be thrown away after each use. In one embodiment, a thin plastic coating material may enclose the clamp design of FIG. **5**A or mouth guard design of FIG. **5**B. The coating material may be inserted before each use, and then after the measurement is exercised the coating material may be peeled off and replaced. The coating or covering material may be selected based on suitable optical properties that do not affect the measurement, or known optical properties that can be calibrated or compensated for during measurement. Such a design may save the dentist or physician or user considerable time, while at the same time provide the business venture with a recurring cost revenue source.

Thus, beyond the problem of other blood constituents or analytes having overlapping spectral features, it may be difficult to observe glucose spectral signatures through the skin and its constituents of water, adipose, collagen and elastin. One approach to overcoming this difficulty may be to try to measure the blood constituents in veins that are located at relatively shallow distances below the skin. Veins may be more beneficial for the measurement than arteries, since arteries tend to be located at deeper levels below the skin. Also, in one embodiment it may be advantageous to use a differential measurement to subtract out some of the interfering absorption lines from the skin. For example, an instrument head may be designed to place one probe above a region of skin over a blood vein, while a second probe may be placed at a region of the skin without a noticeable blood vein below it. Then, by differencing the signals from the two probes, at least part of the skin interference may be cancelled out.

Two representative embodiments for performing such a differential measurement are illustrated in FIG. **6**A and FIG. **6**B. In one embodiment shown in FIG. **6**A, the dorsal of the hand **600** may be used for measuring blood constituents or analytes. The dorsal of the hand **600** may have regions that have distinct veins **601** as well as regions where the veins are not as shallow or pronounced **602**. By stretching the hand and leaning it backwards, the veins **601** may be accentuated in some cases. A near-infrared diffuse reflectance measurement may be performed by placing one probe **603** above the vein-rich region **601**. To turn this into a differential measurement, a second probe **604** may be placed above a region without distinct veins **602**. Then, the outputs from the two probes may be subtracted **605** to at least partially cancel out the features from the skin. The subtraction may be done preferably in the electrical domain, although it can also be performed in the optical domain or digitally/mathematically using sampled data based on the electrical and/or optical signals. Although one example of using the dorsal of the hand **600** is shown, many other parts of the hand can be used within the scope of this disclosure. For example, alternate methods may use transmission through the webbing between the thumb and the fingers **606**, or transmission or diffuse reflection through the tips of the fingers **607**.

In another embodiment, the dorsal of the foot **650** may be used instead of the hand. One advantage of such a configuration may be that for self-testing by a user, the foot may be easier to position the instrument using both hands. One probe **653** may be placed over regions where there are more distinct veins **651**, and a near-infrared diffuse reflectance measurement may be made. For a differential measurement, a second probe **654** may be placed over a region with less prominent veins **652**, and then the two probe signals may be subtracted, either electronically or optically, or may be digitized/sampled and processed mathematically depending on the particular application and implementation. As with the hand, the differential measurements may be intended to compensate for or subtract out (at least in part) the interference from the skin. Since two regions are used in close proximity on the same body part, this may also aid in removing some variability in the skin from environmental effects such as temperature, humidity, or pressure. In addition, it may be advantageous to first treat the skin before the measurement, by perhaps wiping with a cloth or treated cotton ball, applying some sort of cream, or placing an ice cube or chilled bag over the region of interest.

Although two embodiments have been described, many other locations on the body may be used using a single or differential probe within the scope of this disclosure. In yet another embodiment, the wrist may be advantageously used, particularly where a pulse rate is typically monitored. Since the pulse may be easily felt on the wrist, there is underlying the region a distinct blood flow. Other embodiments may use other parts of the body, such as the ear lobes, the tongue, the inner lip, the nails, the eye, or the teeth. Some of these embodiments will be further described below. The ear lobes or the tip of the tongue may be advantageous because they are thinner skin regions, thus permitting transmission rather than diffuse reflection. However, the interference from the skin is still a problem in these embodiments. Other regions such as the inner lip or the bottom of the tongue may be contemplated because distinct veins are observable, but still the interference from the skin may be problematic in these embodiments. The eye may seem as a viable alternative because it is more transparent than skin. However, there are still issues with scattering in the eye. For example, the anterior chamber of the eye (the space between the cornea and the iris) comprises a fluid known as aqueous humor. However, the glucose level in the eye chamber may have a significant temporal lag on changes in the glucose level compared to the blood glucose level.

Light Sources for Near Infrared

There are a number of light sources that may be used in the near infrared. To be more specific, the discussion below will consider light sources operating in the short wave infrared (SWIR), which may cover the wavelength range of approximately 1400 nm to 2500 nm. Other wavelength ranges may also be used for the applications described in this disclosure, so the discussion below is merely provided as exemplary types of light sources. The SWIR wavelength range may be valuable for a number of reasons. First, the SWIR corresponds to a transmission window through water and the atmosphere. Second, the so-called "eye-safe" wavelengths are wavelengths longer than approximately 1400 nm. Third, the SWIR covers the wavelength range for nonlinear combinations of stretching and bending modes as well as the first overtone of C—H stretching modes. Thus, for example, glucose and ketones among other substances may have unique signatures in the SWIR. Moreover, many solids have distinct spectral signatures in the SWIR, so particular solids may be identified using stand-off detection or remote sensing. For instance, many explosives have unique signatures in the SWIR.

Different light sources may be selected for the SWIR based on the needs of the application. Some of the features for selecting a particular light source include power or intensity, wavelength range or bandwidth, spatial or temporal coherence, spatial beam quality for focusing or transmission over long distance, and pulse width or pulse repetition rate. Depending on the application, lamps, light emitting diodes (LEDs), laser diodes (LD's), tunable LD's, super-luminescent laser diodes (SLDs), fiber lasers or super-continuum sources (SC) may be advantageously used. Also, different fibers may be used for transporting the light, such as fused silica fibers, plastic fibers, mid-infrared fibers (e.g., tellurite, chalcogenides, fluorides, ZBLAN, etc), or a hybrid of these fibers.

Lamps may be used if low power or intensity of light is required in the SWIR, and if an incoherent beam is suitable. In one embodiment, in the SWIR an incandescent lamp that can be used is based on tungsten and halogen, which have an emission wavelength between approximately 500 nm to 2500 nm. For low intensity applications, it may also be possible to use thermal sources, where the SWIR radiation is based on the black body radiation from the hot object. Although the thermal and lamp based sources are broadband and have low intensity fluctuations, it may be difficult to achieve a high signal-to-noise ratio due to the low power levels. Also, the lamp based sources tend to be energy inefficient.

In another embodiment, LED's can be used that have a higher power level in the SWIR wavelength range. LED's also produce an incoherent beam, but the power level can be higher than a lamp and with higher energy efficiency. Also, the LED output may more easily be modulated, and the LED provides the option of continuous wave or pulsed mode of operation. LED's are solid state components that emit a wavelength band that is of moderate width, typically between about 20 nm to 40 nm. There are also so-called super-luminescent LEDs that may even emit over a much wider wavelength range. In another embodiment, a wide band light source may be constructed by combining different LEDs that emit in different wavelength bands, some of which could preferably overlap in spectrum. One advantage of LEDs as well as other solid state components is the compact size that they may be packaged into.

In yet another embodiment, various types of laser diodes may be used in the SWIR wavelength range. Just as LEDs may be higher in power but narrower in wavelength emission than lamps and thermal sources, the LDs may be yet higher in power but yet narrower in wavelength emission than LEDs. Different kinds of LDs may be used, including Fabry-Perot LDs, distributed feedback (DFB) LDs, distributed Bragg reflector (DBR) LDs. Since the LDs have relatively narrow wavelength range (typically under 10 nm), in one embodiment a plurality of LDs may be used that are at different wavelengths in the SWIR. The various LDs may be spatially multiplexed, polarization multiplexed, wavelength multiplexed, or a combination of these multiplexing methods. Also, the LDs may be fiber pig-tailed or have one or more lenses on the output to collimate or focus the light. Another advantage of LDs is that they may be packaged compactly and may have a spatially coherent beam output. Moreover, tunable LDs that can tune over a range of wavelengths are also available. The tuning may be done by varying the temperature, or electrical current may be used in particular structures such as distributed Bragg reflector (DBR) LDs, for example. In another embodiment, external cavity LDs may be used that have a tuning element, such as a fiber grating or a bulk grating, in the external cavity.

In another embodiment, super-luminescent laser diodes may provide higher power as well as broad bandwidth. An SLD is typically an edge emitting semiconductor light source based on super-luminescence (e.g., this could be amplified spontaneous emission). SLDs combine the higher power and brightness of LDs with the low coherence of conventional LEDs, and the emission band for SLD's may be 5 to 100 nm wide, preferably in the 60 to 100 nm range. Although currently SLDs are commercially available in the wavelength range of approximately 400 nm to 1700 nm, SLDs could and may in the future be made to cover a broader region of the SWIR.

In yet another embodiment, high power LDs for either direct excitation or to pump fiber lasers and SC light sources may be constructed using one or more laser diode bar stacks. FIG. **7** shows an example of a block diagram **700** or building blocks for constructing the high power LDs. In this embodiment, one or more diode bar stacks **701** may be used, where the diode bar stack may be an array of several single emitter LDs. Since the fast axis (e.g., vertical direction) may be nearly diffraction limited while the slow-axis (e.g., horizontal axis) may be far from diffraction limited, different collimators **702** may be used for the two axes.

Then, the brightness may be increased by spatially combining the beams from multiple stacks **703**. The combiner may include spatial interleaving, it may include wavelength multiplexing, or it may involve a combination of the two. Different spatial interleaving schemes may be used, such as using an array of prisms or mirrors with spacers to bend one array of beams into the beam path of the other. In another embodiment, segmented mirrors with alternate high-reflection and anti-reflection coatings may be used. Moreover, the brightness may be increased by polarization beam combining **704** the two orthogonal polarizations, such as by using a polarization beam splitter. In a particular embodiment, the output may then be focused or coupled into a large diameter core fiber. As an example, typical dimensions for the large diameter core fiber range from diameters of approximately 100 microns to 400 microns or more. Alternatively or in addition, a custom beam shaping module **705** may be used, depending on the particular application. For example, the output of the high power LD may be used directly **706**, or it may be fiber coupled **707** to combine, integrate, or transport the high power LD energy. These high power LDs may grow in importance because the LD powers can rapidly scale up. For example, instead of the power being limited by the power available from a single emitter, the power may increase in multiples depending on the number of diodes multiplexed and the size of the large diameter fiber. Although FIG. **7** is shown as one embodiment, some or all of the elements may be used in a high power LD, or additional elements may also be used.

SWIR Super-Continuum Lasers

Each of the light sources described above have particular strengths, but they also may have limitations. For example, there is typically a trade-off between wavelength range and power output. Also, sources such as lamps, thermal sources, and LEDs produce incoherent beams that may be difficult to focus to a small area and may have difficulty propagating for long distances. An alternative source that may overcome some of these limitations is an SC light source. Some of the advantages of the SC source may include high power and intensity, wide bandwidth, spatially coherent beam that can propagate nearly transform limited over long distances, and easy compatibility with fiber delivery.

Supercontinuum lasers may combine the broadband attributes of lamps with the spatial coherence and high brightness of lasers. By exploiting a modulational instability initiated supercontinuum (SC) mechanism, an all-fiber-integrated SC laser with no moving parts may be built using commercial-off-the-shelf (COTS) components. Moreover, the fiber laser architecture may be a platform where SC in the visible, near-infrared/SWIR, or mid-IR can be generated by appropriate selection of the amplifier technology and the SC generation fiber. But until recently, SC lasers were used primarily in laboratory settings since typically large, table-top, mode-locked lasers were used to pump nonlinear media such as optical fibers to generate SC light. However, those

large pump lasers may now be replaced with diode lasers and fiber amplifiers that gained maturity in the telecommunications industry.

In one embodiment, an all-fiber-integrated, high-powered SC light source **800** may be elegant for its simplicity (FIG. **8**). The light may be first generated from a seed laser diode **801**. For example, the seed LD **801** may be a distributed feedback (DFB) laser diode with a wavelength near 1542 or 1550 nm, with approximately 0.5-2.0 ns pulsed output, and with a pulse repetition rate between about one kilohertz to about 100 MHz or more. The output from the seed laser diode may then be amplified in a multiple-stage fiber amplifier **802** comprising one or more gain fiber segments. In one embodiment, the first stage pre-amplifier **803** may be designed for optimal noise performance. For example, the pre-amplifier **803** may be a standard erbium-doped fiber amplifier or an erbium/ytterbium doped cladding pumped fiber amplifier. Between amplifier stages **803** and **806**, it may be advantageous to use band-pass filters **804** to block amplified spontaneous emission and isolators **805** to prevent spurious reflections. Then, the power amplifier stage **806** may use a cladding-pumped fiber amplifier that may be optimized to minimize nonlinear distortion. The power amplifier fiber **806** may also be an erbium-doped fiber amplifier, if only low or moderate power levels are to be generated.

The SC generation **807** may occur in the relatively short lengths of fiber that follow the pump laser. The SC fiber length may range from around a few millimeters to 100 m or more. In one embodiment, the SC generation may occur in a first fiber **808** where the modulational-instability initiated pulse break-up occurs primarily, followed by a second fiber **809** where the SC generation and spectral broadening occurs primarily.

In one embodiment, one or two meters of standard single-mode fiber (SMF) after the power amplifier stage may be followed by several meters of SC generation fiber. For this example, in the SMF the peak power may be several kilowatts and the pump light may fall in the anomalous group-velocity dispersion regime—often called the soliton regime. For high peak powers in the anomalous dispersion regime, the nanosecond pulses may be unstable due to a phenomenon known as modulational instability, which is basically parametric amplification in which the fiber nonlinearity helps to phase match the pulses. As a consequence, the nanosecond pump pulses may be broken into many shorter pulses as the modulational instability tries to form soliton pulses from the quasi-continuous-wave background. Although the laser diode and amplification process starts with approximately nanosecond-long pulses, modulational instability in the short length of SMF fiber may form approximately 0.5 ps to several-picosecond-long pulses with high intensity. Thus, the few meters of SMF fiber may result in an output similar to that produced by mode-locked lasers, except in a much simpler and cost-effective manner.

The short pulses created through modulational instability may then be coupled into a nonlinear fiber for SC generation. The nonlinear mechanisms leading to broadband SC may include four-wave mixing or self-phase modulation along with the optical Raman effect. Since the Raman effect is self-phase-matched and shifts light to longer wavelengths by emission of optical photons, the SC may spread to longer wavelengths very efficiently. The short-wavelength edge may arise from four-wave mixing, and often times the short wavelength edge may be limited by increasing group-velocity dispersion in the fiber. In many instances, if the particular fiber used has sufficient peak power and SC fiber length, the SC generation process may fill the long-wavelength edge up to the transmission window.

Mature fiber amplifiers for the power amplifier stage **806** include ytterbium-doped fibers (near 1060 nm), erbium-doped fibers (near 1550 nm), erbium/ytterbium-doped fibers (near 1550 nm), or thulium-doped fibers (near 2000 nm). In various embodiments, candidates for SC fiber **809** include fused silica fibers (for generating SC between 0.8-2.7 μm), mid-IR fibers such as fluorides, chalcogenides, or tellurites (for generating SC out to 4.5 μm or longer), photonic crystal fibers (for generating SC between 0.4 and 1.7 μm), or combinations of these fibers. Therefore, by selecting the appropriate fiber-amplifier doping for **806** and nonlinear fiber **809**, SC may be generated in the visible, near-IR/SWIR, or mid-IR wavelength region.

The configuration **800** of FIG. **8** is just one particular example, and other configurations can be used and are intended to be covered by this disclosure. For example, further gain stages may be used, and different types of lossy elements or fiber taps may be used between the amplifier stages. In another embodiment, the SC generation may occur partially in the amplifier fiber and in the pig-tails from the pump combiner or other elements. In yet another embodiment, polarization maintaining fibers may be used, and a polarizer may also be used to enhance the polarization contrast between amplifier stages. Also, not discussed in detail are many accessories that may accompany this set-up, such as driver electronics, pump laser diodes, safety shut-offs, and thermal management and packaging.

In one embodiment, one example of the SC laser that operates in the SWIR is illustrated in FIG. **9**. This SWIR SC source **900** produces an output of up to approximately 5 W over a spectral range of about 1.5 to 2.4 microns, and this particular laser is made out of polarization maintaining components. The seed laser **901** is a distributed feedback (DFB) laser operating near 1542 nm producing approximately 0.5 nsec pulses at an about 8 MHz repetition rate. The pre-amplifier **902** is forward pumped and uses about 2 m length of erbium/ytterbium cladding pumped fiber **903** (often also called dual-core fiber) with an inner core diameter of 12 microns and outer core diameter of 130 microns. The pre-amplifier gain fiber **903** is pumped using a 10 W laser diode near 940 nm **905** that is coupled in using a fiber combiner **904**.

In this particular 5 W unit, the mid-stage between amplifier stages **902** and **906** comprises an isolator **907**, a band-pass filter **908**, a polarizer **909** and a fiber tap **910**. The power amplifier **906** uses an approximately 4 m length of the 12/130 micron erbium/ytterbium doped fiber **911** that is counter-propagating pumped using one or more 30 W laser diodes near 940 nm **912** coupled in through a combiner **913**. An approximately 1-2 meter length of the combiner pig-tail helps to initiate the SC process, and then a length of PM-1550 fiber **915** (polarization maintaining, single-mode, fused silica fiber optimized for 1550 nm) is spliced **914** to the combiner output.

If an output fiber of about 10 m in length is used, then the resulting output spectrum **1000** is shown in FIG. **10**. The details of the output spectrum **1000** depend on the peak power into the fiber, the fiber length, and properties of the fiber such as length and core size, as well as the zero dispersion wavelength and the dispersion properties. For example, if a shorter length of fiber is used, then the spectrum actually reaches to longer wavelengths (e.g., a 2 m length of SC fiber broadens the spectrum to about 2500 nm). Also, if extra-dry fibers are used with less O—H content, then the wavelength edge may also reach to a longer wavelength. To generate more spectra toward the shorter wavelengths, the pump wavelength (in this case ~1542 nm) should be close to the zero dispersion wavelength in the fiber. For example, by using a dispersion shifted fiber or so-called non-zero dispersion shifted fiber, the short wavelength edge may shift to shorter wavelengths.

In one particular embodiment, the SWIR-SC light source of FIG. **9** with output spectrum in FIG. **10** was used in preliminary experiments for examining the reflectance from different dental samples. A schematic of the experimental set-up **1100** for measuring the diffuse reflectance spectroscopy is illustrated in FIG. **11**A. The SC source **1101** in this embodiment was based on the design of FIG. **9** and delivered approximately 1.6 W of light over the wavelength range from about 1500-2400 nm. The output beam **1102** was collimated, and then passed through a chopper **1103** (for lock-in detection at the receiver after the spectrometer **1106**) and an aperture **1104** for localizing the beam on the tooth location. Different teeth **1105** with different lesions and caries were placed in front of the aperture **1104**, and the scattered light was passed through a spectrometer **1106** and collected on a detector, whose signal was sent to a receiver. The tooth samples **1105** were mounted in clay or putty for standing upright. Different types of teeth could be used, including molars, premolars, canine and incisor teeth.

FIG. **11**B shows exemplary reflectance spectra **1150** from a sound enamel region **1151** (e.g., without dental caries), an enamel lesion region **1152**, and a dentine lesion region **1153** of various teeth. The spectra are normalized to have equal value near 2050 nm. In this particular embodiment, the slope from the sound enamel **1151** is steepest between about 1500 and 1950 nm, with a lesser slope in the presence of an enamel lesion **1152**. When there is a sample with dentine lesion **1153**, more features appear in the spectrum from the presence of water absorption lines from water that collects in the dentine. For this experiment, the spectra **1151**, **1152**, and **1153** are flatter in the wavelength region between about 1950 nm and 2350 nm. These are preliminary results, but they show the benefit of using broadband sources such as the SWIR-SC source for diagnosing dental caries. Although the explanation behind the different spectra **1150** of FIG. **11**B may not be understood as yet, it is clear that the spectra **1151**, **1152** and **1153** are distinguishable. Therefore, the broadband reflectance may be used for detection of dental caries and analyzing the region of the caries. Although diffuse reflectance has been used in this experiment, other signals, such as transmission, reflectance or a combination, may also be used and are covered by this disclosure.

Although one particular example of a 5 W SWIR-SC has been described, different components, different fibers, and different configurations may also be used consistent with this disclosure. For instance, another embodiment of the similar configuration **900** in FIG. **9** may be used to generate high powered SC between approximately 1060 and 1800 nm. For this embodiment, the seed laser **901** may be a distributed feedback laser diode of about 1064 nm, the pre-amplifier gain fiber **903** may be a ytterbium-doped fiber amplifier with 10/125 microns dimensions, and the pump laser **905** may be a 10 W laser diode near 915 nm. A mode field adapter may be including in the mid-stage, in addition to the isolator **907**, band pass filter **908**, polarizer **909** and tap **910**. The gain fiber **911** in the power amplifier may be an about 20 m length of ytterbium-doped fiber with 25/400 microns dimension. The pump **912** for the power amplifier may be up to six pump diodes providing 30 W each near 915 nm. For this much pump power, the output power in the SC may be as high as 50 W or more.

In an alternate embodiment, it may be desirous to generate high power SWIR SC over 1.4-1.8 microns and separately 2-2.5 microns (the window between 1.8 and 2 microns may be less important due to the strong water and atmospheric absorption). For example, the SC source of FIG. **12**A can lead to bandwidths ranging from about 1400 nm to 1800 nm or broader, while the SC source of FIG. **12**B can lead to bandwidths ranging from about 1900 nm to 2500 nm or broader. Since these wavelength ranges are shorter than about 2500 nm, the SC fiber can be based on fused silica fiber. Exemplary SC fibers include standard single-mode fiber (SMF), high-nonlinearity fiber, high-NA fiber, dispersion shifted fiber, dispersion compensating fiber, and photonic crystal fibers. Non-fused-silica fibers can also be used for SC generation, including chalcogenides, fluorides, ZBLAN, tellurites, and germanium oxide fibers.

In one embodiment, FIG. **12**A illustrates a block diagram for an SC source **1200** capable of generating light between approximately 1400 nm and 1800 nm or broader. As an example, a pump fiber laser similar to FIG. **9** can be used as the input to a SC fiber **1209**. The seed laser diode **1201** can comprise a DFB laser that generates, for example, several milliwatts of power around 1542 nm or 1553 nm. The fiber pre-amplifier **1202** can comprise an erbium-doped fiber amplifier or an erbium/ytterbium doped double clad fiber. In this example, a mid-stage amplifier **1203** can be used, which can comprise an erbium/ytterbium doped double-clad fiber. A bandpass filter **1205** and isolator **1206** may be used between the pre-amplifier **1202** and mid-stage amplifier **1203**. The power amplifier stage **1204** can comprise a larger core size erbium/ytterbium doped double-clad fiber, and another bandpass filter **1207** and isolator **1208** can be used before the power amplifier **1204**. The output of the power amplifier can be coupled to the SC fiber **1209** to generate the SC output **1210**. This is just one exemplary configuration for an SC source, and other configurations or elements may be used consistent with this disclosure.

In yet another embodiment, FIG. **12**B illustrates a block diagram for an SC source **1250** capable of generating light between approximately 1900 and 2500 nm or broader. As an example, the seed laser diode **1251** can comprise a DFB or DBR laser that generates, for example, several milliwatts of power around 1542 nm or 1553 nm. The fiber pre-amplifier **1252** can comprise an erbium-doped fiber amplifier or an erbium/ytterbium doped double-clad fiber. In this example, a mid-stage amplifier **1253** can be used, which can comprise an erbium/ytterbium doped double-clad fiber. A bandpass filter **1255** and isolator **1256** may be used between the pre-amplifier **1252** and mid-stage amplifier **1253**. The power amplifier stage **1254** can comprise a thulium doped double-clad fiber, and another isolator **1257** can be used before the power amplifier **1254**. Note that the output of the mid-stage amplifier **1253** can be approximately near 1542 nm, while the thulium-doped fiber amplifier **1254** can amplify wavelengths longer than approximately 1900 nm and out to about 2100 nm. Therefore, for this configuration wavelength shifting may be required between 1253 and 1254. In one embodiment, the wavelength shifting can be accomplished using a length of standard single-mode fiber **1258**, which can have a length between approximately 5 and 50 meters, for example. The output of the power amplifier **1254** can be coupled to the SC fiber **1259** to generate the SC output **1260**. This is just one exemplary configuration for an SC source, and other configurations or elements can be used consistent with this disclosure. For example, the various amplifier

stages can comprise different amplifier types, such as erbium doped fibers, ytterbium doped fibers, erbium/ytterbium co-doped fibers and thulium doped fibers.

FIG. **12**C illustrates a reflection-spectroscopy based stand-off detection system having an SC laser source. The set-up **1270** for the reflection-spectroscopy-based stand-off detection system includes an SC source **1271**. First, the diverging SC output is collimated to a 1 cm diameter beam using a 25 mm focal length, 90 degrees off-axis, gold coated, parabolic mirror **1272**. To reduce the effects of chromatic aberration, refractive optics are avoided in the setup. All focusing and collimation is done using metallic mirrors that have almost constant reflectivity and focal length over the entire SC output spectrum. The sample **1274** is kept at a distance from the collimating mirror **1272**, which provides a total round trip path length of twice the distance before reaching the collection optics **1275**. A 12 cm diameter silver coated concave mirror **1275** with a 75 cm focal length is kept 20 cm to the side of the collimation mirror **1272**. The mirror **1275** is used to collect a fraction of the diffusely reflected light from the sample, and focus it into the input slit of a monochromator **1276**. Thus, the beam is incident normally on the sample **1274**, but detected at a reflection angle of $\tan^{-1}(0.2/5)$ or about 2.3 degrees. Appropriate long wavelength pass filters mounted in a motorized rotating filter wheel are placed in the beam path before the input slit **1276** to avoid contribution from higher wavelength orders from the grating (300 grooves/mm, 2 μm blaze). The output slit width is set to 2 mm corresponding to a spectral resolution of 10.8 nm, and the light is detected by a 2 mm×2 mm liquid nitrogen cooled (77K) indium antimonide (InSb) detector **1277**. The detected output is amplified using a trans-impedance pre-amplifier **1277** with a gain of about 105 V/A and connected to a lock-in amplifier **1278** setup for high sensitivity detection. The chopper frequency is 400 Hz, and the lock-in time constant is set to 100 ms corresponding to a noise bandwidth of about 1 Hz. These are exemplary elements and parameter values, but other or different optical elements may be used consistent with this disclosure.

While the above detection systems could be categorized as single path detection systems, it may be advantageous in some cases to use multi-path detection systems. In one embodiment, a detection system from a Fourier transform infrared spectrometer, FTIR, may be used. The received light may be incident on a particular configuration of mirrors, called a Michelson interferometer, that allows some wavelengths to pass through but blocks others due to wave interference. The beam may be modified for each new data point by moving one of the mirrors, which changes the set of wavelengths that pass through. This collected data is called an interferogram. The interferogram is then processed, typically on a computing system, using an algorithm called the Fourier transform. One advantageous feature of FTIR is that it may simultaneously collect spectral data in a wide spectral range.

Another advantage of using the near-infrared or SWIR is that most drug packaging materials are at least partially transparent in this wavelength range, so that drug compositions may be detected and identified through the packaging non-destructively. As an example, SWIR light could be used to see through plastics, since the signature for plastics can be subtracted off and there are large wavelength windows where the plastics are transparent. Because of the hydrocarbon bonds, there are absorption features near 1.7 microns and 2.2-2.5 microns. In general, the absorption bands in the near infrared are due to overtones and combination bands for various functional group vibrations, including signals from

C—H, O—H, C═O, N—H, —COOH, and aromatic C—H groups. It may be difficult to assign an absorption band to a specific functional group due to overlapping of several combinations and overtones. However, with advancements in computational power and chemometrics or multivariate analysis methods, complex systems may be better analyzed. In one embodiment, using software analysis tools the absorption spectrum may be converted to its second derivative equivalent. The spectral differences may permit a fast, accurate, non-destructive and reliable identification of materials. Although particular derivatives are discussed, other mathematical manipulations may be used in the analysis, and these other techniques are also intended to be covered by this disclosure.

In yet another example of multi-beam detection systems, a dual-beam set-up **1280** such as in FIG. **12**D may be used to subtract out (or at least minimize the adverse effects of) light source fluctuations. In one embodiment, the output from an SC source **1281** may be collimated using a CaF2 lens **1282** and then focused into the entrance slit of the monochromator **1283**. At the exit slit, light at the selected wavelength is collimated again and may be passed through a polarizer **1284** before being incident on a calcium fluoride beam splitter **1285**. After passing through the beam splitter **1285**, the light is split into a sample **1286** and reference **1287** arm to enable ratiometric detection that may cancel out effects of intensity fluctuations in the SC source **1281**. The light in the sample arm **1286** passes through the sample of interest and is then focused onto a HgCdTe detector **1288** connected to a pre-amp. A chopper **1282** and lock-in amplifier **1290** setup enable low noise detection of the sample arm signal. The light in the reference arm **1287** passes through an empty container (cuvette, gas cell etc.) of the same kind as used in the sample arm. A substantially identical detector **1289**, pre-amp and lock-in amplifier **1290** is used for detection of the reference arm signal. The signal may then be analyzed using a computer system **1291**. This is one particular example of a method to remove fluctuations from the light source, but other components may be added and other configurations may be used, and these are also intended to be covered by this disclosure.

Although particular examples of detection systems have been described, combinations of these systems or other systems may also be used, and these are also within the scope of this disclosure. As one example, environmental fluctuations (such as turbulence or winds) may lead to fluctuations in the beam for active remote sensing or hyperspectral imaging. A configuration such as FIG. **12**D may be able to remove the effect of environmental fluctuations. Yet another technique may be to "wobble" the light beam after the light source using a vibrating mirror. The motion may lead to the beam moving enough to wash out spatial fluctuations within the beam waist at the sample or detection system. If the vibrating mirror is scanned faster than the integration time of the detectors, then the spatial fluctuations in the beam may be integrated out. Alternately, some sort of synchronous detection system may be used, where the detection is synchronized to the vibrating frequency.

By use of an active illuminator, a number of advantages may be achieved, such as higher signal-to-noise ratios. For example, one way to improve the signal-to-noise ratio would be to use modulation and lock-in techniques. In one embodiment, the light source may be modulated, and then the detection system would be synchronized with the light source. In a particular embodiment, the techniques from lock-in detection may be used, where narrow band filtering around the modulation frequency may be used to reject noise outside the modulation frequency. In an alternate embodiment, change detection schemes may be used, where the detection system captures the signal with the light source on and with the light source off. Again, for this system the light source may be modulated. Then, the signal with and without the light source is differenced. This may enable the sun light changes to be subtracted out. In addition, change detection may help to identify objects that change in the field of view. In the following some exemplary detection systems are described.

One advantage of the SC lasers illustrated in FIGS. **8**, **9**, and **12** is that they may use all-fiber components, so that the SC laser can be all-fiber, monolithically integrated with no moving parts. The all-integrated configuration can consequently be robust and reliable.

FIGS. **8**, **9**, and **12** are examples of SC light sources that may advantageously be used for SWIR light generation in various medical and dental diagnostic and therapeutic applications. However, many other versions of the SC light sources may also be made that are intended to also be covered by this disclosure. For example, the SC generation fiber could be pumped by a mode-locked laser, a gain-switched semiconductor laser, an optically pumped semiconductor laser, a solid state laser, other fiber lasers, or a combination of these types of lasers. Also, rather than using a fiber for SC generation, either a liquid or a gas cell might be used as the nonlinear medium in which the spectrum is to be broadened.

Even within the all-fiber versions illustrated such as in FIG. **9**, different configurations could be used consistent with the disclosure. In an alternate embodiment, it may be desirous to have a lower cost version of the SWIR SC laser of FIG. **9**. One way to lower the cost could be to use a single stage of optical amplification, rather than two stages, which may be feasible if lower output power is required or the gain fiber is optimized. For example, the pre-amplifier stage **902** might be removed, along with at least some of the mid-stage elements. In yet another embodiment, the gain fiber could be double passed to emulate a two stage amplifier. In this example, the pre-amplifier stage **902** might be removed, and perhaps also some of the mid-stage elements. A mirror or fiber grating reflector could be placed after the power amplifier stage **906** that may preferentially reflect light near the wavelength of the seed laser **901**. If the mirror or fiber grating reflector can transmit the pump light near 940 nm, then this could also be used instead of the pump combiner **913** to bring in the pump light **912**. The SC fiber **915** could be placed between the seed laser **901** and the power amplifier stage **906** (SC is only generated after the second pass through the amplifier, since the power level may be sufficiently high at that time). In addition, an output coupler may be placed between the seed laser diode **901** and the SC fiber, which now may be in front of the power amplifier **906**. In a particular embodiment, the output coupler could be a power coupler or divider, a dichroic coupler (e.g., passing seed laser wavelength but outputting the SC wavelengths), or a wavelength division multiplexer coupler. This is just one further example, but a myriad of other combinations of components and architectures could also be used for SC light sources to generate SWIR light that are intended to be covered by this disclosure.

Wireless Link to the Cloud

The non-invasive dental caries measurement device may also benefit from communicating the data output to the "cloud" (e.g., data servers and processors in the web remotely connected) via wireless means. The non-invasive devices may be part of a series of biosensors applied to the patient, and collectively these devices form what might be called a body area network or a personal area network. The biosensors and non-invasive devices may communicate to a smart phone, tablet, personal data assistant, computer and/or other microprocessor-based device, which may in turn wirelessly or over wire and/or fiber optic transmit some or all of the signal or processed data to the internet or cloud. The cloud or internet may in turn send the data to dentists, doctors or health care providers as well as the patients themselves. Thus, it may be possible to have a panoramic, high-definition, relatively comprehensive view of a patient that doctors and dentists can use to assess and manage disease, and that patients can use to help maintain their health and direct their own care.

In a particular embodiment **1300**, the non-invasive measurement device **1301** may comprise a transmitter **1303** to communicate over a first communication link **1304** in the body area network or personal area network to a receiver in a smart phone, tablet, cell phone, PDA, and/or computer **1305**, for example. For the measurement device **1301**, it may also be advantageous to have a processor **1302** to process some of the measured data, since with processing the amount of data to transmit may be less (hence, more energy efficient). The first communication link **1304** may operate through the use of one of many wireless technologies such as Bluetooth, Zigbee, WiFi, IrDA (infrared data association), wireless USB, or Z-wave, to name a few. Alternatively, the communication link **1304** may occur in the wireless medical band between 2360 MHz and 2390 MHz, which the FCC allocated for medical body area network devices, or in other designated medical device or WMTS bands. These are examples of devices that can be used in the body area network and surroundings, but other devices could also be used and are included in the scope of this disclosure.

The personal device **1305** may store, process, display, and transmit some of the data from the measurement device **1301**. The device **1305** may comprise a receiver, transmitter, display, voice control and speakers, and one or more control buttons or knobs and a touch screen. Examples of the device **1305** include smart phones such as the Apple iPhones® or phones operating on the Android or Microsoft systems. In one embodiment, the device **1305** may have an application, software program, or firmware to receive and process the data from the measurement device **1301**. The device **1305** may then transmit some or all of the data or the processed data over a second communication link **1306** to the internet or "cloud" **1307**. The second communication link **1306** may advantageously comprise at least one segment of a wireless transmission link, which may operate using WiFi or the cellular network. The second communication link **1306** may additionally comprise lengths of fiber optic and/or communication over copper wires or cables.

The internet or cloud **1307** may add value to the measurement device **1301** by providing services that augment the measured data collected. In a particular embodiment, some of the functions performed by the cloud include: (a) receive at least a fraction of the data from the device **1305**; (b) buffer or store the data received; (c) process the data using software stored on the cloud; (d) store the resulting processed data; and (e) transmit some or all of the data either upon request or based on an alarm. As an example, the data or processed data may be transmitted **1308** back to the originator (e.g., patient or user), it may be transmitted **1309** to a health care provider or doctor or dentist, or it may be transmitted **1310** to other designated recipients.

Service providers coupled to the cloud **1307** may provide a number of value-add services. For example, the cloud application may store and process the dental data for future reference or during a visit with the dentist or healthcare provider. If a patient has some sort of medical mishap or emergency, the physician can obtain the history of the dental or physiological parameters over a specified period of time. In another embodiment, alarms, warnings or reminders may be delivered to the user **1308**, the healthcare provider **1309**, or other designated recipients **1310**. These are just some of the features that may be offered, but many others may be possible and are intended to be covered by this disclosure. As an example, the device **1305** may also have a GPS sensor, so the cloud **1307** may be able to provide time, date, and position along with the dental or physiological parameters. Thus, if there is a medical or dental emergency, the cloud **1307** could provide the location of the patient to the dental or healthcare provider **1309** or other designated recipients **1310**. Moreover, the digitized data in the cloud **1307** may help to move toward what is often called "personalized medicine." Based on the dental or physiological parameter data history, medication or medical/dental therapies may be prescribed that are customized to the particular patient. Another advantage for commercial entities may be that by leveraging the advances in wireless connectivity and the widespread use of handheld devices such as smart phones that can wirelessly connect to the cloud, businesses can build a recurring cost business model even using non-invasive measurement devices.

Described herein are just some examples of the beneficial use of near-infrared or SWIR lasers for non-invasive measurements of dental caries and early detection of carious regions. However, many other dental or medical procedures can use the near-infrared or SWIR light consistent with this disclosure and are intended to be covered by the disclosure.

Although the present disclosure has been described in several embodiments, a myriad of changes, variations, alterations, transformations, and modifications may be suggested to one skilled in the art, and it is intended that the present disclosure encompass such changes, variations, alterations, transformations, and modifications as falling within the spirit and scope of the appended claims.

While exemplary embodiments are described above, it is not intended that these embodiments describe all possible forms of the disclosure. Rather, the words used in the specification are words of description rather than limitation, and it is understood that various changes may be made without departing from the spirit and scope of the disclosure. Additionally, the features of various implementing embodiments may be combined to form further embodiments of the disclosure. While various embodiments may have been described as providing advantages or being preferred over other embodiments with respect to one or more desired characteristics, as one skilled in the art is aware, one or more characteristics may be compromised to achieve desired system attributes, which depend on the specific application and implementation. These attributes include, but are not limited to: cost, strength, durability, life cycle cost, marketability, appearance, packaging, size, serviceability, weight, manufacturability, ease of assembly, etc. The embodiments described herein that are described as less desirable than other embodiments or prior art implementations with respect to one or more characteristics are not outside the scope of the disclosure and may be desirable for particular applications.

What is claimed is:

1. A wearable device, comprising:

a measurement device including a light source comprising a plurality of light emitting diodes (LEDs) for measuring one or more physiological parameters, the measurement device configured to generate, by modulating at least one of the LEDs having an initial light intensity, an optical beam having a plurality of optical wavelengths, wherein at least a portion of the optical beam includes a near-infrared wavelength between 700 nanometers and 2500 nanometers;

the measurement device comprising one or more lenses configured to receive and to deliver at least a portion of the optical beam to tissue, wherein the tissue reflects at least a portion of the optical beam delivered to the tissue;

the measurement device further comprising a receiver, the receiver having a plurality of spatially separated detectors and one or more analog to digital converters coupled to the spatially separated detectors, the one or more analog to digital converters configured to generate at least two receiver outputs, the receiver configured to:

capture light while the LEDs are off and convert the captured light into a first signal and

capture light while at least one of the LEDs is on and to convert the captured light into a second signal, the captured light including at least a portion of the optical beam reflected from the tissue;

the measurement device configured to improve a signal-to-noise ratio of the optical beam reflected from the tissue by differencing the first signal and the second signal and by differencing the two receiver outputs;

the measurement device configured to further improve the signal-to-noise ratio of the optical beam reflected from the tissue by increasing the light intensity relative to the initial light intensity from at least one of the LEDs;

the measurement device further configured to generate an output signal representing at least in part a non-invasive measurement on blood contained within the tissue, wherein the output signal is generated at least in part by using a Fourier transform of signals from the receiver including at least one of the first and second signals and signals from the at least two receiver outputs; and

wherein the receiver further comprises one or more spectral filters positioned in front of at least some of the plurality of spatially separated detectors.

2. The wearable device of claim 1, wherein the measurement device is adapted to be placed on a wrist of a user.

3. The wearable device of claim 1, wherein the measurement device is adapted to be placed on an ear of a user.

4. The wearable device of claim 1, wherein

the wearable device is configured to communicate with a smart phone or tablet, the smart phone or tablet comprising a wireless receiver, a wireless transmitter, a display, a voice input module, a speaker, and a touch screen, the smart phone or tablet configured to receive and to process at least a portion of the output signal, wherein the smart phone or tablet is configured to store and display the processed output signal, wherein at least a portion of the processed output signal is configured to be transmitted over a wireless transmission link.

5. The wearable device of claim 1, wherein the receiver is configured to be synchronized to the modulation of the at least one of the LEDs.

6. The wearable device of claim 1, wherein the receiver is located a first distance from a first one of the LEDs and a different distance from a second one of the LEDs such that the receiver can capture a third signal from the first LED and a fourth signal from the second LED, and wherein the output signal is generated in part by comparing the third and fourth signals.

7. The wearable device of claim 1, wherein at least one LED emits at a first wavelength and at least another LED emits at a second wavelength, and wherein the first wavelength has a first penetration depth into the tissue and wherein the second wavelength has a second penetration depth into the tissue different from the first penetration depth, and wherein the output signal is generated in part by comparing the reflected light at the first wavelength with the reflected light at the second wavelength.

8. A wearable device, comprising:

a measurement device including a light source comprising a plurality of light emitting diodes (LEDs) for measuring one or more physiological parameters, the measurement device configured to generate, by modulating at least one of the LEDs having an initial light intensity, an optical beam having a plurality of optical wavelengths, wherein at least a portion of the plurality of optical wavelengths is a near-infrared wavelength between 700 nanometers and 2500 nanometers;

the measurement device comprising one or more lenses configured to receive and to deliver a portion of the optical beam to tissue, wherein the tissue reflects at least a portion of the optical beam delivered to the tissue, and wherein the measurement device is adapted to be placed on a wrist or an ear of a user;

the measurement device further comprising a receiver, the receiver having a plurality of spatially separated detectors and one or more analog to digital converters coupled to the spatially separated detectors, the one or more analog to digital converters configured to generate at least two receiver outputs;

the measurement device configured to improve a signal-to-noise ratio of the optical beam reflected from the tissue by differencing the two receiver outputs;

the measurement device configured to further improve the signal-to-noise ratio of the optical beam reflected from the tissue by increasing the light intensity relative to the initial light intensity from at least one of the LEDs;

the measurement device further configured to generate an output signal representing at least in part a non-invasive measurement on blood contained within the tissue, wherein the output signal is generated at least in part by using a Fourier transform of a signal resulting from differencing signals from the at least two receiver outputs; and

wherein the receiver further comprises one or more spectral filters positioned in front of at least some of the plurality of spatially separated detectors.

9. The wearable device of claim 8, wherein at least one LED emits at a first wavelength and at least another LED emits at a second wavelength, and wherein the first wavelength has a first penetration depth into the tissue and wherein the second wavelength has a second penetration depth into the tissue different from the first penetration depth.

10. The wearable device of claim 9, wherein the output signal is generated in part by comparing the reflected light at the first wavelength with the reflected light at the second wavelength.

11. The wearable device of claim **8**, wherein the receiver is further configured to:

capture light while the LEDs are off and convert the captured light into a first signal and

capture light while at least one of the LEDs is on and convert the captured light into a second signal, the captured light including at least a portion of the optical beam reflected from the tissue;

the measurement device configured to further improve a the signal-to-noise ratio of the optical beam reflected from the tissue by differencing the first signal and the second signal.

12. The wearable device of claim **8**, wherein

the wearable device is configured to communicate with a smart phone or tablet, the smart phone or tablet comprising a wireless receiver, a wireless transmitter, a display, a voice input module, a speaker, and a touch screen, the smart phone or tablet configured to receive and to process at least a portion of the output signal, wherein the smart phone or tablet is configured to store and display the processed output signal, wherein at least a portion of the processed output signal is configured to be transmitted over a wireless transmission link.

13. The wearable device of claim **8**, wherein the receiver is configured to be synchronized to the modulation of the at least one of the LEDs.

14. The wearable device of claim **8**, wherein the receiver is located a first distance from a first one of the LEDs and a different distance from a second one of the LEDs such that the receiver can capture a third signal from the first LED and a fourth signal from the second LED, and wherein the output signal is generated in part by comparing the third and fourth signals.

15. A wearable device, comprising:

a measurement device including a light source comprising a plurality of light emitting diodes (LEDs) for measuring one or more physiological parameters, the measurement device configured to generate, by modulating at least one of the LEDs having an initial light intensity, an optical beam having a plurality of optical wavelengths, wherein at least a portion of the plurality of optical wavelengths is a near-infrared wavelength between 700 nanometers and 2500 nanometers;

the measurement device comprising one or more lenses configured to receive and to deliver a portion of the optical beam to tissue, wherein the tissue reflects at least a portion of the optical beam delivered to the tissue, and wherein the measurement device is adapted to be placed on a wrist or an ear of a user;

the measurement device further comprising a receiver, the receiver having a plurality of spatially separated detectors and one or more analog to digital converters coupled to the spatially separated detectors, the one or more analog to digital converters configured to generate at least two receiver outputs, the receiver configured to:

capture light while the LEDs are off and convert the captured light into a first signal and

capture light while at least one of the LEDs is on and convert the captured light into a second signal, the captured light including at least a portion of the optical beam reflected from the tissue;

the measurement device configured to improve a signal-to-noise ratio of the optical beam reflected from the tissue by differencing the first signal and the second signal and by differencing the two receiver outputs;

the measurement device configured to further improve the signal-to-noise ratio of the optical beam reflected from the tissue by increasing the light intensity relative to the initial light intensity from at least one of the LEDs;

the measurement device further configured to generate an output signal representing at least in part a non-invasive measurement on blood contained within the tissue, wherein the output signal is generated at least in part by using a Fourier transform of signals from the receiver including at least one of the first and second signals and signals from the at least two receiver outputs; and

wherein the receiver further comprises one or more spectral filters positioned in front of at least some of the plurality of spatially separated detectors.

16. The wearable device of claim **15**, wherein at least one LED emits at a first wavelength and at least another LED emits at a second wavelength, and wherein the first wavelength has a first penetration depth into the tissue and wherein the second wavelength has a second penetration depth into the tissue different from the first penetration depth.

17. The wearable device of claim **16**, wherein the output signal is generated in part by comparing the reflected light at the first wavelength with the reflected light at the second wavelength.

18. The wearable device of claim **15**, wherein the receiver is configured to be synchronized to the modulating of the at least one of the LEDs.

19. The wearable device of claim **15**, wherein the receiver is located a first distance from a first one of the LEDs and a different distance from a second one of the LEDs such that the receiver can capture a third signal from the first LED and a fourth signal from the second LED, and wherein the output signal is generated in part by comparing the third and fourth signals.

* * * * *

EXHIBIT B

US009861286B1

(12) **United States Patent**
Islam

(10) **Patent No.: US 9,861,286 B1**
(45) **Date of Patent: *Jan. 9, 2018**

(54) **SHORT-WAVE INFRARED SUPER-CONTINUUM LASERS FOR EARLY DETECTION OF DENTAL CARIES**

(71) Applicant: **OMNI MEDSCI, INC.**, Ann Arbor, MI (US)

(72) Inventor: **Mohammed N. Islam**, Ann Arbor, MI (US)

(73) Assignee: **Omni Medsci, Inc.**, Ann Arbor, MI (US)

(*) Notice: Subject to any disclaimer, the term of this patent is extended or adjusted under 35 U.S.C. 154(b) by 0 days.

This patent is subject to a terminal disclaimer.

(21) Appl. No.: **15/686,198**

(22) Filed: **Aug. 25, 2017**

Related U.S. Application Data

(63) Continuation of application No. 15/357,136, filed on Nov. 21, 2016, now Pat. No. 9,757,040, which is a
(Continued)

(51) **Int. Cl.**
G01J 3/00 (2006.01)
A61B 5/00 (2006.01)
(Continued)

(52) **U.S. Cl.**
CPC ***A61B 5/0088*** (2013.01); ***A61B 5/0013*** (2013.01); ***A61B 5/0022*** (2013.01);
(Continued)

(58) **Field of Classification Search**
CPC G01J 3/02; G01J 3/28; G01J 3/42; G01N 21/31; G01N 21/552
(Continued)

(56) **References Cited**

U.S. PATENT DOCUMENTS

4,063,106	A	12/1977	Ashkin et al.
4,158,750	A	6/1979	Sakoe et al.

(Continued)

FOREIGN PATENT DOCUMENTS

DE	102010012987	A1	10/2010
EP	1148666		10/2001

(Continued)

OTHER PUBLICATIONS

Istepanian, Robert H., "The Comparative Performance of Mobile Telemedical Systems based on the IS-54 and GSM Cellular Telephone Standards"; Journal of Telemedicine and Telecare 1999; pp. 97-104.

(Continued)

Primary Examiner — Tarifur Chowdhury
Assistant Examiner — Md M Rahman
(74) *Attorney, Agent, or Firm* — Brooks Kushman P.C.

(57) **ABSTRACT**

A wearable device for use with a smart phone or tablet includes LEDs for measuring physiological parameters by modulating the LEDs and generating a near-infrared multi-wavelength optical beam. At least one LED emits at a first wavelength having a first penetration depth and at least another LED emits at a second wavelength having a second penetration depth into tissue. The device includes lenses that deliver the optical beam to the tissue, which reflects the first and second wavelengths. A receiver is configured to capture light while the LEDs are off and while at least one of the LEDs is on and to difference corresponding signals to improve a signal-to-noise ratio of the optical beam reflected from the tissue. The signal-to-noise ratio is further increased by increasing light intensity of at least one of the LEDs. The device generates an output signal representing a non-invasive measurement on blood within the tissue.

20 Claims, 18 Drawing Sheets

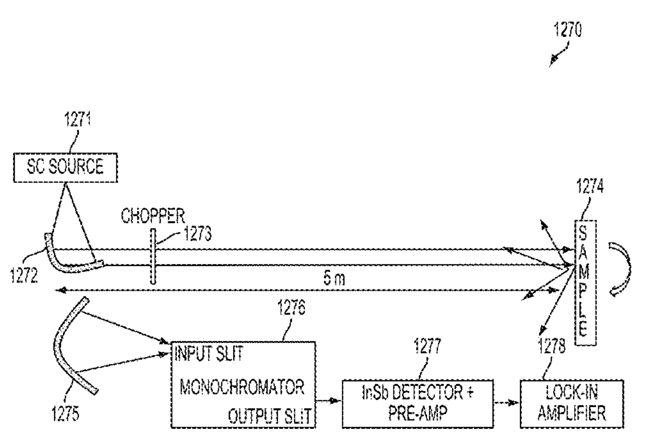

Related U.S. Application Data

continuation of application No. 14/651,367, filed as application No. PCT/US2013/075736 on Dec. 17, 2013, now Pat. No. 9,500,635.

(60) Provisional application No. 61/747,477, filed on Dec. 31, 2012.

(51) **Int. Cl.**

G01N 33/49	(2006.01)
G01N 33/44	(2006.01)
G01N 33/15	(2006.01)
G01N 33/02	(2006.01)
G01N 21/88	(2006.01)
G01N 21/3563	(2014.01)
G01N 21/359	(2014.01)
G01J 3/453	(2006.01)
A61B 5/145	(2006.01)
A61B 5/1455	(2006.01)
H01S 3/30	(2006.01)
G01N 21/39	(2006.01)
G01M 3/38	(2006.01)
G01J 3/28	(2006.01)
G01J 3/10	(2006.01)
G01J 3/18	(2006.01)
G01J 3/14	(2006.01)

(52) **U.S. Cl.**

CPC ***A61B 5/0075*** (2013.01); ***A61B 5/0086*** (2013.01); ***A61B 5/1455*** (2013.01); ***A61B 5/14532*** (2013.01); ***A61B 5/14546*** (2013.01); ***A61B 5/4547*** (2013.01); ***G01J 3/108*** (2013.01); ***G01J 3/28*** (2013.01); ***G01J 3/2823*** (2013.01); ***G01J 3/453*** (2013.01); ***G01N 21/359*** (2013.01); ***G01N 21/3563*** (2013.01); ***G01N 21/39*** (2013.01); ***G01N 21/88*** (2013.01); ***G01N 33/02*** (2013.01); ***G01N 33/15*** (2013.01); ***G01N 33/442*** (2013.01); ***G01N 33/49*** (2013.01); *A61B 2562/0233* (2013.01); *A61B 2562/0238* (2013.01); *A61B 2562/146* (2013.01); *A61B 2576/02* (2013.01); *G01J 3/14* (2013.01); *G01J 3/1838* (2013.01); *G01J 2003/104* (2013.01); *G01J 2003/2826* (2013.01); *G01M 3/38* (2013.01); *G01N 2021/399* (2013.01); *G01N 2201/061* (2013.01); *G01N 2201/062* (2013.01); *G01N 2201/08* (2013.01); *G01N 2201/12* (2013.01); *H01S 3/302* (2013.01)

(58) **Field of Classification Search**

USPC 356/300

See application file for complete search history.

(56) **References Cited**

U.S. PATENT DOCUMENTS

4,221,997	A	9/1980	Flemming
4,275,266	A	6/1981	Lasar
4,374,618	A	2/1983	Howard
4,403,605	A	9/1983	Tanikawa
4,462,080	A	7/1984	Johnstone et al.
4,516,207	A	5/1985	Moriyama et al.
4,523,884	A	6/1985	Clement et al.
4,605,080	A	8/1986	Lemelson
4,641,292	A	2/1987	Tunnell et al.
4,704,696	A	11/1987	Reimer et al.
4,728,974	A	3/1988	Nio et al.
4,762,455	A	8/1988	Coughlan et al.
4,776,016	A	10/1988	Hansen
4,958,910	A	9/1990	Taylor et al.
4,989,253	A	1/1991	Liang et al.
5,078,140	A	1/1992	Kwoh
5,084,880	A	1/1992	Esterowitz et al.
5,086,401	A	2/1992	Glassman et al.
5,134,620	A	7/1992	Huber
5,142,930	A	9/1992	Allen et al.
5,180,378	A	1/1993	Kung et al.
5,191,628	A	3/1993	Byron
5,218,655	A	6/1993	Mizrahi
5,230,023	A	7/1993	Nakano
5,246,004	A	9/1993	Clarke et al.
5,267,152	A	11/1993	Yang et al.
5,267,256	A	11/1993	Saruwatari et al.
5,267,323	A	11/1993	Kimura
5,300,097	A	4/1994	Lerner et al.
5,303,148	A	4/1994	Mattson et al.
5,305,427	A	4/1994	Nagata
5,313,306	A	5/1994	Kuban et al.
5,323,404	A	6/1994	Grubb
5,345,538	A	9/1994	Narayannan et al.
5,400,165	A	3/1995	Gnauck et al.
5,408,409	A	4/1995	Glassman et al.
5,458,122	A	10/1995	Hethuin
5,544,654	A	8/1996	Murphy et al.
5,572,999	A	11/1996	Funda et al.
5,617,871	A	4/1997	Burrows
5,631,758	A	5/1997	Knox et al.
5,687,734	A	11/1997	Dempsey et al.
5,695,493	A	12/1997	Nakajima et al.
5,696,778	A	12/1997	MacPherson
5,704,351	A	1/1998	Mortara et al.
5,718,234	A	2/1998	Warden et al.
5,747,806	A	5/1998	Khalil
5,748,103	A	5/1998	Flach et al.
5,792,204	A	8/1998	Snell
5,812,978	A	9/1998	Nolan
5,855,550	A	1/1999	Lai et al.
5,862,803	A	1/1999	Besson et al.
5,867,305	A	2/1999	Waarts et al.
5,912,749	A	6/1999	Harstead et al.
5,944,659	A	8/1999	Flach et al.
5,950,629	A	9/1999	Taylor et al.
5,957,854	A	9/1999	Besson et al.
5,970,457	A	10/1999	Brant et al.
6,014,249	A	1/2000	Fermann et al.
6,043,927	A	3/2000	Islam
6,115,673	A	9/2000	Malin
6,185,535	B1	2/2001	Hedin et al.
6,200,309	B1	3/2001	Rice et al.
6,224,542	B1	5/2001	Chang et al.
6,246,707	B1	6/2001	Yin et al.
6,246,896	B1	6/2001	Dumoulin
6,273,858	B1	8/2001	Fox et al.
6,278,975	B1	8/2001	Brant et al.
6,281,471	B1	8/2001	Smart
6,285,897	B1	9/2001	Kilcoyne
6,289,238	B1	9/2001	Besson et al.
6,301,271	B1	10/2001	Sanders et al.
6,301,273	B1	10/2001	Sanders et al.
6,333,803	B1	12/2001	Kurotori et al.
6,337,462	B1	1/2002	Smart
6,340,806	B1	1/2002	Smart et al.
6,350,261	B1	2/2002	Domankevitz et al.
6,364,834	B1	4/2002	Reuss et al.
6,374,006	B1	4/2002	Islam et al.
6,381,391	B1	4/2002	Islam et al.
6,402,691	B1	6/2002	Peddicord et al.
6,407,853	B1	6/2002	Samson et al.
6,436,107	B1	8/2002	Wang et al.
6,441,747	B1	8/2002	Khair et al.
6,442,430	B1	8/2002	Ferek-Petric
6,443,890	B1	9/2002	Schulze et al.
6,450,172	B1	9/2002	Hartlaub et al.
6,453,201	B1	9/2002	Daum et al.
6,454,705	B1	9/2002	Cosentino et al.
6,458,120	B1	10/2002	Shen et al.
6,462,500	B1	10/2002	L'Hegarat et al.
6,463,361	B1	10/2002	Wang et al.

(56) **References Cited**

U.S. PATENT DOCUMENTS

6,480,656	B1	11/2002	Islam et al.
6,512,936	B1	1/2003	Monfre
6,534,012	B1	3/2003	Hazen et al.
6,549,702	B2	4/2003	Islam et al.
6,567,431	B2	5/2003	Tabirian et al.
6,587,702	B1	7/2003	Ruchti
6,603,910	B2	8/2003	Islam et al.
6,605,080	B1	8/2003	Altshuler et al.
6,611,643	B2	8/2003	Birk
6,625,180	B2	9/2003	Bufetov et al.
6,631,025	B2	10/2003	Islam et al.
6,640,117	B2	10/2003	Makarewicz
6,659,947	B1	12/2003	Carter et al.
6,659,999	B1	12/2003	Anderson et al.
6,738,652	B2	5/2004	Mattu
6,760,148	B2	7/2004	Islam
6,773,922	B2	8/2004	Jeng
6,788,965	B2	9/2004	Ruchti
6,802,811	B1	10/2004	Slepian
6,816,241	B2	11/2004	Grubisic
6,847,336	B1	1/2005	Lemelson
6,864,978	B1	3/2005	Hazen
6,885,498	B2	4/2005	Islam
6,885,683	B1	4/2005	Fermann et al.
6,943,936	B2	9/2005	Islam et al.
6,990,364	B2	1/2006	Ruchti
7,010,336	B2	3/2006	Lorenz
7,027,467	B2	4/2006	Baev et al.
7,060,061	B2	6/2006	Altshuler et al.
7,133,710	B2	11/2006	Acosta
7,167,300	B2	1/2007	Fermann et al.
7,209,657	B1	4/2007	Islam
7,233,816	B2	6/2007	Blank
7,259,906	B1	8/2007	Islam
7,263,288	B1	8/2007	Islam
7,294,105	B1	11/2007	Islam
7,299,080	B2	11/2007	Acosta
7,317,938	B2	1/2008	Lorenz
7,318,909	B2	1/2008	Lehmann et al.
7,356,364	B1	4/2008	Bullock et al.
7,395,158	B2	7/2008	Monfre
7,433,116	B1	10/2008	Islam
7,519,253	B2	4/2009	Islam
7,519,406	B2	4/2009	Blank
7,620,674	B2	11/2009	Ruchti
7,697,966	B2	4/2010	Monfre
7,787,503	B2	8/2010	Wadsworth
7,787,924	B2	8/2010	Acosta
7,800,818	B2	9/2010	Mattsson
7,807,718	B2	10/2010	Hashim
8,000,574	B2	8/2011	Buchter
8,145,286	B2	3/2012	Arai
8,180,422	B2	5/2012	Rebec
8,472,108	B2	6/2013	Islam
9,207,121	B2	12/2015	Adler
2002/0013518	A1	1/2002	West et al.
2002/0019584	A1	2/2002	Schulze et al.
2002/0032468	A1	3/2002	Hill et al.
2002/0082612	A1	6/2002	Moll et al.
2002/0109621	A1	8/2002	Khair et al.
2002/0115914	A1	8/2002	Russ
2002/0128846	A1	9/2002	Miller
2002/0178003	A1	11/2002	Gehrke et al.
2003/0022126	A1	1/2003	Buchalla
2003/0107739	A1	6/2003	Lehmann et al.
2003/0109055	A1	6/2003	Lehmann et al.
2003/0152307	A1	8/2003	Drasek et al.
2004/0174914	A1	9/2004	Fukatsu
2004/0240037	A1	12/2004	Harter
2005/0111500	A1	5/2005	Harter et al.
2005/0133691	A1	6/2005	Doppke et al.
2006/0223032	A1	10/2006	Fried
2006/0245461	A1	11/2006	Islam
2006/0268393	A1	11/2006	Islam
2006/0283931	A1	12/2006	Polli et al.
2007/0021670	A1	1/2007	Mandelis et al.
2007/0078348	A1	4/2007	Holman
2008/0105665	A1	5/2008	Kondo
2009/0028193	A1	1/2009	Islam
2009/0204110	A1	8/2009	Islam
2010/0046067	A1	2/2010	Fermann et al.
2010/0322490	A1	12/2010	Pan
2010/0331637	A1	12/2010	Ting
2011/0143364	A1	6/2011	Kim
2011/0267688	A1	11/2011	Kleppe et al.
2011/0282167	A1	11/2011	Ridder et al.
2012/0013722	A1	1/2012	Wong
2012/0239013	A1	9/2012	Islam
2013/0274569	A1	10/2013	Islam
2013/0327966	A1	12/2013	Fidler et al.
2014/0078510	A1	3/2014	Rubio Guivernau et al.

FOREIGN PATENT DOCUMENTS

WO	9715240		5/1997
WO	9749340		12/1997
WO	0115959		7/2001
WO	200189362		11/2001
WO	200227640		4/2002
WO	200228123		4/2002
WO	2005013843	A2	2/2005
WO	2007061772	A2	5/2007
WO	2009130464	A1	10/2009
WO	2013012938		1/2013

OTHER PUBLICATIONS

Aris, Ishak Bin, “An Internet-Based Blood Pressure Monitoring System for Patients”; Journal of Telemedicine and Telecare 2001; pp. 51-53.

Sun, Y., C.F. Booker, S. Kumari, R.N. Day, M. Davidson, A. Periasamy, “Characterization of an orange acceptor fluorescent protein for sensitized spectral fluorescence resonant energy transfer microscopy using a white-light laser,” Journal of Biomedical Optics, vol. 14, No. 5, paper 054009 (2009).

Borlinghaus, R., “Colours Count: how the challenge of fluorescence was solved in confocal microscopy,” in Modern Research and Educational Topics in Microscopy, A. Mendez-Vilas and J. Diaz, eds, pp. 890-899, Formatex (2007).

Borlinghaus, R., “The White Confocal: Continuous Spectral Tuning in Excitation and Emission,” in Optical Fluorescence Microscopy, A. Diaspro (Ed), Chapter 2, pp. 37-54, ISBN 978-3-642-15174-3, Springer-Verlag, Berlin (2011).

Borlinghaus, R.T., L. Kuschel, “White Light Laser: The Ultimate Source for Confocal Microscopy,” http://www.leica-microsystems.com/science-lab/white-light-laser (Jun. 27, 2012).

Ziegler, U., A.G. Bittermann, M. Hoechli, “Introduction to Confocal Laser Scanning Microscopy (LEICA),” www.zmb.unizh.ch, May 29, 2013.

Ooi ET, Zhang XQ, Chen JH, Soh PH, Ng K, Yea JH, “Non-invasive glucose measurement using multiple laser diodes,” Optical Diagnostic and Sensing VII, edited by Gerard L. Cote, Alexander V. Priezzhev, Proc. of SPIE vol. 6445, 64450K , (2007).

Schulz, I., J. Putzger, A. Niklas, M. Brandt, A. Jager, A. Hardt, S. Knorzer, K.A. Hiller, S. Loffler, G. Schmalz, S.N. Danilov, S. Giglberger, M. Hirmer, S.D. Ganichev, G. Monkman, “PPG signal acquisition and analysis on in vitro tooth model for dental pulp vitality assessment,” ARC Submission 16, (2012).

Drexler, C., Hirmer, M., Danilov, S., Giglberger, S., Putzger, J., Niklas, A., Jager, A., Hiller, K., Loffler, S., Schmalz, G., Redlich, B., Schulz, I., Monkman, G., Ganichev, S. “Infrared spectroscopy for clinical diagnosis of dental pulp vitality.” Infrared, Millimeter, and Terahertz Waves (IRMMW-THz), 2012 37th International Conference on. IEEE (2012).

Hirmer, Marion, Danilov, Sergey, Giglberger, Stephan, Putzger, Jurgen, Niklas, Andreas, Jager, Andreas, Hiller, Karl-Anton, Loffler, Susanne, Schmalz, Gottfried, Redlich, Britta, Schulz, Irene, Monkman, Gareth, Ganichev, Sergey. “Spectroscopic Study of Human Teeth and Blood from Visible to Terahertz Frequencies for Clinical Diagnosis of Dental Pulp Vitality.” Journal of Infrared, Millimeter, and Terahertz Waves 33.3 (2012): 366-375.

(56) **References Cited**

OTHER PUBLICATIONS

Na, J, J.H. Baek, S.Y. Ryu, C. Lee, B.H. Lee, "Tomographic imaging of incipient dental-caries using optical coherence tomography and comparison with various modalities," ●ptical Review, vol. 16, No. 4, pp. 426-431 (2●●9).

Robert S. Jones et al.; Near-Infrared Transillumination At 131●-nm for the Imaging of Early Dental Decay; vol. 11, No. 18; ●ptics Express 2259; Sep. 8, 2●●3.

Extended European Search Report for European Application No. 13867892.5 dated Jul. 22, 2●16.

Extended European Search Report for European Application No. 13867874.3 dated Jul. 15, 2●16.

Vinay V. Alexander et al.; Modulation Instability High Power All-Fiber Supercontinuum Lasers and Their Applications; ●ptical Fiber Technology 18; 2●12; pp. 349-374.

Final ●ffice Action dated ●ct. 21, 2●16 for U.S. Appl. No. 14/875,7●9.

International Search Report and Written ●pinion for International Application No. PCT/US2●13/●75736 dated Apr. 7, 2●14.

International Preliminary Report on Patentability for International Application No. PCT/US2●13/●75736 dated Jul. 9, 2●15.

Hori, Takashi, et al., "Flatly broadened, wideband and low noise supercontinuum generation in highly nonlinear hybrid fiber", ●ptics Express, vol. 12, No. 2, Jan. 26, 2●●4, pp. 317-324.

Wadsworth, W. J., et al., "Supercontinuum and four-wave mixing with ●-switched pulses in endlessly single-mode photonic crystal fibres", ●ptics Express, vol. 12, No. 2, Jan. 26, 2●●4, pp. 299-3●9.

Hilligsoe, Karen Marie, et al., "Supercontinuum generation in a photonic crystal fiber with two zero dispersion wavelengths", ●ptics Express, vol. 12, No. 6, Mar. 22, 2●●4, pp. 1●45-1●54.

Venugopalan, V., "●ptical Society of America Biomed Topical Meeting Tutorial on Tissue ●ptics", Apr. 27, 2●●4, pp. 1-32.

Slusher, Richart E., et al., "Large Raman gain and nonlinear phase shifts in high-purity As2So3 chalcogenide fibers", J. ●pt. Soc. Am. B, vol. 21, No. 6, Jun. 2●●4, pp. 1146-1155.

Leon-Saval, S. G., et al., "Supercontinuum generation in submicron fibre waveguides", ●ptics Express, vol. 12, No. 13, Jun. 28, 2●●4, pp. 2864-2869.

Nicholson, J. W., et al., "High power, single mode, all-fiber source of femtosecond pulses at 155● nm and its use in supercontinuum generation", ●ptics Express, vol. 12, No. 13, Jun. 28, 2●●4, pp. 3●25-3●34.

Genty, G., et al., "Enhanced bandwidth of supercontinuum generated m microstructured fibers", ●ptics Express, vol. 12, No. 15, Jul. 26, 2●●4, pp. 3471-348●.

Champert, Pierre-Alain, et al., "White-light supercontinuum generation in normally lispersive optical fiber using original multi-wavelength pumping system", ●ptics Express, vol. 12, No. 19, Sep. 2●, 2●●4, pp. 4366-4371.

Nicholson, J. W., "Supercontinuum generation in ultraviolet-irradiated fibers", ●ptics Letters, vol. 29, No. 2●, ●ct. 15, 2●●4, pp. 2363-2365.

Hori, Takashi, et al., "Experimental and numerical analysis of widely broadened supercontinuum generation in highly nonlinear dispersion-shifted fiber with a femtosecond pulse", J. ●pt. Soc. Am. B, vol. 21, No. 11, Nov. 2●●4, pp. 1969-198●.

Demircan, Ayhan, et al., "Supercontinuum generation by the modulation instability", ●ptics Communications 244, 2●●5, pp. 181-185.

Papemyi, S. B., et al., "Sixth-●rder Cascaded Raman Amplification", ●FC/NF●EC, 2●●5, 3 pages.

Tanaka, Keiji, "●ptical nonlinearity in photonic glasses", Journal of Materials Science: Materials in Electronics 16, 2●●5, pp. 633-643.

Westbrook, Paul S., "Improved Supercontinuum Generation Through UV Processing of Highly Nonlinear Fibers", Journal of Lightwave Technology, vol. 23, No. 1, Jan. 2●●5, pp. 13-18.

Abeeluck, Akheelesh K., et al., "Continuous-wave pumping in the anomalous- and normal dispersion regimes of nonlinear fibers for supercontinuum generation", ●ptics Letters, vol. 3●, No. 1, Jan. 1, 2●●5, pp. 61-63.

Kutz, J. Nathan, et al., "Enhanced Supercontinuum Generation through Dispersion-Management", ●ptics Express, vol. 13, No. 11, May 3●, 2●●5, pp. 3989-3998.

Lee, Ju Han, et al., "Experimental performance comparison for various continuous-wave supercontinuum schemes: ring cavity and single pass structures", ●ptics Express, vol. 13, No. 13, Jun. 27, 2●●5, pp. 4848-4853.

Saliminia, A., et al., "Ultra-broad and coherent white light generation in silica glass by focused femtosecond pulses at 1.5pm", ●ptics Express, vol. 13, No. 15, Jul. 25, 2●●5, pp. 5731-5738.

Takushima, Yuichi, High average power, depolarized super-continuum generation using a 1.55-um ASE noise source, ●ptics Express, vol. 13, No. 15, Jul. 25, 2●●5, pp. 5871.-5877.

Travers, J. C., et al., "Extended continuous-wave supercontinuum generation in a low-water-loss holey fiber", ●ptics Letters, vol. 3●, No. 15, Aug. 1, 2●●5, pp. 1938-194●.

Kobtsev, Serguei M., et al., "Modelling of high-power supercontinuum generation in highly nonlinear, dispersion shifted fibers at CW pump", ●ptics Express, vol. 13, No. 18, Sep. 5, 2●●5, pp. 6912-6918.

Falk, Peter, et al., "Supercontinuum generation in a photonic crystal fiber with two zero-dispersion wavelengths tapered to normal dispersion at all wavelengths", ●ptics Express, vol. 13, No. 19, Sep. 19, 2●●5, pp. 7535-754●.

Tombelaine, Vincent, et al., "Ultra wide band supercontinuum generation in air-silica holey fibers by SHG-induced modulation instabilities", ●ptics Express, vol. 13, No. 19, Sep. 19, 2●●5, pp. 7399-74●4.

Hazen, K.H., M.A. Arnold, G.W. Small, "Measurement of glucose and other analytes in undiluted human serum with near-infrared transmission spectroscopy," Analytica Chimica Acta, vol. 371, pp. 255-267 (1998).

Malin, S.F., T.L. Ruchti, T.L. Blank, S.N. Thennadil, S.L. Monfre, "Noninvasive prediction of glucose by near-infrared diffuse reflectance spectroscopy," Clinical Chemistry, vol. 45, No. 9, pp. 1651-1658 (1999).

Thennadil, S.N., J.L. Rennert, B.J. Wenzel, K.H. Hazen, T.L. Ruchti, M.B. Block, "Comparison of glucose concentration in interstitial fluid, and capillary and venous blood during rapid changes in blood glucose levels," Diabetes Technology & Therapeutics, vol. 3, No. 3, pp. 357-365 (2●●1).

Troy, T.L., S.N. Thennadil, "●ptical properties of human skin in the near infrared wavelength range of 1●●● to 22●●nm," Journal of Biomedical ●ptics, vol. 6, No. 2, pp. 167-176, (2●●1).

Blank, T.B., T.L. Ruchti, A.D. Lorenz, S.L. Monfre, M.R. Makarewicz, M. Mattu, K.H. Hazen, "Clinical results from a non-invasive blood glucose monitor," ●ptical Diagnostics and Sensing of Biological Fluids and Glucose and Cholesterol Monitoring II, A.V. Priezzhev and G.L. Cote, Editors, Proceedings of SPIE, vol. 4624, pp. 1●19 (2●●2).

Yeh, S-J, C.F. Hanna, ●.S. Khalil, "Monitoring blood glucose changes in cutaneous tissue by temperature-modulated localized reflectance measurements," Clinical Chemistry, vol. 49, No. 6, pp. 924-934 (2●●3).

Marbach, R., T. Koschinsky, F.A. Gries, H.M. Heise, "Noninvasive blood glucose assay by near-infrared diffuse reflectance spectroscopy of the human inner lip," Applied Spectroscopy, vol. 47, No. 7, pp. 875-881 (1993).

Enejder, A.M.K., T.G. Scecina, J. ●h, M. Hunter, W.C. Shih, S. Sasic, G.L. Horowitz, M.S. Feld, "Raman spectroscopy for noninvasive glucose measurements," Journal of Biomedical ●ptics, vol. 1●, No. 3, ●31114 (2●●5).

●lesberg, J.T., L. Liu, V.V. Zee, M.A. Arnold, "In vivo near-infrared spectroscopy of rat skin tissue with varying blood glucose levels," Analytic Chemistry, vol. 78, No. 1, pp. 215-223 (2●●6).

●lesberg, J.T., M.A. Arnold, C. Mermelstein, J. Schmitz, J. Wagner, "Tunable laser diode system for noninvasive blood glucose measurements," Applied Spectroscopy, vol. 59, No. 12, pp. 148●-1484 (2●●5).

Harman-Boehm, I. A. Gal, A.M. Raykhman, J.D. Zahn, E. Naidis, Y. Mayzel, "Noninvasive glucose monitoring: a novel approach," Journal of Diabetes Science and Technology, vol. 3, No. 2 pp. 253-26● (2●●9).

(56) **References Cited**

OTHER PUBLICATIONS

Kim-K.D. G.S. Son, S.S. Lim, S.S. Lee, "Measurement of glucose level exploiting a relative optical absorption at discrete probe wavelengths," Japanese Journal of Applied Physics, vol. 48, ●77●●1 (2●●9).
Smith, J.L., "The Pursuit of Noninvasive Glucose: Hunting the Deceitfil Turkey," 2nd Edition, pp. 1-141 (2●11).
Pezzaniti, J.L., T.W. Jeng, L. McDowell, G.M. ●osta, "Preliminary investigation of near-infrared spectroscopic measurements of urea, creatinine, glucose, protein and ketone in urine," Clinical Biochemistry, vol. 34, pp. 239-246 (2●●1).
Lussi, A., R. Hibst, R. Paulus, "Diagnodent: An optical method for caries detection," Journal of Dental Research, vol. 83, special issue C, pp. C8●-C83 (2●●4).
Reese, E.L, E.E. Fisher, D.A. Horowitz, "Photoelectric densitometry of the circulation of the human dental pulp," The Journal of the Baltimore College of Dental Surgery, vol. 26, No. 1, pp. 6-18 (1971).
Zakian, C., I. Pretty, R. Ellwood, "Near-infrared hyperspectral imaging of teeth for dental caries detection," Journal of Biomedical ●ptics, vol. 16, No. 6, ●64●47 (2●●9).
Belikov, A.V., A.V. Skripnik, K.V. Shatilova, "Study of the dynamics of the absorption spectra of human tooth enamel and dentine under heating and ablation by submillisecond pulse radiation of an erbium laser with a generation wavelength of 2.79 um," ●ptics and Spectroscopy, vol. 1●9, No. 2, pp. 211-216 (2●1●).
Karlsson, L. "Caries detection methods based on changes in optical properties between healthy and carious issue," International Journal of Dentistry, vol. 2●1●, Article ID 27●729, 9 pages (2●1●).
Fried, D. M. Staninec, C.L. Darling, "Near-infrared imaging of dental decay at 131●nm," Journal of Laser Dentistry, vol. 18, No. 1, pp. 8-16 (2●1●).
Burmen, M. P. Usenik, A. Fidler, F. Pernus, B. Likar, "A construction of standardized near infrared hyper-spectral teeth database—a first step in the development of reliable diagnostic tool for quantification and early detection of caries," Lasers in Dentistry XVII, edited by P. Rechmann, D. Fried, Proceedings of SPIE, vol. 7884, Paper 7884●E (2●11).
Maia, A., L. Karlsson, W. Margulis, A. Gomes, "Evaluation of two imaging techniques: near-infrared transillumination and dental radiographs for the detection of early approximal enamel caries," Dentomaxillofacial Radiology, vol. 4●, pp. 429-433 (2●11).
Chung, S., D. Fried, M. Staninec, C.L. Darling, "Multispectral near-IR reflectance and transillumination imaging of teeth," Biomedical ●ptics Express, vol. 2, No. 1●, pp. 28●4-2814 (2●11).
Chung, S., D. Fried, M. Staninec, C.L. Darling, "Near infrared imaging of teeth at wavelengths between 12●● and 16●●nm," Proceedings of the Society of Photo ●ptical Instrument Engineering, paper 7884 (2●11).
Staninec, M., S.M. Douglas, C.L. Darling, K. Chan, H. Kang, R. C. Lee, D. Fried, "Nondestructive clinical assessment of occlusal caries lesions using near-IR imaging methods," Lasers in Surgery and Medicine, vol. 43, No. 1●, pp. 951-959 (2●11).
Nishizawa, N., "Generation and application of high-quality supercontinuum sources," ●ptical Fiber Technology, vol. 18, pp. 394-4●2 (2●12).
Islam, M. N., et al., "Broad bandwidths from frequency-shifting solitons in fibers", ●ptics Letters, vol. 14, No. 7, Apr. 1, 1989, pp. 37●-372.
Islam, M. N., et al., "Femtosecond distributed soliton spectrum in fibers", J. ●pt. Soc. Am. B, vol. 6, No. 6, Jun. 1989, pp. 1149-1158.
Busse, Lynda E., et al., "Design Parameters for Fluoride Multimode Fibers", Journal of Lightwave Technology, vol. 9, No. 7, Jul. 1991, pp. 828-831.
Wuthrich, Stefan, et al., "●ptical damage thresholds at 2.94 um in fluoride glass fibers", Applied ●ptics, vol. 31, No. 27, Sep. 2●, 1992, pp. 5833-5837.
Inoue, H., et al., "Computer simulation of the vibrational spectra and properties of fluoride glasses based on ZrF4", Journal of Non-Crystalline Solids, vol. 161, 1993, pp. 118-122.
Mizunami, Toru, et al., "Gain saturation characteristics of Raman amplification in silica and fluoride glass optical fibers", ●ptics Communications 97, 1993, pp. 74-78.
Desthieux, B., et al., "111 kW (●. 5 mJ) pulse amplification at 1.5 um using a gated cascade of three erbium-doped fiber amplifiers," Appl. Phys. Lett. vol. 63, Aug. 2, 1993, pp. 586-588.
Edwards, Glenn, et al., "Tissue ablation by a free-electron laser tuned to the amide II band", Nature, vol. 371, Sep. 29, 1994, pp. 416-419.
Borrelli, N. F., et al., "Resonant and non-resonant effects in photonic glasses", Journal of Non-Crystalline Solids 185, 1995, pp. 1●9-122.
Asobe, Masaki, et al., "Third-order nonlinear spectroscopy in As2S3 chalcogenide glass fibers", J. Appl. Phys. 77 (11), Jun. 1, 1995, pp. 5518-5523.
Jarman, Richard H., "Novel optical fiber lasers", Current ●pinion in Solid State and Materials Science, 1996, pp. 199-2●3.
Iatridis, James C., et al., "Is the Nucleus Pulposus a Solid or a Fluid? Mechanical Behaviors of the Nucleus Pulposus of the Human Intervertebral Disc", Spine, vol. 21(1●), May 15, 1996, pp. 1174-1184.
Asobe, Masaki, "Nonlinear ●ptical Properties of Chalcogenide Glass Fibers and Their Application to All-●ptical Switching", ●ptical Fiber Technology, vol. 3, Article No. ●F97●214, 1997, pp. 142-148.
Smektala, F., et al., "Chalcogenide glasses with large non-linear refractive indices", Journal of Non-Crystalline Solids 239, 1998, pp. 139-142.
Hamilton, James D., et al., "High Frequency Ultrasound Imaging with ●ptical Arrays", IEEE Transactions on Ultrasonics, Ferroelectrics, and Frequency Control, vol. 45, No. 1, Jan. 1998, pp. 216-235.
Hamilton, James D., et al., "High Frequency Ultrasound Imaging Using an Active ●ptical Detector", IEEE Transactions on Ultrasonics, Ferroelectrics, and Frequency Control, vol. 15, No. 3, May 1998, pp. 719-727.
Nowak, G. A., et al., "Low-power high-efficiency wavelength conversion based on modulational instability in high-nonlinearity fiber," ●ptics Letters, vol. 23, No. 12, Jun. 15, 1998, pp. 936-938.
Cardinal, T., et al., "Non-linear optical properties of chalcogenide glasses in the system As-S-Se", Journal of Non-Crystalline Solids 256 & 257, 1999, pp. 353-36●.
Lucas, Jacques, "Infrared glasses", Current ●pinion in Solid State & Materials Science 4, 1999. pp. 181-187.
Sanghera, J. S., et al., Active and passive chalcogenide glass optical fibers for IR applications: a review, Journal of Non-Crystalline Solids 256 & 257, 1999, pp. 6-16.
Nishida, Yoshiki, et al., "Reliability of Fluoride Fiber Module for ●ptical Amplifier Use", IEEE Photonics Technology Letters, vol. 11, No. 12, Dec. 1999, pp. 1596-1598.
Nowak, George A., et al., "Stable supercontinuum generation in short lengths of conventional dispersion-shifted fiber", Applied ●ptics, vol. 38, No. 36, Dec. 2●, 1999, pp. 7364-7369.
Urban, J. P. G., et al., "The Nucleus of the Intervertebral Disc from Development to Degeneration" Amer. Zool., vol. 4●, 2●●●, pp. 53-61.
Hamilton, James D., et al., "High Frequency ●ptoacoustic Arrays Using Etalon Detection", IEEE Transactions on Ultrasonics, Ferroelectrics, and Frequency Control, vol. 47, No. 1, Jan. 2●●●, pp. 16●-169.
Ranka, Jinendra K., et al., "Visible continuum generation in air-silica microstructure optical fibers with anomalous dispersion at 8●● nm", ●ptics Letters, vol. 25, No. 1, Jan. 1, 2●●●, pp. 25-27.
Boult, Maggi, et al., "Systematic Review of Percutaneous Endoscopic Laser Discectomy: Update and Re-appraisal", Australian Safety and Efficacy Register of New Interventional Procedures—Surgical Report No. 5, Feb. 2●●●, 49 pages.
Boult, Maggi, et aL, "Percutaneous Endoscopic Laser Discectomy", Systematic Review, Aust. N.Z.J. Surg., vol. 7●, Apr. 7, 2●●●, pp. 475-479.
Camacho, Nancy P., et al., "FTIR Microscopic Imaging of Collagen and Proteoglycan in Bovine Cartilage," Biopolymers (Biospectroscopy), vol. 62, 2●●1, pp. 1-8.

(56) **References Cited**

OTHER PUBLICATIONS

Choi, Joon Y., et al, "Thermal, Mechanical, ●ptical, and Morphologic Changes in Bovine Nucleus Pulposus Induced by Nd:YAG (λ=1.32 um) Laser Irradiation", Lasers in Surgery and Medicine, vol. 28, 2●●1, pp. 248-254.

Hafez, M. I., et al., "The Effect of Irrigation on Peak Temperatures in Nerve Root, Dura, and Intervertebral Disc During Laser-Assisted Foraminoplasty", Lasers in Surgery and Medicine, vol. 29, 2●●1, pp. 33-37.

Jackson, Stuart D., et al., "Theory and numerical simulation of nth-order cascaded Raman fiber lasers", J. ●pt. Soc. Am. B, vol. 18, No. 9, Sep. 2●●1, pp. 1297-13●6.

Werle, Peter, et al., "Near- and mid-infrared laser-optical sensors for gas analysis", ●ptics and Lasers in Engineering 37, 2●●2, pp. 1●1-114.

Beck, Mattias, et al., "Continuous Wave ●peration of a Mid-Infrared Semiconductor Laser at Room Temperature," Science vol. 295, www.sciencemag.org, Jan. 11, 2●●2, pp. 3●1-3●5.

Harbold, J. M., et al., "Highly nonlinear As—S—Se glasses for all-optical switching", ●ptics Letters, vol. 27, No. 2, Jan. 15, 2●●2, pp. 119-121.

Coen, Stephane, et al., "Supercontinuum generation by stimulated Raman scattering and parametric four-wave mixing in photonic crystal fibers", J. ●pt. Soc. Am. B, vol. 19, No. 4, Apr. 2●●2, pp. 753-764.

Dudley, John M., et al., "Supercontinuum generation in air-silica microstructured fibers with nanosecond and femtosecond pulse pumping", J. ●pt. Soc. Am. B, vol. 19, No. 4, Apr. 2●●2, pp. 765-771.

Harbold, Jeffrey M., et al., "Highly Nonlinear Ge—As—Se and. Ge—As—S—Se Glasses for All-●ptical Switching", IEEE Photonics Technology Letters, vol. 14, No. 6, Jun. 2●●2, pp. 822-824.

Husakou, Anton V., et al, "Supercontinuum generation, four-wave mixing, and fission of iigher-order solitons in photonic-crystal fibers", J. ●pt. Soc. Am. B, vol. 19, No. 9, Sep. 2●●2, pp. 2171-2182.

Wadsworth, William J., et al., "Supercontinuum generation in photonic crystal fibers and optical fiber tapers: a novel light source", J. ●pt. Soc. Am. B, vol. 19, No. 9, Sep. 2●●2, pp. 2148-2155.

Kumar, V.V. Ravi Kanth, et al, "Extruded soft glass photonic crystal fiber for ultrabroad supercontinuum generation", ●ptics Express, vol. 1●, No. 25, Dec. 16, 2●●2, pp. 152●-1525.

Edwards, Glenn S., et al., "Advantage of the Mark-III FEL for biophysical research and biomedical applications", J. Synchrotron Rad. vol. 1●, 2●●3, pp. 354-357.

Nicholson, J. W., et al., "Pulsed and continuous-wave supercontinuum generation in highly nonlinear, dispersion-shifted fibers", Applied Physics B 77, 2●●3, pp. 211-218.

Sobol, Emil, et al., "Time-resolved, light scattering measurements of cartilage and cornea denaturation due to free electron laser radiation", Journal of Biomedical ●ptics, vol. 8, No. 2, Apr. 2●●3, pp. 216-222.

Nicholson, J. W., et al., "All-fiber, octave-spanning supercontinuum", ●ptics Letters, vol. 28, No. 8, Apr. 15, 2●●3, pp. 643-645.

Faralli, S., et al., "Impact of Double Rayleigh Scattering Noise in Distributed Higher ●rder Raman Pumping Schemes", IEEE Photonics Technology Letters, vol. 15, No. 6, Jun. 2●●3, pp. 8●4-8●6.

"New and Emerging Techniques—Surgical, Rapid Review, Laser Discectomy", Australian Safety and Efficacy Register of New Interventional Procedures—Surgical, Jun. 2●●3, 12 pages.

Avdokhin, A. V., et al, "Continuous-wave, high-power, Raman continuum generation in holey fibers", ●ptics Letters, vol. 28, No. 15, Aug. 1, 2●●3, pp. 1353-1355.

Mussot, Arnaud, et al., "Generation of a broadband single-mode supercontinuum in a conventional dispersion-shifted fiber by use of a subnanosecond microchip laser", ●ptics Letters, vol. 28, No. 19, ●ct. 1, 2●●3, pp. 182●-1822.

Slusher, Richard, et al., "Highly nonlinear composite chalcogenide/polymer fibers", ●SA 2●●4, 1 page.

Thongtrangan, Issada, et al., "Minimally invasive spinal surgery: a historical perspective", Neurosurg. Focus, vol. 16, Article 13, Jan. 2●●4, pp. 1-1●.

Lee, Ju Han, et al., "Continuous-wave supercontinuum laser based on an erbium-doped fiber ring cavity incorporating a highly nonlinear optical fiber", ●ptics Letters, vol. 3●, No. 19, ●ct. 1, 2●●5, pp. 2599-26●1.

Genty, G., et al., "Supercontinuum generation in large mode-area microstructured fibers", ●ptics Express, vol. 13, No. 21, ●ct. 17, 2●●5, pp. 8625-8633.

Schreiber, T., et al., "Supercontinuum generation by femtosecond single and dual wavelength pumping in photonic crystal fibers with two zero dispersion wavelengths", ●ptics Express, vol. 13, No. 23, Nov. 14, 2●●5, pp. 9556-9569.

Travers, J. C., et al., "Extended blue supercontinuum generation in cascaded holey fibers", ●ptics Letters, vol. 3●, No. 23, Dec. 1, 2●●5, pp. 3132-3134.

Hagen, C. L., et al., "Generation of a Continuum Extending to the Midinfrared by Pumping ZBLAN Fiber With an Ultrafast 155●-nm Source", IEEE Photonics Technology Letters, vol. 18, No. 1, Jan. 1, 2●●6, pp. 91-93.

Moon, Sucbei, et al., "Generation of octave-spanning supercontinuum with 155●-nm amplified diode-laser pulses and a dispersion-shifted fiber", ●ptics Express, vol. 14, No. 1, Jan. 9, 2●●6, pp. 27●-278.

Fedotova, ●., et al., "Supercontinuum generation in planar rib waveguides enabled by anomalous dispersion", ●ptics Express, vol. 14, No. 4, Feb. 2●, 2●●6, pp. 1512-1517.

Harrington, James A., "Infrared Fiber ●ptics", ●SA Handbook, vol. III, white paper, to be published by McGraw Hill, Undated, 13 pages.

Aaviksoo, J., et al., "●bservation of optical precursors at pulse propagation in GaAs", Physical Review A, vol. 44, No. 9, Nov. 1, 1991, pp. R5353-R5356.

Boppart, Stephen A., et al., "Imaging developing neural morphology using optical coherence tomography", Journal of Neuroscience Methods 7●, 1996, pp. 65-72.

Boppart, Stephen A., et al., "Noninvasive assessment of the developing Xenopus cardiovascular system using optical coherence tomography", Prec. Natl. Acad. Sci. USA, vol. 94, Apr. 1997, pp. 4256-4261.

Tearney, Guillermo J., et al., "In vivo Endoscopic ●ptical Biopsy with ●ptical Coherence Tomography", Science, New Series, vol. 276, Jun. 27, 1997, pp. 2●37-2●39.

de Boer, Johannes F., et al., "Imaging thermally damaged tissue by polarization sensitive optical coherence tomography", ●ptics Express 212, vol. 3, No. 6, Sep. 14, 1998, pp. 212-218.

Roggan, Andre, et al., "●ptical Properties of Circulating Human Blood in the Wavelength Range 4●●-25●● NM", Journal of Biomedical ●ptics, vol. 4, No. 1, Jan. 1999, pp. 36-46.

de Boer, Johannes F., et al., "Determination of the depth-resolved Stokes parameters of light backscattered from turbid media by use of polarization-sensitive optical coherence tomography", ●ptics Letters, vol. 24, No. 5; Mar. 1, 1999, pp. 3●●-3●2.

Rollins, Andrew M., et al., "Real-time in vivo imaging of human gastrointestinal ultrastructure by use of endoscopic optical coherence tomography with a novel efficient interferometer design", ●ptics Letters, vol. 24, No. 19, ●ct. 1, 1999, pp. 1358-136●.

D'Amico, Anthony V., et al., "●ptical Coherence Tomography As a Method for Identifying Benign and Malignant Microscopic Structures in the Prostate Gland", Basic Science, Urology 55 (5), 2●●●, pp. 783-787.

Li, Xingde, et al., "Imaging needle for optical coherence tomography", ●ptics Letters, vol. 25, No. 2●, ●ct. 15, 2●●●, pp. 152●-1522.

●ughstun, Kurt E., "Influence of precursor fields on ultrashort pulse autocorrelation measurements and pulse width evolution", ●ptics Express, vol. 8, No. 8, Apr. 9, 2●●1, pp. 481-491.

Kowalevicz, Andrew M., et al., "Ultrahigh resolution optical coherence tomography using a superluminescent light source" ●ptics Express 349, vol. 1●, No. 7, Apr. 8, 2●●2, pp. 349-353.

Povazay, B., et al., "Submicrometer axial resolution optical coherence tomography", ●ptics Letters, vol. 27, No. 2●, ●ct. 15, 2●●2, pp. 18●●-18●2.

(56) **References Cited**

OTHER PUBLICATIONS

Xie, T.-Q., et al., "Detection of tumorigenesis in urinary bladder with optical coherence tomography: optical characterization of morphological changes", Optics Express, vol. 10, No. 24, Dec. 2, 2002, 2003, pp. 1431-1443.
Seefeldt, Michael, et al., "Compact white-light source with an average output power of 2.4 Wand 900 nm spectral bandwidth", Optics Communications 216, pp. 199-202.
Wang, Yimin, et al., "Ultrahigh-resolution optical coherence tomography by broadband continuum generation from a photonic crystal fiber", Optics Letters, vol. 28, No. 3, Feb. 1, 2003, pp. 182-184.
Bizheva, K, et al., "Compact, broad-bandwidth fiberlaserforsub-2-pm axial resolution optical coherence tomography in the 1300-nm wavelength region," Optics Letters, vol. 28, No. 9, May 1, 2003, pp. 707-709.
Pan, Yingtian, et al., "Hand-held arthroscopic optical coherence tomography for in vivo high-resolution imaging of articular cartilage", Journal of Biomedical Optics 8(4), Oct. 2003, pp. 648-654.
Xie, Tuqiang, et al., "Endoscopic optical coherence tomography with a modified microelectromechanical systems mirror for detection of bladder cancers", Applied Optics, vol. 42, No. 31, Nov. 1, 2003, pp. 6422-6426.
Dubois, A., et al., "Three-dimensional cellular-level imaging using fill-field optical coherence tomography", Physics in Medicine and Biology, Phys. Med. Biol. 49, 2004, pp. 1227-1234.
Park, Jesung, et al., "Analysis of birefringent image in the retinal nerve fiber layer by polarization sensitive optical coherence tomography", Ophthalmic Technologies XIV, Proceedings of SPIE, vol. 5314, 2004, pp. 188-194.
Unterhuber, A., et al., "Advances in broad bandwidth light sources for ultrahigh resolution optical coherence tomography", Physics in Medicine and Biology, Phys. Med. Biol. 49, 2004, pp. 1235-1246.
Drexler, Wolfgang, "Ultrahigh-resolution optical coherence tomography", Journal of Biomedical Optics, vol. 9, No. 1, Jan./Feb. 2004, pp. 47-74.
Schmitt, Joseph, et al., "Intravascular Optical Coherence Tomography Opens a Window Onto Coronary Artery Disease", Optics & Photonics News, Feb. 2004, pp. 20-25.
Nassif, N.A., et al., "In vivo high-resolution video-rate spectral-domain optical coherence tomography of the human retina and optic nerve", Optics Express, vol. 12, No. 3, Feb. 9, 2004, pp. 367-376.
Choi, Seung-Ho, et al., "Observation of Optical Precursors in Water", Physical Review Letters, vol. 92, No. 19, May 14, 2004, pp. 193903-1-193903-3.
Pierce, Mark C., et al., "Advances in Optical Coherence Tomography imaging for Dermatology", Optical Coherence Tomography Advances, The Journal of Investigative Dermatology, Sep. 3, 2004, pp. 458-463.
"State-Specific Trends in Chronic Kidney Failure—United States, 1990-2001", Morbidity and Mortality Weekly Report, Department of Health and Human Services Centers for Disease Control and Prevention, vol. 53, No. 39, copied from internet: file://C:\Documents and Settings\eturlo\Desktop\State-Specific Trends in Chronic Kidney . . . Feb. 12, 2010, Oct. 8, 2004, pp. 918-920.
I.B. Ads, A.A.E. Wagie, N.B. Mariun, A.B.E. Janunal, "An Internet-based blood pressure monitoring system for patients," Journal of Telemedicine and Telecare, 2001, pp. 51-53.
R.H. Istepanian, B. Woodward, P.A. Bales, S. Chen, B. Luk, "The comparative performance of mobile telemediCal systems based on the IS-54 and GSM cellular telephone standards," Journal of Telemedicine and Telecare, 1999, pp. 97-104.
Shaw, et al, IR Supercontinuum Generation in As—Se Photonic Crystal Fiber, Optical Society of America, Copyright 2005, 3 pages.
PCT/US06/44451, Notification of Transmittal of the International Search Report and the Written Opinion of the International Searching Authority, or the Declaration, dated Nov. 29, 2007, 12 pages.
G.S. Edwards et al., "Free-electron-laser-based biophysical and biomedical instrumentation," American Institute of Physics, vol. 74, No. 7, Jul. 2003, pp. 3207-3245.
Computer Motion, Inc., "501(k) Summary-ZEUS® MicroWrist™ Surgical System and Accessories," Sep. 24, 2002, 6 pages.
Computer Motion, Inc. "HERMES™ O.R. Control Center—510(k) Summary of Safety and Effectiveness," Oct. 11, 2002, 5 pages.
K.M. Joos, et al. "Optic Nerve Sheath Fenestration with a Novel Wavelength Produced by the Free Electron Laser (FEL)," Lasers in Surgery and Medicine, 27: 2000,191-205.
J. Sanghera, I. Aggarwal, "IR Fiber Optics at NRL," undated, 10 pages.
J. Sanghera, L.B. Shaw, I.D. Aggarwal, "Applications of chalcogenide glass optical fibers," Academic of Science, 2003, pp. 1-11.
B. Rigas, P.T.T. Wong, "Human Colon Adenocarcinoma Cell Lines Display Infrared Spectroscopic Features," Cancer Research, Jan. 1, 1992, pp. 84-88.
G. Edwards, et al., "Comparison of OPA and Mark-III FEL for Tissue Ablation at 6.45 Microns," Department of Physics and Free Electron Laser Laboratory, Duke University, 2002, 7 pages.
Glenn Edwards, "Biomedical and potential clinical applications for pulsed lasers operating near 6.45 um," Society of Photo-Optical Instrumentation Engineers, 1995, 2 pages.
Passat, "Solid-State Lasers and Optical Components," Jul. 14, 2003, 5 pages.
P.A. Thielen and L.B. Shaw, et al., "Small-core As—Se fiber for Raman amplification," Optics Leti-Ers, vol. 28, No. 16, Aug. 15, 2003, 3 pages.
R.Rox Anderson, et al., "Selective Photothermolysis: Precise Microsurgery by Selective Absorption of Pulsed Radiation," Department of Dermatology, Harvard Medical School, Science, vol. 220, Apr. 29, 1983, 4 pages.
U.S. Appl. No. 10/652,276, "System and Method for Voice Control of Medical devices," by Mohanuned N. Islam, abandoned (074036.0129) filed Aug. 29, 2003.
U.S. Appl. No. 10/757,341, "System and Method for Voice Control of Medical Devices," by Mohanuned N. Islam, issued (074036.0132) filed Jan. 13, 2004.
U.S. Appl. No. 12/206,432, "System and Method for Voice Control of Medical Devices," by Mohanuned N. Islam, pending (074036.0154) filed Sep. 8, 2008.
U.S. Patent and Trademark Office, Office Action for U.S. Appl. No. 12/206,432, filed Sep. 8, 2008, Mohanuned N. Islam, Date filed: Mar. 12, 2009.
U.S. Patent and Trademark Office, Notice of Allowance and Fee(s) Due for U.S. Appl. No. 12/206,432, filed Sep. 8, 2008, Mohanuned N. Islam, Date filed: Aug. 28, 2009.

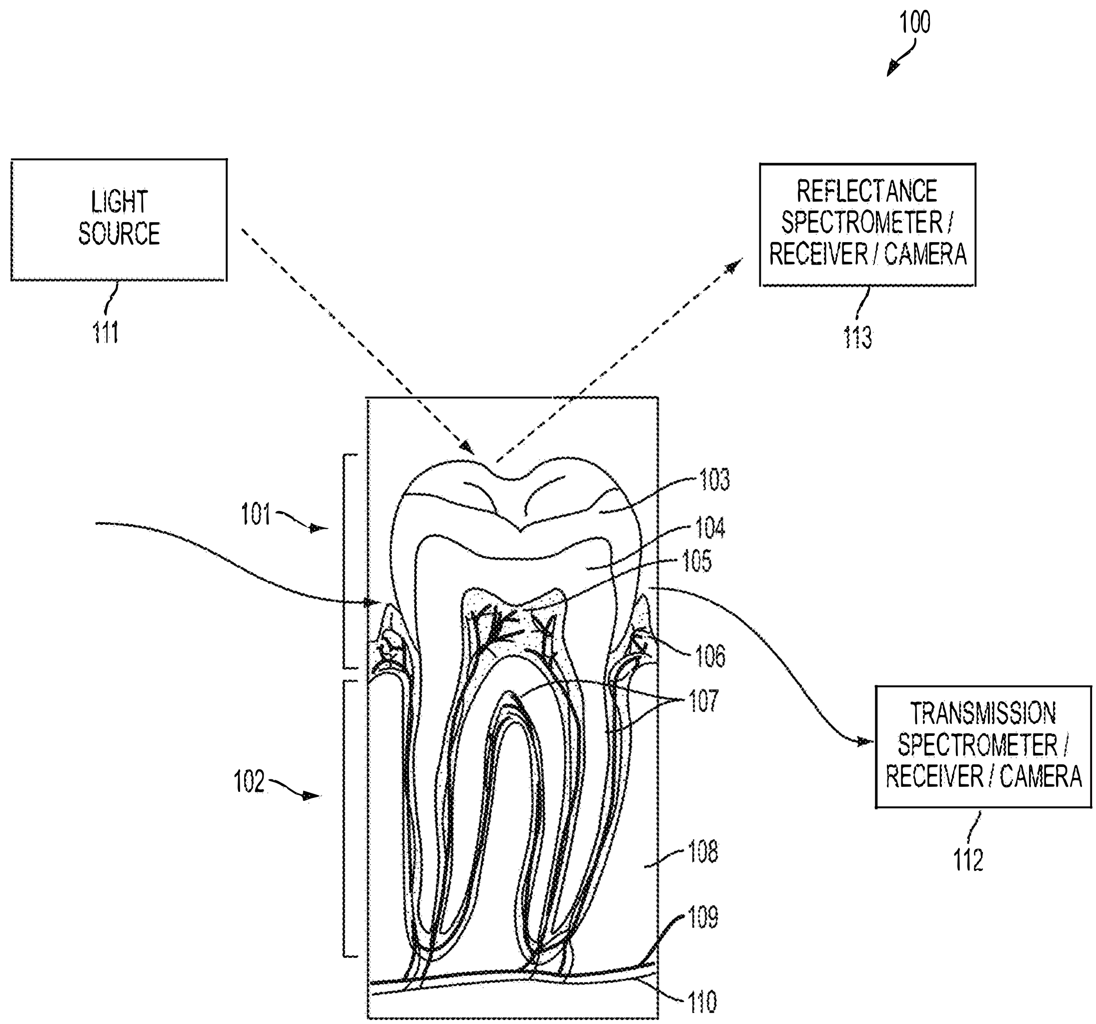
100
LIGHT SOURCE
111
REFLECTANCE SPECTROMETER / RECEIVER / CAMERA
113
101
102
103
104
105
106
107
108
109
110
TRANSMISSION SPECTROMETER / RECEIVER / CAMERA
112

FIG. 1

200

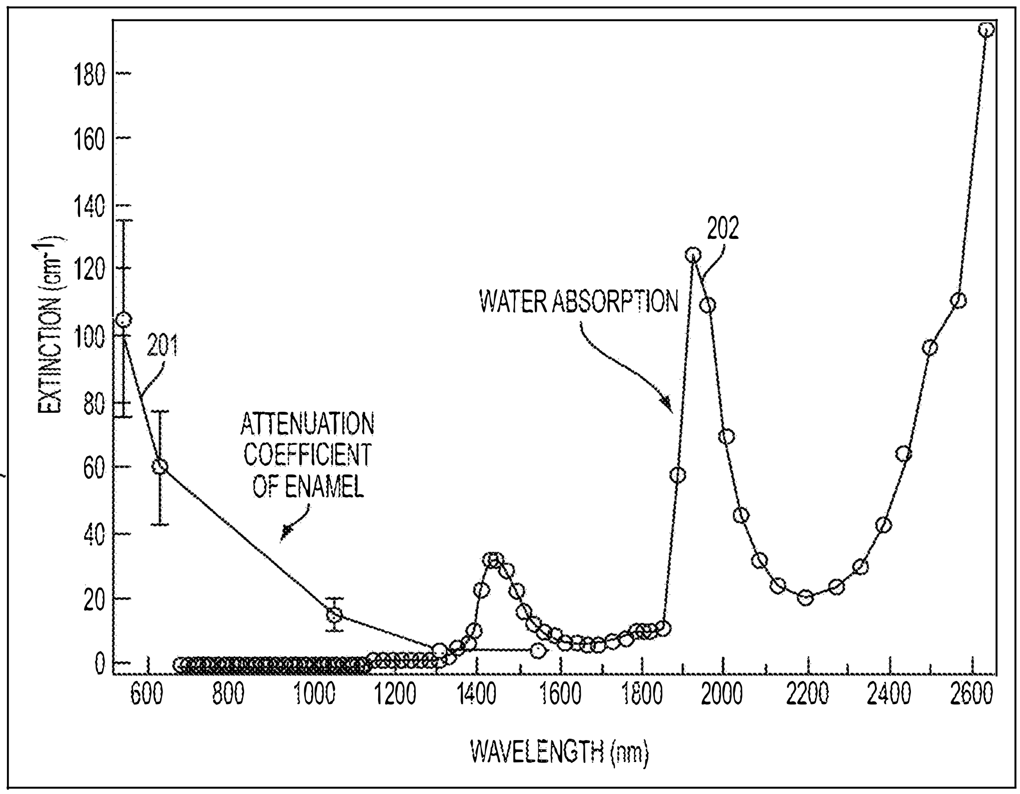

180
160
140
120
100
80
60
40
20
0
EXTINCTION (cm-1)
600
800
1000
1200
1400
1600
1800
2000
2200
2400
2600
WAVELENGTH (nm)
201
202
ATTENUATION COEFFICIENT OF ENAMEL
WATER ABSORPTION

FIG. 2A

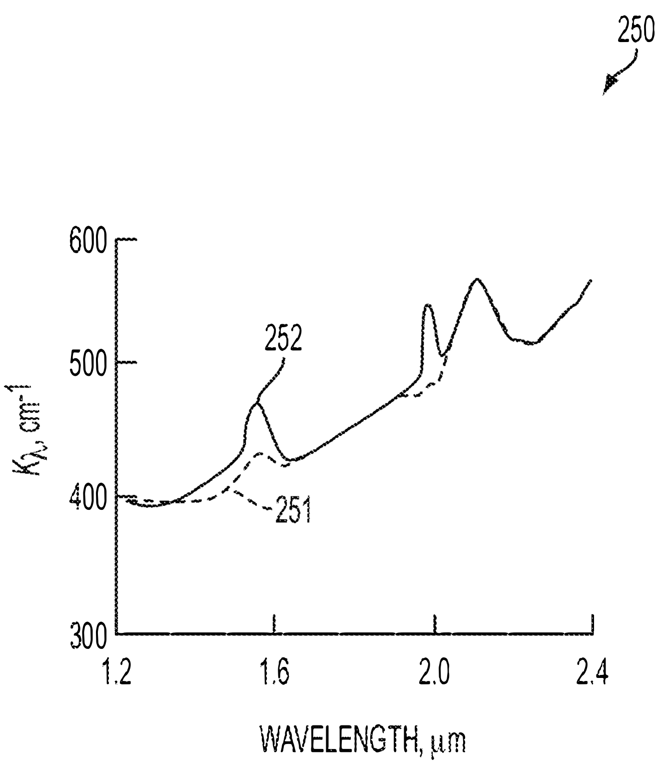
250
600
500
400
300
252
251
K_λ, cm^{-1}
1.2
1.6
2.0
2.4
WAVELENGTH, μm

FIG. 2B

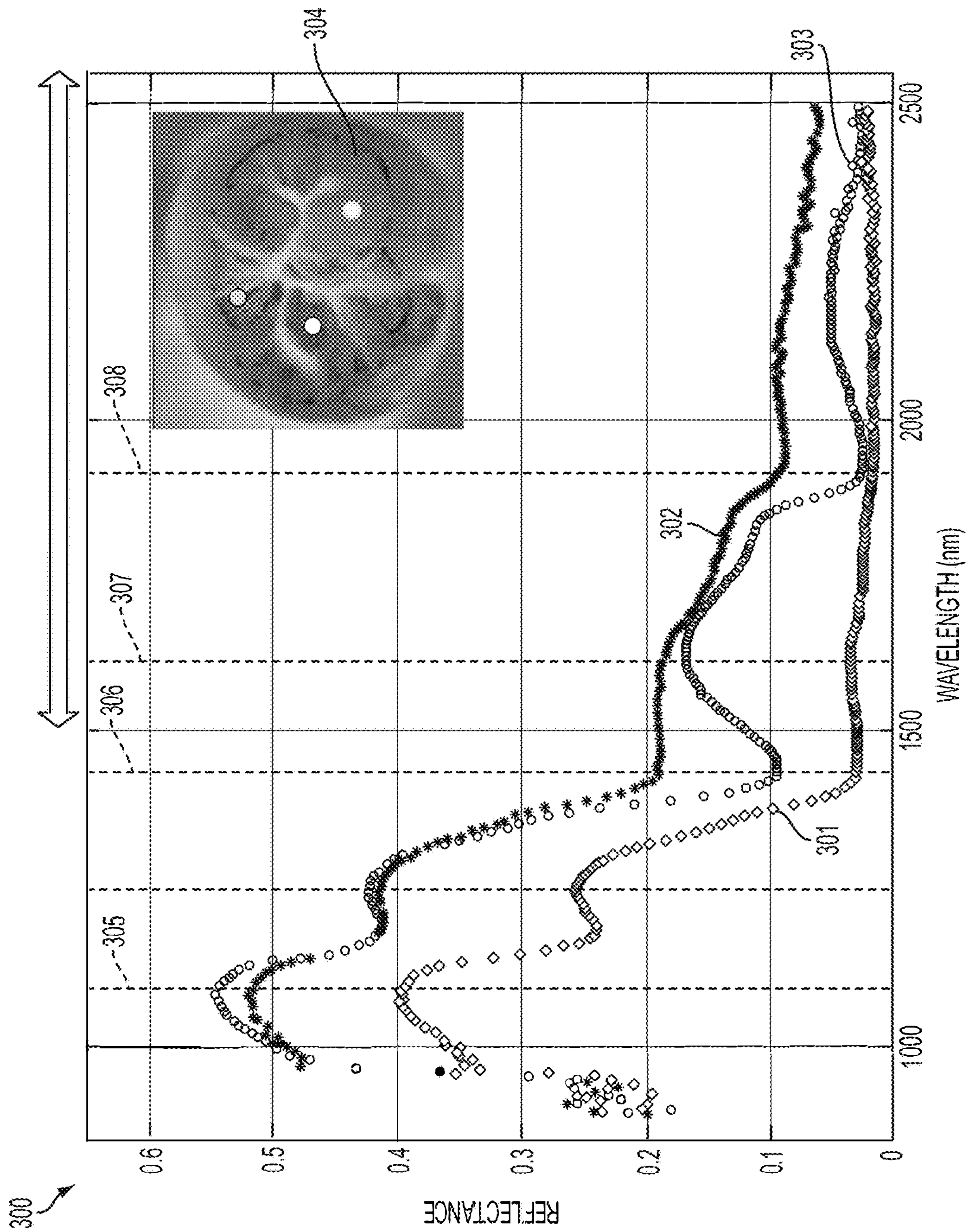
300
REFLECTANCE
0.6
0.5
0.4
0.3
0.2
0.1
0
1000
1500
2000
2500
WAVELENGTH (nm)
301
302
303
304
305
306
307
308

FIG. 3

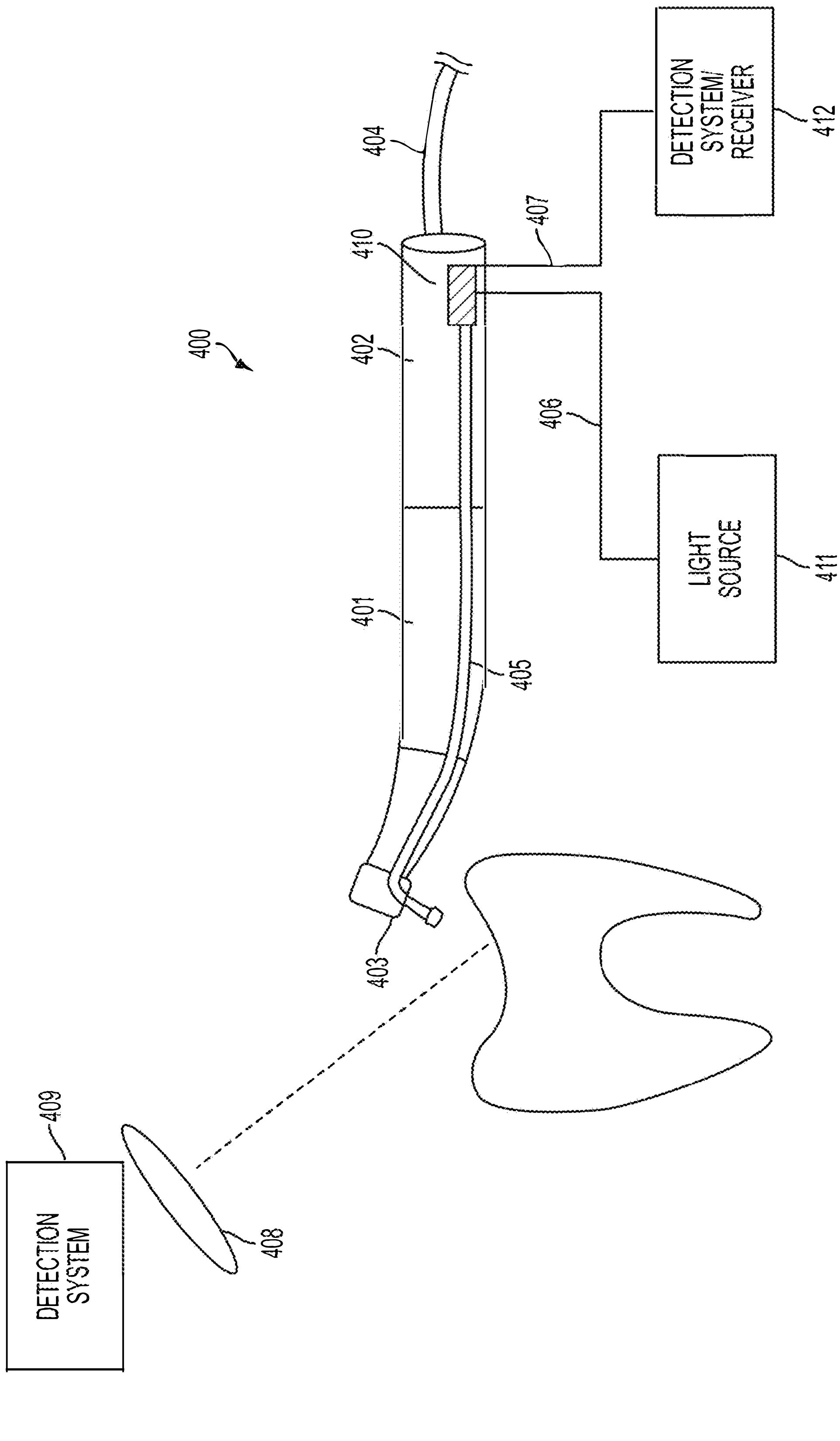
400
404
410
407
402
DETECTION SYSTEM/ RECEIVER
412
406
LIGHT SOURCE
411
401
405
403
409
DETECTION SYSTEM
408

FIG. 4

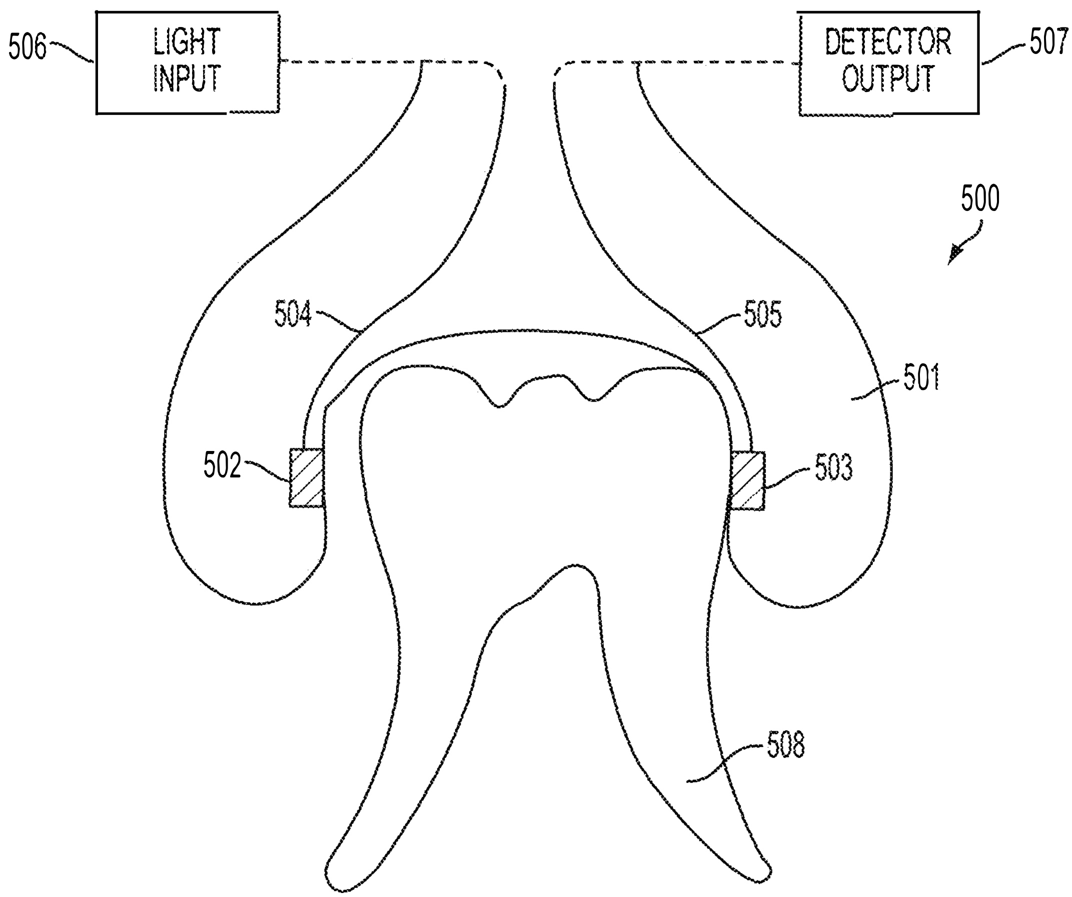
506
LIGHT INPUT
DETECTOR OUTPUT
507
500
504
505
501
502
503
508

FIG. 5A

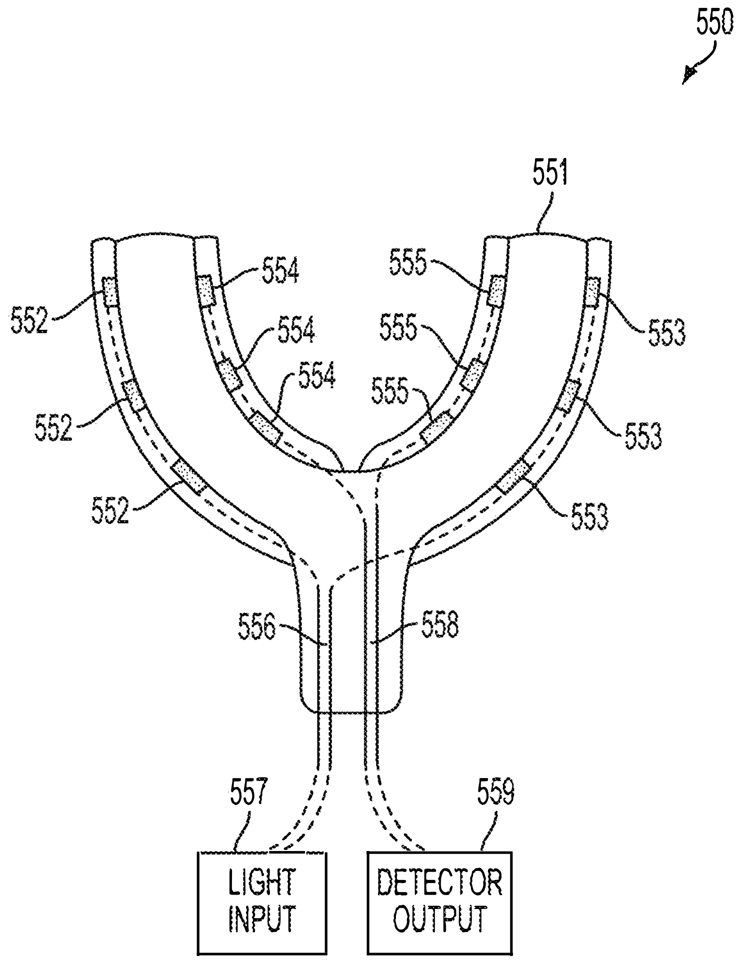
550
551
552
552
552
553
553
553
554
554
554
555
555
555
556
558
557
559
LIGHT INPUT
DETECTOR OUTPUT

FIG. 5B

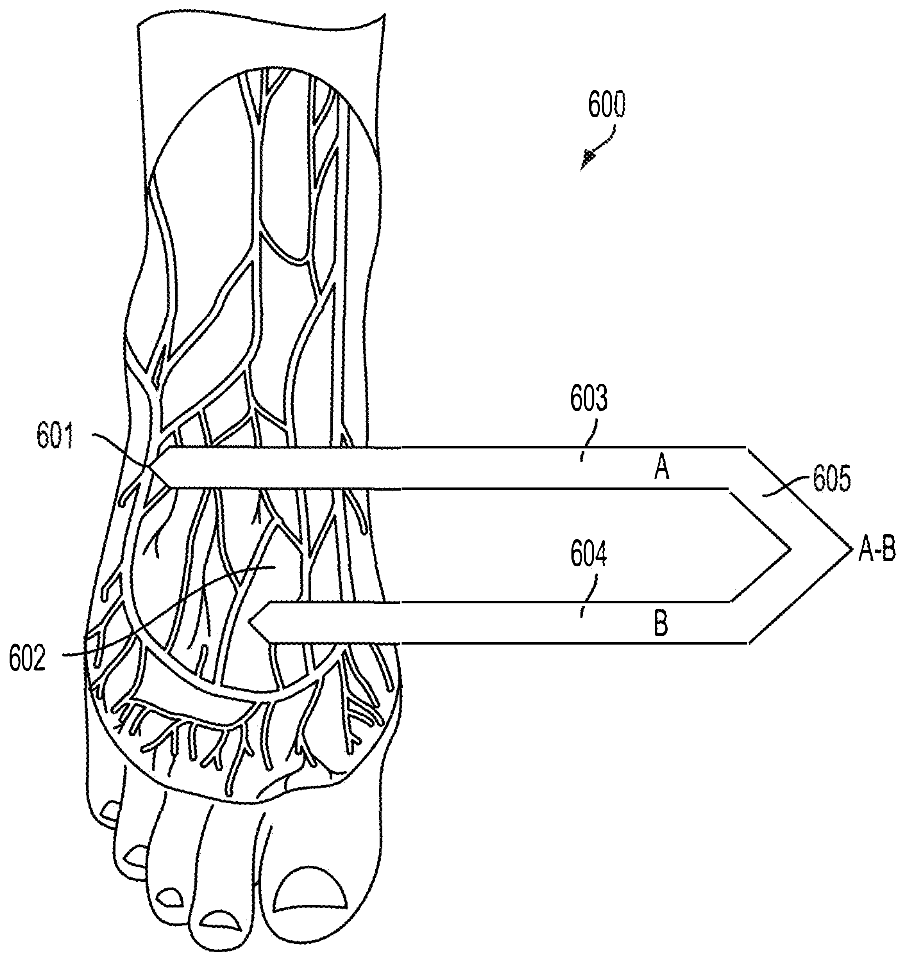

FIG. 6A

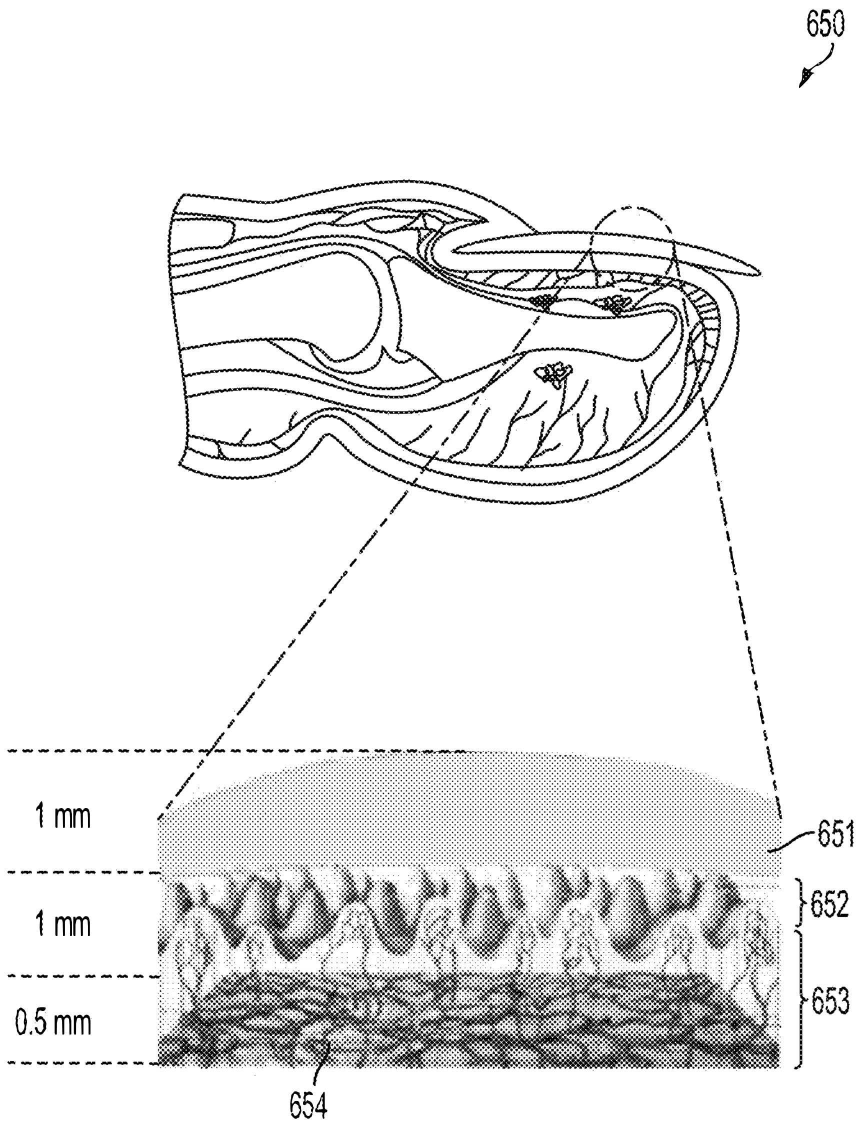

FIG. 6B

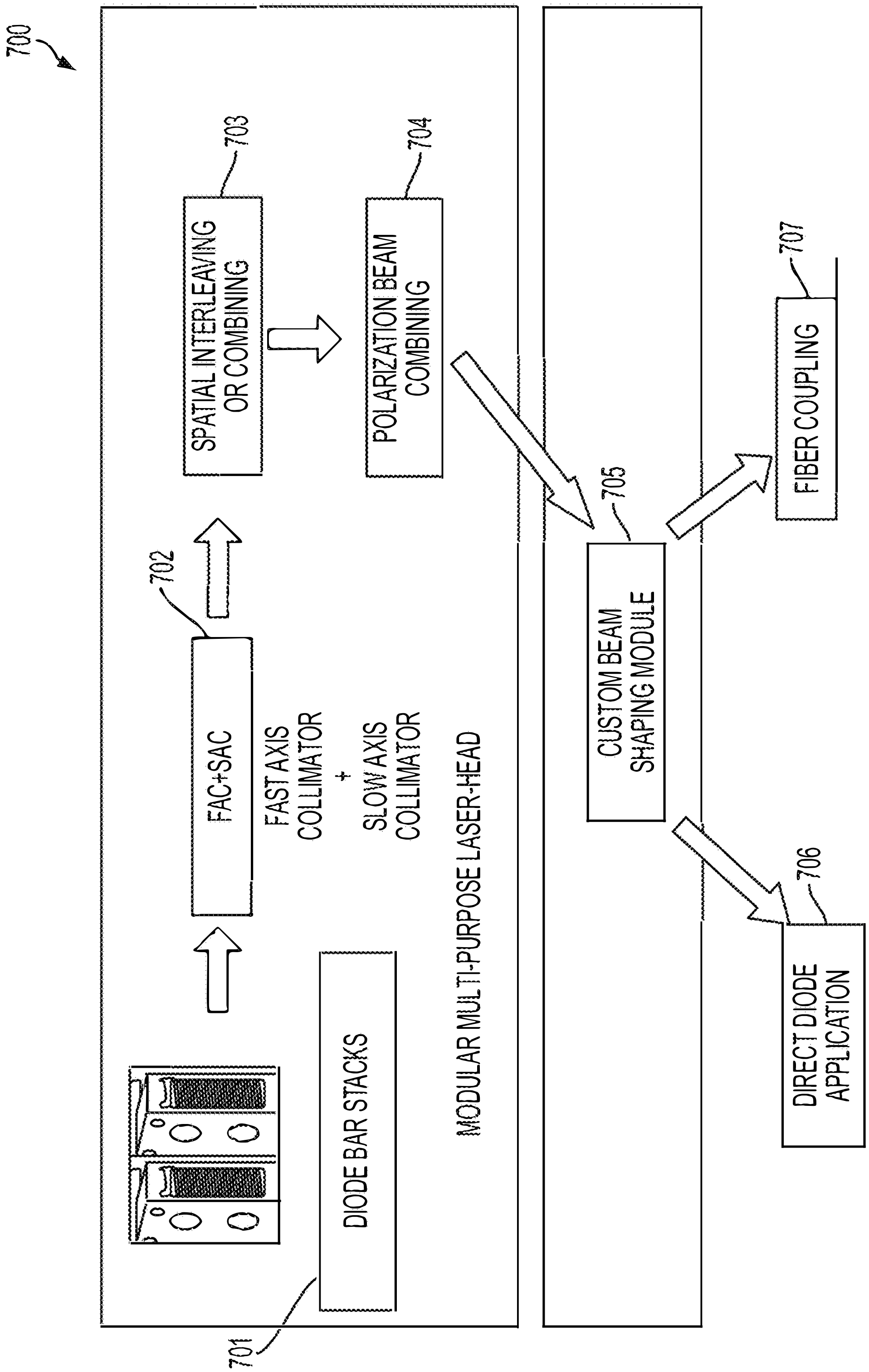
700
701
DIODE BAR STACKS
702
FAC+SAC
FAST AXIS COLLIMATOR
+
SLOW AXIS COLLIMATOR
703
SPATIAL INTERLEAVING OR COMBINING
704
POLARIZATION BEAM COMBINING
MODULAR MULTI-PURPOSE LASER-HEAD
705
CUSTOM BEAM SHAPING MODULE
706
DIRECT DIODE APPLICATION
707
FIBER COUPLING

FIG. 7

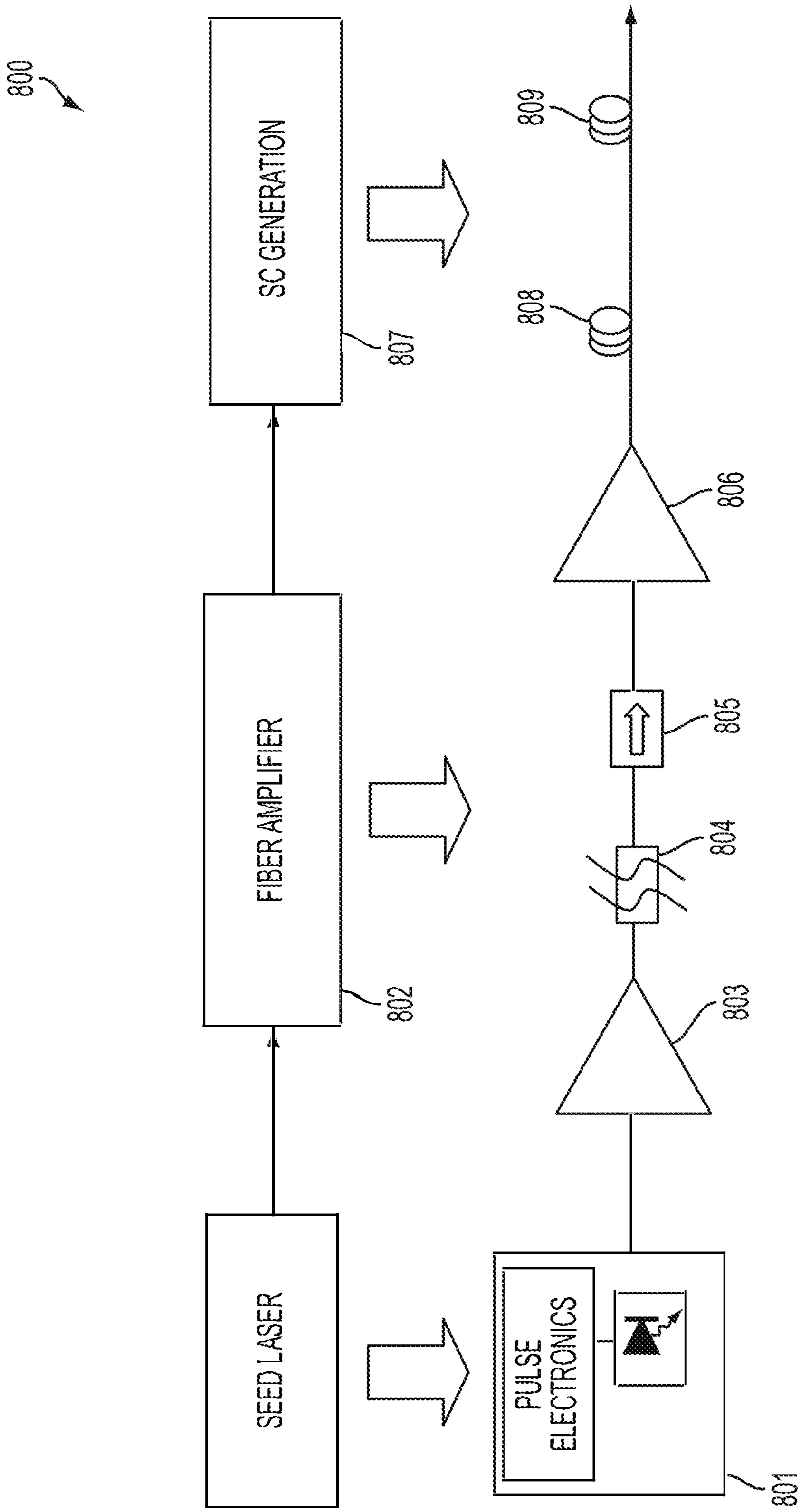
800
SC GENERATION
807
FIBER AMPLIFIER
802
SEED LASER
809
808
806
805
804
803
PULSE
ELECTRONICS
801

FIG. 8

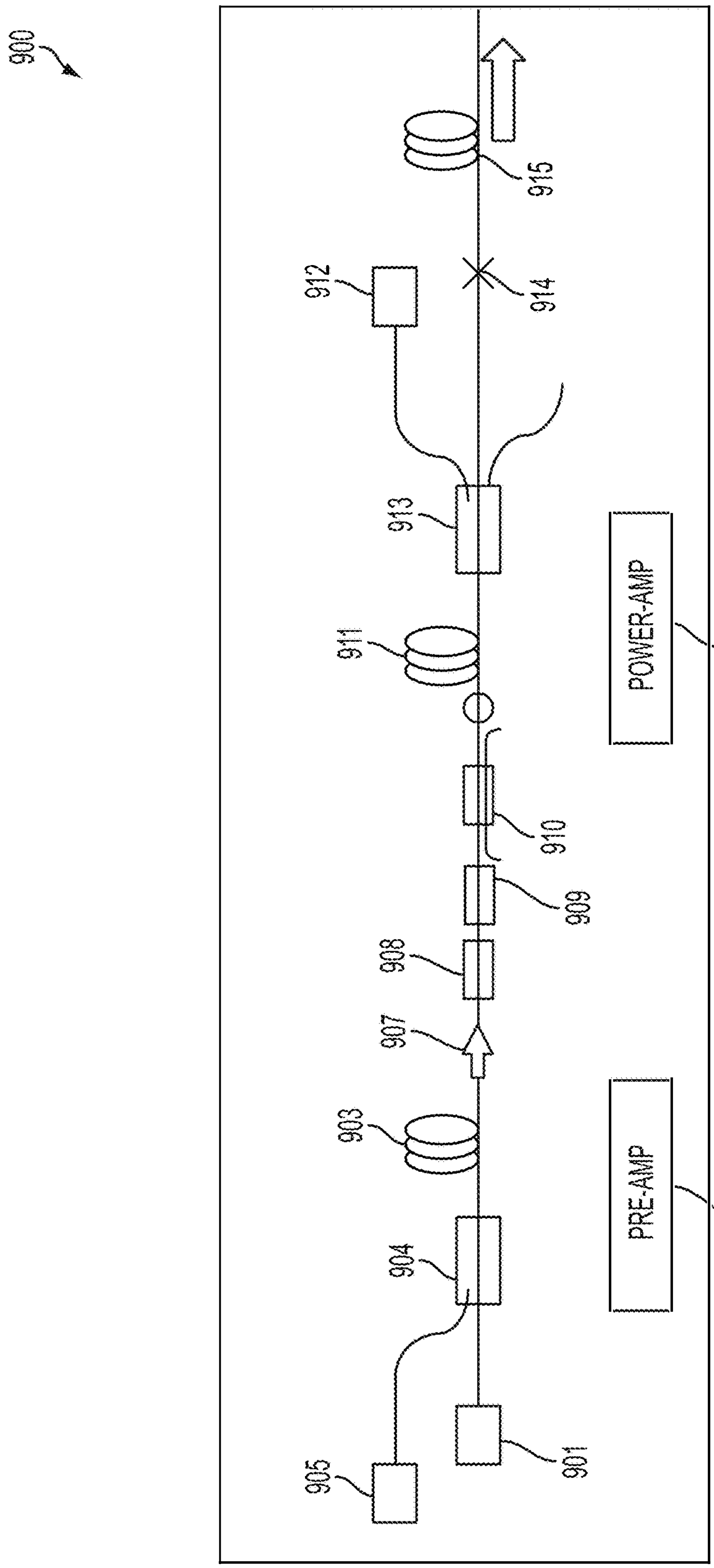
900
901
902
903
904
905
906
907
908
909
910
911
912
913
914
915
PRE-AMP
POWER-AMP

FIG. 9

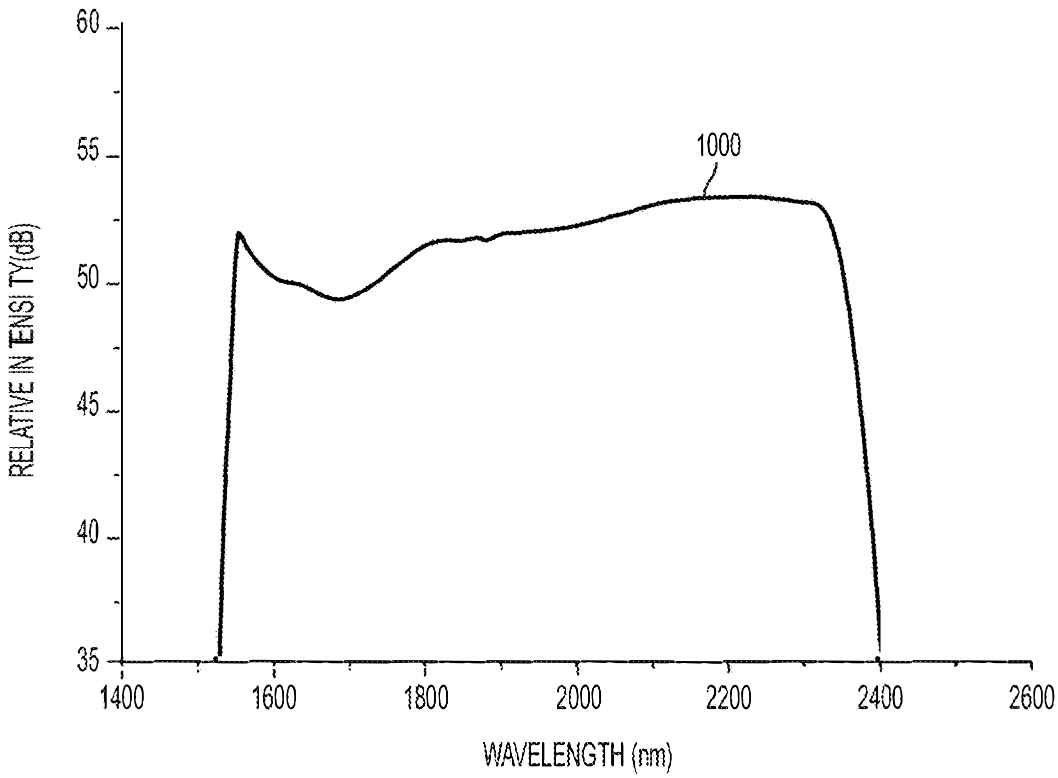
60
55
50
45
40
35
RELATIVE IN TENSI TY(dB)
1000
1400
1600
1800
2000
2200
2400
2600
WAVELENGTH (nm)

FIG. 10

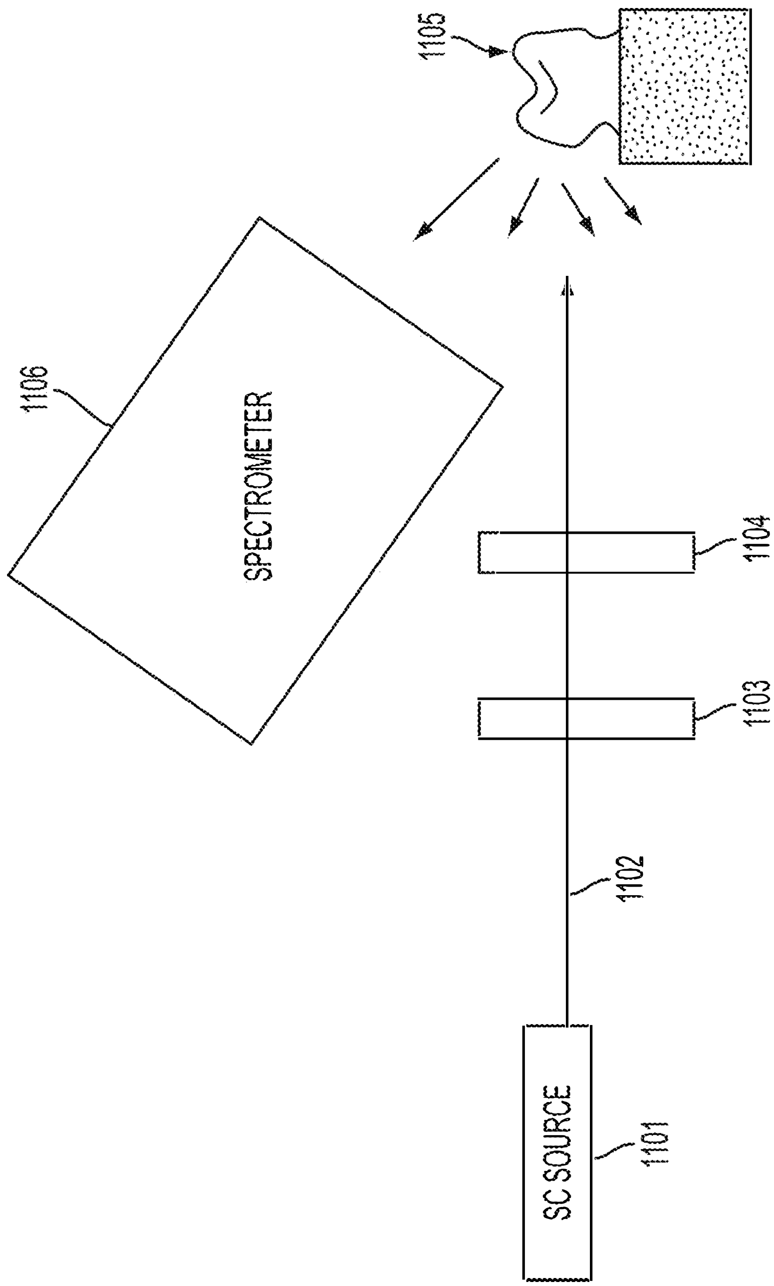

FIG. 11A

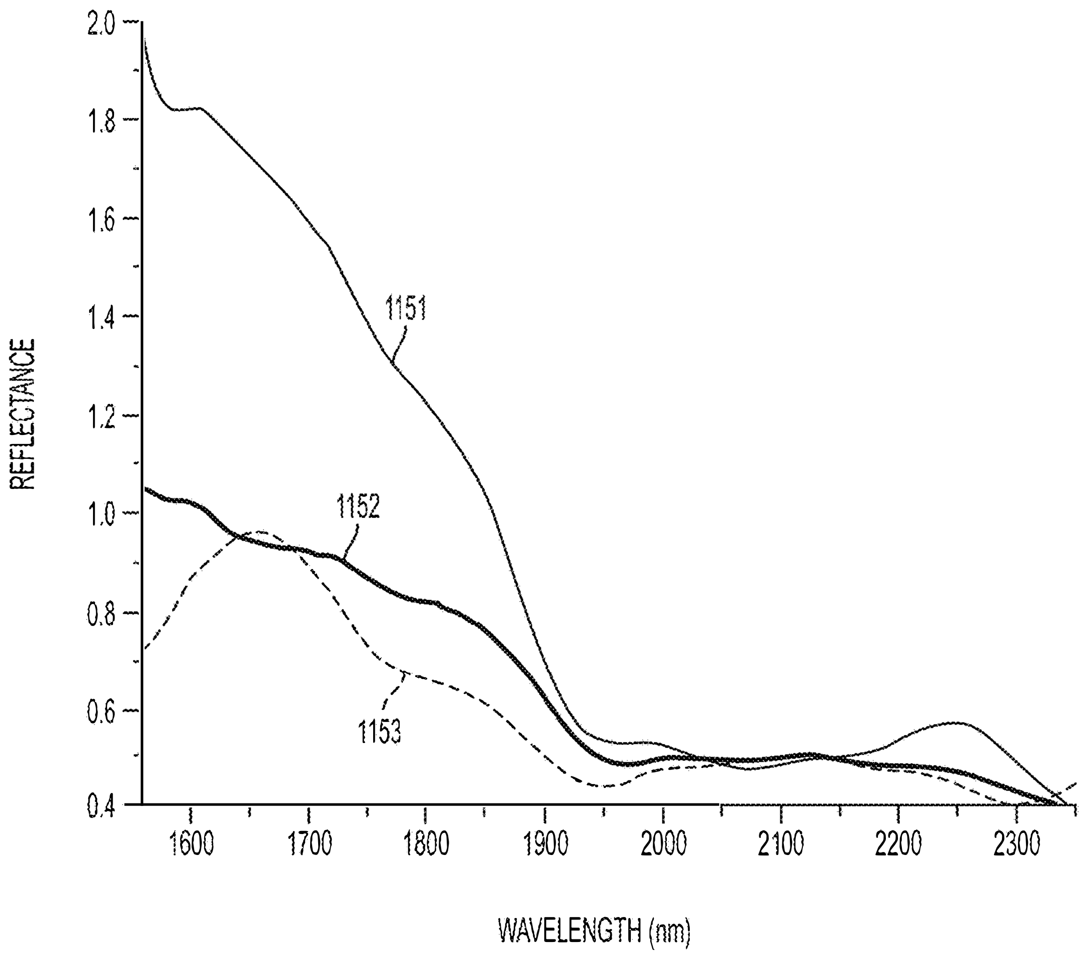
2.0
1.8
1.6
1.4
1.2
1.0
0.8
0.6
0.4
REFLECTANCE
1151
1152
1153
1600
1700
1800
1900
2000
2100
2200
2300
WAVELENGTH (nm)

FIG. 11B

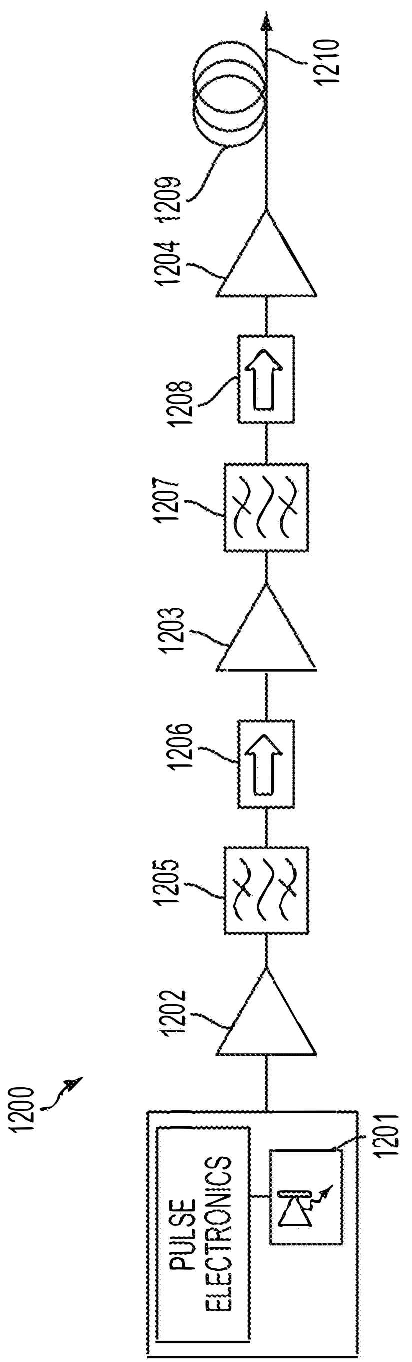

FIG. 12A

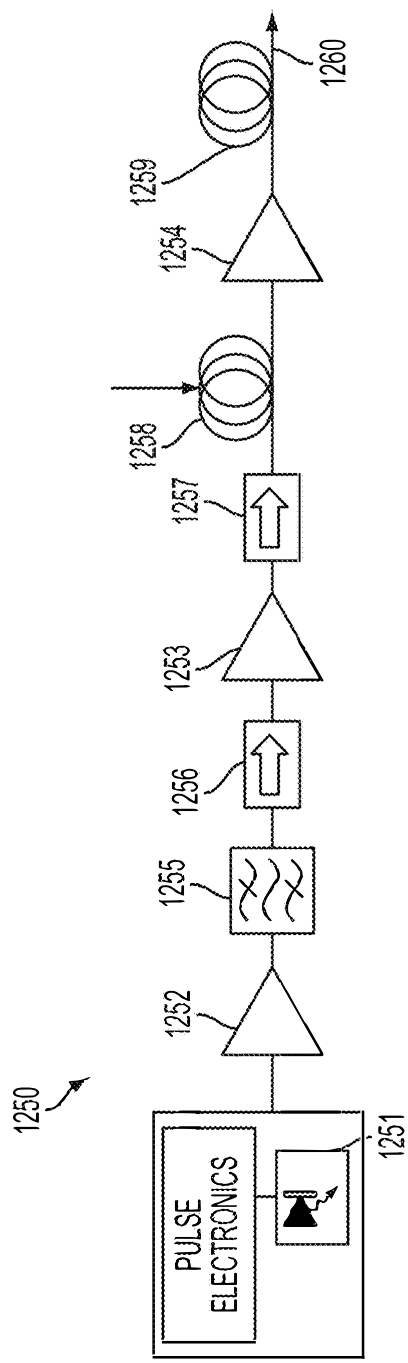

FIG. 12B

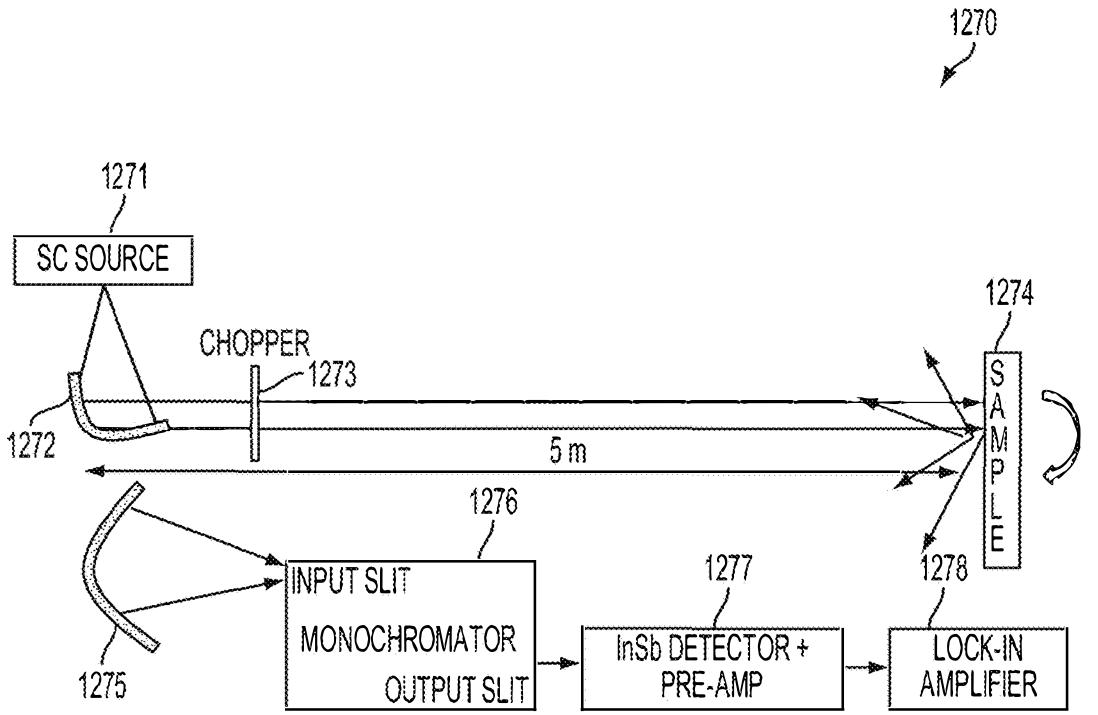
1270
1271
SC SOURCE
CHOPPER
1273
1274
SAMPLE
1272
5 m
1276
INPUT SLIT
MONOCHROMATOR
OUTPUT SLIT
1277
InSb DETECTOR +
PRE-AMP
1278
LOCK-IN
AMPLIFIER
1275

FIG. 12C

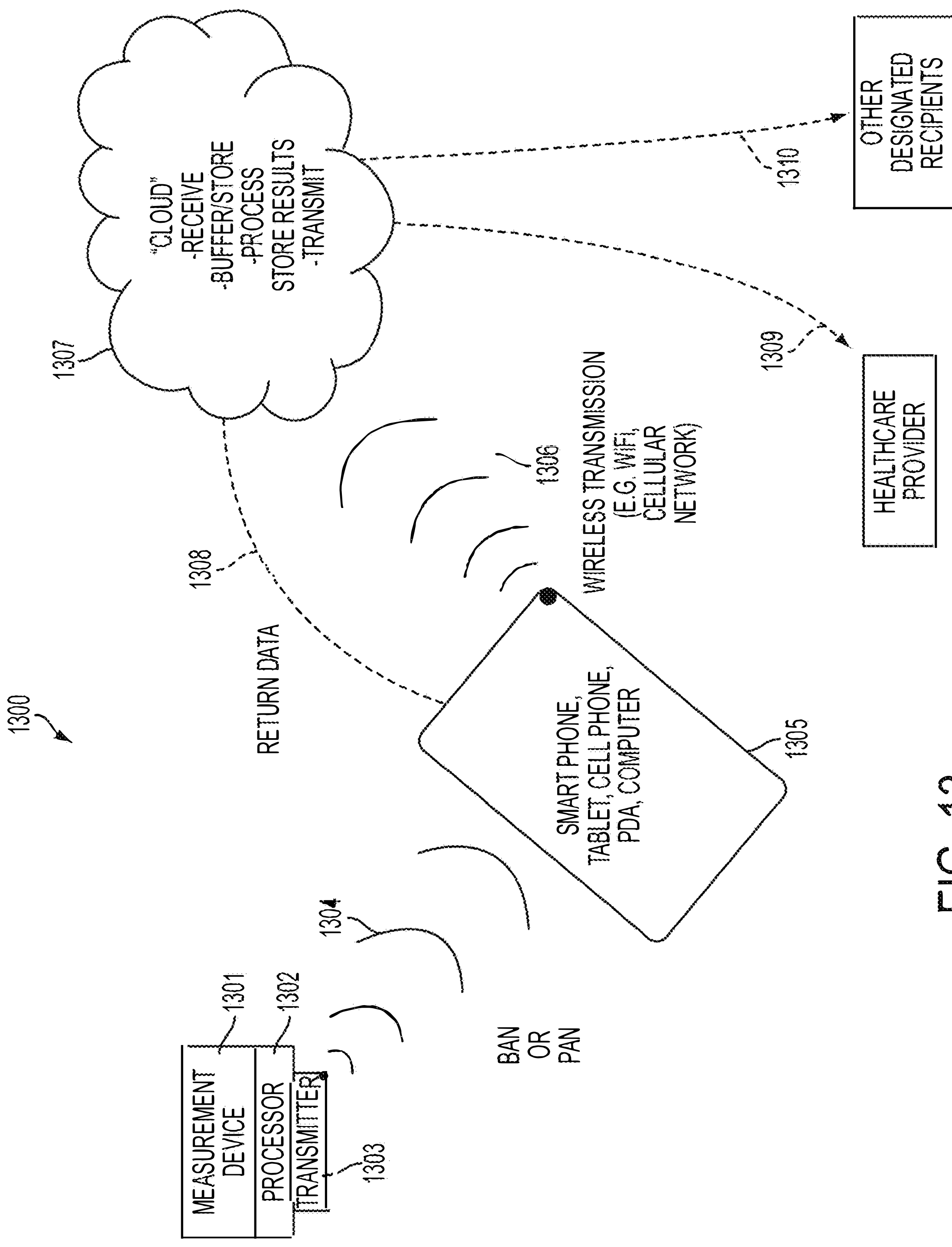
1300
MEASUREMENT DEVICE
PROCESSOR
TRANSMITTER
1301
1302
1303
1304
BAN OR PAN
SMART PHONE, TABLET, CELL PHONE, PDA, COMPUTER
1305
RETURN DATA
1308
WIRELESS TRANSMISSION (E.G. WIFI, CELLULAR NETWORK)
1306
"CLOUD"
-RECEIVE
-BUFFER/STORE
-PROCESS
STORE RESULTS
-TRANSMIT
1307
1309
HEALTHCARE PROVIDER
1310
OTHER DESIGNATED RECIPIENTS

FIG. 13

SHORT-WAVE INFRARED SUPER-CONTINUUM LASERS FOR EARLY DETECTION OF DENTAL CARIES

CROSS-REFERENCE TO RELATED APPLICATIONS

This application is a Continuation of U.S. application Ser. No. 15/357,136 filed Nov. 21, 2016, which is a Continuation of U.S. application Ser. No. 14/651,367 filed Jun. 11, 2015, which is the U.S. national phase of PCT Application No. PCT/US2013/075736 filed Dec. 17, 2013, which claims the benefit of U.S. provisional application Ser. No. 61/747,477 filed Dec. 31, 2012 and U.S. provisional application Ser. No. 61/754,698 filed Jan. 21, 2013, the disclosures of which are hereby incorporated by reference in their entirety.

This application is related to U.S. provisional application Ser. No. 61/747,472 filed Dec. 31, 2012; Ser. No. 61/747,481 filed Dec. 31, 2012; Ser. No. 61/747,485 filed Dec. 31, 2012; Ser. No. 61/747,487 filed Dec. 31, 2012; Ser. No. 61/747,492 filed Dec. 31, 2012; and Ser. No. 61/747,553 filed Dec. 31, 2012, the disclosures of which are hereby incorporated in their entirety in their entirety by reference herein.

This application has a common priority date with commonly owned U.S. application Ser. No. 14/650,897 filed Jun. 10, 2015, which is the U.S. national phase of International Application PCT/US2013/075700 entitled Near-Infrared Lasers For Non-Invasive Monitoring Of Glucose, Ketones, HBA1C, And Other Blood Constituents; U.S. application Ser. No. 14/108,995 filed Dec. 17, 2013, now U.S. Pat. No. 9,164,032 entitled Focused Near-Infrared Lasers For Non-Invasive Vasectomy And Other Thermal Coagulation Or Occlusion Procedures; U.S. application Ser. No. 14/650,981 filed Jun. 10, 2015, which is the U.S. national phase of International Application PCT/US2013/075767 entitled Short-Wave Infrared Super-Continuum Lasers For Natural Gas Leak Detection, Exploration, And Other Active Remote Sensing Applications; U.S. application Ser. No. 14/108,986 filed Dec. 17, 2013 entitled Short-Wave Infrared Super-Continuum Lasers For Detecting Counterfeit Or Illicit Drugs And Pharmaceutical Process Control; U.S. application Ser. No. 14/108,974 filed Dec. 17, 2013 entitled Non-Invasive Treatment Of Varicose Veins; and U.S. application Ser. No. 14/109,007 filed Dec. 17, 2013 entitled Near-Infrared Super-Continuum Lasers For Early Detection Of Breast And Other Cancers, the disclosures of which are hereby incorporated in their entirety by reference herein.

TECHNICAL FIELD

This disclosure relates to lasers and light sources for healthcare, medical, dental, or bio-technology applications, including systems and methods for using near-infrared or short-wave infrared light sources for early detection of dental caries, often called cavities.

BACKGROUND AND SUMMARY

Dental care and the prevention of dental decay or dental caries has changed in the United States over the past several decades, due to the introduction of fluoride to drinking water, the use of fluoride dentifrices and rinses, application of topical fluoride in the dental office, and improved dental hygiene. Despite these advances, dental decay continues to be the leading cause of tooth loss. With the improvements over the past several decades, the majority of newly discovered carious lesions tend to be localized to the occlusal pits and fissures of the posterior dentition and the proximal contact sites. These early carious lesions may be often obscured in the complex and convoluted topography of the pits and fissures or may be concealed by debris that frequently accumulates in those regions of the posterior teeth. Moreover, such lesions are difficult to detect in the early stages of development.

Dental caries may be a dynamic disease that is characterized by tooth demineralization leading to an increase in the porosity of the enamel surface. Leaving these lesions untreated may potentially lead to cavities reaching the dentine and pulp and perhaps eventually causing tooth loss. Occlusal surfaces (bite surfaces) and approximal surfaces (between the teeth) are among the most susceptible sites of demineralization due to acid attack from bacterial by-products in the biofilm. Therefore, there is a need for detection of lesions at an early stage, so that preventive agents may be used to inhibit or reverse the demineralization.

Traditional methods for caries detection include visual examination and tactile probing with a sharp dental exploration tool, often assisted by radiographic (x-ray) imaging. However, detection using these methods may be somewhat subjective; and, by the time that caries are evident under visual and tactile examination, the disease may have already progressed to an advanced stage. Also, because of the ionizing nature of x-rays, they are dangerous to use (limited use with adults, and even less used with children). Although x-ray methods are suitable for approximal surface lesion detection, they offer reduced utility for screening early caries in occlusal surfaces due to their lack of sensitivity at very early stages of the disease.

Some of the current imaging methods are based on the observation of the changes of the light transport within the tooth, namely absorption, scattering, transmission, reflection and/or fluorescence of light. Porous media may scatter light more than uniform media. Taking advantage of this effect, the Fiber-optic trans-illumination is a qualitative method used to highlight the lesions within teeth by observing the patterns formed when white light, pumped from one side of the tooth, is scattered away and/or absorbed by the lesion. This technique may be difficult to quantify due to an uneven light distribution inside the tooth.

Another method called quantitative light-induced fluorescence—QLF—relies on different fluorescence from solid teeth and caries regions when excited with bright light in the visible. For example, when excited by relatively high intensity blue light, healthy tooth enamel yields a higher intensity of fluorescence than does demineralized enamel that has been damaged by caries infection or any other cause. On the other hand, for excitation by relatively high intensity of red light, the opposite magnitude change occurs, since this is the region of the spectrum for which bacteria and bacterial by-products in carious regions absorb and fluoresce more pronouncedly than do healthy areas. However, the image provided by QLF may be difficult to assess due to relatively poor contrast between healthy and infected areas. Moreover, QLF may have difficulty discriminating between white spots and stains because both produce similar effects. Stains on teeth are commonly observed in the occlusal sites of teeth, and this obscures the detection of caries using visible light.

As described in this disclosure, the near-infrared region of the spectrum offers a novel approach to imaging carious regions because scattering is reduced and absorption by stains is low. For example, it has been demonstrated that the scattering by enamel tissues reduces in the form of $1/(\text{wavelength})^3$, e.g., inversely as the cube of wavelength. By using a broadband light source in the short-wave infrared (SWIR) part of the spectrum, which corresponds approximately to 1400 nm to 2500 nm, lesions in the enamel and dentine may be observed. In one embodiment, intact teeth have low reflection over the SWIR wavelength range. In the presence of caries, the scattering increases, and the scattering is a function of wavelength; hence, the reflected signal decreases with increasing wavelength. Moreover, particularly when caries exist in the dentine region, water build up may occur, and dips in the SWIR spectrum corresponding to the water absorption lines may be observed. The scattering and water absorption as a function of wavelength may thus be used for early detection of caries and for quantifying the degree of demineralization.

SWIR light may be generated by light sources such as lamps, light emitting diodes, one or more laser diodes, super-luminescent laser diodes, and fiber-based super-continuum sources. The SWIR super-continuum light sources advantageously may produce high intensity and power, as well as being a nearly transform-limited beam that may also be modulated. Also, apparatuses for caries detection may include C-clamps over teeth, a handheld device with light input and light detection, which may also be attached to other dental equipment such as drills. Alternatively, a mouth-guard type apparatus may be used to simultaneously illuminate one or more teeth. Fiber optics may be conveniently used to guide the light to the patient as well as to transport the signal back to one or more detectors and receivers.

In one embodiment, a wearable device for use with a smart phone or tablet comprises a measurement device including a light source comprising a plurality of light emitting diodes (LEDs) for measuring one or more physiological parameters, the measurement device configured to generate, by modulating at least one of the LEDs having an initial light intensity, an optical beam having a plurality of optical wavelengths. At least one of the LEDs emits at a first wavelength having a first penetration depth into tissue and at least another of the LEDs emits at a second wavelength having a second penetration depth into the tissue, wherein at least a portion of the optical beam includes a near-infrared wavelength between 700 nanometers and 2500 nanometers. The measurement device comprises one or more lenses configured to receive and to deliver at least a portion of each of the first and of the second wavelengths to tissue, wherein the tissue reflects at least a portion of each of the first and of the second wavelengths. The measurement device further comprises a receiver configured to capture light while the LEDs are off and convert the captured light into a first signal and capture light while at least one of the LEDs is on and to convert the captured light into a second signal, the captured light including at least a portion of one of the first or second wavelengths reflected from the tissue. The measurement device is configured to improve a signal-to-noise ratio of the optical beam reflected from the tissue by differencing the first signal and the second signal. The light source is configured to further improve the signal-to-noise ratio of the optical beam reflected from the tissue by increasing the light intensity relative to the initial light intensity from at least one of the LEDs. The measurement device is further configured to generate an output signal representing at least in part a non-invasive measurement on blood contained within the tissue.

In another embodiment, a wearable device for use with a smart phone or tablet comprises a measurement device including a light source comprising a plurality of light emitting diodes (LEDs) for measuring one or more physiological parameters, the measurement device configured to generate, by modulating at least one of the LEDs having an initial light intensity, an optical beam having a plurality of optical wavelengths, wherein at least a portion of the plurality of optical wavelengths is a near-infrared wavelength between 700 nanometers and 2500 nanometers. The measurement device comprises one or more lenses configured to receive and to deliver a portion of the optical beam to tissue, wherein the tissue reflects at least a portion of the optical beam delivered to the tissue, and wherein the measurement device is adapted to be placed on a wrist or an ear of a user. The measurement device further comprises a receiver configured to capture light while the LEDs are off and convert the captured light into a first signal and capture light while at least one of the LEDs is on and convert the captured light into a second signal, the captured light including at least a portion of the optical beam reflected from the tissue. The measurement device is configured to improve a signal-to-noise ratio of the optical beam reflected from the tissue by differencing the first signal and the second signal. The light source is configured to further improve the signal-to-noise ratio of the optical beam reflected from the tissue by increasing the light intensity relative to the initial light intensity from at least one of the LEDs. The measurement device is further configured to generate an output signal representing at least in part a non-invasive measurement on blood contained within the tissue.

In one embodiment, a wearable device for use with a smart phone or tablet comprises a measurement device including a light source comprising a plurality of light emitting diodes (LEDs) for measuring one or more physiological parameters, the measurement device configured to generate, by modulating at least one of the LEDs having an initial light intensity, an optical beam having a plurality of optical wavelengths, wherein at least a portion of the plurality of optical wavelengths is a near-infrared wavelength between 700 nanometers and 2500 nanometers. The measurement device comprises one or more lenses configured to receive and to deliver a portion of the optical beam to tissue, wherein the tissue reflects at least a portion of the optical beam delivered to the tissue, and wherein the measurement device is adapted to be placed on a wrist or an ear of a user. The measurement device further comprises a receiver configured to capture light while the LEDs are off and convert the captured light into a first signal and capture light while at least one of the LEDs is on and convert the captured light into a second signal, the captured light including at least a portion of the optical beam reflected from the tissue. The measurement device is configured to improve a signal-to-noise ratio of the optical beam reflected from the tissue by differencing the first signal and the second signal. The light source is configured to further improve the signal-to-noise ratio of the optical beam reflected from the tissue by increasing the light intensity relative to the initial light intensity from at least one of the LEDs. The measurement device is further configured to generate an output signal representing at least in part a non-invasive measurement on blood contained within the tissue. The receiver includes a plurality of spatially separated detectors, wherein at least one analog to digital converter is coupled to the spatially separated detectors.

In one embodiment, a wearable device for use with a smart phone or tablet includes a measurement device including a light source comprising a plurality of light emitting diodes for measuring one or more physiological parameters, the measurement device configured to generate an input optical beam with one or more optical wavelengths, wherein at least a portion of the one or more optical wavelengths is a near-infrared wavelength between 700 nanometers and 2500 nanometers. The measurement device comprises one or more lenses configured to receive and to deliver a portion of the input optical beam to a sample comprising skin or tissue, wherein the sample reflects at least a portion of the input optical beam delivered to the sample. The measurement device further comprises a reflective surface configured to receive and redirect at least a portion of light reflected from the sample, and a receiver configured to receive at least a portion of the input optical beam reflected from the sample. The light source is configured to increase a signal-to-noise ratio of the input optical beam reflected from the sample, wherein the increased signal-to-noise ratio results from an increase to the light intensity from at least one of the plurality of light emitting diodes and from modulation of at least one of the plurality of light emitting diodes. The measurement device is configured to generate an output signal representing at least in part a non-invasive measurement on blood contained within the sample. The wearable device is configured to communicate with the smart phone or tablet, the smart phone or tablet comprising a wireless receiver, a wireless transmitter, a display, a voice input module, a speaker, and a touch screen. The smart phone or tablet is configured to receive and to process at least a portion of the output signal, wherein the smart phone or tablet is configured to store and display the processed output signal, and wherein at least a portion of the processed output signal is configured to be transmitted over a wireless transmission link.

In another embodiment, a wearable device for use with a smart phone or tablet includes a measurement device including a light source comprising a plurality of light emitting diodes for measuring one or more physiological parameters, the measurement device configured to generate an input optical beam with one or more optical wavelengths, wherein at least a portion of the one or more optical wavelengths is a near-infrared wavelength between 700 nanometers and 2500 nanometers. The measurement device comprises one or more lenses configured to receive and to deliver a portion of the input optical beam to a sample comprising skin or tissue, wherein the sample reflects at least a portion of the input optical beam delivered to the sample. The measurement device further comprises a reflective surface configured to receive and redirect at least a portion of light reflected from the sample. The measurement device further comprises a receiver configured to receive at least a portion of the input optical beam reflected from the sample, the receiver being located a first distance from a first one of the plurality of light emitting diodes and a different distance from a second one of the plurality of light emitting diodes such that the receiver receives a first signal from the first light emitting diode and a second signal from the second light emitting diode. The measurement device is configured to generate an output signal representing at least in part a non-invasive measurement on blood contained within the sample. The wearable device is configured to communicate with the smart phone or tablet. The smart phone or tablet comprises a wireless receiver, a wireless transmitter, a display, a voice input module, a speaker, and a touch screen, and is configured to receive and to process at least a portion of the output signal. The smart phone or tablet is configured to store and display the processed output signal, wherein at least a portion of the processed output signal is configured to be transmitted over a wireless transmission link.

In one embodiment, a method of measuring physiological information comprises providing a wearable device for use with a smart phone or tablet, the smart phone or tablet comprising a wireless receiver, a wireless transmitter, a display, a voice input module, a speaker, and a touch screen. The wearable device is capable of performing all of the steps comprising: generating an input optical beam having one or more optical wavelengths using a light source comprising a plurality of light emitting diodes, wherein at least a portion of the one or more optical wavelengths is a near-infrared wavelength between 700 nanometers and 2500 nanometers; delivering a portion of the input optical beam to a sample comprising skin or tissue using one or more lenses; receiving and reflecting at least a portion of the input optical beam reflected from the sample; receiving a portion of the input optical beam reflected from the sample to generate an output signal representing at least in part a non-invasive measurement on blood contained within the sample; increasing the signal-to-noise ratio of the input optical beam reflected from the sample by increasing a light intensity from at least one of the plurality of light emitting diodes and by modulating at least one of the plurality of light emitting diodes; and transmitting at least a portion of the output signal to the smart phone or tablet for processing to generate a processed output signal and for transmitting from the smart phone or tablet at least a portion of the processed output signal over a wireless transmission link.

In another embodiment, a method of measuring physiological information comprises providing a wearable device for use with a smart phone or tablet, the smart phone or tablet comprising a wireless receiver, a wireless transmitter, a display, a voice input module, a speaker, and a touch screen. The wearable device is capable of performing all of the steps comprising: generating a first and a second input optical beam each having one or more optical wavelengths using a light source comprising a plurality of light emitting diodes, wherein at least a portion of the one or more optical wavelengths is a near-infrared wavelength between 700 nanometers and 2500 nanometers; delivering a portion of the first input optical beam and a portion of the second input optical beam to a sample comprising skin or tissue using one or more lenses; receiving and reflecting at least a portion of the input optical beam reflected from the sample; receiving a portion of the first input optical beam reflected from the sample from a first one of the plurality of light emitting diodes located at a first distance and receiving a portion of the second input optical beam reflected from the sample from a different one of the plurality of light emitting diodes located at a distance different from the first distance to generate an output signal representing at least in part a non-invasive measurement on blood contained within the sample; and transmitting at least a portion of the output signal to the smart phone or tablet for processing to generate a processed output signal and for transmitting from the smart phone or tablet at least a portion of the processed output signal over a wireless transmission link.

BRIEF DESCRIPTION OF THE DRAWINGS

For a more complete understanding of the present disclosure, and for further features and advantages thereof, reference is now made to the following description taken in conjunction with the accompanying drawings, in which:

FIG. **1** illustrates the structure of a tooth.

FIG. **2A** shows the attenuation coefficient for dental enamel and water versus wavelength from approximately 600 nm to 2600 nm.

FIG. **2**B illustrates the absorption spectrum of intact enamel and dentine in the wavelength range of approximately 1.2 to 2.4 microns.

FIG. **3** shows the near infrared spectral reflectance over the wavelength range of approximately 800 nm to 2500 nm from an occlusal tooth surface. The black diamonds correspond to the reflectance from a sound, intact tooth section. The asterisks correspond to a tooth section with an enamel lesion. The circles correspond to a tooth section with a dentine lesion.

FIG. **4** illustrates a hand-held dental tool design of a human interface that may also be coupled with other dental tools.

FIG. **5**A illustrates a clamp design of a human interface to cap over one or more teeth and perform a non-invasive measurement for dental caries.

FIG. **5**B shows a mouth guard design of a human interface to perform a non-invasive measurement for dental caries.

FIG. **6**A illustrates the dorsal of a hand for performing a differential measurement for measuring blood constituents or analytes.

FIG. **6**B illustrates the dorsal of a foot for performing a differential measurement for measuring blood constituents or analytes.

FIG. **7** illustrates a block diagram or building blocks for constructing high power laser diode assemblies.

FIG. **8** shows a platform architecture for different wavelength ranges for an all-fiber-integrated, high powered, super-continuum light source.

FIG. **9** illustrates one embodiment for a short-wave infrared super-continuum light source.

FIG. **10** shows the output spectrum from the SWIR SC laser of FIG. **9** when about 10 m length of fiber for SC generation is used. This fiber is a single-mode, non-dispersion shifted fiber that is optimized for operation near 1550 nm.

FIG. **11**A illustrates a schematic of the experimental set-up for measuring the diffuse reflectance spectroscopy using the SWIR-SC light source of FIGS. **9** and **10**.

FIG. **11**B shows exemplary reflectance from a sound enamel region, an enamel lesion region, and a dentine lesion region. The spectra are normalized to have equal value near 2050 nm.

FIGS. **12**A-B illustrate high power SWIR-SC lasers that may generate light between approximately 1.4-1.8 microns (FIG. **12**A) or approximately 2-2.5 microns (FIG. **12**B).

FIG. **12**C shows a reflection-spectroscopy based stand-off detection system having an SC laser source.

FIG. **13** schematically shows that the medical measurement device can be part of a personal or body area network that communicates with another device (e.g., smart phone or tablet) that communicates with the cloud. The cloud may in turn communicate information with the user, dental or healthcare providers, or other designated recipients.

DETAILED DESCRIPTION OF EXAMPLE EMBODIMENTS

As required, detailed embodiments of the present disclosure are disclosed herein; however, it is to be understood that the disclosed embodiments are merely exemplary of the disclosure that may be embodied in various and alternative forms. The figures are not necessarily to scale; some features may be exaggerated or minimized to show details of particular components. Therefore, specific structural and functional details disclosed herein are not to be interpreted as limiting, but merely as a representative basis for teaching one skilled in the art to variously employ the present disclosure.

Near-infrared (NIR) and SWIR light may be preferred for caries detection compared to visible light imaging because the NIR/SWIR wavelengths generally have lower absorption by stains and deeper penetration into teeth. Hence, NIR/SWIR light may provide a caries detection method that can be non-invasive, non-contact and relatively stain insensitive. Broadband light may provide further advantages because carious regions may demonstrate spectral signatures from water absorption and the wavelength dependence of porosity in the scattering of light.

The wavelength of light should be selected appropriately to achieve a non-invasive procedure. For example, the light should be able to penetrate deep enough to reach through the dermis and subcutaneous fat layers to reach varicose veins. For example, the penetration depth may be defined as the inverse of the absorption coefficient, although it may also be necessary to include the scattering for the calculation. To achieve penetration deep enough to reach the varicose veins, wavelengths may correspond to local minima in water **501** and adipose **502** absorption, as well as potentially local minima in collagen **503** and elastin **504** absorption. For example, wavelengths near approximately 1100 nm, 1310 nm, or 1650 nm may be advantageous for non-invasive procedures. More generally, wavelength ranges of approximately 900 nm to 1150 nm, 1280 nm to 1340 nm, or 1550 nm to 1680 nm may be advantageous for non-invasive procedures.

In general, the near-infrared region of the electromagnetic spectrum covers between approximately 0.7 microns (700 nm) to about 2.5 microns (2500 nm). However, it may also be advantageous to use just the short-wave infrared between approximately 1.4 microns (1400 nm) and about 2.5 microns (2500 nm). One reason for preferring the SWIR over the entire NIR may be to operate in the so-called "eye safe" window, which corresponds to wavelengths longer than about 1400 nm. Therefore, for the remainder of the disclosure the SWIR will be used for illustrative purposes. However, it should be clear that the discussion that follows could also apply to using the NIR wavelength range, or other wavelength bands.

In particular, wavelengths in the eye safe window may not transmit down to the retina of the eye, and therefore, these wavelengths may be less likely to create permanent eye damage from inadvertent exposure. The near-infrared wavelengths have the potential to be dangerous, because the eye cannot see the wavelengths (as it can in the visible), yet they can penetrate and cause damage to the eye. Even if a practitioner is not looking directly at the laser beam, the practitioner's eyes may receive stray light from a reflection or scattering from some surface. Hence, it can always be a good practice to use eye protection when working around lasers. Since wavelengths longer than about 1400 nm are substantially not transmitted to the retina or substantially absorbed in the retina, this wavelength range is known as the eye safe window. For wavelengths longer than 1400 nm, in general only the cornea of the eye may receive or absorb the light radiation.

FIG. **1** illustrates the structure of an exemplary cross-section of a tooth **100**. The tooth **100** has a top layer called the crown **101** and below that a root **102** that reaches well into the gum **106** and bone **108** of the mouth. The exterior of the crown **101** is an enamel layer **103**, and below the enamel is a layer of dentine **104** that sits atop a layer of cementum **107**. Below the dentine **104** is a pulp region **105**, which comprises within it blood vessels **109** and nerves **110**. If the light can penetrate the enamel **103** and dentine **104**, then the blood flow and blood constituents may be measured through the blood vessels in the dental pulp **105**. While the amount of blood flow in the capillaries of the dental pulp **105** may be less than an artery or vein, the smaller blood flow could still be advantageous for detecting or measuring blood constituents as compared to detection through the skin if there is less interfering spectral features from the tooth. Although the structure of a molar tooth is illustrated in FIG. **1**, other types of teeth also have similar structure. For example, different types of teeth include molars, pre-molars, canine and incisor teeth.

As used throughout this document, the term "couple" and or "coupled" refers to any direct or indirect communication between two or more elements, whether or not those elements are physically connected to one another. As used throughout this disclosure, the term "spectroscopy" means that a tissue or sample is inspected by comparing different features, such as wavelength (or frequency), spatial location, transmission, absorption, reflectivity, scattering, refractive index, or opacity. In one embodiment, "spectroscopy" may mean that the wavelength of the light source is varied, and the transmission, absorption, or reflectivity of the tissue or sample is measured as a function of wavelength. In another embodiment, "spectroscopy" may mean that the wavelength dependence of the transmission, absorption or reflectivity is compared between different spatial locations on a tissue or sample. As an illustration, the "spectroscopy" may be performed by varying the wavelength of the light source, or by using a broadband light source and analyzing the signal using a spectrometer, wavemeter, or optical spectrum analyzer.

As used throughout this disclosure, the term "fiber laser" refers to a laser or oscillator that has as an output light or an optical beam, wherein at least a part of the laser comprises an optical fiber. For instance, the fiber in the "fiber laser" may comprise one of or a combination of a single mode fiber, a multi-mode fiber, a mid-infrared fiber, a photonic crystal fiber, a doped fiber, a gain fiber, or, more generally, an approximately cylindrically shaped waveguide or light-pipe. In one embodiment, the gain fiber may be doped with rare earth material, such as ytterbium, erbium, and/or thulium, for example. In another embodiment, the mid-infrared fiber may comprise one or a combination of fluoride fiber, ZBLAN fiber, chalcogenide fiber, tellurite fiber, or germanium doped fiber. In yet another embodiment, the single mode fiber may include standard single-mode fiber, dispersion shifted fiber, non-zero dispersion shifted fiber, high-nonlinearity fiber, and small core size fibers.

As used throughout this disclosure, the term "pump laser" refers to a laser or oscillator that has as an output light or an optical beam, wherein the output light or optical beam is coupled to a gain medium to excite the gain medium, which in turn may amplify another input optical signal or beam. In one particular example, the gain medium may be a doped fiber, such as a fiber doped with ytterbium, erbium, and/or thulium. In one embodiment, the "pump laser" may be a fiber laser, a solid state laser, a laser involving a nonlinear crystal, an optical parametric oscillator, a semiconductor laser, or a plurality of semiconductor lasers that may be multiplexed together. In another embodiment, the "pump laser" may be coupled to the gain medium by using a fiber coupler, a dichroic mirror, a multiplexer, a wavelength division multiplexer, a grating, or a fused fiber coupler.

As used throughout this document, the term "super-continuum" and or "supercontinuum" and or "SC" refers to

a broadband light beam or output that comprises a plurality of wavelengths. In a particular example, the plurality of wavelengths may be adjacent to one-another, so that the spectrum of the light beam or output appears as a continuous band when measured with a spectrometer. In one embodiment, the broadband light beam may have a bandwidth or at least 10 nm. In another embodiment, the "super-continuum" may be generated through nonlinear optical interactions in a medium, such as an optical fiber or nonlinear crystal. For example, the "super-continuum" may be generated through one or a combination of nonlinear activities such as four-wave mixing, the Raman effect, modulational instability, and self-phase modulation.

As used throughout this disclosure, the terms "optical light" and or "optical beam" and or "light beam" refer to photons or light transmitted to a particular location in space. The "optical light" and or "optical beam" and or "light beam" may be modulated or unmodulated, which also means that they may or may not contain information. In one embodiment, the "optical light" and or "optical beam" and or "light beam" may originate from a fiber, a fiber laser, a laser, a light emitting diode, a lamp, a pump laser, or a light source.

Transmission or Reflection Through Teeth

The transmission, absorption and reflection from teeth has been studied in the near infrared, and, although there are some features, the enamel and dentine appear to be fairly transparent in the near infrared (particularly SWIR wavelengths between about 1400 and 2500 nm). For example, the absorption or extinction ratio for light transmission has been studied. FIG. **2**A illustrates the attenuation coefficient **200** for dental enamel **201** (filled circles) and the absorption coefficient of water **202** (open circles) versus wavelength. Near-infrared light may penetrate much further without scattering through all the tooth enamel, due to the reduced scattering coefficient in normal enamel. Scattering in enamel may be fairly strong in the visible, but decreases as approximately $1/(\text{wavelength})^3$ [i.e., inverse of the cube of the wavelength] with increasing wavelength to a value of only 2-3 cm-1 at 1310 nm and 1550 nm in the near infrared. Therefore, enamel may be virtually transparent in the near infrared with optical attenuation 1-2 orders of magnitude less than in the visible range.

As another example, FIG. **2**B illustrates the absorption spectrum **250** of intact enamel **251** (dashed line) and dentine **252** (solid line) in the wavelength range of approximately 1.2 to 2.4 microns. In the near infrared there are two absorption bands in the areas of about 1.5 and 2 microns. The band with a peak around 1.57 microns may be attributed to the overtone of valent vibration of water present in both enamel and dentine. In this band, the absorption is greater for dentine than for enamel, which may be related to the large water content in this tissue. In the region of 2 microns, dentine may have two absorption bands, and enamel one. The band with a maximum near 2.1 microns may belong to the overtone of vibration of PO hydroxyapatite groups, which is the main substance of both enamel and dentine. Moreover, the band with a peak near 1.96 microns in dentine may correspond to water absorption (dentine may contain substantially higher water than enamel).

In addition to the absorption coefficient, the reflectance from intact teeth and teeth with dental caries (e.g., cavities) has been studied. In one embodiment, FIG. **3** shows the near infrared spectral reflectance **300** over the wavelength range of approximately 800 nm to 2500 nm from an occlusal (e.g., top) tooth surface **304**. The curve with black diamonds **301** corresponds to the reflectance from a sound, intact tooth section. The curve with asterisks (*) **302** corresponds to a tooth section with an enamel lesion. The curve with circles **303** corresponds to a tooth section with a dentine lesion. Thus, when there is a lesion, more scattering occurs and there may be an increase in the reflected light.

For wavelengths shorter than approximately 1400 nm, the shapes of the spectra remain similar, but the amplitude of the reflection changes with lesions. Between approximately 1400 nm and 2500 nm, an intact tooth **301** has low reflectance (e.g., high transmission), and the reflectance appears to be more or less independent of wavelength. On the other hand, in the presence of lesions **302** and **303**, there is increased scattering, and the scattering loss may be wavelength dependent. For example, the scattering loss may decrease as the inverse of some power of wavelength, such as $1/(\text{wavelength})^3$—so, the scattering loss decreases with longer wavelengths. When there is a lesion in the dentine **303**, more water can accumulate in the area, so there is also increased water absorption. For example, the dips near 1450 nm and 1900 nm may correspond to water absorption, and the reflectance dips are particularly pronounced in the dentine lesion **303**.

FIG. **3** may point to several novel techniques for early detection and quantification of carious regions. One method may be to use a relatively narrow wavelength range (for example, from a laser diode or super-luminescent laser diode) in the wavelength window below 1400 nm. In one embodiment, wavelengths in the vicinity of 1310 nm may be used, which is a standard telecommunications wavelength where appropriate light sources are available. Also, it may be advantageous to use a super-luminescent laser diode rather than a laser diode, because the broader bandwidth may avoid the production of laser speckle that can produce interference patterns due to light's scattering after striking irregular surfaces. As FIG. **3** shows, the amplitude of the reflected light (which may also be proportional to the inverse of the transmission) may increase with dental caries. Hence, comparing the reflected light from a known intact region with a suspect region may help identify carious regions. However, one difficulty with using a relatively narrow wavelength range and relying on amplitude changes may be the calibration of the measurement. For example, the amplitude of the reflected light may depend on many factors, such as irregularities in the dental surface, placement of the light source and detector, distance of the measurement instrument from the tooth, etc.

In one embodiment, use of a plurality of wavelengths can help to better calibrate the dental caries measurement. For example, a plurality of laser diodes or super-luminescent laser diodes may be used at different center wavelengths. Alternately, a lamp or alternate broadband light source may be used followed by appropriate filters, which may be placed after the light source or before the detectors. In one example, wavelengths near 1090 nm, 1440 nm and 1610 nm may be employed. The reflection from the tooth **305** appears to reach a local maximum near 1090 nm in the representative embodiment illustrated. Also, the reflectance near 1440 nm **306** is higher for dental caries, with a distinct dip particularly for dentine caries **303**. Near 1610 nm **307**, the reflection is also higher for carious regions. By using a plurality of wavelengths, the values at different wavelengths may help quantify a caries score. In one embodiment, the degree of enamel lesions may be proportional to the ratio of the reflectance near 1610 nm divided by the reflectance near 1090 nm. Also, the degree of dentine lesion may be proportional to the difference between the reflectance near 1610 nm and 1440 nm, with the difference then divided by the reflectance near 1090 nm. Although one set of wavelengths has been described, other wavelengths may also be used and are intended to be covered by this disclosure.

In yet another embodiment, it may be further advantageous to use all of some fraction of the SWIR between approximately 1400 and 2500 nm. For example, a SWIR super-continuum light source could be used, or a lamp source could be used. On the receiver side, a spectrometer and/or dispersive element could be used to discriminate the various wavelengths. As FIG. **3** shows, an intact tooth **301** has a relatively low and featureless reflectance over the SWIR. On the other hand, with a carious region there is more scattering, so the reflectance **302**,**303** increases in amplitude. Since the scattering is inversely proportional to wavelength or some power of wavelength, the carious region reflectance **302**, **303** also decreases with increasing wavelength. Moreover, the carious region may contain more water, so there are dips in the reflectance near the water absorption lines **306** and **308**. The degree of caries or caries score may be quantified by the shape of the spectrum over the SWIR, taking ratios of different parts of the spectrum, or some combination of this and other spectral processing methods.

Although several methods of early caries detection using spectral reflectance have been described, other techniques could also be used and are intended to be covered by this disclosure. For example, transmittance may be used rather than reflectance, or a combination of the two could be used. Moreover, the transmittance, reflectance and/or absorbance could also be combined with other techniques, such as quantitative light-induced fluorescence or fiber-optic trans-illumination. Also, the SWIR could be advantageous, but other parts of the infrared, near-infrared or visible wavelengths may also be used consistent with this disclosure.

One other benefit of the absorption, transmission or reflectance in the near infrared and SWIR may be that stains and non-calcified plaque are not visible in this wavelength range, enabling better discrimination of defects, cracks, and demineralized areas. For example, dental calculus, accumulated plaque, and organic stains and debris may interfere significantly with visual diagnosis and fluorescence-based caries detection schemes in occlusal surfaces. In the case of using quantitative light-induced fluorescence, such confounding factors typically may need to be removed by prophylaxis (abrasive cleaning) before reliable measurements can be taken. Surface staining at visible wavelengths may further complicate the problem, and it may be difficult to determine whether pits and fissures are simply stained or demineralized. On the other hand, staining and pigmentation generally interfere less with NIR or SWIR imaging. For example, NIR and SWIR light may not be absorbed by melanin and porphyrins produced by bacteria and those found in food dyes that accumulate in dental plaque and are responsible for the pigmentation.

Human Interface for Measurement System

A number of different types of measurements may be used to image for dental caries, particularly early detection of dental caries. A basic feature of the measurements may be that the optical properties are measured as a function of wavelength at a plurality of wavelengths. As further described below, the light source may output a plurality of wavelengths, or a continuous spectrum over a range of wavelengths. In one embodiment, the light source may cover some or all of the wavelength range between approximately 1400 nm and 2500 nm. The signal may be received at a receiver, which may also comprise a spectrometer or filters to discriminate between different wavelengths. The signal may also be received at a camera, which may also comprise filters or a spectrometer. In one embodiment, the spectral discrimination using filters or a spectrometer may be placed after the light source rather than at the receiver. The receiver usually comprises one or more detectors (optical-to-electrical conversion element) and electrical circuitry. The receiver may also be coupled to analog to digital converters, particularly if the signal is to be fed to a digital device.

Referring to FIG. **1**, one or more light sources **111** may be used for illumination. In one embodiment, a transmission measurement may be performed by directing the light source output **111** to the region near the interface between the gum **106** and dentine **104**. In one embodiment, the light may be directed using a light guide or a fiber optic. The light may then propagate through the dental pulp **105** to the other side, where the light may be incident on one or more detectors or another light guide to transport the signal to **112** a spectrometer, receiver, and/or camera, for example. In one embodiment, the light source may be directed to one or more locations near the interface between the gum **106** and dentine **104** (in one example, could be from the two sides of the tooth). The transmitted light may then be detected in the occlusal surface above the tooth using a **112** spectrometer, receiver, or camera, for example. In another embodiment, a reflectance measurement may be conducted by directing the light source output **111** to, for example, the occlusal surface of the tooth, and then detecting the reflectance at a **113** spectrometer, receiver or camera. Although a few embodiments for imaging the tooth are described, other embodiments and techniques may also be used and are intended to be covered by this disclosure. These optical techniques may measure optical properties such as reflectance, transmittance, absorption, or luminescence.

In one embodiment, FIG. **4** shows that the light source and/or detection system may be integrated with a dental hand-piece **400**. The hand-piece **400** may also include other dental equipment, such as a drill, pick, air spray or water cooling stream. The dental hand-piece **400** may include a housing **401** and a motor housing **402** (in some embodiments such as with a drill, a motor may be placed in this section). The end of hand-piece **403** that interfaces with the tooth may be detachable, and it may also have the light input and output end. The dental hand-piece **400** may also have an umbilical cord **404** for connecting to power supplies, diagnostics, or other equipment, for example.

A light guide **405** may be integrated with the hand-piece **400**, either inside the housing **401**, **402** or adjacent to the housing. In one embodiment, a light source **410** may be contained within the housing **401**, **402**. In an alternative embodiment, the hand-piece **400** may have a coupler **410** to couple to an external light source **411** and/or detection system or receiver **412**. The light source **411** may be coupled to the hand-piece **400** using a light guide or fiber optic cable **406**. In addition, the detection system or receiver **412** may be coupled to the hand-piece **400** using one or more light guides, fiber optic cable or a bundle of fibers **407**.

The light incident on the tooth may exit the hand-piece **400** through the end **403**. The end **403** may also have a lens system or curved mirror system to collimate or focus the light. In one embodiment, if the light source is integrated with a tool such as a drill, then the light may reach the tooth at the same point as the tip of the drill. The reflected or transmitted light from the tooth may then be observed externally and/or guided back through the light guide **405** in the hand-piece **400**. If observed externally, there may be a lens system **408** for collecting the light and a detection system **409** that may have one or more detectors and electronics. If the light is to be guided back through the hand-piece **400**, then the reflected light may transmit through the light guide **405** back to the detection system or receiver **412**. In one embodiment, the incident light may be guided by a fiber optic through the light guide **405**, and the reflected light may be captured by a series of fibers forming a bundle adjacent to or surrounding the incident light fiber.

In another embodiment, a "clamp" design **500** may be used as a cap over one or more teeth, as illustrated in FIG. **5**A. The clamp design may be different for different types of teeth, or it may be flexible enough to fit over different types of teeth. For example, different types of teeth include the molars (toward the back of the mouth), the premolars, the canine, and the incisors (toward the front of the mouth). One embodiment of the clamp-type design is illustrated in FIG. **5**A for a molar tooth **508**. The C-clamp **501** may be made of a plastic or rubber material, and it may comprise a light source input **502** and a detector output **503** on the front or back of the tooth, for example.

The light source input **502** may comprise a light source directly, or it may have light guided to it from an external light source. Also, the light source input **502** may comprise a lens system to collimate or focus the light across the tooth. The detector output **503** may comprise a detector directly, or it may have a light guide to transport the signal to an external detector element. The light source input **502** may be coupled electrically or optically through **504** to a light input **506**. For example, if the light source is external in **506**, then the coupling element **504** may be a light guide, such as a fiber optic. Alternately, if the light source is contained in **502**, then the coupling element **504** may be electrical wires connecting to a power supply in **506**. Similarly, the detector output **503** may be coupled to a detector output unit **507** with a coupling element **505**, which may be one or more electrical wires or a light guide, such as a fiber optic. This is just one example of a clamp over one or more teeth, but other embodiments may also be used and are intended to be covered by this disclosure. For example, if reflectance from the teeth is to be used in the measurement, then the light input **502** and detected light input **503** may be on the same side of the tooth.

In yet another embodiment, one or more light source ports and sensor ports may be used in a mouth-guard type design. For example, one embodiment of a dental mouth guard **550** is illustrated in FIG. **5**B. The structure of the mouth guard **551** may be similar to mouth guards used in sports (e.g., when playing football or boxing) or in dental trays used for applying fluoride treatment, and the mouth guard may be made from plastic, rubber, or any other suitable materials. As an example, the mouth guard may have one or more light source input ports **552**, **553** and one or more detector output ports **554**, **555**. Although six input and output ports are illustrated, any number of ports may be used.

Similar to the clamp design described above, the light source inputs **552**, **553** may comprise one or more light sources directly, or they may have light guided to them from an external light source. Also, the light source inputs **552**, **553** may comprise lens systems to collimate or focus the light across the teeth. The detector outputs **554**, **555** may comprise one or more detectors directly, or they may have one or more light guides to transport the signals to an external detector element. The light source inputs **552**, **553** may be coupled electrically or optically through **556** to a light input **557**. For example, if the light source is external in **557**, then the one or more coupling elements **556** may be one or more light guides, such as a fiber optic. Alternately, if the light sources are contained in **552**, **553**, then the coupling element **556** may be one or more electrical wires connecting to a power supply in **557**. Similarly, the detector outputs **554**, **555** may be coupled to a detector output unit **559** with one or more coupling elements **558**, which may be one or more electrical wires or one or more light guides, such as a fiber optic. This is just one example of a mouth guard design covering a plurality of teeth, but other embodiments may also be used and are intended to be covered by this disclosure. For instance, the position of the light source inputs and detector output ports could be exchanged, or some mixture of locations of light source inputs and detector output ports could be used. Also, if reflectance from the teeth is to be measured, then the light sources and detectors may be on the same side of the tooth. Moreover, it may be advantageous to pulse the light source with a particular pulse width and pulse repetition rate, and then the detection system can measure the pulsed light returned from or transmitted through the tooth. Using a lock-in type technique (e.g., detecting at the same frequency as the pulsed light source and also possibly phase locked to the same signal), the detection system may be able to reject background or spurious signals and increase the signal-to-noise ratio of the measurement.

Other elements may be added to the human interface designs of FIGS. **4**-**6** and are also intended to be covered by this disclosure. For instance, in one embodiment it may be desirable to have replaceable inserts that may be disposable. Particularly in a dentist's or doctor's office or hospital setting, the same instrument may be used with a plurality of patients. Rather than disinfecting the human interface after each use, it may be preferable to have disposable inserts that can be thrown away after each use. In one embodiment, a thin plastic coating material may enclose the clamp design of FIG. **5**A or mouth guard design of FIG. **5**B. The coating material may be inserted before each use, and then after the measurement is exercised the coating material may be peeled off and replaced. The coating or covering material may be selected based on suitable optical properties that do not affect the measurement, or known optical properties that can be calibrated or compensated for during measurement. Such a design may save the dentist or physician or user considerable time, while at the same time provide the business venture with a recurring cost revenue source.

Thus, beyond the problem of other blood constituents or analytes having overlapping spectral features, it may be difficult to observe glucose spectral signatures through the skin and its constituents of water, adipose, collagen and elastin. One approach to overcoming this difficulty may be to try to measure the blood constituents in veins that are located at relatively shallow distances below the skin. Veins may be more beneficial for the measurement than arteries, since arteries tend to be located at deeper levels below the skin. Also, in one embodiment it may be advantageous to use a differential measurement to subtract out some of the interfering absorption lines from the skin. For example, an instrument head may be designed to place one probe above a region of skin over a blood vein, while a second probe may be placed at a region of the skin without a noticeable blood vein below it. Then, by differencing the signals from the two probes, at least part of the skin interference may be cancelled out.

Two representative embodiments for performing such a differential measurement are illustrated in FIG. **6**A and FIG. **6**B. In one embodiment shown in FIG. **6**A, the dorsal of the hand **600** may be used for measuring blood constituents or analytes. The dorsal of the hand **600** may have regions that have distinct veins **601** as well as regions where the veins are not as shallow or pronounced **602**. By stretching the hand and leaning it backwards, the veins **601** may be accentuated in some cases. A near-infrared diffuse reflectance measurement may be performed by placing one probe **603** above the vein-rich region **601**. To turn this into a differential measurement, a second probe **604** may be placed above a region without distinct veins **602**. Then, the outputs from the two probes may be subtracted **605** to at least partially cancel out the features from the skin. The subtraction may be done preferably in the electrical domain, although it can also be performed in the optical domain or digitally/mathematically using sampled data based on the electrical and/or optical signals. Although one example of using the dorsal of the hand **600** is shown, many other parts of the hand can be used within the scope of this disclosure. For example, alternate methods may use transmission through the webbing between the thumb and the fingers **606**, or transmission or diffuse reflection through the tips of the fingers **607**.

In another embodiment, the dorsal of the foot **650** may be used instead of the hand. One advantage of such a configuration may be that for self-testing by a user, the foot may be easier to position the instrument using both hands. One probe **653** may be placed over regions where there are more distinct veins **651**, and a near-infrared diffuse reflectance measurement may be made. For a differential measurement, a second probe **654** may be placed over a region with less prominent veins **652**, and then the two probe signals may be subtracted, either electronically or optically, or may be digitized/sampled and processed mathematically depending on the particular application and implementation. As with the hand, the differential measurements may be intended to compensate for or subtract out (at least in part) the interference from the skin. Since two regions are used in close proximity on the same body part, this may also aid in removing some variability in the skin from environmental effects such as temperature, humidity, or pressure. In addition, it may be advantageous to first treat the skin before the measurement, by perhaps wiping with a cloth or treated cotton ball, applying some sort of cream, or placing an ice cube or chilled bag over the region of interest.

Although two embodiments have been described, many other locations on the body may be used using a single or differential probe within the scope of this disclosure. In yet another embodiment, the wrist may be advantageously used, particularly where a pulse rate is typically monitored. Since the pulse may be easily felt on the wrist, there is underlying the region a distinct blood flow. Other embodiments may use other parts of the body, such as the ear lobes, the tongue, the inner lip, the nails, the eye, or the teeth. Some of these embodiments will be further described below. The ear lobes or the tip of the tongue may be advantageous because they are thinner skin regions, thus permitting transmission rather than diffuse reflection. However, the interference from the skin is still a problem in these embodiments. Other regions such as the inner lip or the bottom of the tongue may be contemplated because distinct veins are observable, but still the interference from the skin may be problematic in these embodiments. The eye may seem as a viable alternative because it is more transparent than skin. However, there are still issues with scattering in the eye. For example, the anterior chamber of the eye (the space between the cornea and the iris) comprises a fluid known as aqueous humor. However, the glucose level in the eye chamber may have a significant temporal lag on changes in the glucose level compared to the blood glucose level.

Light Sources for Near Infrared

There are a number of light sources that may be used in the near infrared. To be more specific, the discussion below will consider light sources operating in the short wave infrared (SWIR), which may cover the wavelength range of approximately 1400 nm to 2500 nm. Other wavelength ranges may also be used for the applications described in this disclosure, so the discussion below is merely provided as exemplary types of light sources. The SWIR wavelength range may be valuable for a number of reasons. First, the SWIR corresponds to a transmission window through water and the atmosphere. Second, the so-called "eye-safe" wavelengths are wavelengths longer than approximately 1400 nm. Third, the SWIR covers the wavelength range for nonlinear combinations of stretching and bending modes as well as the first overtone of C-H stretching modes. Thus, for example, glucose and ketones among other substances may have unique signatures in the SWIR. Moreover, many solids have distinct spectral signatures in the SWIR, so particular solids may be identified using stand-off detection or remote sensing. For instance, many explosives have unique signatures in the SWIR.

Different light sources may be selected for the SWIR based on the needs of the application. Some of the features for selecting a particular light source include power or intensity, wavelength range or bandwidth, spatial or temporal coherence, spatial beam quality for focusing or transmission over long distance, and pulse width or pulse repetition rate. Depending on the application, lamps, light emitting diodes (LEDs), laser diodes (LD's), tunable LD's, super-luminescent laser diodes (SLDs), fiber lasers or super-continuum sources (SC) may be advantageously used. Also, different fibers may be used for transporting the light, such as fused silica fibers, plastic fibers, mid-infrared fibers (e.g., tellurite, chalcogenides, fluorides, ZBLAN, etc), or a hybrid of these fibers.

Lamps may be used if low power or intensity of light is required in the SWIR, and if an incoherent beam is suitable. In one embodiment, in the SWIR an incandescent lamp that can be used is based on tungsten and halogen, which have an emission wavelength between approximately 500 nm to 2500 nm. For low intensity applications, it may also be possible to use thermal sources, where the SWIR radiation is based on the black body radiation from the hot object. Although the thermal and lamp based sources are broadband and have low intensity fluctuations, it may be difficult to achieve a high signal-to-noise ratio due to the low power levels. Also, the lamp based sources tend to be energy inefficient.

In another embodiment, LED's can be used that have a higher power level in the SWIR wavelength range. LED's also produce an incoherent beam, but the power level can be higher than a lamp and with higher energy efficiency. Also, the LED output may more easily be modulated, and the LED provides the option of continuous wave or pulsed mode of operation. LED's are solid state components that emit a wavelength band that is of moderate width, typically between about 20 nm to 40 nm. There are also so-called super-luminescent LEDs that may even emit over a much wider wavelength range. In another embodiment, a wide band light source may be constructed by combining different LEDs that emit in different wavelength bands, some of which could preferably overlap in spectrum. One advantage

of LEDs as well as other solid state components is the compact size that they may be packaged into.

In yet another embodiment, various types of laser diodes may be used in the SWIR wavelength range. Just as LEDs may be higher in power but narrower in wavelength emission than lamps and thermal sources, the LDs may be yet higher in power but yet narrower in wavelength emission than LEDs. Different kinds of LDs may be used, including Fabry-Perot LDs, distributed feedback (DFB) LDs, distributed Bragg reflector (DBR) LDs. Since the LDs have relatively narrow wavelength range (typically under 10 nm), in one embodiment a plurality of LDs may be used that are at different wavelengths in the SWIR. The various LDs may be spatially multiplexed, polarization multiplexed, wavelength multiplexed, or a combination of these multiplexing methods. Also, the LDs may be fiber pig-tailed or have one or more lenses on the output to collimate or focus the light. Another advantage of LDs is that they may be packaged compactly and may have a spatially coherent beam output. Moreover, tunable LDs that can tune over a range of wavelengths are also available. The tuning may be done by varying the temperature, or electrical current may be used in particular structures such as distributed Bragg reflector (DBR) LDs, for example. In another embodiment, external cavity LDs may be used that have a tuning element, such as a fiber grating or a bulk grating, in the external cavity.

In another embodiment, super-luminescent laser diodes may provide higher power as well as broad bandwidth. An SLD is typically an edge emitting semiconductor light source based on super-luminescence (e.g., this could be amplified spontaneous emission). SLDs combine the higher power and brightness of LDs with the low coherence of conventional LEDs, and the emission band for SLD's may be 5 to 100 nm wide, preferably in the 60 to 100 nm range. Although currently SLDs are commercially available in the wavelength range of approximately 400 nm to 1700 nm, SLDs could and may in the future be made to cover a broader region of the SWIR.

In yet another embodiment, high power LDs for either direct excitation or to pump fiber lasers and SC light sources may be constructed using one or more laser diode bar stacks. FIG. **7** shows an example of a block diagram **700** or building blocks for constructing the high power LDs. In this embodiment, one or more diode bar stacks **701** may be used, where the diode bar stack may be an array of several single emitter LDs. Since the fast axis (e.g., vertical direction) may be nearly diffraction limited while the slow-axis (e.g., horizontal axis) may be far from diffraction limited, different collimators **702** may be used for the two axes.

Then, the brightness may be increased by spatially combining the beams from multiple stacks **703**. The combiner may include spatial interleaving, it may include wavelength multiplexing, or it may involve a combination of the two. Different spatial interleaving schemes may be used, such as using an array of prisms or mirrors with spacers to bend one array of beams into the beam path of the other. In another embodiment, segmented mirrors with alternate high-reflection and anti-reflection coatings may be used. Moreover, the brightness may be increased by polarization beam combining **704** the two orthogonal polarizations, such as by using a polarization beam splitter. In a particular embodiment, the output may then be focused or coupled into a large diameter core fiber. As an example, typical dimensions for the large diameter core fiber range from diameters of approximately 100 microns to 400 microns or more. Alternatively or in addition, a custom beam shaping module **705** may be used, depending on the particular application. For example, the output of the high power LD may be used directly **706**, or it may be fiber coupled **707** to combine, integrate, or transport the high power LD energy. These high power LDs may grow in importance because the LD powers can rapidly scale up. For example, instead of the power being limited by the power available from a single emitter, the power may increase in multiples depending on the number of diodes multiplexed and the size of the large diameter fiber. Although FIG. **7** is shown as one embodiment, some or all of the elements may be used in a high power LD, or additional elements may also be used.

SWIR Super-Continuum Lasers

Each of the light sources described above have particular strengths, but they also may have limitations. For example, there is typically a trade-off between wavelength range and power output. Also, sources such as lamps, thermal sources, and LEDs produce incoherent beams that may be difficult to focus to a small area and may have difficulty propagating for long distances. An alternative source that may overcome some of these limitations is an SC light source. Some of the advantages of the SC source may include high power and intensity, wide bandwidth, spatially coherent beam that can propagate nearly transform limited over long distances, and easy compatibility with fiber delivery.

Supercontinuum lasers may combine the broadband attributes of lamps with the spatial coherence and high brightness of lasers. By exploiting a modulational instability initiated supercontinuum (SC) mechanism, an all-fiber-integrated SC laser with no moving parts may be built using commercial-off-the-shelf (COTS) components. Moreover, the fiber laser architecture may be a platform where SC in the visible, near-infrared/SWIR, or mid-IR can be generated by appropriate selection of the amplifier technology and the SC generation fiber. But until recently, SC lasers were used primarily in laboratory settings since typically large, table-top, mode-locked lasers were used to pump nonlinear media such as optical fibers to generate SC light. However, those large pump lasers may now be replaced with diode lasers and fiber amplifiers that gained maturity in the telecommunications industry.

In one embodiment, an all-fiber-integrated, high-powered SC light source **800** may be elegant for its simplicity (FIG. **8**). The light may be first generated from a seed laser diode **801**. For example, the seed LD **801** may be a distributed feedback (DFB) laser diode with a wavelength near 1542 or 1550 nm, with approximately 0.5-2.0 ns pulsed output, and with a pulse repetition rate between about one kilohertz to about 100 MHz or more. The output from the seed laser diode may then be amplified in a multiple-stage fiber amplifier **802** comprising one or more gain fiber segments. In one embodiment, the first stage pre-amplifier **803** may be designed for optimal noise performance. For example, the pre-amplifier **803** may be a standard erbium-doped fiber amplifier or an erbium/ytterbium doped cladding pumped fiber amplifier. Between amplifier stages **803** and **806**, it may be advantageous to use band-pass filters **804** to block amplified spontaneous emission and isolators **805** to prevent spurious reflections. Then, the power amplifier stage **806** may use a cladding-pumped fiber amplifier that may be optimized to minimize nonlinear distortion. The power amplifier fiber **806** may also be an erbium-doped fiber amplifier, if only low or moderate power levels are to be generated.

The SC generation **807** may occur in the relatively short lengths of fiber that follow the pump laser. The SC fiber length may range from around a few millimeters to 100 m or more. In one embodiment, the SC generation may occur in a first fiber **808** where the modulational-instability initiated pulse break-up occurs primarily, followed by a second fiber **809** where the SC generation and spectral broadening occurs primarily.

In one embodiment, one or two meters of standard single-mode fiber (SMF) after the power amplifier stage may be followed by several meters of SC generation fiber. For this example, in the SMF the peak power may be several kilowatts and the pump light may fall in the anomalous group-velocity dispersion regime---often called the soliton regime. For high peak powers in the anomalous dispersion regime, the nanosecond pulses may be unstable due to a phenomenon known as modulational instability, which is basically parametric amplification in which the fiber nonlinearity helps to phase match the pulses. As a consequence, the nanosecond pump pulses may be broken into many shorter pulses as the modulational instability tries to form soliton pulses from the quasi-continuous-wave background. Although the laser diode and amplification process starts with approximately nanosecond-long pulses, modulational instability in the short length of SMF fiber may form approximately 0.5 ps to several-picosecond-long pulses with high intensity. Thus, the few meters of SMF fiber may result in an output similar to that produced by mode-locked lasers, except in a much simpler and cost-effective manner.

The short pulses created through modulational instability may then be coupled into a nonlinear fiber for SC generation. The nonlinear mechanisms leading to broadband SC may include four-wave mixing or self-phase modulation along with the optical Raman effect. Since the Raman effect is self-phase-matched and shifts light to longer wavelengths by emission of optical photons, the SC may spread to longer wavelengths very efficiently. The short-wavelength edge may arise from four-wave mixing, and often times the short wavelength edge may be limited by increasing group-velocity dispersion in the fiber. In many instances, if the particular fiber used has sufficient peak power and SC fiber length, the SC generation process may fill the long-wavelength edge up to the transmission window.

Mature fiber amplifiers for the power amplifier stage **806** include ytterbium-doped fibers (near 1060 nm), erbium-doped fibers (near 1550 nm), erbium/ytterbium-doped fibers (near 1550 nm), or thulium-doped fibers (near 2000 nm). In various embodiments, candidates for SC fiber **809** include fused silica fibers (for generating SC between 0.8-2.7 μm), mid-IR fibers such as fluorides, chalcogenides, or tellurites (for generating SC out to 4.5 μm or longer), photonic crystal fibers (for generating SC between 0.4 and 1.7 μm), or combinations of these fibers. Therefore, by selecting the appropriate fiber-amplifier doping for **806** and nonlinear fiber **809**, SC may be generated in the visible, near-IR/SWIR, or mid-IR wavelength region.

The configuration **800** of FIG. **8** is just one particular example, and other configurations can be used and are intended to be covered by this disclosure. For example, further gain stages may be used, and different types of lossy elements or fiber taps may be used between the amplifier stages. In another embodiment, the SC generation may occur partially in the amplifier fiber and in the pig-tails from the pump combiner or other elements. In yet another embodiment, polarization maintaining fibers may be used, and a polarizer may also be used to enhance the polarization contrast between amplifier stages. Also, not discussed in detail are many accessories that may accompany this set-up, such as driver electronics, pump laser diodes, safety shut-offs, and thermal management and packaging.

In one embodiment, one example of the SC laser that operates in the SWIR is illustrated in FIG. **9**. This SWIR SC source **900** produces an output of up to approximately 5 W over a spectral range of about 1.5 to 2.4 microns, and this particular laser is made out of polarization maintaining components. The seed laser **901** is a distributed feedback (DFB) laser operating near 1542 nm producing approximately 0.5 nsec pulses at an about 8 MHz repetition rate. The pre-amplifier **902** is forward pumped and uses about 2 m length of erbium/ytterbium cladding pumped fiber **903** (often also called dual-core fiber) with an inner core diameter of 12 microns and outer core diameter of 130 microns. The pre-amplifier gain fiber **903** is pumped using a 10 W laser diode near 940 nm **905** that is coupled in using a fiber combiner **904**.

In this particular 5 W unit, the mid-stage between amplifier stages **902** and **906** comprises an isolator **907**, a band-pass filter **908**, a polarizer **909** and a fiber tap **910**. The power amplifier **906** uses an approximately 4 m length of the 12/130 micron erbium/ytterbium doped fiber **911** that is counter-propagating pumped using one or more 30 W laser diodes near 940 nm **912** coupled in through a combiner **913**. An approximately 1-2 meter length of the combiner pig-tail helps to initiate the SC process, and then a length of PM-1550 fiber **915** (polarization maintaining, single-mode, fused silica fiber optimized for 1550 nm) is spliced **914** to the combiner output.

If an output fiber of about 10 m in length is used, then the resulting output spectrum **1000** is shown in FIG. **10**. The details of the output spectrum **1000** depend on the peak power into the fiber, the fiber length, and properties of the fiber such as length and core size, as well as the zero dispersion wavelength and the dispersion properties. For example, if a shorter length of fiber is used, then the spectrum actually reaches to longer wavelengths (e.g., a 2 m length of SC fiber broadens the spectrum to about 2500 nm). Also, if extra-dry fibers are used with less O-H content, then the wavelength edge may also reach to a longer wavelength. To generate more spectra toward the shorter wavelengths, the pump wavelength (in this case ~1542 nm) should be close to the zero dispersion wavelength in the fiber. For example, by using a dispersion shifted fiber or so-called non-zero dispersion shifted fiber, the short wavelength edge may shift to shorter wavelengths.

In one particular embodiment, the SWIR-SC light source of FIG. **9** with output spectrum in FIG. **10** was used in preliminary experiments for examining the reflectance from different dental samples. A schematic of the experimental set-up 1100 for measuring the diffuse reflectance spectroscopy is illustrated in FIG. **11**A. The SC source **1101** in this embodiment was based on the design of FIG. **9** and delivered approximately 1.6 W of light over the wavelength range from about 1500-2400 nm. The output beam **1102** was collimated, and then passed through a chopper **1103** (for lock-in detection at the receiver after the spectrometer **1106**) and an aperture **1104** for localizing the beam on the tooth location. Different teeth **1105** with different lesions and caries were placed in front of the aperture **1104**, and the scattered light was passed through a spectrometer **1106** and collected on a detector, whose signal was sent to a receiver. The tooth samples **1105** were mounted in clay or putty for standing upright. Different types of teeth could be used, including molars, premolars, canine and incisor teeth.

FIG. **11**B shows exemplary reflectance spectra **1150** from a sound enamel region **1151** (e.g., without dental caries), an enamel lesion region **1152**, and a dentine lesion region **1153** of various teeth. The spectra are normalized to have equal value near 2050 nm. In this particular embodiment, the slope from the sound enamel **1151** is steepest between about 1500 and 1950 nm, with a lesser slope in the presence of an enamel lesion **1152**. When there is a sample with dentine lesion **1153**, more features appear in the spectrum from the presence of water absorption lines from water that collects in the dentine. For this experiment, the spectra **1151**, **1152**, and **1153** are flatter in the wavelength region between about 1950 nm and 2350 nm. These are preliminary results, but they show the benefit of using broadband sources such as the SWIR-SC source for diagnosing dental caries. Although the explanation behind the different spectra **1150** of FIG. **11**B may not be understood as yet, it is clear that the spectra **1151**, **1152** and **1153** are distinguishable. Therefore, the broadband reflectance may be used for detection of dental caries and analyzing the region of the caries. Although diffuse reflectance has been used in this experiment, other signals, such as transmission, reflectance or a combination, may also be used and are covered by this disclosure.

Although one particular example of a 5 W SWIR-SC has been described, different components, different fibers, and different configurations may also be used consistent with this disclosure. For instance, another embodiment of the similar configuration **900** in FIG. **9** may be used to generate high powered SC between approximately 1060 and 1800 nm. For this embodiment, the seed laser **901** may be a distributed feedback laser diode of about 1064 nm, the pre-amplifier gain fiber **903** may be a ytterbium-doped fiber amplifier with 10/125 microns dimensions, and the pump laser **905** may be a 10 W laser diode near 915 nm. A mode field adapter may be including in the mid-stage, in addition to the isolator **907**, band pass filter **908**, polarizer **909** and tap **910**. The gain fiber **911** in the power amplifier may be an about 20 m length of ytterbium-doped fiber with 25/400 microns dimension. The pump **912** for the power amplifier may be up to six pump diodes providing 30 W each near 915 nm. For this much pump power, the output power in the SC may be as high as 50 W or more.

In an alternate embodiment, it may be desirous to generate high power SWIR SC over 1.4-1.8 microns and separately 2-2.5 microns (the window between 1.8 and 2 microns may be less important due to the strong water and atmospheric absorption). For example, the SC source of FIG. **12**A can lead to bandwidths ranging from about 1400 nm to 1800 nm or broader, while the SC source of FIG. **12**B can lead to bandwidths ranging from about 1900 nm to 2500 nm or broader. Since these wavelength ranges are shorter than about 2500 nm, the SC fiber can be based on fused silica fiber. Exemplary SC fibers include standard single-mode fiber (SMF), high-nonlinearity fiber, high-NA fiber, dispersion shifted fiber, dispersion compensating fiber, and photonic crystal fibers. Non-fused-silica fibers can also be used for SC generation, including chalcogenides, fluorides, ZBLAN, tellurites, and germanium oxide fibers.

In one embodiment, FIG. **12**A illustrates a block diagram for an SC source **1200** capable of generating light between approximately 1400 and 1800 nm or broader. As an example, a pump fiber laser similar to FIG. **9** can be used as the input to a SC fiber **1209**. The seed laser diode **1201** can comprise a DFB laser that generates, for example, several milliwatts of power around 1542 nm or 1553 nm. The fiber pre-amplifier **1202** can comprise an erbium-doped fiber amplifier or an erbium/ytterbium doped double clad fiber. In this example a mid-stage amplifier **1203** can be used, which can comprise an erbium/ytterbium doped double-clad fiber.

A bandpass filter **1205** and isolator **1206** may be used between the pre-amplifier **1202** and mid-stage amplifier **1203**. The power amplifier stage **1204** can comprise a larger core size erbium/ytterbium doped double-clad fiber, and another bandpass filter **1207** and isolator **1208** can be used before the power amplifier **1204**. The output of the power amplifier can be coupled to the SC fiber **1209** to generate the SC output **1210**. This is just one exemplary configuration for an SC source, and other configurations or elements may be used consistent with this disclosure.

In yet another embodiment, FIG. **12**B illustrates a block diagram for an SC source **1250** capable of generating light between approximately 1900 and 2500 nm or broader. As an example, the seed laser diode **1251** can comprise a DFB or DBR laser that generates, for example, several milliwatts of power around 1542 nm or 1553 nm. The fiber pre-amplifier **1252** can comprise an erbium-doped fiber amplifier or an erbium/ytterbium doped double-clad fiber. In this example a mid-stage amplifier **1253** can be used, which can comprise an erbium/ytterbium doped double-clad fiber. A bandpass filter **1255** and isolator **1256** may be used between the pre-amplifier **1252** and mid-stage amplifier **1253**. The power amplifier stage **1254** can comprise a thulium doped double-clad fiber, and another isolator **1257** can be used before the power amplifier **1254**. Note that the output of the mid-stage amplifier **1253** can be approximately near 1542 nm, while the thulium-doped fiber amplifier **1254** can amplify wavelengths longer than approximately 1900 nm and out to about 2100 nm. Therefore, for this configuration wavelength shifting may be required between 1253 and 1254. In one embodiment, the wavelength shifting can be accomplished using a length of standard single-mode fiber **1258**, which can have a length between approximately 5 and 50 meters, for example. The output of the power amplifier **1254** can be coupled to the SC fiber **1259** to generate the SC output **1260**. This is just one exemplary configuration for an SC source, and other configurations or elements can be used consistent with this disclosure. For example, the various amplifier stages can comprise different amplifier types, such as erbium doped fibers, ytterbium doped fibers, erbium/ytterbium co-doped fibers and thulium doped fibers.

FIG. **12**C illustrates a reflection-spectroscopy based stand-off detection system having an SC laser source. The set-up 1270 for the reflection-spectroscopy-based stand-off detection system includes an SC source **1271**. First, the diverging SC output is collimated to a 1 cm diameter beam using a 25 mm focal length, 90 degrees off-axis, gold coated, parabolic mirror **1272**. To reduce the effects of chromatic aberration, refractive optics are avoided in the setup. All focusing and collimation is done using metallic mirrors that have almost constant reflectivity and focal length over the entire SC output spectrum. The sample **1274** is kept at a distance from the collimating mirror **1272**, which provides a total round trip path length of twice the distance before reaching the collection optics **1275**. A 12 cm diameter silver coated concave mirror **1275** with a 75 cm focal length is kept 20 cm to the side of the collimation mirror **1272**. The mirror **1275** is used to collect a fraction of the diffusely reflected light from the sample, and focus it into the input slit of a monochromator **1276**. Thus, the beam is incident normally on the sample **1274**, but detected at a reflection angle of $\tan^{-1}$ (0.2/5) or about 2.3 degrees. Appropriate long wavelength pass filters mounted in a motorized rotating filter wheel are placed in the beam path before the input slit **1276** to avoid contribution from higher wavelength orders from the grating (300 grooves/mm, 2 μm blaze). The output slit width is set to 2 mm corresponding to a spectral resolution of 10.8 nm, and the light is detected by a 2 mm×2 mm liquid nitrogen cooled (**77**K) indium antimonide (InSb) detector **1277**. The detected output is amplified using a trans-impedance pre-amplifier **1277** with a gain of about 105V/A and connected to a lock-in amplifier **1278** setup for high sensitivity detection. The chopper frequency is 400 Hz, and the lock-in time constant is set to 100 ms corresponding to a noise bandwidth of about 1 Hz. These are exemplary elements and parameter values, but other or different optical elements may be used consistent with this disclosure.

By use of an active illuminator, a number of advantages may be achieved, such as higher signal-to-noise ratios. For example, one way to improve the signal-to-noise ratio would be to use modulation and lock-in techniques. In one embodiment, the light source may be modulated, and then the detection system would be synchronized with the light source. In a particular embodiment, the techniques from lock-in detection may be used, where narrow band filtering around the modulation frequency may be used to reject noise outside the modulation frequency. In an alternate embodiment, change detection schemes may be used, where the detection system captures the signal with the light source on and with the light source off. Again, for this system the light source may be modulated. Then, the signal with and without the light source is differenced. This may enable the sun light changes to be subtracted out. In addition, change detection may help to identify objects that change in the field of view. In the following some exemplary detection systems are described.

One advantage of the SC lasers illustrated in FIGS. **8**, **9**, and **12** is that they may use all-fiber components, so that the SC laser can be all-fiber, monolithically integrated with no moving parts. The all-integrated configuration can consequently be robust and reliable.

FIGS. **8**, **9**, and **12** are examples of SC light sources that may advantageously be used for SWIR light generation in various medical and dental diagnostic and therapeutic applications. However, many other versions of the SC light sources may also be made that are intended to also be covered by this disclosure. For example, the SC generation fiber could be pumped by a mode-locked laser, a gain-switched semiconductor laser, an optically pumped semiconductor laser, a solid state laser, other fiber lasers, or a combination of these types of lasers. Also, rather than using a fiber for SC generation, either a liquid or a gas cell might be used as the nonlinear medium in which the spectrum is to be broadened.

Even within the all-fiber versions illustrated such as in FIG. **9**, different configurations could be used consistent with the disclosure. In an alternate embodiment, it may be desirous to have a lower cost version of the SWIR SC laser of FIG. **9**. One way to lower the cost could be to use a single stage of optical amplification, rather than two stages, which may be feasible if lower output power is required or the gain fiber is optimized. For example, the pre-amplifier stage **902** might be removed, along with at least some of the mid-stage elements. In yet another embodiment, the gain fiber could be double passed to emulate a two stage amplifier. In this example, the pre-amplifier stage **902** might be removed, and perhaps also some of the mid-stage elements. A mirror or fiber grating reflector could be placed after the power amplifier stage **906** that may preferentially reflect light near the wavelength of the seed laser **901**. If the mirror or fiber grating reflector can transmit the pump light near 940 nm, then this could also be used instead of the pump combiner **913** to bring in the pump light **912**. The SC fiber **915** could be placed between the seed laser **901** and the power amplifier stage **906** (SC is only generated after the second pass through the amplifier, since the power level may be sufficiently high at that time). In addition, an output coupler may be placed between the seed laser diode **901** and the SC fiber, which now may be in front of the power amplifier **906**. In a particular embodiment, the output coupler could be a power coupler or divider, a dichroic coupler (e.g., passing seed laser wavelength but outputting the SC wavelengths), or a wavelength division multiplexer coupler. This is just one further example, but a myriad of other combinations of components and architectures could also be used for SC light sources to generate SWIR light that are intended to be covered by this disclosure.

Wireless Link to the Cloud

The non-invasive dental caries measurement device may also benefit from communicating the data output to the "cloud" (e.g., data servers and processors in the web remotely connected) via wireless means. The non-invasive devices may be part of a series of biosensors applied to the patient, and collectively these devices form what might be called a body area network or a personal area network. The biosensors and non-invasive devices may communicate to a smart phone, tablet, personal data assistant, computer and/or other microprocessor-based device, which may in turn wirelessly or over wire and/or fiber optic transmit some or all of the signal or processed data to the internet or cloud. The cloud or internet may in turn send the data to dentists, doctors or health care providers as well as the patients themselves. Thus, it may be possible to have a panoramic, high-definition, relatively comprehensive view of a patient that doctors and dentists can use to assess and manage disease, and that patients can use to help maintain their health and direct their own care.

In a particular embodiment **1300**, the non-invasive measurement device **1301** may comprise a transmitter **1303** to communicate over a first communication link **1304** in the body area network or personal area network to a receiver in a smart phone, tablet, cell phone, PDA, and/or computer **1305**, for example. For the measurement device **1301**, it may also be advantageous to have a processor **1302** to process some of the measured data, since with processing the amount of data to transmit may be less (hence, more energy efficient). The first communication link **1304** may operate through the use of one of many wireless technologies such as Bluetooth, Zigbee, WiFi, IrDA (infrared data association), wireless USB, or Z-wave, to name a few. Alternatively, the communication link **1304** may occur in the wireless medical band between 2360 MHz and 2390 MHz, which the FCC allocated for medical body area network devices, or in other designated medical device or WMTS bands. These are examples of devices that can be used in the body area network and surroundings, but other devices could also be used and are included in the scope of this disclosure.

The personal device **1305** may store, process, display, and transmit some of the data from the measurement device **1301**. The device **1305** may comprise a receiver, transmitter, display, voice control and speakers, and one or more control buttons or knobs and a touch screen. Examples of the device **1305** include smart phones such as the Apple iPhones® or phones operating on the Android or Microsoft systems. In one embodiment, the device **1305** may have an application, software program, or firmware to receive and process the data from the measurement device **1301**. The device **1305** may then transmit some or all of the data or the processed data over a second communication link **1306** to the internet or "cloud" **1307**. The second communication link **1306** may advantageously comprise at least one segment of a wireless transmission link, which may operate using WiFi or the cellular network. The second communication link **1306** may additionally comprise lengths of fiber optic and/or communication over copper wires or cables.

The internet or cloud **1307** may add value to the measurement device **1301** by providing services that augment the measured data collected. In a particular embodiment, some of the functions performed by the cloud include: (a) receive at least a fraction of the data from the device **1305**; (b) buffer or store the data received; (c) process the data using software stored on the cloud; (d) store the resulting processed data; and (e) transmit some or all of the data either upon request or based on an alarm. As an example, the data or processed data may be transmitted **1308** back to the originator (e.g., patient or user), it may be transmitted **1309** to a health care provider or doctor or dentist, or it may be transmitted **1310** to other designated recipients.

Service providers coupled to the cloud **1307** may provide a number of value-add services. For example, the cloud application may store and process the dental data for future reference or during a visit with the dentist or healthcare provider. If a patient has some sort of medical mishap or emergency, the physician can obtain the history of the dental or physiological parameters over a specified period of time. In another embodiment, alarms, warnings or reminders may be delivered to the user **1308**, the healthcare provider **1309**, or other designated recipients **1310**. These are just some of the features that may be offered, but many others may be possible and are intended to be covered by this disclosure. As an example, the device **1305** may also have a GPS sensor, so the cloud **1307** may be able to provide time, date, and position along with the dental or physiological parameters. Thus, if there is a medical or dental emergency, the cloud **1307** could provide the location of the patient to the dental or healthcare provider **1309** or other designated recipients **1310**. Moreover, the digitized data in the cloud **1307** may help to move toward what is often called "personalized medicine." Based on the dental or physiological parameter data history, medication or medical/dental therapies may be prescribed that are customized to the particular patient. Another advantage for commercial entities may be that by leveraging the advances in wireless connectivity and the widespread use of handheld devices such as smart phones that can wirelessly connect to the cloud, businesses can build a recurring cost business model even using non-invasive measurement devices.

Described herein are just some examples of the beneficial use of near-infrared or SWIR lasers for non-invasive measurements of dental caries and early detection of carious regions. However, many other dental or medical procedures can use the near-infrared or SWIR light consistent with this disclosure and are intended to be covered by the disclosure.

Although the present disclosure has been described in several embodiments, a myriad of changes, variations, alterations, transformations, and modifications may be suggested to one skilled in the art, and it is intended that the present disclosure encompass such changes, variations, alterations, transformations, and modifications as falling within the spirit and scope of the appended claims.

While exemplary embodiments are described above, it is not intended that these embodiments describe all possible forms of the disclosure. Rather, the words used in the specification are words of description rather than limitation, and it is understood that various changes may be made without departing from the spirit and scope of the disclosure.

Additionally, the features of various implementing embodiments may be combined to form further embodiments of the disclosure. While various embodiments may have been described as providing advantages or being preferred over other embodiments with respect to one or more desired characteristics, as one skilled in the art is aware, one or more characteristics may be compromised to achieve desired system attributes, which depend on the specific application and implementation. These attributes include, but are not limited to: cost, strength, durability, life cycle cost, marketability, appearance, packaging, size, serviceability, weight, manufacturability, ease of assembly, etc. The embodiments described herein that are described as less desirable than other embodiments or prior art implementations with respect to one or more characteristics are not outside the scope of the disclosure and may be desirable for particular applications.

What is claimed is:

1. A wearable device for use with a smart phone or tablet, the wearable device comprising:

a measurement device including a light source comprising a plurality of light emitting diodes (LEDs) for measuring one or more physiological parameters, the measurement device configured to generate, by modulating at least one of the LEDs having an initial light intensity, an optical beam having a plurality of optical wavelengths, wherein at least one of the LEDs emits at a first wavelength having a first penetration depth into tissue and at least another of the LEDs emits at a second wavelength having a second penetration depth into the tissue different from the first penetration depth, wherein at least a portion of the optical beam includes a near-infrared wavelength between 700 nanometers and 2500 nanometers;

the measurement device comprising one or more lenses configured to receive and to deliver at least a portion of each of the first and of the second wavelengths to tissue, wherein the tissue reflects at least a portion of each of the first and of the second wavelengths;

the measurement device further comprising a receiver configured to:

capture light while the LEDs are off and convert the captured light into a first signal and

capture light while at least one of the LEDs is on and to convert the captured light into a second signal, the captured light including at least a portion of one of the first or second wavelengths reflected from the tissue;

the measurement device configured to improve a signal-to-noise ratio of the optical beam reflected from the tissue by differencing the first signal and the second signal;

the light source configured to further improve the signal-to-noise ratio of the optical beam reflected from the tissue by increasing the light intensity relative to the initial light intensity from at least one of the LEDs;

the measurement device further configured to generate an output signal representing at least in part a non-invasive measurement on blood contained within the tissue.

2. The wearable device of claim **1**, wherein the measurement device is adapted to be placed on a wrist of a user.

3. The wearable device of claim **1**, wherein the measurement device is adapted to be placed on an ear of a user.

4. The wearable device of claim **1**, wherein the second wavelength is between 900 nanometers and 1150 nanometers.

5. The wearable device of claim **1**, wherein

the wearable device is configured to communicate with the smart phone or tablet, the smart phone or tablet comprising a wireless receiver, a wireless transmitter, a display, a voice input module, a speaker, and a touch screen, the smart phone or tablet configured to receive and to process at least a portion of the output signal, wherein the smart phone or tablet is configured to store and display the processed output signal, wherein at least a portion of the processed output signal is configured to be transmitted over a wireless transmission link.

6. The wearable device of claim **1**, wherein the receiver is configured to be synchronized to the modulation of at least one of the LEDs.

7. The wearable device of claim **1**, wherein the receiver is located a first distance from a first one of the LEDs and a different distance from a second one of the LEDs such that the receiver can capture a third signal from the first LED and a fourth signal from the second LED, and wherein the output signal is generated in part by comparing the third and fourth signals.

8. The wearable device of claim **1**, wherein the output signal is generated in part by comparing the reflected light at the first wavelength with the reflected light at the second wavelength.

9. A wearable device for use with a smart phone or tablet, the wearable device comprising:

a measurement device including a light source comprising a plurality of light emitting diodes (LEDs) for measuring one or more physiological parameters, the measurement device configured to generate, by modulating at least one of the LEDs having an initial light intensity, an optical beam having a plurality of optical wavelengths, wherein at least a portion of the plurality of optical wavelengths is a near-infrared wavelength between 700 nanometers and 2500 nanometers;

the measurement device comprising one or more lenses configured to receive and to deliver a portion of the optical beam to tissue, wherein the tissue reflects at least a portion of the optical beam delivered to the tissue, and wherein the measurement device is adapted to be placed on a wrist or an ear of a user;

the measurement device further comprising a receiver configured to:

capture light while the LEDs are off and convert the captured light into a first signal and

capture light while at least one of the LEDs is on and convert the captured light into a second signal, the captured light including at least a portion of the optical beam reflected from the tissue;

the measurement device configured to improve a signal-to-noise ratio of the optical beam reflected from the tissue by differencing the first signal and the second signal;

the light source configured to further improve the signal-to-noise ratio of the optical beam reflected from the tissue by increasing the light intensity relative to the initial light intensity from at least one of the LEDs;

the measurement device further configured to generate an output signal representing at least in part a non-invasive measurement on blood contained within the tissue.

10. The wearable device of claim **9**, wherein at least one LED emits at a first wavelength and at least another LED emits at a second wavelength, and wherein the first wavelength has a first penetration depth into the tissue and wherein the second wavelength has a second penetration depth into the tissue different from the first penetration depth.

11. The wearable device of claim **10**, wherein the output signal is generated in part by comparing the reflected light at the first wavelength with the reflected light at the second wavelength.

12. The wearable device of claim **10**, wherein the second wavelength is between 900 nanometers and 1150 nanometers.

13. The wearable device of claim **9**, wherein

the wearable device is configured to communicate with the smart phone or tablet, the smart phone or tablet comprising a wireless receiver, a wireless transmitter, a display, a voice input module, a speaker, and a touch screen, the smart phone or tablet configured to receive and to process at least a portion of the output signal, wherein the smart phone or tablet is configured to store and display the processed output signal, wherein at least a portion of the processed output signal is configured to be transmitted over a wireless transmission link.

14. The wearable device of claim **9**, wherein the receiver is configured to be synchronized to the modulation of the at least one of the LEDs.

15. The wearable device of claim **9**, wherein the receiver is located a first distance from a first one of the LEDs and a different distance from a second one of the LEDs such that the receiver can capture a third signal from the first LED and a fourth signal from the second LED, and wherein the output signal is generated in part by comparing the third and fourth signals.

16. A wearable device for use with a smart phone or tablet, the wearable device comprising:

a measurement device including a light source comprising a plurality of light emitting diodes (LEDs) for measuring one or more physiological parameters, the measurement device configured to generate, by modulating at least one of the LEDs having an initial light intensity, an optical beam having a plurality of optical wavelengths, wherein at least a portion of the plurality of optical wavelengths is a near-infrared wavelength between 700 nanometers and 2500 nanometers;

the measurement device comprising one or more lenses configured to receive and to deliver a portion of the optical beam to tissue, wherein the tissue reflects at least a portion of the optical beam delivered to the tissue, and wherein the measurement device is adapted to be placed on a wrist or an ear of a user;

the measurement device further comprising a receiver configured to:

capture light while the LEDs are off and convert the captured light into a first signal and

capture light while at least one of the LEDs is on and convert the captured light into a second signal, the captured light including at least a portion of the optical beam reflected from the tissue;

the measurement device configured to improve a signal-to-noise ratio of the optical beam reflected from the tissue by differencing the first signal and the second signal;

the light source configured to further improve the signal-to-noise ratio of the optical beam reflected from the tissue by increasing the light intensity relative to the initial light intensity from at least one of the LEDs;

the measurement device further configured to generate an output signal representing at least in part a non-invasive measurement on blood contained within the tissue; and

wherein the receiver includes a plurality of spatially separated detectors, wherein at least one analog to digital converter is coupled to the spatially separated detectors.

17. The wearable device of claim **16**, wherein at least one LED emits at a first wavelength and at least another LED emits at a second wavelength, and wherein the first wavelength has a first penetration depth into the tissue and wherein the second wavelength has a second penetration depth into the tissue different from the first penetration depth.

18. The wearable device of claim **17**, wherein the output signal is generated in part by comparing the reflected light at the first wavelength with the reflected light at the second wavelength.

19. The wearable device of claim **16**, wherein the receiver is configured to be synchronized to the modulating of at least one of the LEDs.

20. The wearable device of claim **16**, wherein the receiver is located a first distance from a first one of the LEDs and a different distance from a second one of the LEDs such that the receiver can capture a third signal from the first LED and a fourth signal from the second LED, and wherein the output signal is generated in part by comparing the third and fourth signals.

* * * * *

EXHIBIT C

US009885698B2

(12) **United States Patent**
Islam

(10) **Patent No.: US 9,885,698 B2**
(45) **Date of Patent: *Feb. 6, 2018**

(54) **NEAR-INFRARED LASERS FOR NON-INVASIVE MONITORING OF GLUCOSE, KETONES, HBA1C, AND OTHER BLOOD CONSTITUENTS**

(71) Applicant: **OMNI MEDSCI, INC.**, Ann Arbor, MI (US)

(72) Inventor: **Mohammed N. Islam**, Ann Arbor, MI (US)

(73) Assignee: **Omni Medsci, Inc.**, Ann Arbor, MI (US)

(*) Notice: Subject to any disclaimer, the term of this patent is extended or adjusted under 35 U.S.C. 154(b) by 0 days.

This patent is subject to a terminal disclaimer.

(21) Appl. No.: **15/212,549**

(22) Filed: **Jul. 18, 2016**

(65) **Prior Publication Data**

US 2016/0327476 A1 Nov. 10, 2016

Related U.S. Application Data

(63) Continuation of application No. 14/650,897, filed as application No. PCT/US2013/075700 on Dec. 17, 2013, now Pat. No. 9,494,567.

(Continued)

(51) **Int. Cl.**
G01J 3/00 (2006.01)
G01N 33/15 (2006.01)

(Continued)

(52) **U.S. Cl.**
CPC ***G01N 33/15*** (2013.01); ***A61B 5/0013*** (2013.01); ***A61B 5/0022*** (2013.01);

(Continued)

(58) **Field of Classification Search**
CPC G01J 3/02; G01J 3/28; G01J 3/42; G01N 21/31; G01N 21/552

(Continued)

(56) **References Cited**

U.S. PATENT DOCUMENTS

4,063,106 A 12/1977 Ashkin et al.
4,158,750 A 6/1979 Sakoe et al.

(Continued)

FOREIGN PATENT DOCUMENTS

CN 101849821 B 7/2013
DE 102010012987 A1 10/2010

(Continued)

OTHER PUBLICATIONS

Istepanian Robert H., "The Comparative Performance of Mobile Telemedical Systems based on the IS-54 and GSM Cellular Telephone Standards"; Journal of Telemedicine and Telecare 1999; pp. 97-104.

(Continued)

Primary Examiner — Tarifur Chowdhury
Assistant Examiner — Md M Rahman
(74) *Attorney, Agent, or Firm* — Brooks Kushman P.C.

(57) **ABSTRACT**

A wearable device for use with a smart phone or tablet includes a measurement device having a light source with a plurality of light emitting diodes (LEDs) for measuring physiological parameters and configured to generate an optical beam with wavelengths including a near-infrared wavelength between 700 and 2500 nanometers. The measurement device includes lenses configured to deliver the optical beam to a sample of skin or tissue, which reflects the optical beam to a receiver located a first distance from one of the LEDs and a different distance from another of the LEDs, and is also configured to generate an output signal representing a non-invasive measurement on blood con-

(Continued)

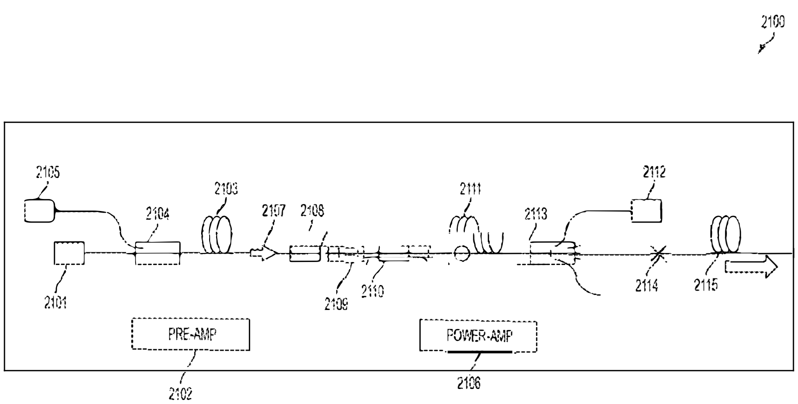

tained within the sample. The wearable device is configured to communicate with the smart phone or tablet, which receives, processes, stores and displays the output signal with the processed output signal configured to be transmitted over a wireless transmission link.

18 Claims, 31 Drawing Sheets

Related U.S. Application Data

(60) Provisional application No. 61/747,472, filed on Dec. 31, 2012.

(51) **Int. Cl.**

A61B 5/1455	(2006.01)
A61B 5/00	(2006.01)
G01J 3/10	(2006.01)
G01J 3/28	(2006.01)
G01J 3/453	(2006.01)
G01N 21/359	(2014.01)
G01J 3/14	(2006.01)
A61B 5/145	(2006.01)
G01N 33/49	(2006.01)
G01N 21/3563	(2014.01)
G01N 21/39	(2006.01)
G01N 33/02	(2006.01)
G01N 33/44	(2006.01)
G01N 21/88	(2006.01)
G01J 3/42	(2006.01)
G01J 3/02	(2006.01)
H01S 3/30	(2006.01)
G01J 3/18	(2006.01)
G01M 3/38	(2006.01)
G01J 3/12	(2006.01)
G01N 21/35	(2014.01)
G01N 21/85	(2006.01)
G01N 21/95	(2006.01)
H01S 3/067	(2006.01)
H01S 3/00	(2006.01)

(52) **U.S. Cl.**

CPC ***A61B 5/0075*** (2013.01); ***A61B 5/0086*** (2013.01); ***A61B 5/0088*** (2013.01); ***A61B 5/1455*** (2013.01); ***A61B 5/14532*** (2013.01); ***A61B 5/14546*** (2013.01); ***A61B 5/4547*** (2013.01); ***A61B 5/6801*** (2013.01); ***A61B 5/7257*** (2013.01); ***A61B 5/742*** (2013.01); ***A61B 5/7405*** (2013.01); ***G01J 3/0218*** (2013.01); ***G01J 3/108*** (2013.01); ***G01J 3/14*** (2013.01); ***G01J 3/28*** (2013.01); ***G01J 3/2823*** (2013.01); ***G01J 3/42*** (2013.01); ***G01J 3/453*** (2013.01); ***G01N 21/35*** (2013.01); ***G01N 21/359*** (2013.01); ***G01N 21/3563*** (2013.01); ***G01N 21/39*** (2013.01); ***G01N 21/88*** (2013.01); ***G01N 33/02*** (2013.01); ***G01N 33/025*** (2013.01); ***G01N 33/442*** (2013.01); ***G01N 33/49*** (2013.01); *A61B 2562/0233* (2013.01); *A61B 2562/0238* (2013.01); *A61B 2562/146* (2013.01); *A61B 2576/02* (2013.01); *G01J 3/1838* (2013.01); *G01J 2003/104* (2013.01); *G01J 2003/1208* (2013.01); *G01J 2003/2826* (2013.01); *G01M 3/38* (2013.01); *G01N 21/85* (2013.01); *G01N 21/9508* (2013.01); *G01N 2021/3595* (2013.01); *G01N 2021/399* (2013.01); *G01N 2201/061* (2013.01); *G01N 2201/062* (2013.01); *G01N 2201/06113* (2013.01); *G01N 2201/08* (2013.01); *G01N 2201/12* (2013.01); *G01N 2201/129* (2013.01); *H01S 3/0092* (2013.01); *H01S 3/06758* (2013.01); *H01S 3/302* (2013.01)

(58) **Field of Classification Search**
USPC 356/300
See application file for complete search history.

(56) **References Cited**

U.S. PATENT DOCUMENTS

4,221,997	A	9/1980	Flemming
4,275,266	A	6/1981	Lasar
4,374,618	A	2/1983	Howard
4,403,605	A	9/1983	Tanikawa
4,462,080	A	7/1984	Johnstone et al.
4,516,207	A	5/1985	Moriyama et al.
4,523,884	A	6/1985	Clement et al.
4,605,080	A	8/1986	Lemelson
4,641,292	A	2/1987	Tunnell et al.
4,704,696	A	11/1987	Reimer et al.
4,728,974	A	3/1988	Nio et al.
4,762,455	A	8/1988	Coughlan et al.
4,776,016	A	10/1988	Hansen
4,958,910	A	9/1990	Taylor et al.
4,989,253	A	1/1991	Liang et al.
5,078,140	A	1/1992	Kwoh
5,084,880	A	1/1992	Esterowitz et al.
5,086,401	A	2/1992	Glassman et al.
5,134,620	A	7/1992	Huber
5,142,930	A	9/1992	Allen et al.
5,180,378	A	1/1993	Kung et al.
5,191,628	A	3/1993	Byron
5,218,655	A	6/1993	Mizrahi
5,230,023	A	7/1993	Nakano
5,246,004	A	9/1993	Clarke et al.
5,267,152	A	11/1993	Yang et al.
5,267,256	A	11/1993	Saruwatari et al.
5,267,323	A	11/1993	Kimura
5,300,097	A	4/1994	Lerner et al.
5,303,148	A	4/1994	Mattson et al.
5,305,427	A	4/1994	Nagata
5,313,306	A	5/1994	Kuban et al.
5,323,404	A	6/1994	Grubb
5,345,538	A	9/1994	Narayannan et al.
5,400,165	A	3/1995	Gnauck et al.
5,408,409	A	4/1995	Glassman et al.
5,458,122	A	10/1995	Hethuin
5,544,654	A	8/1996	Murphy et al.
5,572,999	A	11/1996	Funda et al.
5,617,871	A	4/1997	Burrows
5,631,758	A	5/1997	Knox et al.
5,687,734	A	11/1997	Dempsey et al.
5,695,493	A	12/1997	Nakajima et al.
5,696,778	A	12/1997	MacPherson
5,704,351	A	1/1998	Mortara et al.
5,718,234	A	2/1998	Warden et al.
5,747,806	A	5/1998	Khalil
5,748,103	A	5/1998	Flach et al.
5,792,204	A	8/1998	Snell
5,812,978	A	9/1998	Nolan
5,855,550	A	1/1999	Lai et al.
5,862,803	A	1/1999	Besson et al.
5,867,305	A	2/1999	Waarts et al.
5,912,749	A	6/1999	Harstead et al.
5,944,659	A	8/1999	Flach et al.
5,950,629	A	9/1999	Taylor et al.
5,957,854	A	9/1999	Besson et al.
5,970,457	A	10/1999	Brant et al.
6,014,249	A	1/2000	Fermann et al.
6,043,927	A	3/2000	Islam
6,115,673	A	9/2000	Malin
6,181,414	B1	1/2001	Raz et al.
6,185,535	B1	2/2001	Hedin et al.

(56) **References Cited**

U.S. PATENT DOCUMENTS

6,200,309	B1	3/2001	Rice et al.
6,212,310	B1	4/2001	Waarts et al.
6,224,542	B1	5/2001	Chang et al.
6,246,707	B1	6/2001	Yin et al.
6,246,896	B1	6/2001	Dumoulin
6,273,858	B1	8/2001	Fox et al.
6,278,975	B1	8/2001	Brant et al.
6,281,471	B1	8/2001	Smart
6,285,897	B1	9/2001	Kilcoyne
6,289,238	B1	9/2001	Besson et al.
6,301,271	B1	10/2001	Sanders et al.
6,301,273	B1	10/2001	Sanders et al.
6,333,803	B1	12/2001	Kurotori et al.
6,337,462	B1	1/2002	Smart
6,340,806	B1	1/2002	Smart et al.
6,350,261	B1	2/2002	Domankevitz et al.
6,364,834	B1	4/2002	Reuss et al.
6,374,006	B1	4/2002	Islam et al.
6,381,391	B1	4/2002	Islam et al.
6,402,691	B1	6/2002	Peddicord et al.
6,407,853	B1	6/2002	Samson et al.
6,436,107	B1	8/2002	Wang et al.
6,441,747	B1	8/2002	Khair et al.
6,442,430	B1	8/2002	Ferek-Petric
6,443,890	B1	9/2002	Schulze et al.
6,450,172	B1	9/2002	Hartlaub et al.
6,453,201	B1	9/2002	Daum et al.
6,454,705	B1	9/2002	Cosentino et al.
6,458,120	B1	10/2002	Shen et al.
6,462,500	B1	10/2002	L'Hegarat et al.
6,463,361	B1	10/2002	Wang et al.
6,480,656	B1	11/2002	Islam et al.
6,512,936	B1	1/2003	Monfre
6,534,012	B1	4/2003	Viswanathan
6,549,702	B2	4/2003	Islam et al.
6,567,431	B2	5/2003	Tabirian et al.
6,587,702	B1	7/2003	Ruchti
6,603,910	B2	8/2003	Islam et al.
6,605,080	B1	8/2003	Altshuler et al.
6,611,643	B2	8/2003	Birk
6,619,835	B2	9/2003	Kita
6,625,180	B2	9/2003	Bufetov et al.
6,631,025	B2	10/2003	Islam et al.
6,640,117	B2	10/2003	Makarewicz
6,659,947	B1	12/2003	Carter et al.
6,659,999	B1	12/2003	Anderson et al.
6,738,652	B2	5/2004	Mattu
6,760,148	B2	7/2004	Islam
6,773,922	B2	8/2004	Jeng
6,788,965	B2	9/2004	Ruchti
6,802,811	B1	10/2004	Slepian
6,816,241	B2	11/2004	Grubisic
6,847,336	B1	1/2005	Lemelson
6,864,978	B1	3/2005	Hazen
6,885,498	B2	4/2005	Islam
6,885,683	B1	4/2005	Fermann et al.
6,943,936	B2	9/2005	Islam et al.
6,990,364	B2	1/2006	Ruchti
7,010,336	B2	3/2006	Lorenz
7,027,467	B2	4/2006	Baev et al.
7,060,061	B2	6/2006	Altshuler et al.
7,105,823	B2	9/2006	Abrahamsson et al.
7,133,710	B2	11/2006	Acosta
7,167,300	B2	1/2007	Fermann et al.
7,209,657	B1	4/2007	Islam
7,233,816	B2	6/2007	Blank
7,259,906	B1	8/2007	Islam
7,263,288	B1	8/2007	Islam
7,294,105	B1	11/2007	Islam
7,299,080	B2	11/2007	Acosta
7,317,938	B2	1/2008	Lorenz
7,356,364	B1	4/2008	Bullock et al.
7,395,158	B2	7/2008	Monfre
7,433,116	B1	10/2008	Islam
7,519,253	B2	4/2009	Islam
7,519,406	B2	4/2009	Blank
7,620,674	B2	11/2009	Ruchti
7,697,966	B2	4/2010	Monfre
7,771,320	B2	8/2010	Riley et al.
7,787,503	B2	8/2010	Wadsworth
7,787,924	B2	8/2010	Acosta
7,800,818	B2	9/2010	Mattsson
7,807,718	B2	10/2010	Hashim
7,848,605	B2	12/2010	Ridder et al.
7,890,158	B2	2/2011	Rowe et al.
8,000,574	B2	8/2011	Buchter
8,145,286	B2	3/2012	Arai
8,157,730	B2	4/2012	LeBoeuf et al.
8,158,493	B2	4/2012	Shah et al.
8,180,422	B2	5/2012	Rebec
8,213,007	B2	7/2012	Wang et al.
8,430,310	B1	4/2013	Ho et al.
8,472,108	B2	6/2013	Islam
8,509,882	B2	8/2013	Albert et al.
8,788,002	B2	7/2014	LeBoeuf et al.
8,948,832	B2	2/2015	Hong et al.
9,164,032	B2	10/2015	Islam
9,326,712	B1	5/2016	Kiani
2002/0013518	A1	1/2002	West et al.
2002/0019584	A1	2/2002	Schulze et al.
2002/0032468	A1	3/2002	Hill et al.
2002/0082612	A1	6/2002	Moll et al.
2002/0109621	A1	8/2002	Khair et al.
2002/0115914	A1	8/2002	Russ
2002/0128846	A1	9/2002	Miller
2002/0178003	A1	11/2002	Gehrke et al.
2003/0022126	A1	1/2003	Buchalla
2004/0174914	A1	9/2004	Fukatsu
2004/0240037	A1	12/2004	Harter
2005/0111500	A1	5/2005	Harter et al.
2005/0133691	A1	6/2005	Doppke et al.
2006/0058683	A1	3/2006	Chance
2006/0198397	A1	9/2006	Korolev et al.
2006/0223032	A1	10/2006	Fried
2006/0245461	A1	11/2006	Islam
2006/0268393	A1	11/2006	Islam
2006/0281982	A1	12/2006	Grata et al.
2006/0283931	A1	12/2006	Polli et al.
2007/0021670	A1	1/2007	Mandelis et al.
2007/0078348	A1	4/2007	Holman
2008/0086318	A1	4/2008	Gilley et al.
2008/0105665	A1	5/2008	Kondo
2009/0028193	A1	1/2009	Islam
2009/0105605	A1	4/2009	Abreu
2009/0204110	A1	8/2009	Islam
2009/0244288	A1	10/2009	Fujimoto et al.
2009/0287067	A1	11/2009	Dorogusker et al.
2010/0046067	A1	2/2010	Fermann et al.
2010/0160794	A1	6/2010	Banet et al.
2010/0160798	A1	6/2010	Banet et al.
2010/0217102	A1	8/2010	LeBoeuf et al.
2010/0322490	A1	12/2010	Pan
2010/0331637	A1	12/2010	Ting
2011/0040197	A1	2/2011	Welch et al.
2011/0143364	A1	6/2011	Kim
2011/0208015	A1	8/2011	Welch et al.
2011/0267688	A1	11/2011	Kleppe et al.
2011/0282167	A1	11/2011	Ridder et al.
2011/0292376	A1	12/2011	Kukushkin et al.
2012/0013722	A1	1/2012	Wong
2012/0239013	A1	9/2012	Islam
2012/0245439	A1	9/2012	Andre et al.
2012/0310062	A1	12/2012	Li et al.
2012/0316455	A1	12/2012	Rahman et al.
2013/0274569	A1	10/2013	Islam
2013/0281795	A1	10/2013	Varadan
2013/0327966	A1	12/2013	Fidler et al.
2014/0078510	A1	3/2014	Rubio Guivernau et al.
2014/0081100	A1	3/2014	Muhsin et al.
2014/0236021	A1	8/2014	Islam
2014/0249427	A1	9/2014	Liu
2014/0275852	A1	9/2014	Hong et al.
2014/0275854	A1	9/2014	Venkatraman et al.

(56) **References Cited**

U.S. PATENT DOCUMENTS

2015/0011851	A1	1/2015	Mehta et al.
2016/0045118	A1	2/2016	Kiani
2016/0327476	A1	11/2016	Islam

FOREIGN PATENT DOCUMENTS

EP	1148666		10/2001
WO	WO0971524O		5/1997
WO	WO9749340		12/1997
WO	WO0115O959		7/2001
WO	2001189362		11/2001
WO	2002276400		4/2002
WO	200228123		4/2002
WO	2005013843	A2	2/2005
WO	2007061772	A2	5/2007
WO	2009130464	A1	10/2009
WO	2012135952	A1	10/2012
WO	2013012938		1/2013
WO	2015084376		6/2015

OTHER PUBLICATIONS

Aris, Ishak Bin, "An Internet-Based Blood Pressure Monitoring System for Patients"; Journal of Telemedicine and Telecare 2001; pp. 51-53.

Sun, Y., C.F. Booker, S. Kumari, R.N. Day, M. Davidson, A. Periasamy, "Characterization of an orange acceptor fluorescent protein for sensitized spectral fluorescence resonant energy transfer microscopy using a white-light laser," Journal of Biomedical Optics, vol. 14, No. 5, paper 054009 (2009).

Borlinghaus, R., "Colours Count: how the challenge of fluorescence was solved in confocal microscopy," in Modern Research and Educational Topics in Microscopy, A. Mendez-Vilas and J. Diaz, eds, pp. 890-899, Formatex (2007).

Borlinghaus, R., "The White Confocal: Continuous Spectral Tuning in Excitation and Emission," in Optical Fluorescence Microscopy, A. Diaspro (Ed), Chapter 2, pp. 37-54, ISBN 978-3-642-15174-3, Springer-Verlag, Berlin (2011).

Borlinghaus, R.T., L. Kuschel, "White Light Laser: The Ultimate Source for Confocal Microscopy," http://www.leica-microsystems.com/science-lab/white-light-laser (Jun. 27, 2012).

Ziegler, U., A.G. Bittermann, M. Hoechli, "Introduction to Confocal Laser Scanning Microscopy (LEICA)," www.zmb.unizh.ch, May 29, 2013.

"Application Brief The role of infrared microprobe analysis in forensic drug analysis," www.smithsdetection.com, Jun. 27, 2005.

Jasco Application Note No. 200DR0188-E, "Rapid Identification of illegal drug using NIR (identification of MDMA tablet)", Sep. 4, 2008.

Palou, A. J. Cruz, M. Blanco, J. Tomas, J. De Los Rios, M. Alcala, "Determination of drug, excipients and coating distribution in pharmaceutical tablets using NIR-CI," Journal of Pharmaceutical Analysis, vol. 2, No. 2, pp. 90-97 (2012).

Arnold, T., M. De Biasio, R. Leitner, "Near-Infrared Imaging Spectroscopy for Counterfeit Drug Detection," Next Generation Spectroscopic Technologies IV, edited by M. A. Druy, R.A. Crocombe, Proceedings of SPIE, vol. 8032, 80320Y-1 to 7, (2011).

Wedding, B.B., C. Wright, S. Grauf, R.D. White, "The application of near infrared spectroscopy for the assessment of avocado quality attributes," Infrared Spectroscopy—Life and Biomedical Sciences, pp. 211-230 (2011).

Michaels, C.A., T. Masiello, P.M. Chu, "Fourier transform spectrometry with a near infrared supercontinuum source," Optical Society of America, CLEO/IQEC Conference, paper CMDD6 (2009).

Michaels, C.A., T. Masiello, P.M. Chu, "Fourier transform spectrometry with a near-infrared supercontinuum source," Applied Spectroscopy, vol. 63, No. 5, pp. 538-543 (2009).

Moros,J., J. Kuligowski, G. Quintas, S. Garrigues, M. DeLa Guardia, "New cut-off criterion for uninformative variable elimination in multivariate calibration of near-infrared spectra for the determination of heroin in illicit street drugs," Analytica Chimica Acta, vol. 630, pp. 150-160 (2008).

Moros, J. N. Gallpienso, R. Vilches, S. Garrigues, M. DeLa Guardia, "Nondestructive direct determination of heroin in seized illicit street drugs by diffuse reflectance near-infrared spectroscopy," Analytical Chemistry, vol. 80, No. 19, pp. 7257-7265 (Oct. 1, 2008).

Roggo, Y. P. Chalus, L. Maurer, C. Lema-Martinez, A. Edmond, N. Jent, "A review of near infrared spectroscopy and chemometrics in pharmaceutical technologies," Journal of Pharmaceutical and Biomedical Analysis, vol. 44, pp. 683-700 (2007).

Pojic, M. J. Mastilovic, N. Majcen, "The application of near infrared spectroscopy in wheat quality control," Infrared Spectroscopy—Life and Biomedical Sciences, pp. 167-184 (2012).

Reich, G. "Near-infrared spectroscopy and imaging: basic principles and pharmaceutical applications," Advanced Drug Delivery Reviews, vol. 57, pp. 1109-1143 (2005).

Rodionova, O.Y., L.P. Houmoller, A.L. Pomerantsev, P. Geladi, J. Burger, V.L. Dorofeyev, A.P. Arzamastsev, "NIR spectrometry for counterfeit drug detection: a feasibility study," Analytica Chimica Acta, vol. 549, pp. 151-158 (2005).

Schneider, R.C., K.A. Kovar, "Analysis of ecstasy tablets: comparison of reflectance and transmittance near infrared spectroscopy," Forensic Science International, vol. 134, pp. 187-195 (2003).

Olsen, B.A., M.W. Borer, F.M. Perry, R.A. Forbes, "Screening for counterfeit drugs using near-infrared spectroscopy," Pharmaceutical Technology, pp. 62-71 (Jun. 2002).

Scafi, S.H.F., C. Pasquini, "Identification of counterfeit drugs using near-infrared spectroscopy," Analyst, vol. 126, pp. 2218-2224 (2001).

Sondermann, N., K.A. Kovar, "Identification of ecstasy in complex matrices using near-infrared spectroscopy," Forensic Science International, vol. 102, pp. 133-147 (1999).

Rambla, F.J., S. Garrigues, M. DeLa Guardia, "PLS-NIR determination of total sugar, glucose, fructose and sucrose in aqueous solutions of fruit juices," Analytica Chimica Acta, vol. 344, pp. 41-53 (1997).

Bizheva, K, et al., "Compact, broad-bandwidth fiberlaserforsub-2-pm axial resolution optical coherence tomography in the 1300-nm wavelength region," Optics Letters, vol. 28, No. 9, May 1, 2003, pp. 707-709.

Wang, Yimin, et al., "Ultrahigh-resolution optical coherence tomography by broadband continuum generation from a photonic crystal fiber", Optics Letters, vol. 28, No. 3, Feb. 1, 2003, pp. 182-184.

Seefeldt, Michael, et al., "Compact white-light source with an average output power of 2.4 Wand 900 nm spectral bandwidth", Optics Communications 216, pp. 199-202.

Xie, T.-Q., et al., "Detection of tumorigenesis in urinary bladder with optical coherence tomography: optical characterization of morphological changes", Optics Express, vol. 10, No. 24, Dec. 2, 2002, 2003, pp. 1431-1443.

Povazay, B., et al., "Submicrometer axial resolution optical coherence tomography", Optics Letters, vol. 27, No. 20, Oct. 15, 2002, pp. 1800-1802.

Kowalevicz, Andrew M., et al., "Ultrahigh resolution optical coherence tomography using a superluminescent light source" Optics Express 349, vol. 10, No. 7, Apr. 8, 2002, pp. 349-353.

Oughstun, Kurt E., "Influence of precursor fields on ultrashort pulse autocorrelation measurements and pulse width evolution", Optics Express, vol. 8, No. 8, Apr. 9, 2001, pp. 481-491.

Li, Xingde, et al., "Imaging needle for optical coherence tomography", Optics Letters, vol. 25, No. 20, Oct. 15, 2000, pp. 1520-1522.

D'Amico, Anthony V., et al., "Optical Coherence Tomography As a Method for Identifying Benign and Malignant Microscopic Structures in the Prostate Gland", Basic Science, Urology 55 (5), 2000, pp. 783-787.

Rollins, Andrew M., et al., "Real-time in vivo imaging of human gastrointestinal ultrastructure by use of endoscopic optical coherence tomography with a novel efficient interferometer design", Optics Letters, vol. 24, No. 19, Oct. 1, 1999, pp. 1358-1360.

(56) **References Cited**

OTHER PUBLICATIONS

De Boer, Johannes F., et al., "Determination of the depth-resolved Stokes parameters of light backscattered from turbid media by use of polarization-sensitive optical coherence tomography", Optics Letters, vol. 24, No. 5; Mar. 1, 1999, pp. 300-302.
Roggan, Andre, et al., "Optical Properties of Circulating Human Blood in the Wavelength Range 400-2500 NM", Journal of Biomedical Optics, vol. 4, No. 1, Jan. 1999, pp. 36-46.
De Boer, Johannes F., et al., "Imaging thermally damaged tissue by polarization sensitive optical coherence tomography", Optics Express 212, vol. 3, No. 6, Sep. 14, 1998, pp. 212-218.
Tearney, Guillermo J., et al., "In vivo Endoscopic Optical Biopsy with Optical Coherence Tomography", Science, New Series, vol. 276, Jun. 27, 1997, pp. 2037-2039.
Boppart, Stephen A., et al., "Noninvasive assessment of the developing Xenopus cardiovascular system using optical coherence tomography", Prec. Natl. Acad. Sci. USA, vol. 94, Apr. 1997, pp. 4256-4261.
Boppart, Stephen A., et al., "Imaging developing neural morphology using optical coherence tomography", Journal of Neuroscience Methods 70, 1996, pp. 65-72.
Aaviksoo, J., et al., "Observation of optical precursors at pulse propagation in GaAs", Physical Review A, vol. 44, No. 9, Nov. 1, 1991, pp. R5353-R5356.
Harrington, James A., "Infrared Fiber Optics", OSA Handbook, vol. III, white paper, to be published by McGraw Hill, Undated, 13 pages.
Fedotova, O., et al., "Supercontinuum generation in planar rib waveguides enabled by anomalous dispersion", Optics Express, vol. 14, No. 4, Feb. 20, 2006, pp. 1512-1517.
Moon, Sucbei, et al., "Generation of octave-spanning supercontinuum with 1550-nm amplified diode-laser pulses and a dispersion-shifted fiber", Optics Express, vol. 14, No. 1, Jan. 9, 2006, pp. 270-278.
Hagen, C. L., et al., "Generation of a Continuum Extending to the Midinfrared by Pumping ZBLAN Fiber With an Ultrafast 1550-nm Source", IEEE Photonics Technology Letters, vol. 18, No. 1, Jan. 1, 2006, pp. 91-93.
Travers, J. C., et al., "Extended blue supercontinuum generation in cascaded holey fibers", Optics Letters, vol. 30, No. 23, Dec. 1, 2005, pp. 3132-3134.
Schreiber, T., et al., "Supercontinuum generation by femtosecond single and dual wavelength pumping in photonic crystal fibers with two zero dispersion wavelengths", Optics Express, vol. 13, No. 23, Nov. 14, 2005, pp. 9556-9569.
Genty, G., et al., "Supercontinuum generation in large mode-area microstructured fibers", Optics Express, vol. 13, No. 21, Oct. 17, 2005, pp. 8625-8633.
Lee, Ju Han, et al., "Continuous-wave supercontinuum laser based on an erbium-doped fiber ring cavity incorporating a highly nonlinear optical fiber", Optics Letters, vol. 30, No. 19, Oct. 1, 2005, pp. 2599-2601.
Hori, Takashi, et al., "Flatly broadened, wideband and low noise supercontinuum generation in highly nonlinear hybrid fiber", Optics Express, vol. 12, No. 2, Jan. 26, 2004, pp. 317-324.
Wadsworth, W. J., et al., "Supercontinuum and four-wave mixing with Q-switched pulses in endlessly single-mode photonic crystal fibres", Optics Express, vol. 12, No. 2, Jan. 26, 2004, pp. 299-309.
Hilligsoe, Karen Marie, et al., "Supercontinuum generation in a photonic crystal fiber with two zero dispersion wavelengths", Optics Express, vol. 12, No. 6, Mar. 22, 2004, pp. 1045-1054.
Venugopalan, V., "Optical Society of America BIOMED Topical Meeting Tutorial on Tissue Optics", Apr. 27, 2004, pp. 1-32.
Slusher, Richart E., et al., "Large Raman gain and nonlinear phase shifts in high-purity As2So3 chalcogenide fibers", J. Opt. Soc. Am. B, vol. 21, No. 6, Jun. 2004, pp. 1146-1155.
Leon-Saval, S. G., et al., "Supercontinuum generation in submicron fibre waveguides", Optics Express, vol. 12, No. 13, Jun. 28, 2004, pp. 2864-2869.
Nicholson, J. W., et al., "High power, single mode, all-fiber source of femtosecond pulses at 1550 nm and its use in supercontinuum generation", Optics Express, vol. 12, No. 13, Jun. 28, 2004, pp. 3025-3034.
Genty, G., et al., "Enhanced bandwidth of supercontinuum generated m microstructured fibers", Optics Express, vol. 12, No. 15, Jul. 26, 2004, pp. 3471-3480.
Champert, Pierre-Alain, et al., "White-light supercontinuum generation in normally dispersive optical fiber using original multi-wavelength pumping system", Optics Express, vol. 12, No. 19, Sep. 20, 2004, pp. 4366-4371.
Nicholson, J. W., "Supercontinuum generation in ultraviolet-irradiated fibers", Optics Letters, vol. 29, No. 20, Oct. 15, 2004, pp. 2363-2365.
Hori, Takashi, et al., "Experimental and numerical analysis of widely broadened supercontinuum generation in highly nonlinear dispersion-shifted fiber with a femtosecond pulse", J. Opt. Soc. Am. B, vol. 21, No. 11, Nov. 2004, pp. 1969-1980.
Demircan, Ayhan, et al., "Supercontinuum generation by the modulation instability", Optics Communications 244, 2005, pp. 181-185.
Papernyi, S. B., et al., "Sixth-Order Cascaded Raman Amplification", OFC/NFOEC, 2005, 3 pages.
Tanaka, Keiji, "Optical nonlinearity in photonic glasses", Journal of Materials Science: Materials in Electronics 16, 2005, pp. 633-643.
Westbrook, Paul S., "Improved Supercontinuum Generation Through UV Processing of Highly Nonlinear Fibers", Journal of Lightwave Technology, vol. 23, No. 1, Jan. 2005, pp. 13-18.
Abeeluck, Akheelesh K., et al., "Continuous-wave pumping in the anomalous- and normal dispersion regimes of nonlinear fibers for supercontinuum generation", Optics Letters, vol. 30, No. 1, Jan. 1, 2005, pp. 61-63.
Kutz, J. Nathan, et al., Enhanced Supercontinuum Generation through Dispersion-Management, Optics Express, vol. 13, No. 11, May 30, 2005, pp. 3989-3998.
Lee, Ju Han, et al., "Experimental performance comparison for various continuous-wave supercontinuum schemes: ring cavity and single pass structures", Optics Express, vol. 13, No. 13, Jun. 27, 2005, pp. 4848-4853.
Saliminia, A., et al., "Ultra-broad and coherent white light generation in silica glass by focused femtosecond pulses at 1.5pm", Optics Express, vol. 13, No. 15, Jul. 25, 2005, pp. 5731-5738.
Takushima, Yuichi, High average power, depolarized super-continuum generation using a 1.55-um ASE noise source, Optics Express, vol. 13, No. 15, Jul. 25, 2005, pp. 5871.-5877.
Travers, J. C., et al., "Extended continuous-wave supercontinuum generation in a low-water-loss holey fiber", Optics Letters, vol. 30, No. 15, Aug. 1, 2005, pp. 1938-1940.
Kobtsev, Serguei M., et al., "Modelling of high-power supercontinuum generation in highly nonlinear, dispersion shifted fibers at CW pump", Optics Express, vol. 13, No. 18, Sep. 5, 2005, pp. 6912-6918.
Falk, Peter, et al., "Supercontinuum generation in a photonic crystal fiber with two zero-dispersion wavelengths tapered to normal dispersion at all wavelengths", Optics Express, vol. 13, No. 19, Sep. 19, 2005, pp. 7535-7540.
Tombelaine, Vincent, et al., "Ultra wide band supercontinuum generation in air-silica holey fibers by SHG-induced modulation instabilities", Optics Express, vol. 13, No. 19, Sep. 19, 2005, pp. 7399-7404.
Hazen, K.H., M.A. Arnold, G.W. Small, "Measurement of glucose and other analytes in undiluted human serum with near-infrared transmission spectroscopy," Analytica Chimica Acta, vol. 371, pp. 255-267 (1998).
Malin S.F., T.L. Ruchti, T.B. Blank, S.N. Thennadil, S.L. Monfre, "Noninvasive prediction of glucose by near-infrared diffuse reflectance spectroscopy," Clinical Chemistry, vol. 45, No. 9, pp. 1651-1658 (1999).
Thennadil, S.N., J.L. Rennert, B.J. Wenzel, K.H. Hazen, T.L. Ruchti, M.B. Block, "Comparison of glucose concentration in interstitial fluid, and capillary and venous blood during rapid changes in blood glucose levels," Diabetes Technology & Therapeutics, vol. 3, No. 3, pp. 357-365 (2001).

(56) **References Cited**

OTHER PUBLICATIONS

Troy, T.L., S.N. Thennadil, "Optical properties of human skin in the near infrared wavelength range of 1000 to 2200nm," Journal of Biomedical Optics, vol. 6, No. 2, pp. 167-176, (2001).
Blank, T.B., T.L. Ruchti, A.D. Lorenz, S.L. Monfre, M.R. Makarewicz, M. Mattu, K.H. Hazen, "Clinical results from a non-invasive blood glucose monitor," Optical Diagnostics and Sensing of Biological Fluids and Glucose and Cholesterol Monitoring II, A.V. Priezzhev and G.L. Cote, Editors, Proceedings of SPIE, vol. 4624, pp. 1019 (2002).
Yeh, S-J, C.F. Hanna, O.S. Khalil, "Monitoring blood glucose changes in cutaneous tissue by temperature-modulated localized reflectance measurements," Clinical Chemistry, vol. 49, No. 6, pp. 924-934 (2003).
Marbach, R., T. Koschinsky, F.A. Gries, H.M. Heise, "Noninvasive blood glucose assay by near-infrared diffuse reflectance spectroscopy of the human inner lip," Applied Spectroscopy, vol. 47, No. 7, pp. 875-881 (1993).
Enejder, A.M.K., T.G. Scecina, J. Oh, M. Hunter, W.C. Shih, S. Sasic, G.L. Horowitz, M.S. Feld, "Raman spectroscopy for noninvasive glucose measurements," Journal of Biomedical Optics, vol. 10, No. 3, 031114 (2005).
Olesberg, J.T., L. Liu, V.V. Zee, M.A. Arnold, "In vivo near-infrared spectroscopy of rat skin tissue with varying blood glucose levels," Analytic Chemistry, vol. 78, No. 1, pp. 215-223 (2006).
Olesberg, J.T., M.A. Arnold, C. Mermelstein, J. Schmitz, J. Wagner, "Tunable laser diode system for noninvasive blood glucose measurements," Applied Spectroscopy, vol. 59, No. 12, pp. 1480-1484 (2005).
Harman-Boehm, I. A. Gal, A.M. Raykhman, J.D. Zahn, E. Naidis, Y. Mayzel, "Noninvasive glucose monitoring: a novel approach," Journal of Diabetes Science and Technology, vol. 3, No. 2 pp. 253-260 (2009).
Kim-K. D. G.S. Son, S.S. Lim, S.S. Lee, "Measurement of glucose level exploiting a relative optical absorption at discrete probe wavelengths," Japanese Journal of Applied Physics, vol. 48, 077001 (2009).
Smith, J.L., "The Pursuit of Noninvasive Glucose: Hunting the Deceitfil Turkey," 2nd Edition, pp. 1-141 (2011).
Pezzaniti, J.L., T.W. Jeng, L. McDowell, G.M. Oosta, "Preliminary investigation of near-infrared spectroscopic measurements of urea, creatinine, glucose, protein and ketone in urine," Clinical Biochemistry, vol. 34, pp. 239-246 (2001).
Lussi, A., R. Hibst, R. Paulus, "Diagnodent: An optical method for caries detection," Journal of Dental Research, vol. 83, special issue C, pp. C80-C83 (2004).
Reese, E.L, E.E. Fisher, D.A. Horowitz, "Photoelectric densitometry of the circulation of the human dental pulp," The Journal of the Baltimore College of Dental Surgery, vol. 26, No. 1, pp. 6-18 (1971).
Zakian, C., I. Pretty, R. Ellwood, "Near-infrared hyperspectral imaging of teeth for dental caries detection," Journal of Biomedical Optics, vol. 16, No. 6, 064047 (2009).
Belikov, A.V., A.V. Skripnik, K.V. Shatilova, "Study of the dynamics of the absorption spectra of human tooth enamel and dentine under heating and ablation by submillisecond pulse radiation of an erbium laser with a generation wavelength of 2.79 um," Optics and Spectroscopy, vol. 109, No. 2, pp. 211-216 (2010).
Karlsson, L. "Caries detection methods based on changes in optical properties between healthy and carious tissue," International Journal of Dentistry, vol. 2010, Article ID 270729, 9 pages (2010).
Fried, D. M. Staninec, C.L. Darling, "Near-infrared imaging of dental decay at 1310nm," Journal of Laser Dentistry, vol. 18, No. 1, pp. 8-16 (2010).
Burmen, M. P. Usenik, A. Fidler, F. Pernus, B. Likar, "A construction of standardized near infrared hyper-spectral teeth database—a first step in the development of reliable diagnostic tool for quantification and early detection of caries," Lasers in Dentistry XVII, edited by P. Rechmann, D. Fried, Proceedings of SPIE, vol. 7884, Paper 78840E (2011).
Maia, A., L. Karlsson, W. Margulis, A. Gomes, "Evaluation of two imaging techniques: near-infrared transillumination and dental radiographs for the detection of early approximal enamel caries," Dentomaxillofacial Radiology, vol. 40, pp. 429-433 (2011).
Chung, S., D. Fried, M. Staninec, C.L. Darling, "Multispectral near-IR reflectance and transillumination imaging of teeth," Biomedical Optics Express, vol. 2, No. 10, pp. 2804-2814 (2011).
Chung, S., D. Fried, M. Staninec, C.L. Darling, "Near infrared imaging of teeth at wavelengths between 1200 and 1600nm," Proceedings of the Society of Photo Optical Instrument Engineering, paper 7884 (2011).
Staninec, M., S.M. Douglas, C.L. Darling, K. Chan, H. Kang, R. C. Lee, D. Fried, "Nondestructive clinical assessment of occlusal caries lesions using near-IR imaging methods," Lasers in Surgery and Medicine, vol. 43, No. 10, pp. 951-959 (2011).
Nishizawa, N., "Generation and application of high-quality supercontinuum sources," Optical Fiber Technology, vol. 18, pp. 394-402 (2012).
Islam, M. N., et al., "Broad bandwidths from frequency-shifting solitons in fibers", Optics Letters, vol. 14, No. 7, Apr. 1, 1989, pp. 370-372.
Islam, M. N., et al., "Femtosecond distributed soliton spectrum in fibers", J. Opt. Soc. Am. B, vol. 6, No. 6, Jun. 1989, pp. 1149-1158.
Busse, Lynda E., et al., "Design Parameters for Fluoride Multimode Fibers", Journal of Lightwave Technology, vol. 9, No. 7, Jul. 1991, pp. 828-831.
Wuthrich, Stefan, et al., "Optical damage thresholds at 2.94 um in fluoride glass fibers", Applied Optics, vol. 31, No. 27, Sep. 20, 1992, pp. 5833-5837.
Inoue, H., et al., "Computer simulation of the vibrational spectra and properties of fluoride glasses based on ZrF4", Journal of Non-Crystalline Solids, vol. 161, 1993, pp. 118-122.
Mizunami, Toru, et al., "Gain saturation characteristics of Raman amplification in silica and fluoride glass optical fibers", Optics Communications 97, 1993, pp. 74-78.
Desthieux, B., et al., "111 kW (0. 5 mJ) pulse amplification at 1.5 um using a gated cascade of three erbium-doped fiber amplifiers," Appl. Phys. Lett. vol. 63, Aug. 2, 1993, pp. 586-588.
Edwards, Glenn, et al., Tissue ablation by a free-electron laser tuned to the amide II band, Nature, vol. 371, Sep. 29, 1994, pp. 416-419.
Borrelli, N. F., et al., "Resonant and non-resonant effects in photonic glasses", Journal of Non-Crystalline Solids 185, 1995, pp. 109-122.
Asobe, Masaki, et al., "Third-order nonlinear spectroscopy in As2S3 chalcogenide glass fibers", J. Appl. Phys. 77 (11), Jun. 1, 1995, pp. 5518-5523.
Jarman, Richard H., "Novel optical fiber lasers", Current Opinion in Solid State and Materials Science, 1996, pp. 199-203.
Iatridis, James C., et al., "Is the Nucleus Pulposus a Solid or a Fluid? Mechanical Behaviors of the Nucleus Pulposus of the Human Intervertebral Disc", Spine, vol. 21(10), May 15, 1996, pp. 1174-1184.
Asobe, Masaki, "Nonlinear Optical Properties of Chalcogenide Glass Fibers and Their Application to All-Optical Switching", Optical Fiber Technology, vol. 3, Article No. OF970214, 1997, pp. 142-148.
Smektala, F., et al., "Chalcogenide glasses with large non-linear refractive indices", Journal of Non-Crystalline Solids 239, 1998, pp. 139-142.
Hamilton, James D., et al., "High Frequency Ultrasound Imaging with Optical Arrays", IEEE Transactions on Ultrasonics, Ferroelectrics, and Frequency Control, vol. 45, No. 1, Jan. 1998, pp. 216-235.
Hamilton, James D., et al., "High Frequency Ultrasound Imaging Using an Active Optical Detector", IEEE Transactions on Ultrasonics, Ferroelectrics, and Frequency Control, vol. 45, No. 3, May 1998, pp. 719-727.
Nowak, G. A., et al., "Low-power high-efficiency wavelength conversion based on modulational instability in high-nonlinearity fiber," Optics Letters, vol. 23, No. 12, Jun. 15, 1998, pp. 936-938.
Cardinal, T., et al., "Non-linear optical properties of chalcogenide glasses in the system As—S—Se", Journal of Non-Crystalline Solids 256 & 257, 1999, pp. 353-360.

(56) **References Cited**

OTHER PUBLICATIONS

Lucas, Jacques, "Infrared glasses", Current ●pinion in Solid State & Materials Science 4, 1999. pp. 181-187.
Sanghera, J. S., et al., Active and passive chalcogenide glass optical fibers for IR applications: a review, Journal of Non-Crystalline Solids 256 & 257, 1999, pp. 6-16.
Nishida, Yoshiki, et al., "Reliability of Fluoride Fiber Module for ●ptical Amplifier Use", IEEE Photonics Technology Letters, vol. 11, No. 12, Dec. 1999, pp. 1596-1598.
Nowak, George A., et al., "Stable supercontinuum generation in short lengths of conventional dispersion-shifted fiber", Applied ●ptics, vol. 38, No. 36, Dec. 2●, 1999, pp. 7364-7369.
Urban, J. P. G., et al., "The Nucleus of the Intervertebral Disc from Development to Degeneration" Amer. Zool., vol. 4●, 2●●●, pp. 53-61.
Hamilton, James D., et al., "High Frequency ●ptoacoustic Arrays Using Etalon Detection", IEEE Transactions on Ultrasonics, Ferroelectrics, and Frequency Control, vol. 47, No. 1, Jan. 2●●●, pp. 16●-169.
Ranka, Jinendra K., et al., "Visible continuum generation in air-silica microstructure optical fibers with anomalous dispersion at 8●● nm", ●ptics Letters, vol. 25, No. 1, Jan. 1, 2●●●, pp. 25-27.
Boult, Maggi, et al., "Systematic Review of Percutaneous Endoscopic Laser Discectomy: Update and Re-appraisal", Australian Safety and Efficacy Register of New Interventional Procedures—Surgical Report No. 5, Feb. 2●●●, 49 pages.
Boult, Maggi, et aL, "Percutaneous Endoscopic Laser Discectomy", Systematic Review, Aust. N.Z.J. Surg., vol. 7●, Apr. 7, 2●●●, pp. 475-479.
Camacho, Nancy P., et al., "FTIR Microscopic Imaging of Collagen and Proteoglycan in Bovine Cartilage," Biopolymers (Biospectroscopy), vol. 62, 2●●1, pp. 1-8.
Choi, Joon Y., et al, "Thermal, Mechanical, ●ptical, and Morphologic Changes in Bovine Nucleus Pulposus Induced by Nd:YAG (λ=1.32 um) Laser Irradiation", Lasers in Surgery and Medicine, vol. 28, 2●●1, pp. 248-254.
Hafez, M. I., et al., "The Effect of Irrigation on Peak Temperatures in Nerve Root, Dura, and Intervertebral Disc During Laser-Assisted Foraminoplasty", Lasers in Surgery and Medicine, vol. 29, 2●●1, pp. 33-37.
Jackson, Stuart D., et al., "Theory and numerical simulation of nth-order cascaded Raman fiber lasers", J. ●pt. Soc. Am. B, vol. 18, No. 9, Sep. 2●●1, pp. 1297-13●6.
Werle, Peter, et a!., "Near- and mid-infrared laser-optical sensors for gas analysis", ●ptics and Lasers in Engineering 37, 2●●2, pp. 1●1-114.
Beck, Mattias, et al., "Continuous Wave ●peration of a Mid-Infrared Semiconductor Laser at Room Temperature," Science vol. 295, www.sciencemag.org, Jan. 11, 2●●2, pp. 3●1-3●5.
Harbold, J. M., et al., "Highly nonlinear As—S—Se glasses for all-optical switching", ●ptics Letters, vol. 27, No. 2, Jan. 15, 2●●2, pp. 119-121.
Coen, Stephane, et al., "Supercontinuum generation by stimulated Raman scattering and parametric four-wave mixing in photonic crystal fibers", J. ●pt. Soc. Am. B, vol. 19, No. 4, Apr. 2●●2, pp. 753-764.
Dudley, John M., et al., "Supercontinuum generation in air-silica microstructured fibers with nanosecond and femtosecond pulse pumping", J. ●pt. Soc. Am. B, vol. 19, No. 4, Apr. 2●●2, pp. 765-771.
Harbold, Jeffrey M., et al., "Highly Nonlinear Ge—As—Se and. Ge—As—S—Se Glasses for All-●ptical Switching", IEEE Photonics Technology Letters, vol. 14, No. 6, Jun. 2●●2, pp. 822-824.
Husakou, Anton V., et al, "Supercontinuum generation, four-wave mixing, and fission of higher-order solitons in photonic-crystal fibers", J. ●pt. Soc. Am. B, vol. 19, No. 9, Sep. 2●●2, pp. 2171-2182.
Wadsworth, William J., et al., "Supercontinuum generation in photonic crystal fibers and optical fiber tapers: a novel light source", J. ●pt. Soc. Am. B, vol. 19, No. 9, Sep. 2●●2, pp. 2148-2155.
Kumar, V.V. Ravi Kanth, et al, "Extruded soft glass photonic crystal fiber for ultrabroad supercontinuum generation", ●ptics Express, vol. 1●, No. 25, Dec. 16, 2●●2, pp. 152●-1525.
Edwards, Glenn S., et al., "Advantage of the Mark-III FEL for biophysical research and biomedical applications", J. Synchrotron Rad. vol. 1●, 2●●3, pp. 354-357.
Nicholson, J. W., et al., "Pulsed and continuous-wave supercontinuum generation in highly nonlinear, dispersion-shifted fibers", Applied Physics B 77, 2●●3, pp. 211-218.
Sobol, Emil, et al., "Time-resolved, light scattering measurements of cartilage and cornea denaturation due to free electron laser radiation", Journal of Biomedical ●ptics, vol. 8, No. 2, Apr. 2●●3, pp. 216-222.
Nicholson, J. W., et al., "All-fiber, octave-spanning supercontinuum", ●ptics Letters, vol. 28, No. 8, Apr. 15, 2●●3, pp. 643-645.
Faralli, S., et al., "Impact of Double Rayleigh Scattering Noise in Distributed Higher ●rder Raman Pumping Schemes", IEEE Photonics Technology Letters, vol. 15, No. 6, Jun. 2●●3, pp. 8●4-8●6.
"New and Emerging Techniques—Surgical, Rapid Review, Laser Discectomy", Australian Safety and Efficacy Register of New Interventional Procedures—Surgical, Jun. 2●●3, 12 pages.
Avdokhin, A. V., et al, "Continuous-wave, high-power, Raman continuum generation in holey fibers", ●ptics Letters, vol. 28, No. 15, Aug. 1, 2●●3, pp. 1353-1355.
Mussot, Arnaud, et al., "Generation of a broadband single-mode supercontinuum in a conventional dispersion-shifted fiber by use of a subnanosecond microchip laser", ●ptics Letters, vol. 28, No. 19, ●ct. 1, 2●●3, pp. 182●-1822.
Slusher, Richard, et al., "Highly nonlinear composite chalcogenide/polymer fibers", ●SA 2●●4, 1 page.
Thongtrangan, Issada, et al., "Minimally invasive spinal surgery: a historical perspective", Neurosurg. Focus, vol. 16, Article 13, Jan. 2●●4, pp. 1-1●.
Pan, Yingtian, et al., "Hand-held arthroscopic optical coherence tomography for in vivo high-resolution imaging of articular cartilage", Journal of Biomedical ●ptics 8(4), ●ct. 2●●3, pp. 648-654.
Xie, Tuqiang, et al., "Endoscopic optical coherence tomography with a modified microelectromechanical systems mirror for detection of bladder cancers", Applied ●ptics, vol. 42, No. 31, Nov. 1, 2●●3, pp. 6422-6426.
Dubois, A., et al., "Three-dimensional cellular-level imaging using fiill-field optical coherence tomography", Physics in Medicine and Biology, Phys. Med. Biol. 49, 2●●4, pp. 1227-1234.
Park, Jesung, et al., "Analysis of birefringent image in the retinal nerve fiber layer by polarization sensitive optical coherence tomography", ●phthalmic Technologies XIV, Proceedings of SPIE, vol. 5314, 2●●4, pp. 188-194.
Unterhuber, A., et al., "Advances in broad bandwidth light sources for ultrahigh resolution optical coherence tomography", Physics in Medicine and Biology, Phys. Med. Biol. 49, 2●●4, pp. 1235-1246.
Drexler, Wolfgang, "Ultrahigh-resolution optical coherence tomography", Journal of Biomedical ●ptics, vol. 9, No. 1, Jan./Feb. 2●●4, pp. 47-74.
Schmitt, Joseph, et al., "Intravascular ●ptical Coherence Tomography ●pens a Window ●nto Coronary Artery Disease", ●ptics & Photonics News, Feb. 2●●4, pp. 2●-25.
Nassif, N.A., et al., "In vivo high-resolution video-rate spectral-domain optical coherence tomography of the human retina and optic nerve", ●ptics Express, vol. 12, No. 3, Feb. 9, 2●●4, pp. 367-376.
Choi, Seung-Ho, et al., "●bservation of ●ptical Precursors in Water", Physical Review Letters, vol. 92, No. 19, May 14, 2●●4, pp. 1939●3-1-1939●3-.3.
Pierce, Mark C., et al., "Advances in ●ptical Coherence Tomography imaging for Dermatology", ●ptical Coherence Tomography Advances, The Journal of Investigative Dermatology, Sep. 3, 2●●4, pp. 458-461.
"State-Specific Trends in chronic Kidney Failure—United states, 199●-2●●1", Morbidity and Mortality Weekly Report, Department of Health and Human Services Centers for Disease Control and Prevention, vol. 53, No. 39, copied from internet: file://C:\Documents and Settings\eturlo\Desktop\State-Specific Trends in Chronic Kidney . . . Feb. 12, 2●1●, ●ct. 8, 2●●4, pp. 918-92●.

(56) **References Cited**

OTHER PUBLICATIONS

I.B. Ads, A.A.E. Wagie, N.B. Mariun, A.B.E. Jammal, "An Internet-based blood pressure monitoring system for patients," Journal of Telemedicine and Telecare, 2001, pp. 51-53.
R.H. Istepanian, B. Woodward, P.A. Bales, S. Chen, B. Luk, "The comparative performance of mobile telemediCal systems based on the IS-54 and GSM cellular telephone standards," Journal of Telemedicine and Telecare, 1999, pp. 97-104.
Shaw, et al, IR Supercontinuum Generation in As—Se Photonic Crystal Fiber, Optical Society of America, Copyright 2005, 3 pages.
PCT/US06/44451, Notification of Transmittal of the International Search Report and the Written Opinion of the International Searching Authority, or the Declaration, dated Nov. 29, 2007, 12 pages.
G.S. Edwards et al., "Free-electron-laser-based biophysical and biomedical instrumentation," American Institute of Physics, vol. 74, No. 7, Jul. 2003, pp. 3207-3245.
Computer Motion, Inc., "501(k) Summary—ZEUS® MicroWrist™ Surgical System and Accessories," Sep. 24, 2002, 6 pages.
Computer Motion, Inc. "HERMES™ O.R. Control Center—510(k) Sununary of Safety and Effectiveness," Oct. 11, 2002, 5 pages.
K.M. Joos, et al. "Optic Nerve Sheath Fenestration with a Novel Wavelength Produced by the Free Electron Laser (FEL)," Lasers in Surgery and Medicine, 27: 2000,191-205.
J. Sanghera, I. Aggarwal, "IR Fiber Optics at NRL," undated, 10 pages.
J. Sanghera, L.B. Shaw, I.D. Aggarwal, "Applications of chalcogenide glass optical fibers," Academic of Science, 2003, pp. 1-11.
B. Rigas, P.T.T. Wong, "Human Colon Adenocarcinoma Cell Lines Display Infrared Spectroscopic Features," Cancer Research, Jan. 1, 1992, pp. 84-88.
G. Edwards, et al., "Comparison of OPA and Mark-III FEL for Tissue Ablation at 6.45 Microns," Department of Physics and Free Electron Laser Laboratory, Duke University, 2002, 7 pages.
Glenn Edwards, "Biomedical and potential clinical applications for pulsed lasers operating near 6.45 um," Society of Photo-Optical Instrumentation Engineers, 1995, 2 pages.
Passat, "Solid-State Lasers and Optical Components," Jul. 14, 2003, 5 pages.
P.A. Thielen and L.B. Shaw, et al., "Small-core As—Se fiber for Raman amplification," Optics Leti-ers, vol. 28, No. 16, Aug. 15, 2003, 3 pages.
R.Rox Anderson, et al., "Selective Photothermolysis: Precise Microsurgery by Selective Absorption of Pulsed Radiation," Department of Dermatology, Harvard Medical School, Science, vol. 220, Apr. 29, 1983, 4 pages.
U.S. Appl. No. 10/652,276, "System and Method for Voice Control of Medical Devices," by Mohammed N. Islam, abandoned filed Aug. 29, 2003.
U.S. Appl. No. 10/757,341, "System and Method for Voice Control of Medical devices," by Mohammed N. Islam, issued filed Jan. 13, 2004.
U.S. Appl. No. 12/206,432, "System and Method for Voice Control of Medical Devices," by Mohammed N. Islam, pending filed Sep. 8, 2008.
U.S. Patent and Trademark Office, Office Action for U.S. Appl. No. 12/206,432, filed Sep. 8, 2008, Mohammed N, Islam, filed Mar. 12, 2009.
U.S. Patent and Trademark Office, Notice of Allowance and Fee(s) Due for U.S. Appl. No. 12/206,432, filed Sep. 8, 2008, Mohammed N. Islam, filed Aug. 28, 2009.
International Search Report and Written Opinion for International Application No. PCT/US2013/075700 dated Apr. 24, 2014.
International Preliminary Report on Patentability for International Application No. PCT/US2013/075700 dated Jul. 9, 2015.
U.S. Appl. No. 61/350,673; titled: Opticoustic Sensor; Inventor: Massi Joe E. Kiani; filed Jun. 2, 2010.
Non-Final Office Action for U.S. Appl. No. 14/875,709 dated May 26, 2016.
Ooi ET, Zhang XQ, Chen JH, Soh PH, Ng K, Yea JH, "Non-invasive glucose measurement using multiple laser Jiodes," Optical Diagnostic and Sensing VII, edited by Gerard L. Cote, Alexander V. Priezzhev, Proc. of SPIE vol. 6445, 64450K , (2007).
Schulz, I., J. Putzger, A. Niklas, M. Brandt, A. Jager, A. Hardt, S. Knorzer, K.A. Hiller, S. Loffler, G. Schmalz, S.N. Danilov, S. Giglberger, M. Hirmer, S.D. Ganichev, G. Monkman, "PPG signal acquisition and analysis on in vitro tooth model for dental pulp vitality assessment," ARC Submission 16, (2012).
Drexler, C., Hirmer, M., Danilov, S., Giglberger, S., Putzger, J., Niklas, A., Jager, A., Hiller, K., Loffler, S., Schmalz, G., Redlich, B., Schulz, I., Monkman, G., Ganichev, S. "Infrared spectroscopy for clinical diagnosis of dental pulp vitality." Infrared, Millimeter, and Terahertz Waves (IRMMW-THz), 2012 37th International Conference on. IEEE (2012).
Hirmer, Marion, Danilov, Sergey, Giglberger, Stephan, Putzger, Jurgen, Niklas, Andreas, Jager, Andreas, Hiller, Karl-Anton, Loffler, Susanne, Schmalz, Gottfried, Redlich, Britta, Schulz, Irene, Monkman, Gareth, Ganichev, Sergey. "Spectroscopic Study of Human Teeth and Blood from Visible to Terahertz Frequencies for Clinical Diagnosis of Dental Pulp Vitality." Journal of Infrared, Millimeter, and Terahertz Waves 33.3 (2012): 366-375.
Na, J, J.H. Baek, S.Y. Ryu, C. Lee, B.H. Lee, "Tomographic imaging of incipient dental-caries using optical coherence tomography and comparison with various modalities," Optical Review, vol. 16, No. 4, pp. 426-431 (2009).
Vinay V. Alexander et al.; Modulation Instability High Power All-Fiber Supercontinuum Lasers and Their Applications; Optical Fiber Technology 18; 2012; pp. 349-374.
Robert S. Jones et al.; Near-Infrared Transillumination At 1310-nm for the Imaging of Early Dental Decay; vol. 11; No. 18; Optics Express 2259; Sep. 8, 2003.
Extended European Search Report for European Application No. 13867874.3 dated Jul. 15, 2016.
Extended European Search Report for European Application No. 13867892.5 dated Jul. 22, 2016.
Final Office Action dated Oct. 21, 2016 for U.S. Appl. No. 14/875,709.
Notice of Allowance for U.S. Appl. No. 14/875,709 dated Jan. 10, 2017.
Extended European Search Report for European Application No. 17156625.0 dated Mar. 20, 2017.
Extended European Search Report for European Application No. 17155541.0 dated May 24, 2017.

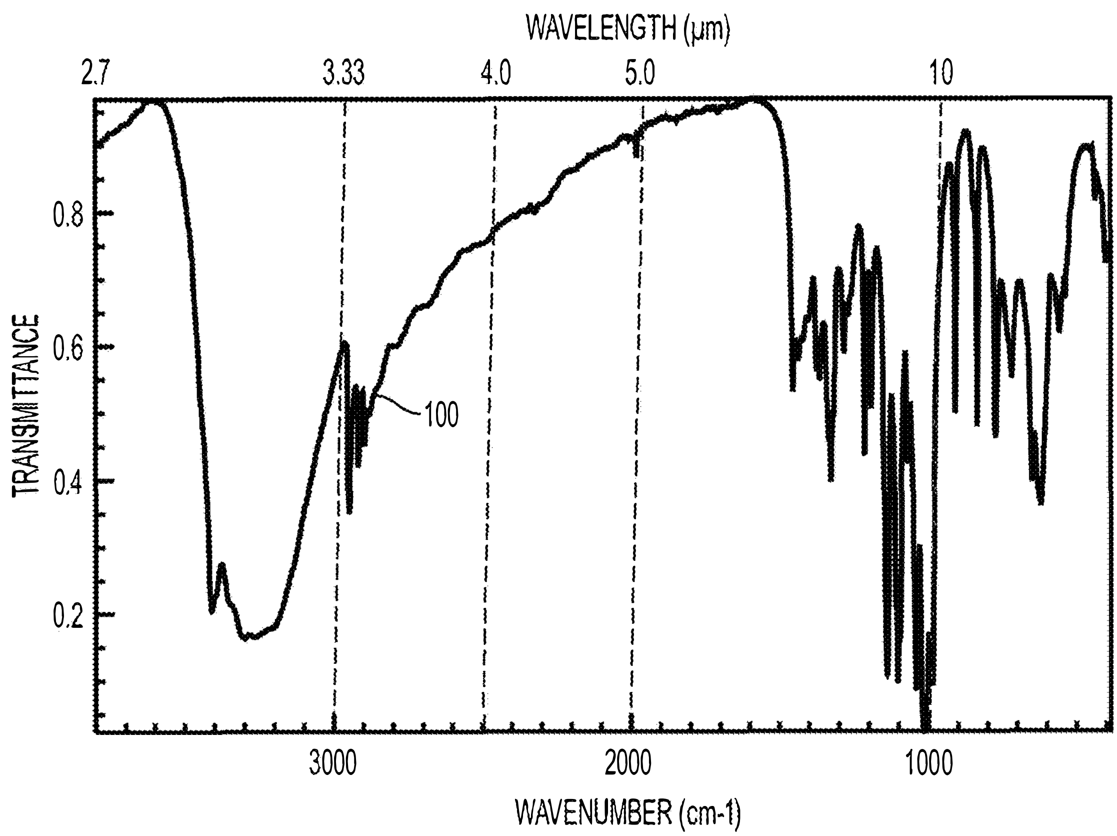
WAVELENGTH (μm)
2.7
3.33
4.0
5.0
10
TRANSMITTANCE
0.8
0.6
0.4
0.2
100
3000
2000
1000
WAVENUMBER (cm-1)

FIG. 1

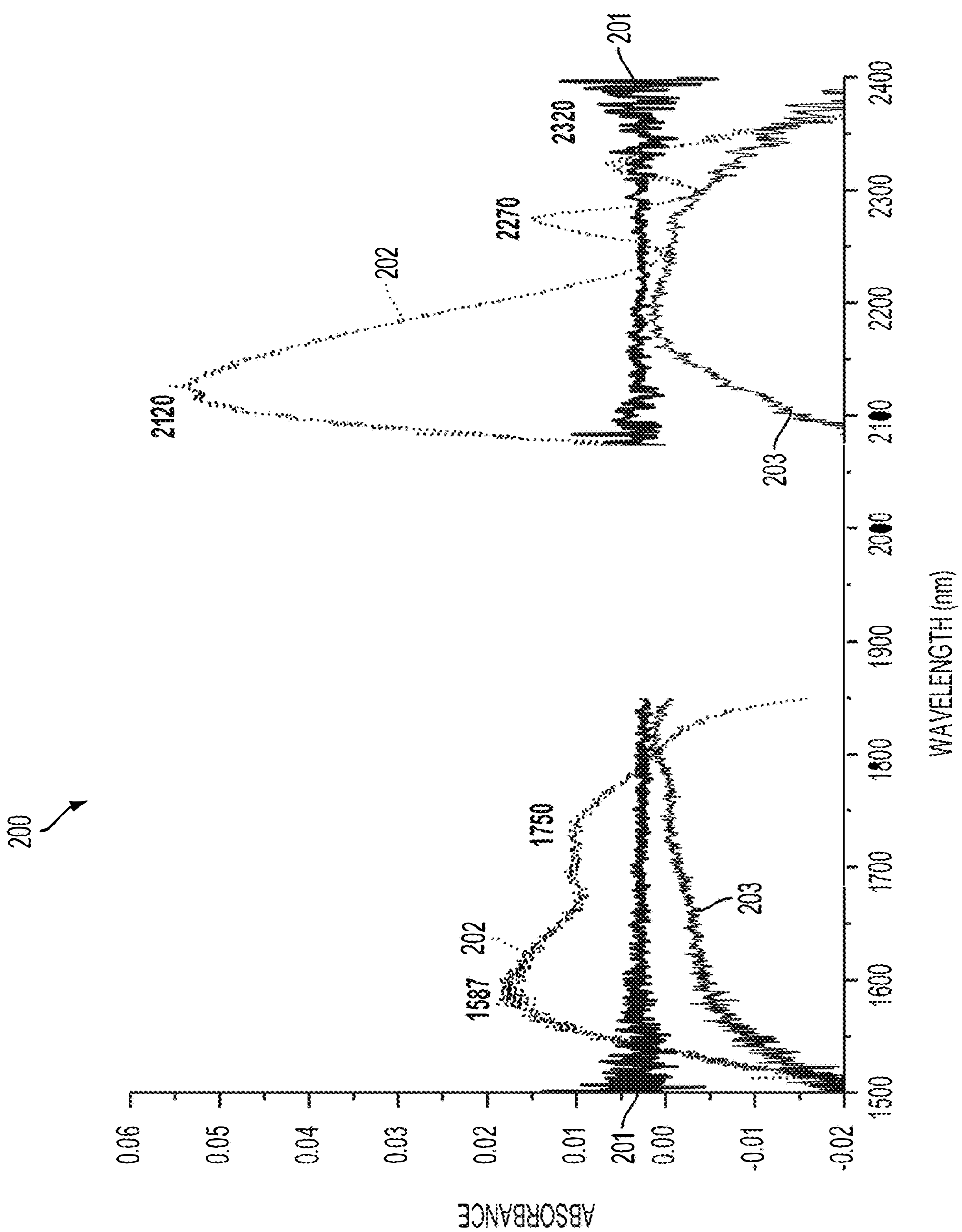
200
ABSORBANCE
0.06
0.05
0.04
0.03
0.02
0.01
0.00
-0.01
-0.02
201
202
203
1587
1750
2120
2270
2320
1500
1600
1700
1800
1900
2000
2100
2200
2300
2400
WAVELENGTH (nm)

FIG. 2

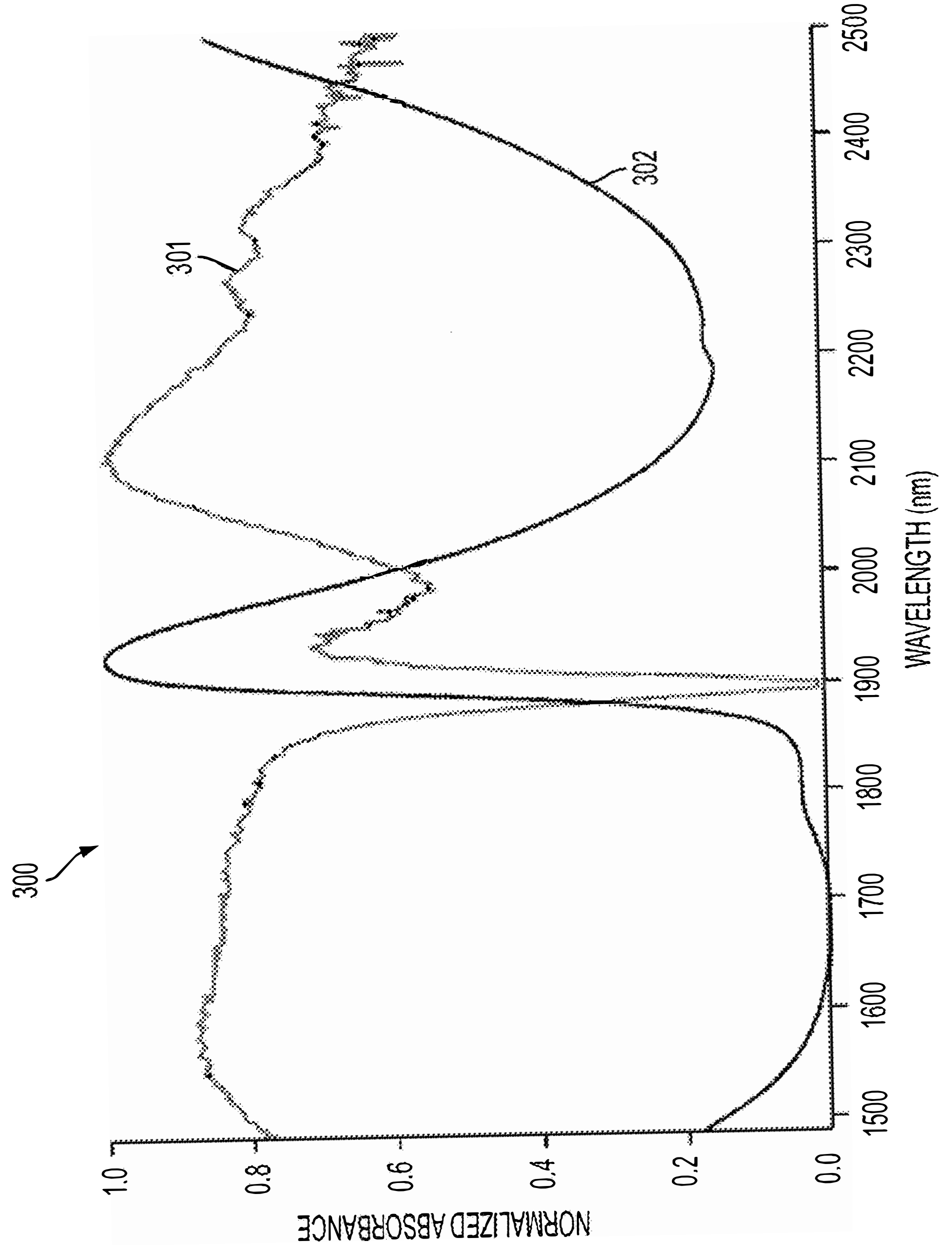
300
301
302
NORMALIZED ABSORBANCE
1.0
0.8
0.6
0.4
0.2
0.0
1500
1600
1700
1800
1900
2000
2100
2200
2300
2400
2500
WAVELENGTH (nm)

FIG. 3A

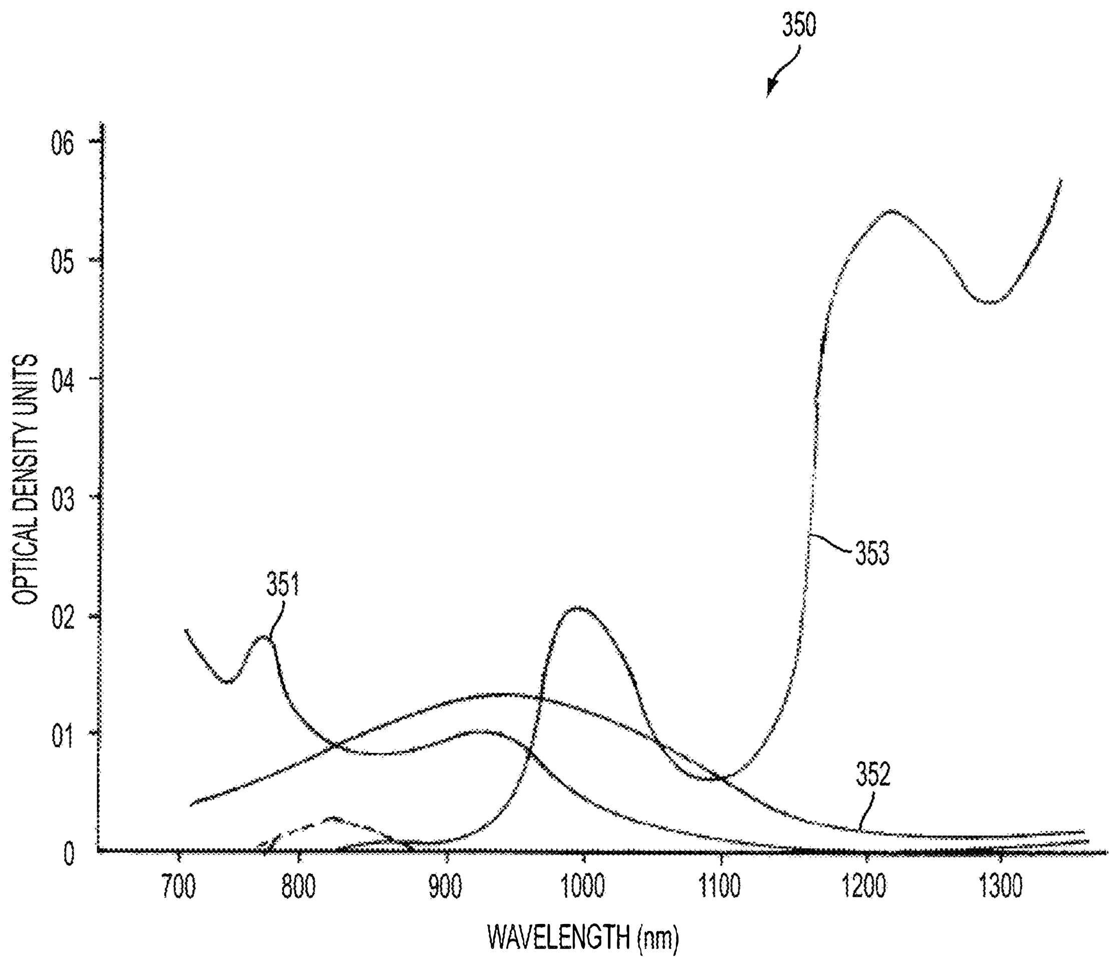
350
06
05
04
03
02
01
0
OPTICAL DENSITY UNITS
351
352
353
700
800
900
1000
1100
1200
1300
WAVELENGTH (nm)

FIG. 3B

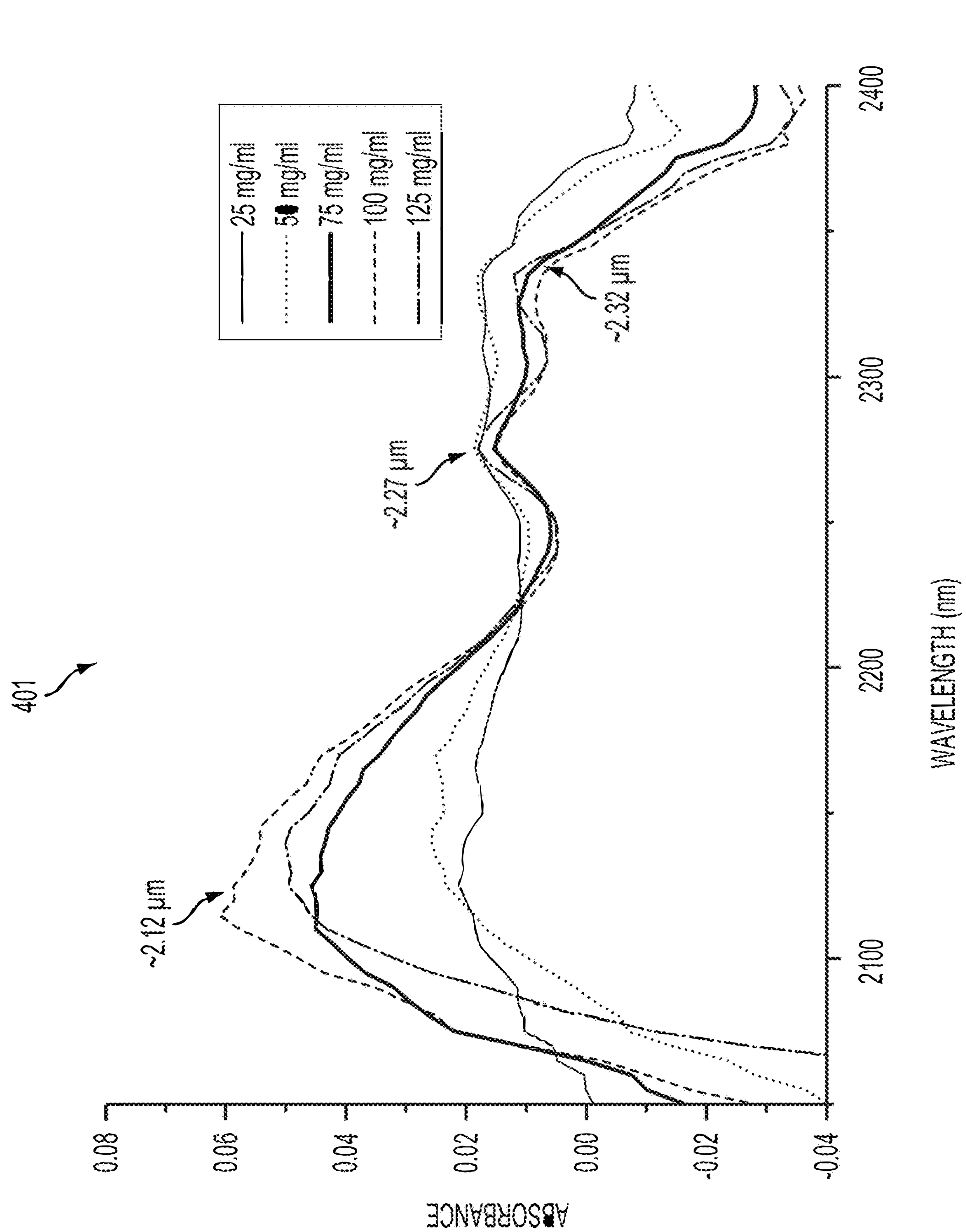
401
~2.12 µm
~2.27 µm
~2.32 µm
25 mg/ml
50 mg/ml
75 mg/ml
100 mg/ml
125 mg/ml
ABSORBANCE
0.08
0.06
0.04
0.02
0.00
-0.02
-0.04
2100
2200
2300
2400
WAVELENGTH (nm)

FIG. 4A

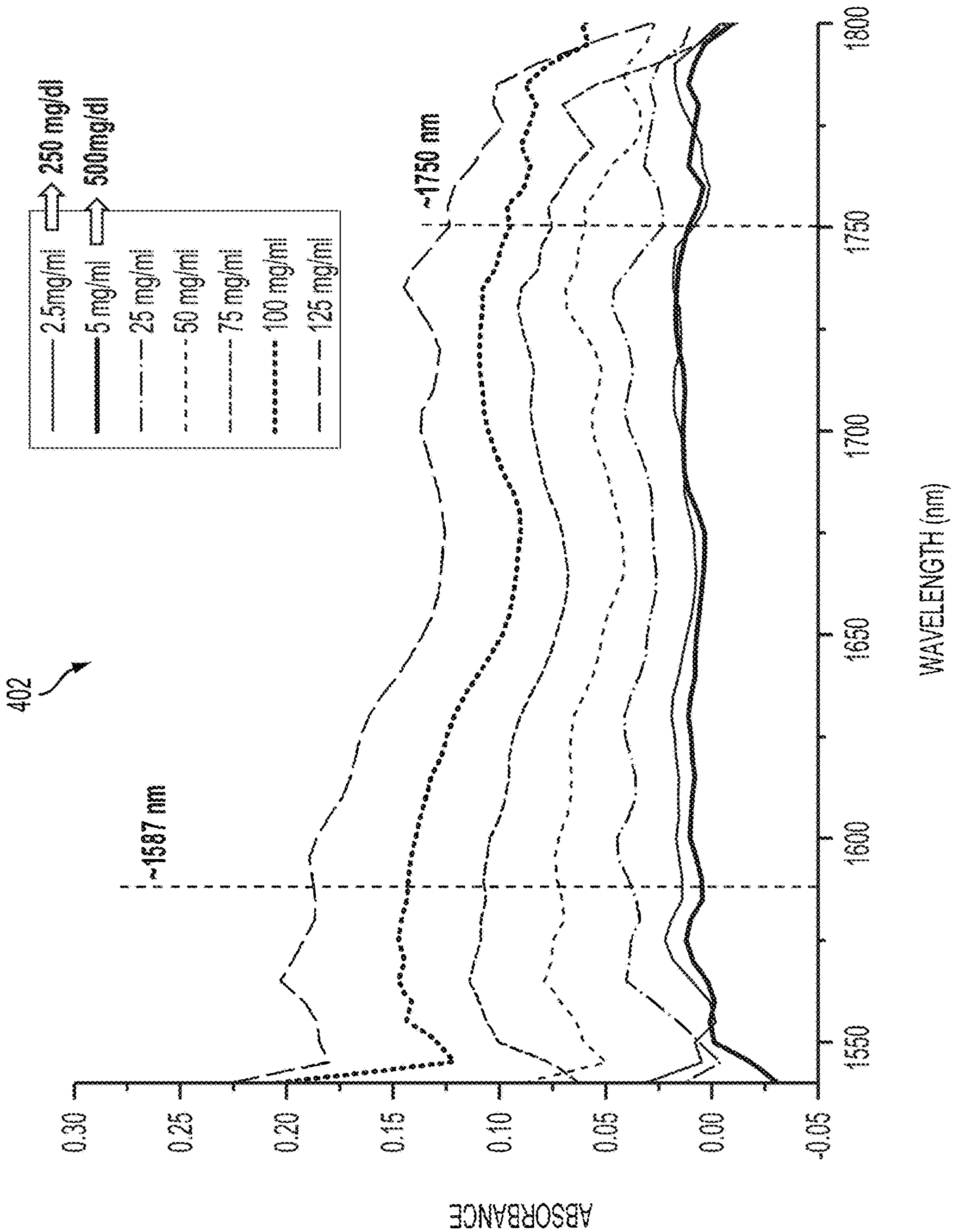
402
~1587 nm
~1750 nm
2.5mg/ml
5 mg/ml
25 mg/ml
50 mg/ml
75 mg/ml
100 mg/ml
125 mg/ml
250 mg/dl
500mg/dl
ABSORBANCE
0.30
0.25
0.20
0.15
0.10
0.05
0.00
-0.05
1550
1600
1650
1700
1750
1800
WAVELENGTH (nm)

FIG. 4B

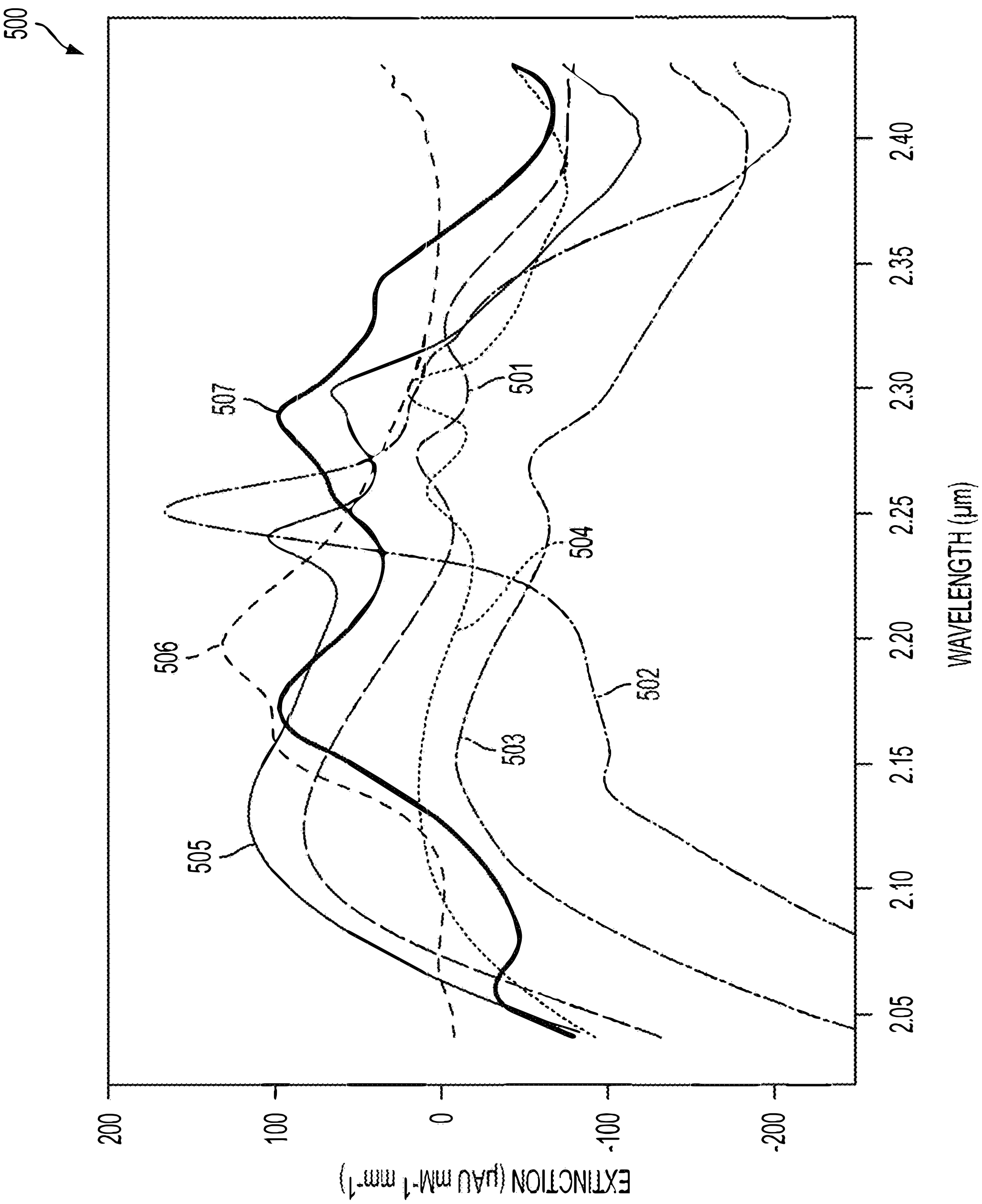
500
501
502
503
504
505
506
507
200
100
0
-100
-200
EXTINCTION (μAU mM-1 mm-1)
2.05
2.10
2.15
2.20
2.25
2.30
2.35
2.40
WAVELENGTH (μm)

FIG. 5

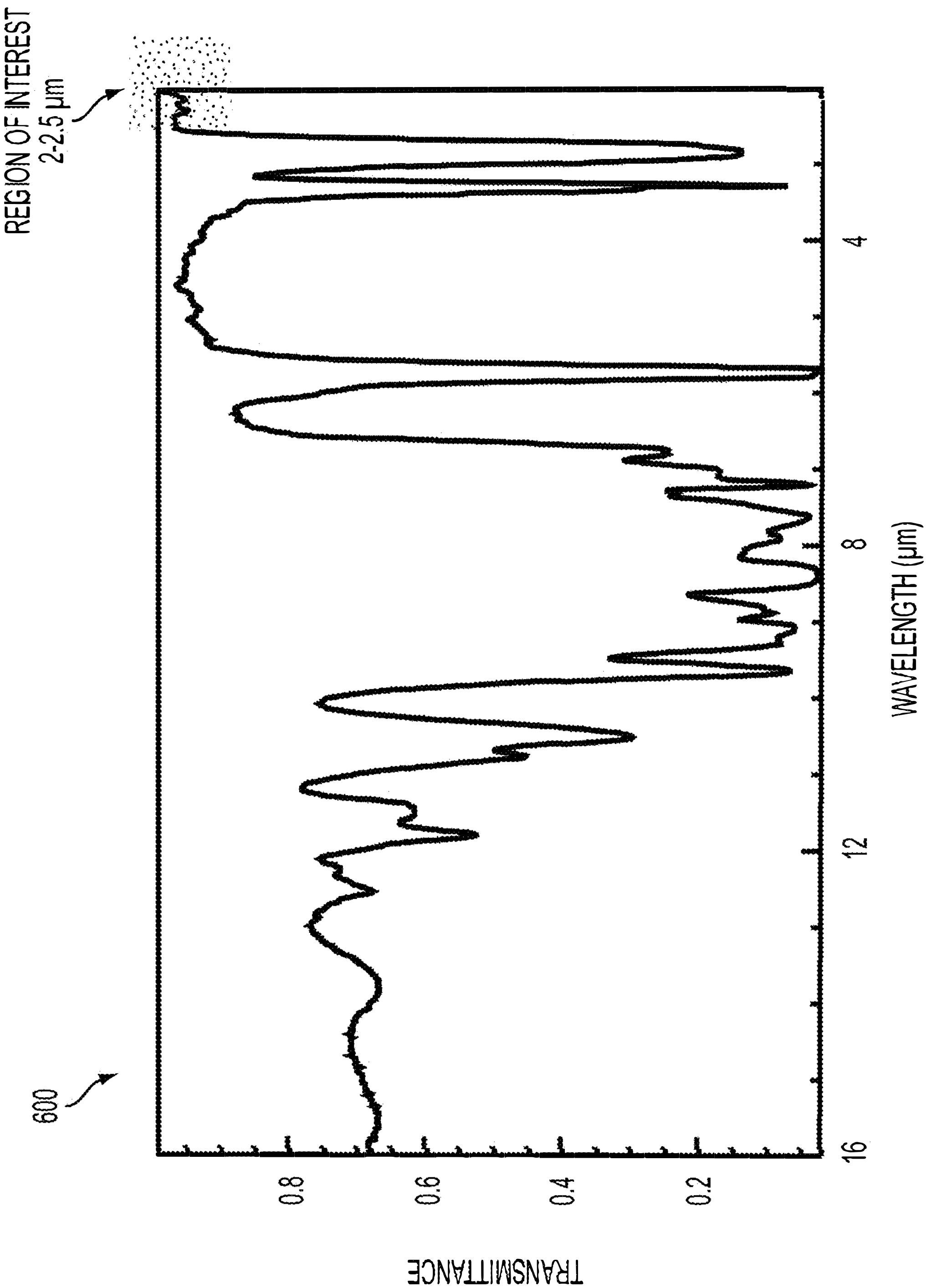
REGION OF INTEREST
2-2.5 µm
600
TRANSMITTANCE
0.8
0.6
0.4
0.2
WAVELENGTH (µm)
4
8
12
16

FIG. 6

FIG. 7

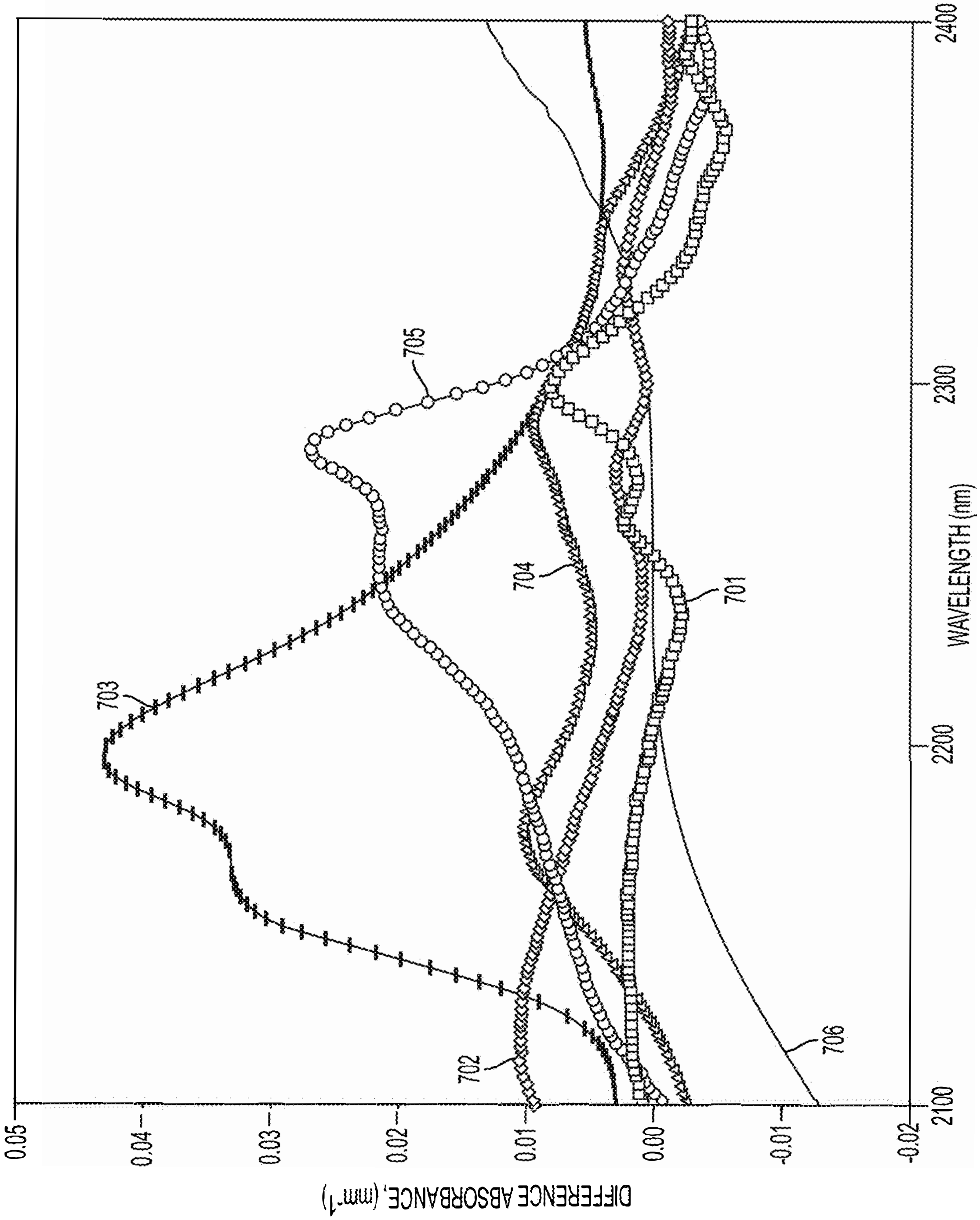
701
702
703
704
705
706
0.05
0.04
0.03
0.02
0.01
0.00
-0.01
-0.02
2100
2200
2300
2400
WAVELENGTH (nm)
DIFFERENCE ABSORBANCE, (mm-1)

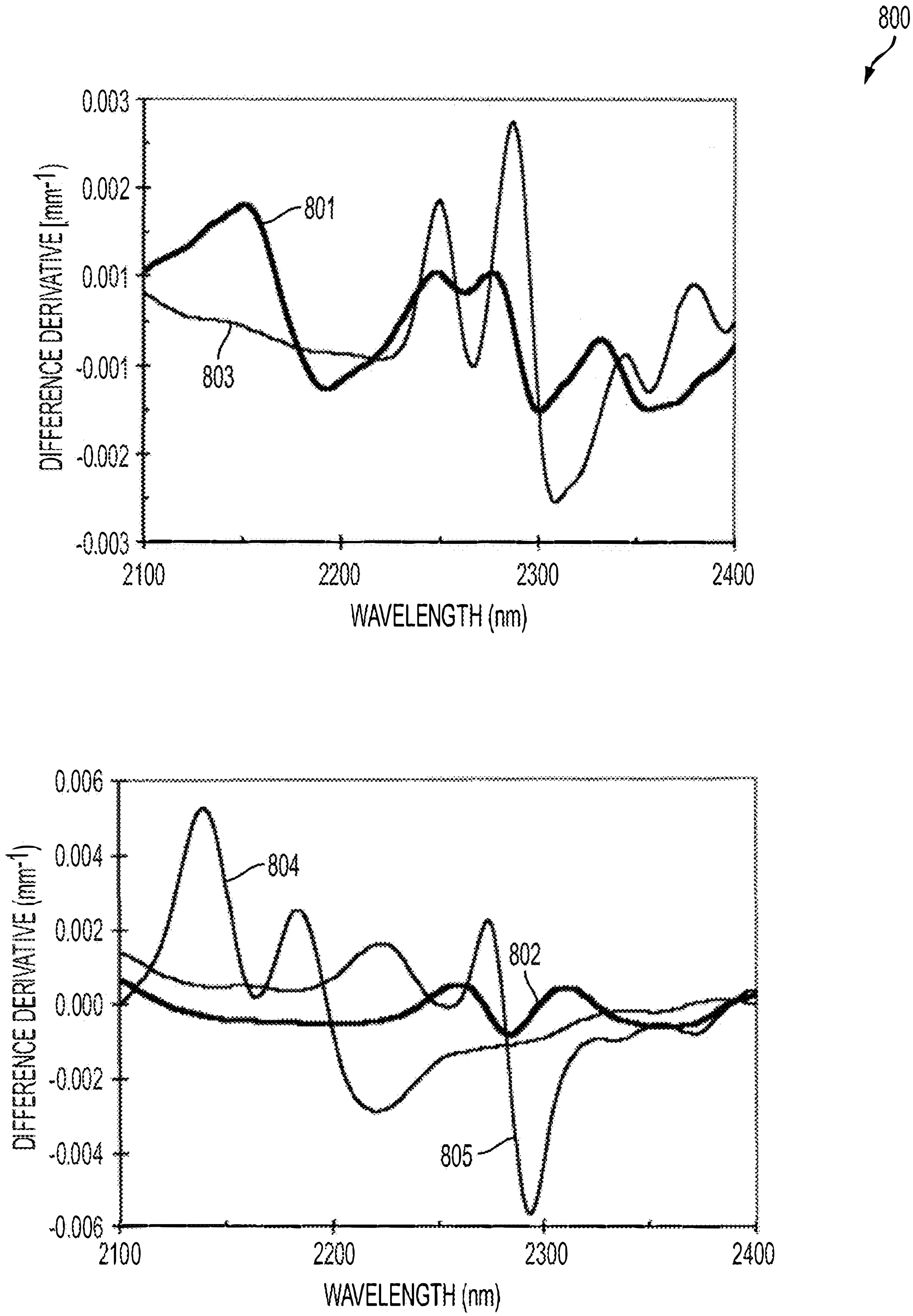
800
0.003
0.002
0.001
-0.001
-0.002
-0.003
DIFFERENCE DERIVATIVE [mm-1]
801
803
2100
2200
2300
2400
WAVELENGTH (nm)
0.006
0.004
0.002
0.000
-0.002
-0.004
-0.006
DIFFERENCE DERIVATIVE (mm-1)
804
802
805
2100
2200
2300
2400
WAVELENGTH (nm)

FIG. 8A

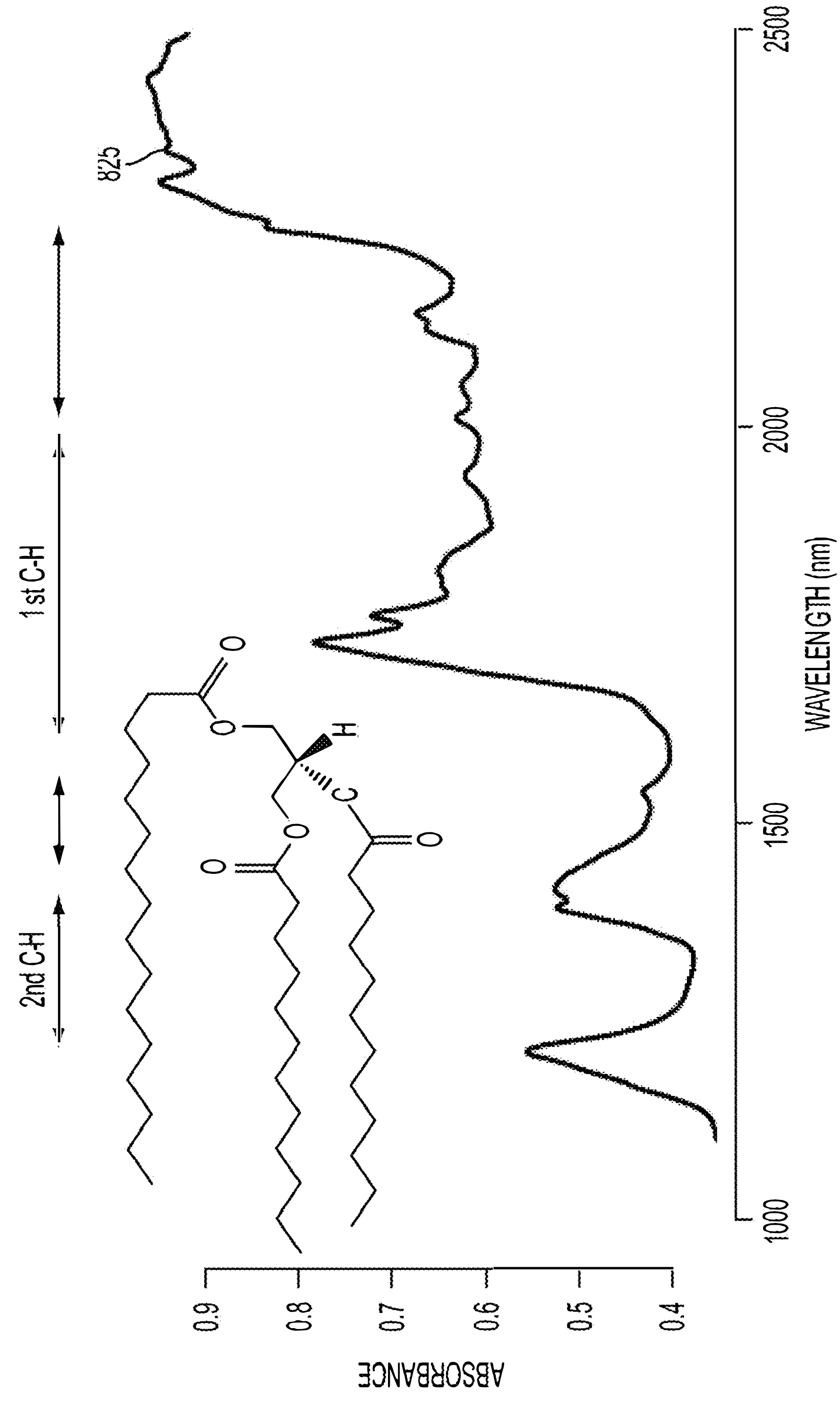
1st C-H
2nd C-H
825
2500
2000
1500
1000
WAVELENGTH (nm)
ABSORBANCE
0.9
0.8
0.7
0.6
0.5
0.4
O
H
C

FIG. 8B

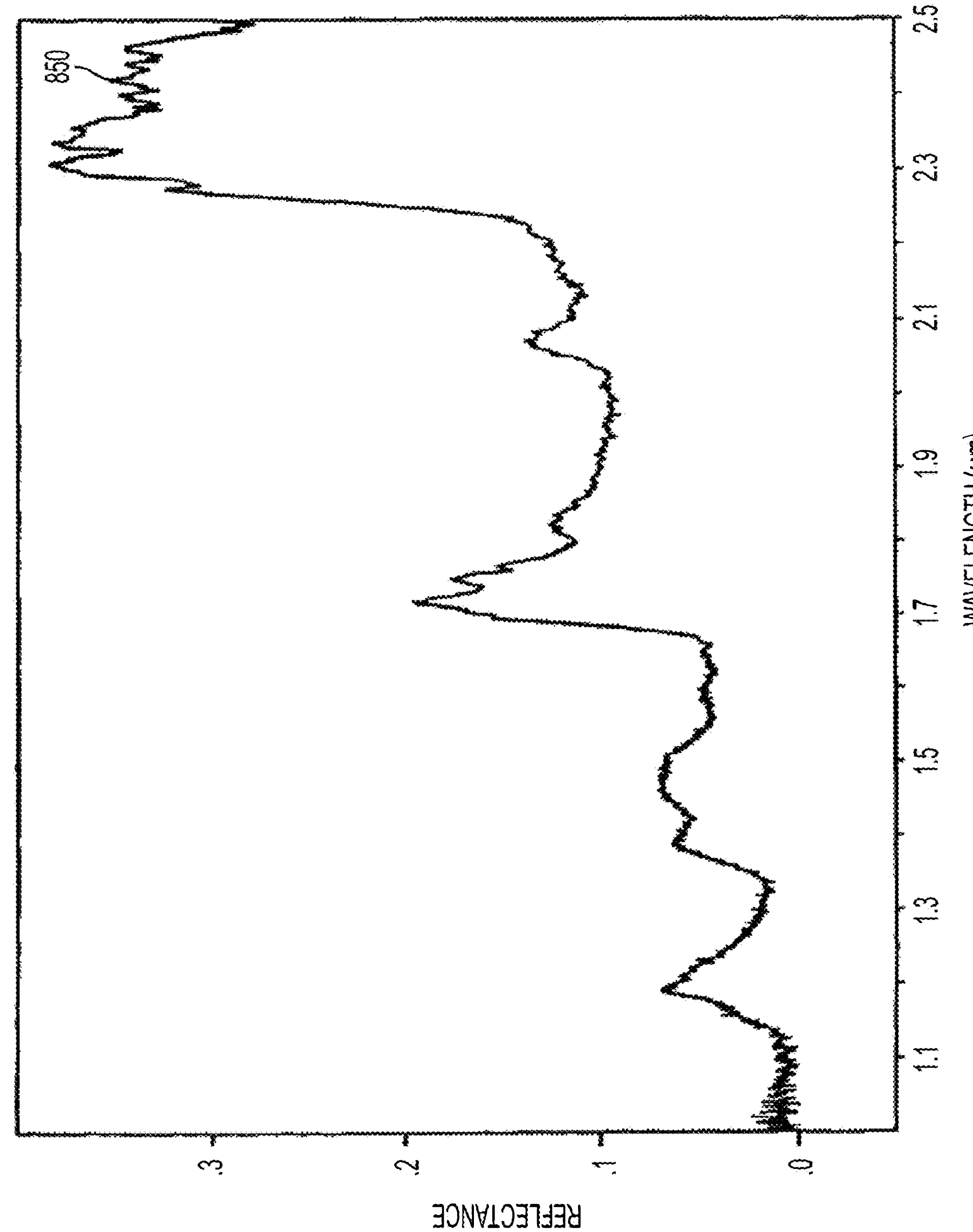

FIG. 8C

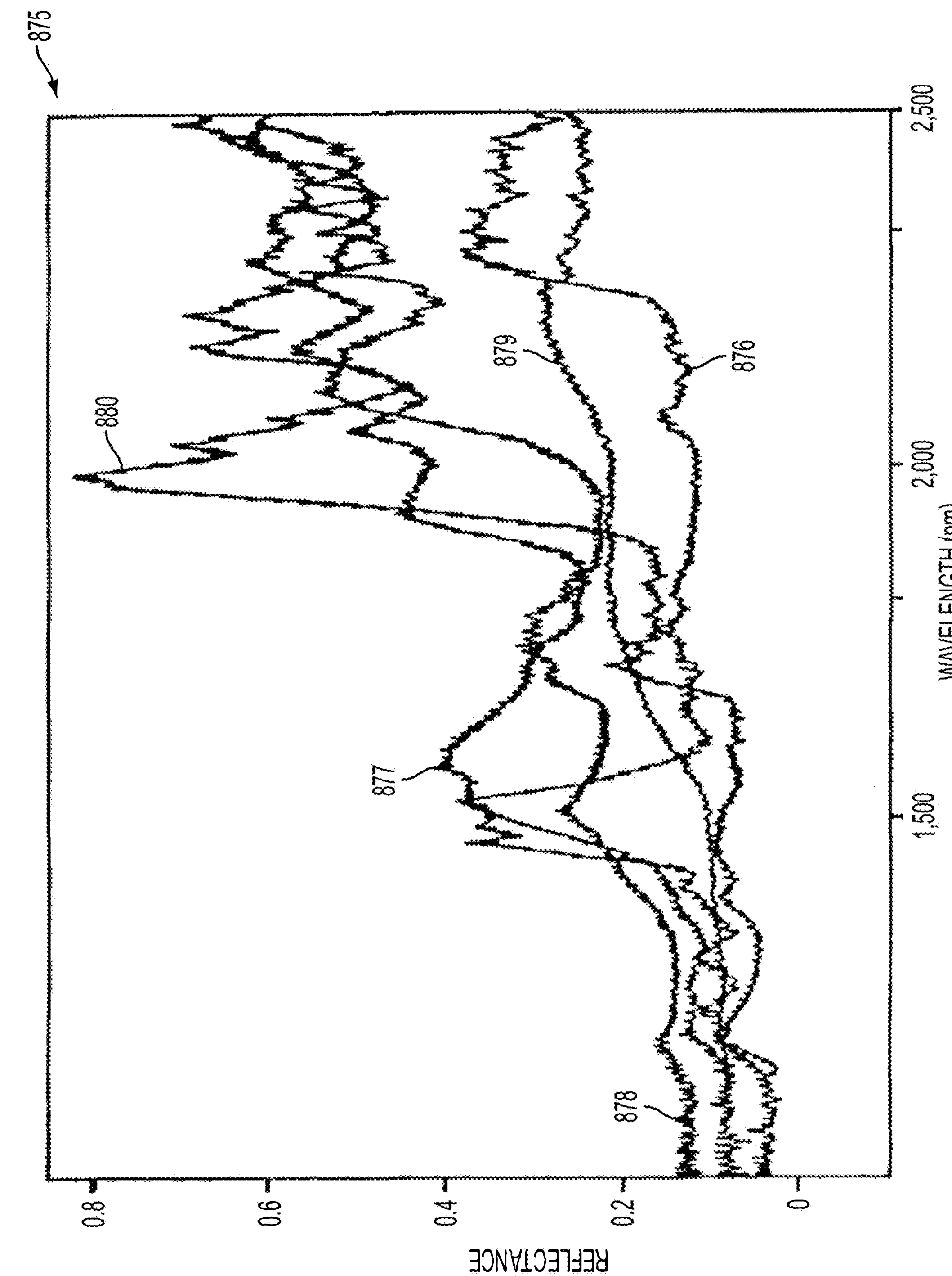
875
880
877
878
879
876
REFLECTANCE
0.8
0.6
0.4
0.2
0
WAVELENGTH (nm)
1,500
2,000
2,500

FIG. 8D

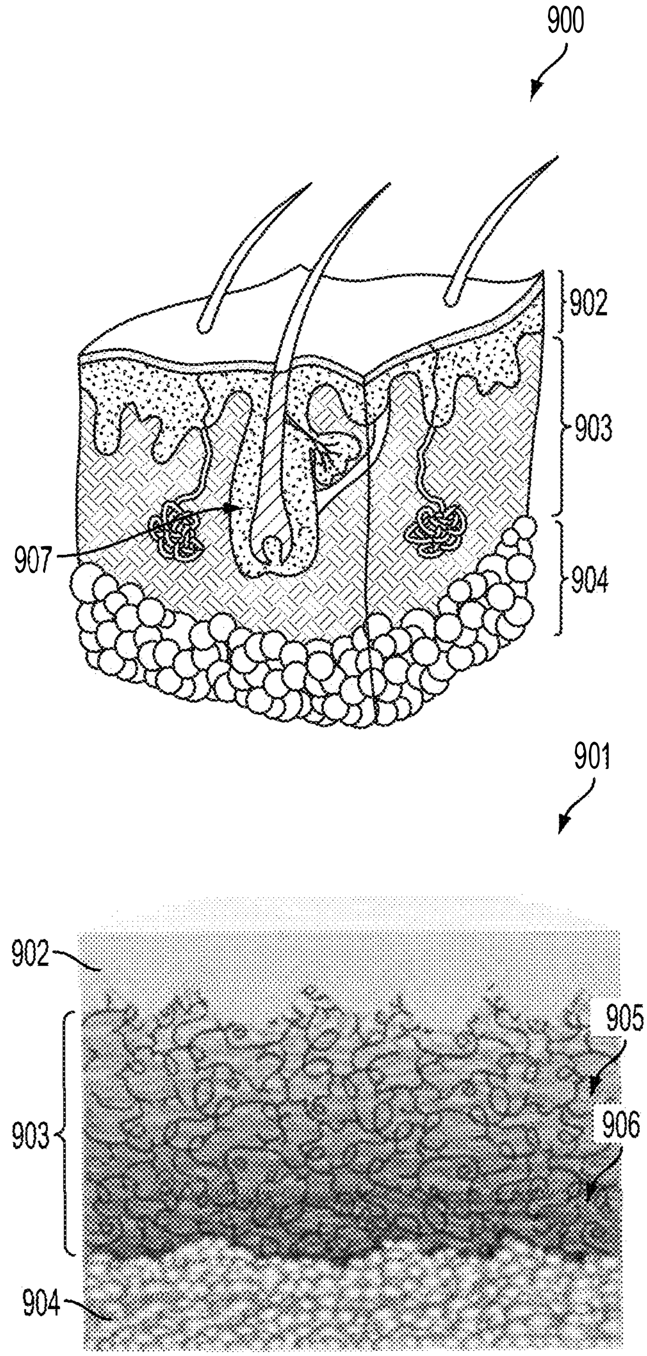

FIG. 9

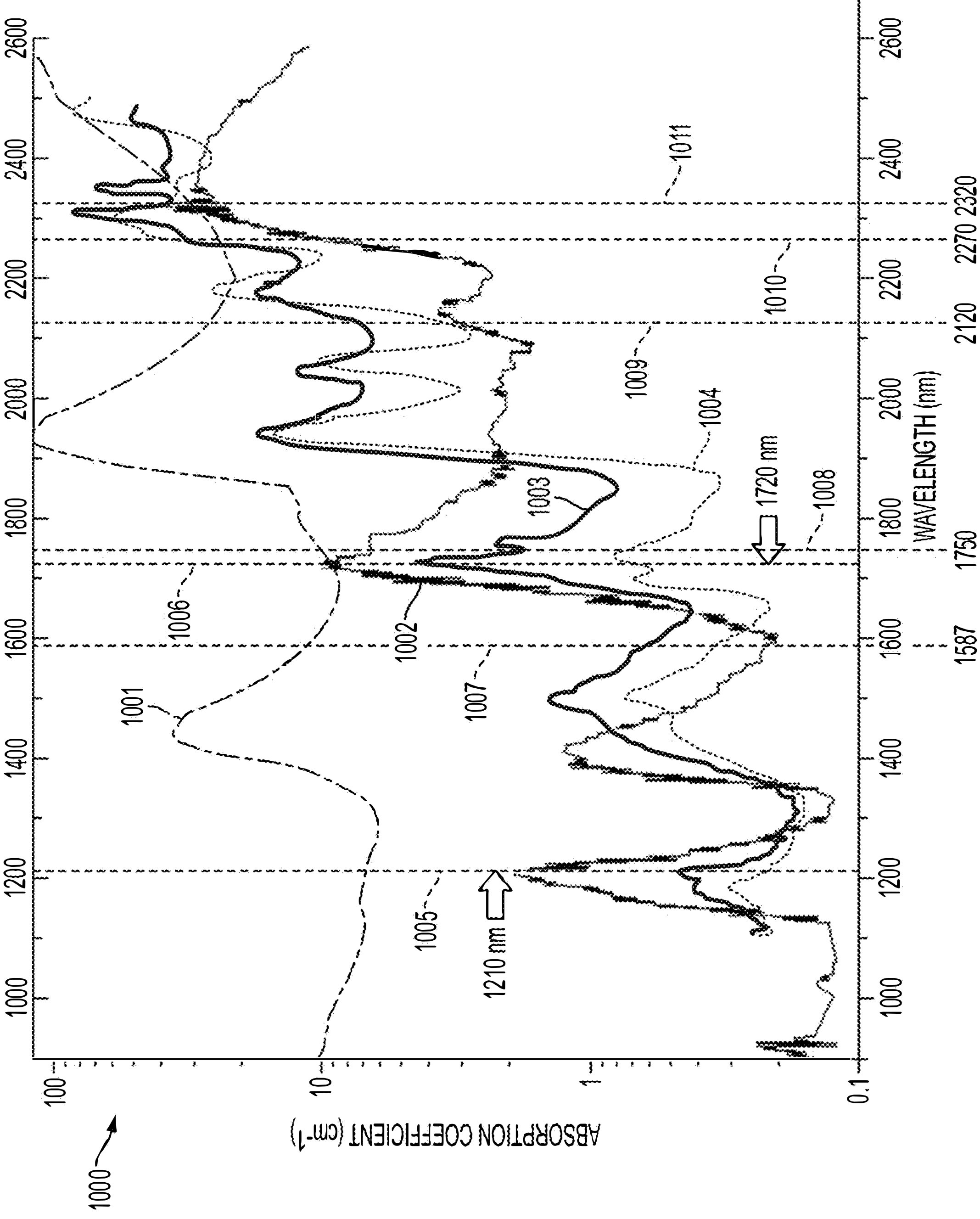

1000
ABSORPTION COEFFICIENT (cm-1)
100
10
1
0.1
WAVELENGTH (nm)
1000
1200
1400
1600
1800
2000
2200
2400
2600
1587
1750
2120
2270 2320
1210 nm
1720 nm
1001
1002
1003
1004
1005
1006
1007
1008
1009
1010
1011

FIG. 10

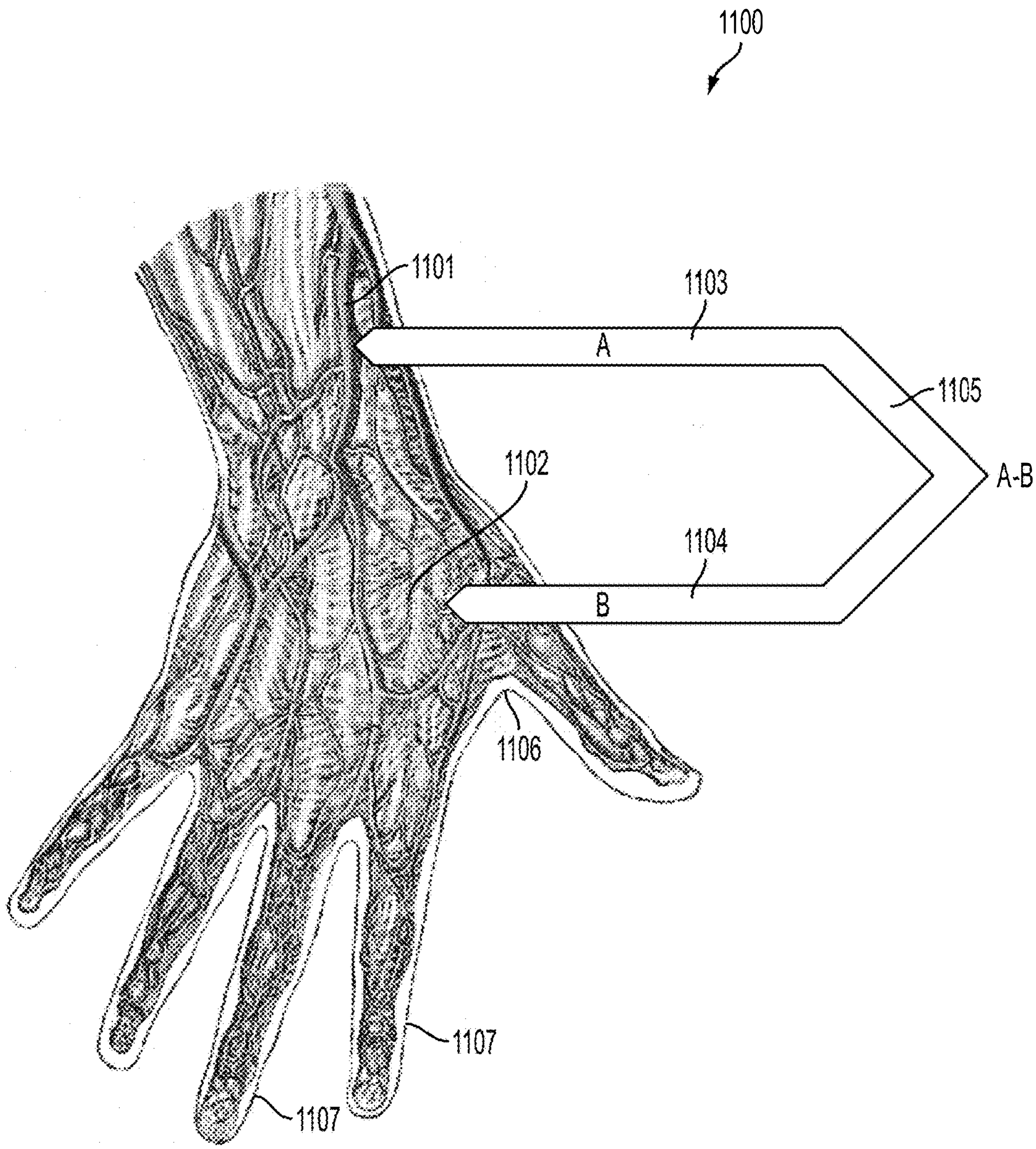

FIG. 11

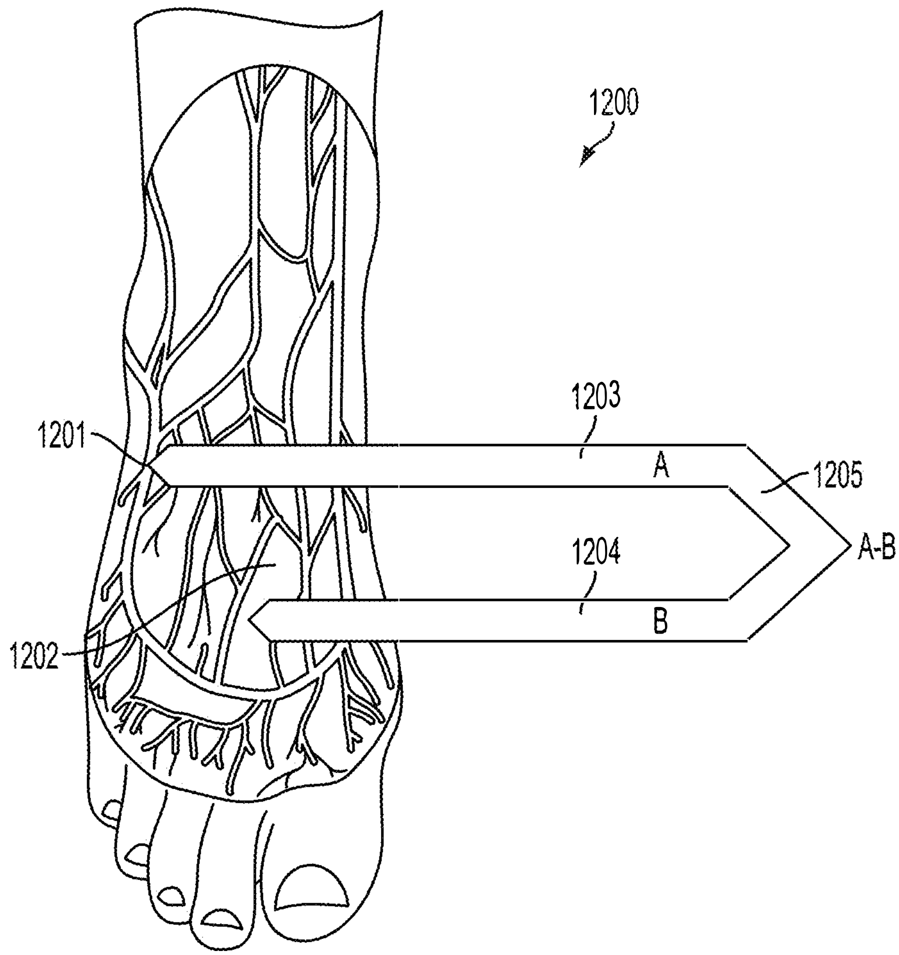

FIG. 12

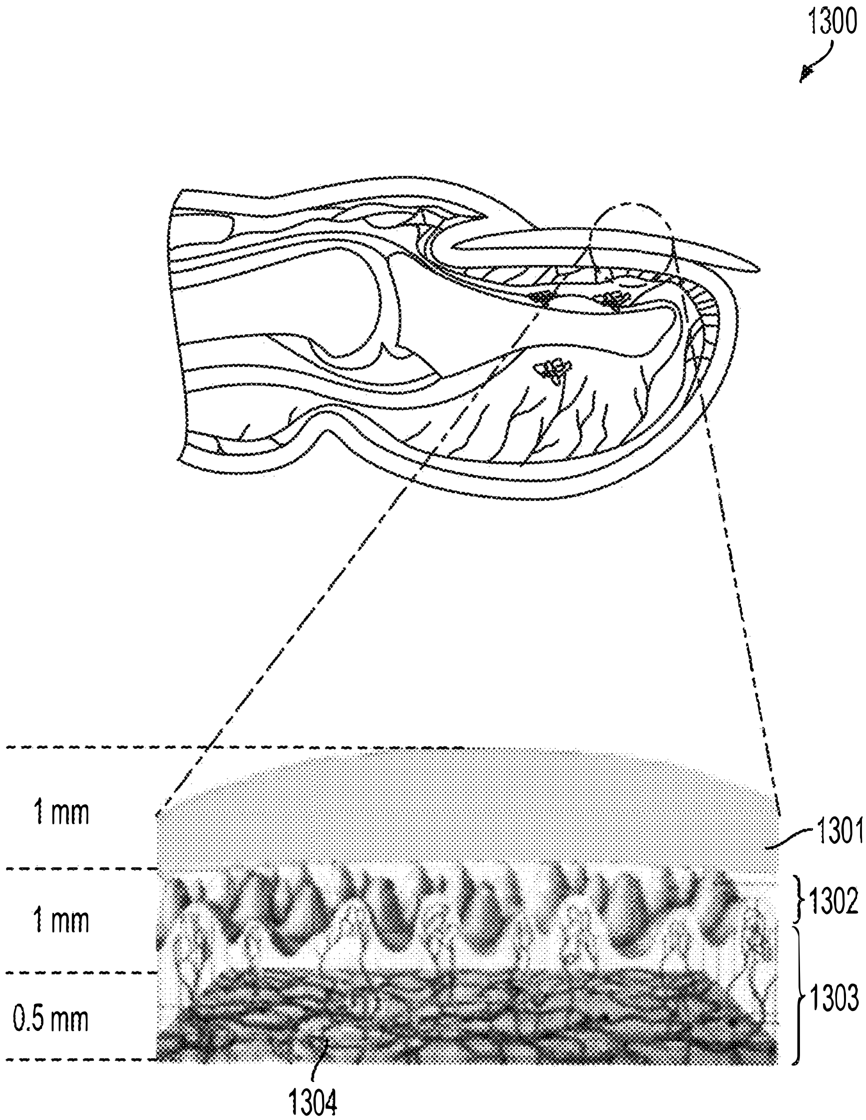

FIG. 13

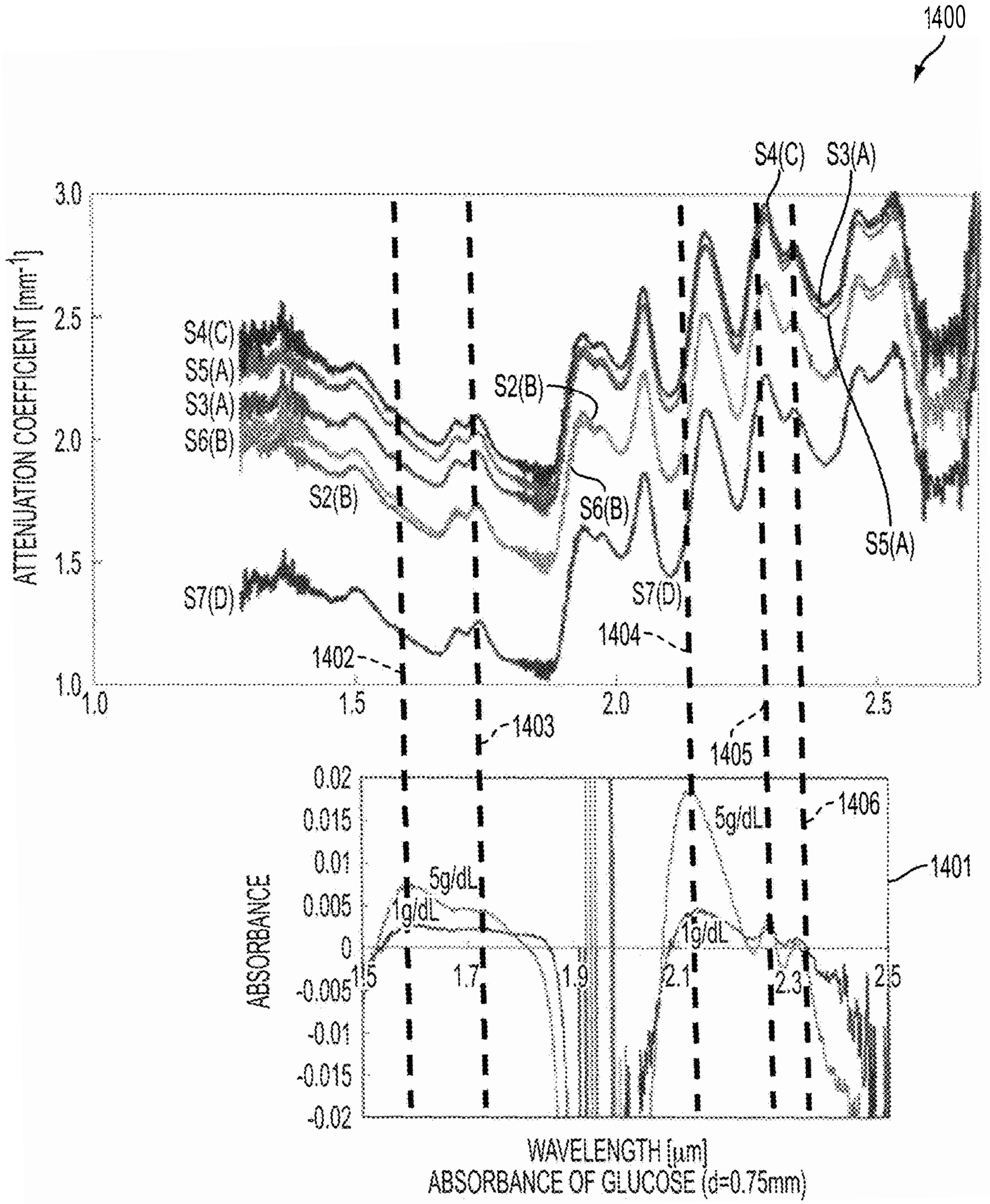
1400
S4(C)
S3(A)
3.0
2.5
2.0
1.5
1.0
ATTENUATION COEFFICIENT [mm⁻¹]
S4(C)
S5(A)
S3(A)
S6(B)
S2(B)
S2(B)
S6(B)
S5(A)
S7(D)
S7(D)
1402
1404
1.0
1.5
2.0
2.5
1403
1405
1406
1401
0.02
0.015
0.01
0.005
0
-0.005
-0.01
-0.015
-0.02
ABSORBANCE
5g/dL
1g/dL
5g/dL
1g/dL
1.5
1.7
1.9
2.1
2.3
2.5
WAVELENGTH [µm]
ABSORBANCE OF GLUCOSE (d=0.75mm)

FIG. 14

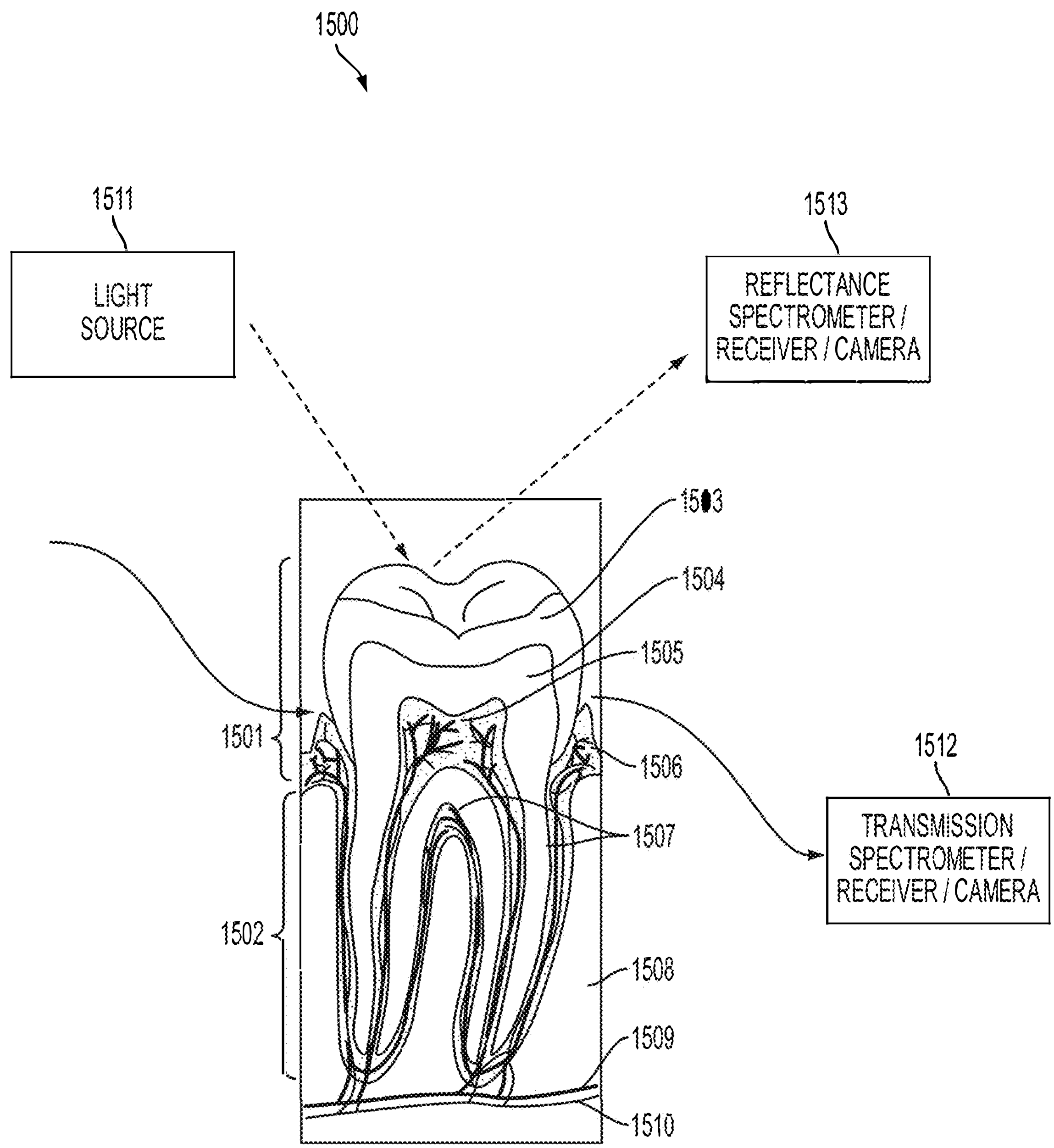
1500
1511
LIGHT SOURCE
1513
REFLECTANCE SPECTROMETER / RECEIVER / CAMERA
1503
1504
1505
1501
1506
1512
TRANSMISSION SPECTROMETER / RECEIVER / CAMERA
1507
1502
1508
1509
1510

FIG. 15

1600

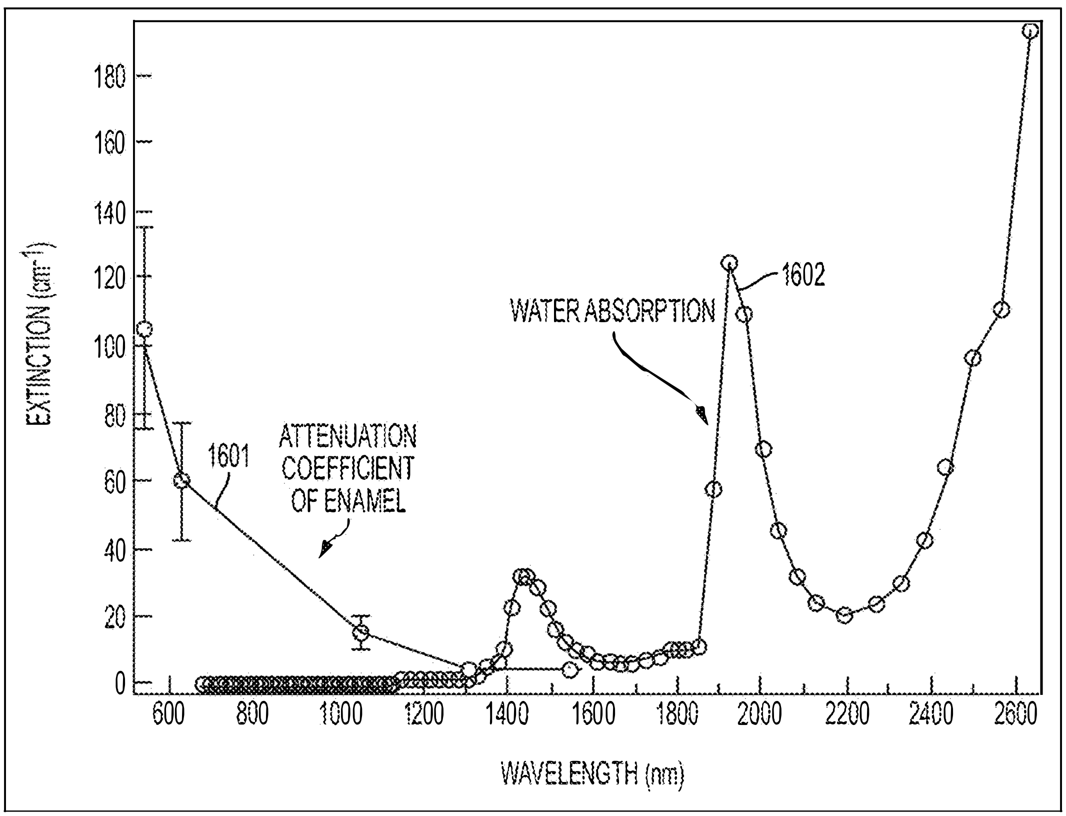
180
160
140
120
100
80
60
40
20
0
EXTINCTION (cm⁻¹)
600
800
1000
1200
1400
1600
1800
2000
2200
2400
2600
WAVELENGTH (nm)
1601
ATTENUATION COEFFICIENT OF ENAMEL
WATER ABSORPTION
1602

FIG. 16A

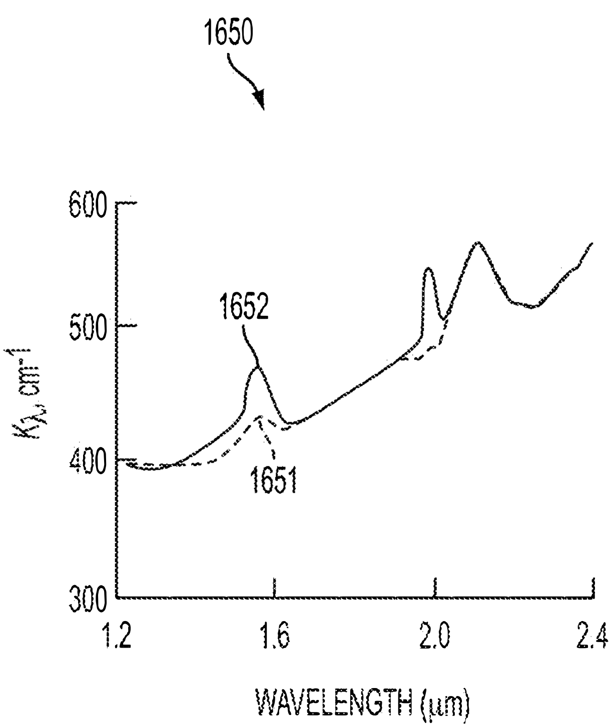

1650
600
500
400
300
1652
1651
K_λ, cm^{-1}
1.2
1.6
2.0
2.4
WAVELENGTH (µm)

FIG. 16B

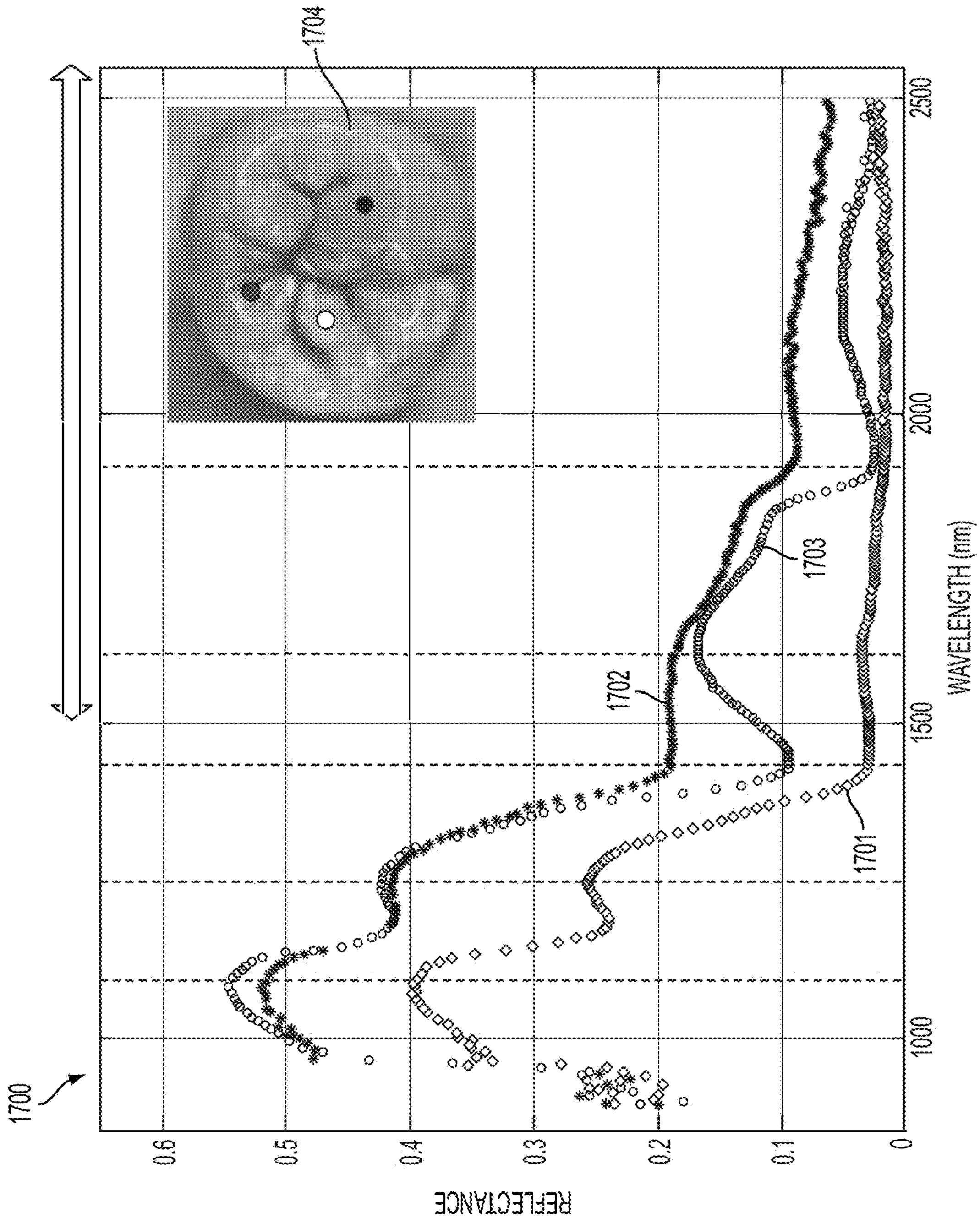
1700
1701
1702
1703
1704
REFLECTANCE
0
0.1
0.2
0.3
0.4
0.5
0.6
WAVELENGTH (nm)
1000
1500
2000
2500

FIG. 17

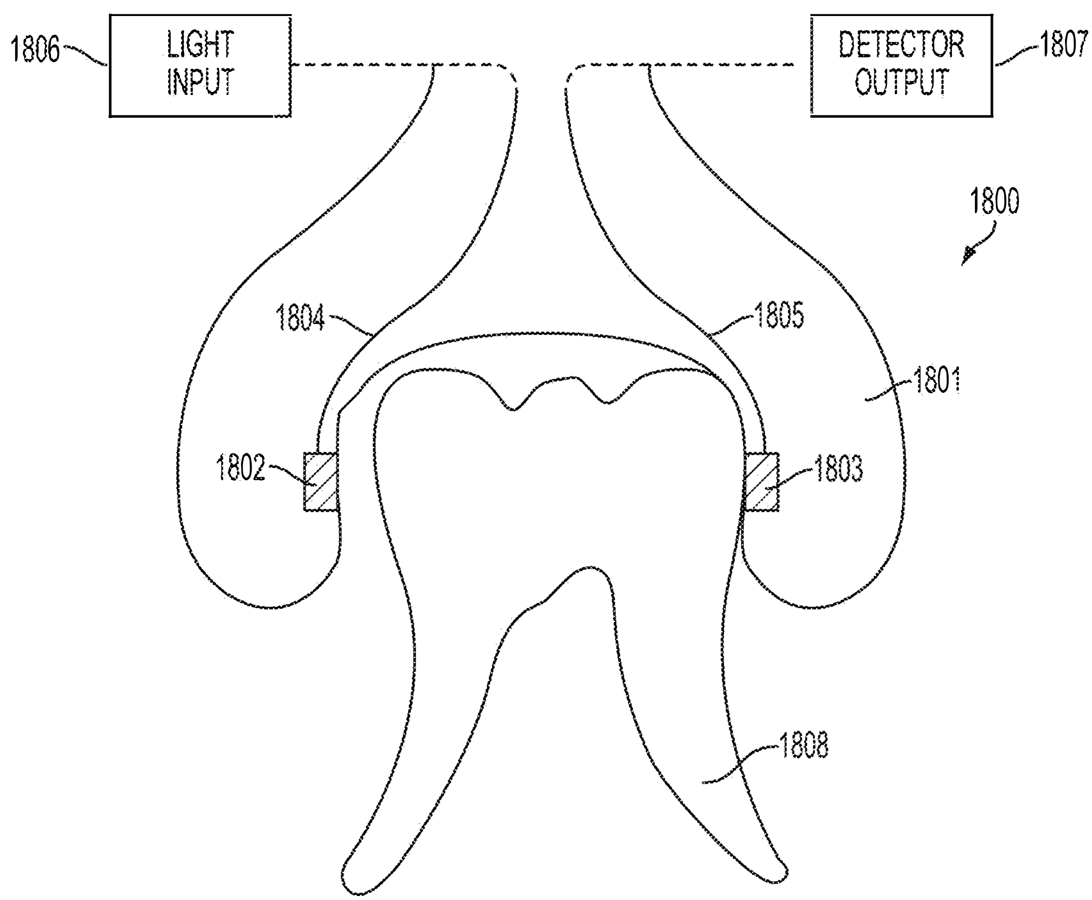
1806
LIGHT INPUT
DETECTOR OUTPUT
1807
1800
1804
1805
1801
1802
1803
1808

FIG. 18A

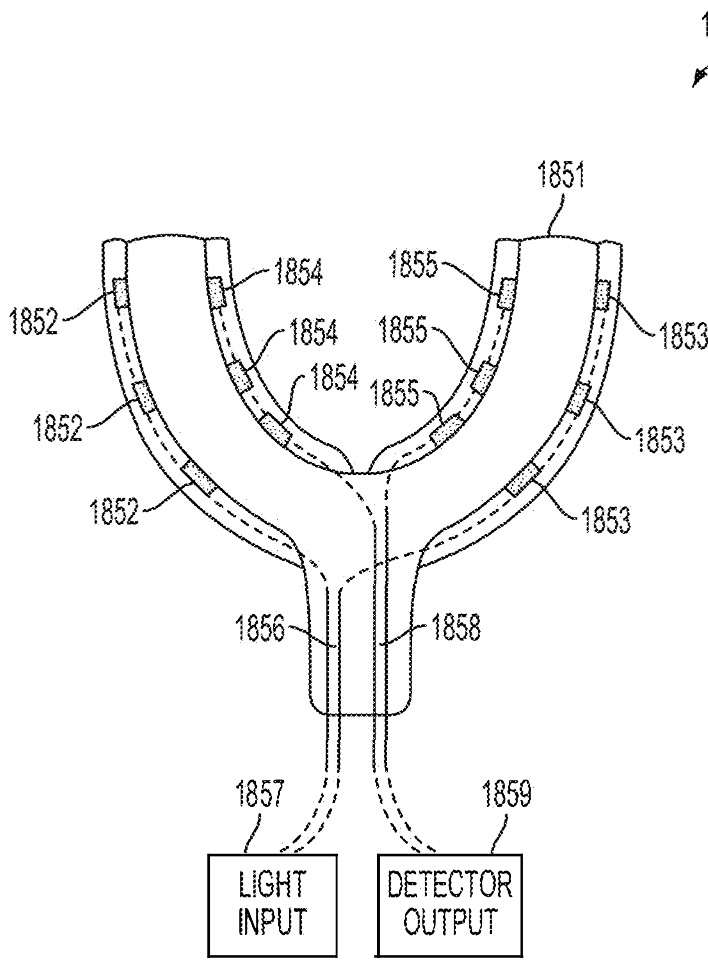
1850
1851
1852
1852
1852
1853
1853
1853
1854
1854
1854
1855
1855
1855
1856
1858
1857
1859
LIGHT INPUT
DETECTOR OUTPUT

FIG. 18B

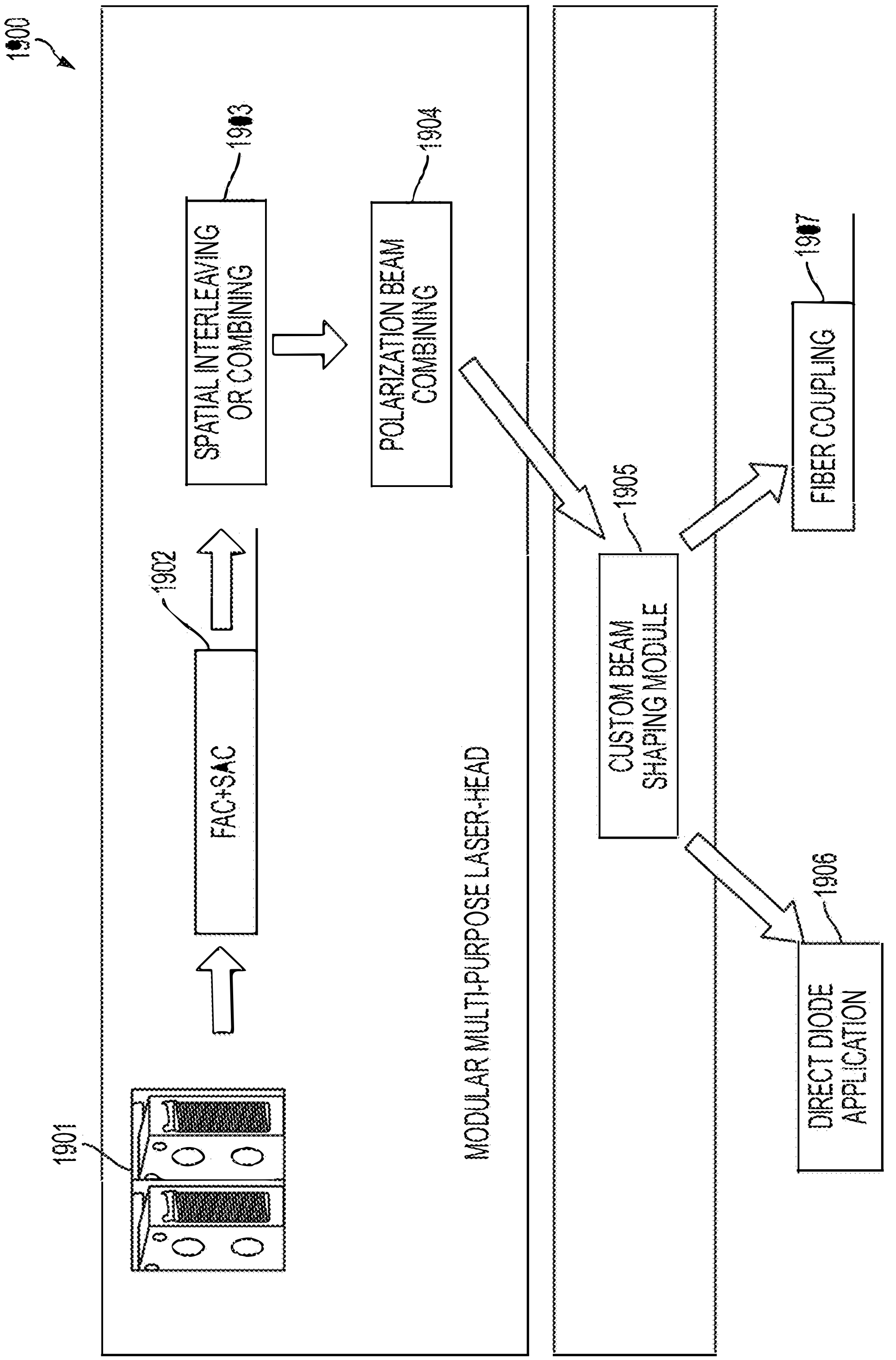
1900
1901
1902
FAC+SAC
1903
SPATIAL INTERLEAVING OR COMBINING
1904
POLARIZATION BEAM COMBINING
MODULAR MULTI-PURPOSE LASER-HEAD
1905
CUSTOM BEAM SHAPING MODULE
1906
DIRECT DIODE APPLICATION
1907
FIBER COUPLING

FIG. 19

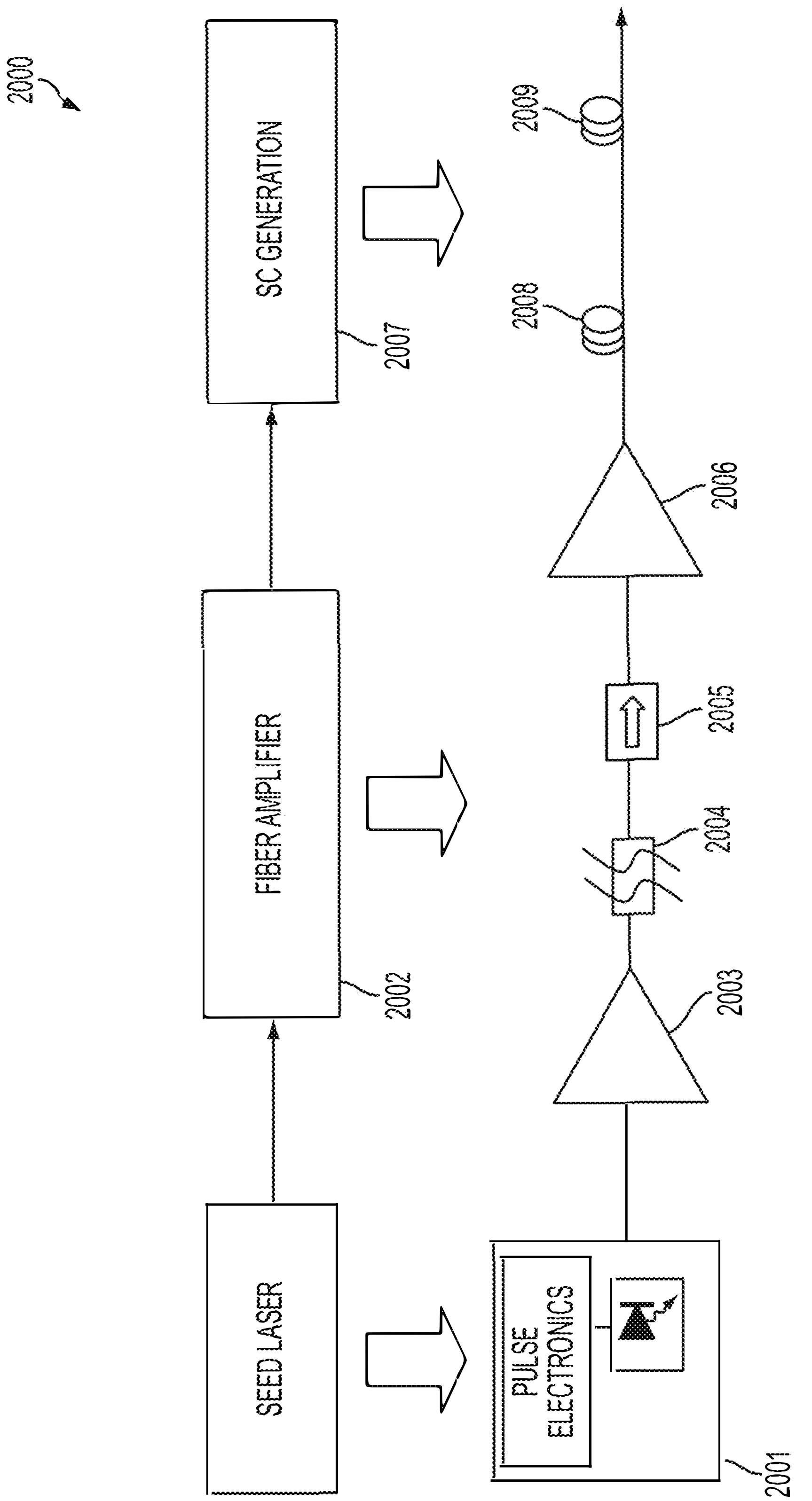
2000
SEED LASER
FIBER AMPLIFIER
SC GENERATION
2002
2007
PULSE ELECTRONICS
2001
2003
2004
2005
2006
2008
2009

FIG. 20

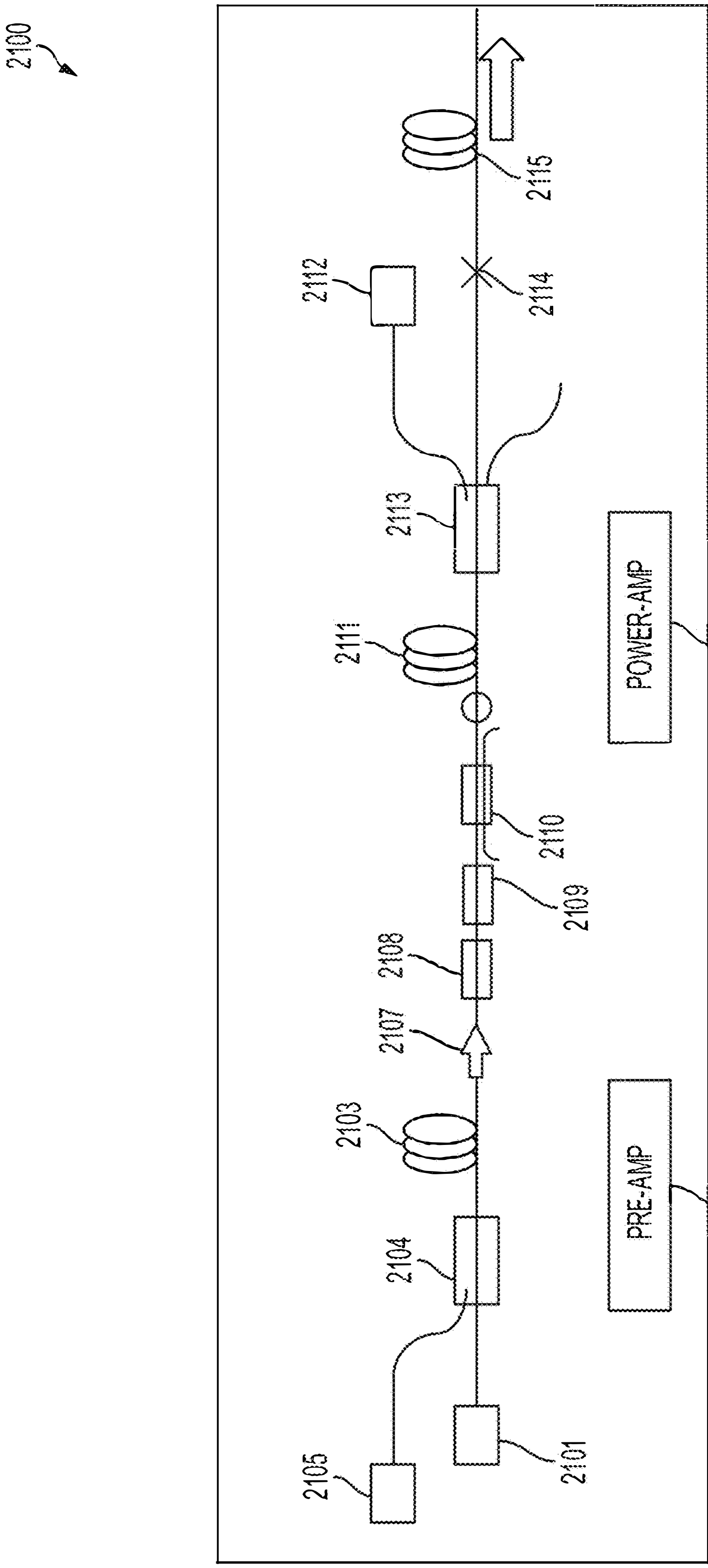
2100
2105
2101
2104
2103
2107
2108
2109
2110
2111
2113
2112
2114
2115
PRE-AMP
2102
POWER-AMP
2106

FIG. 21

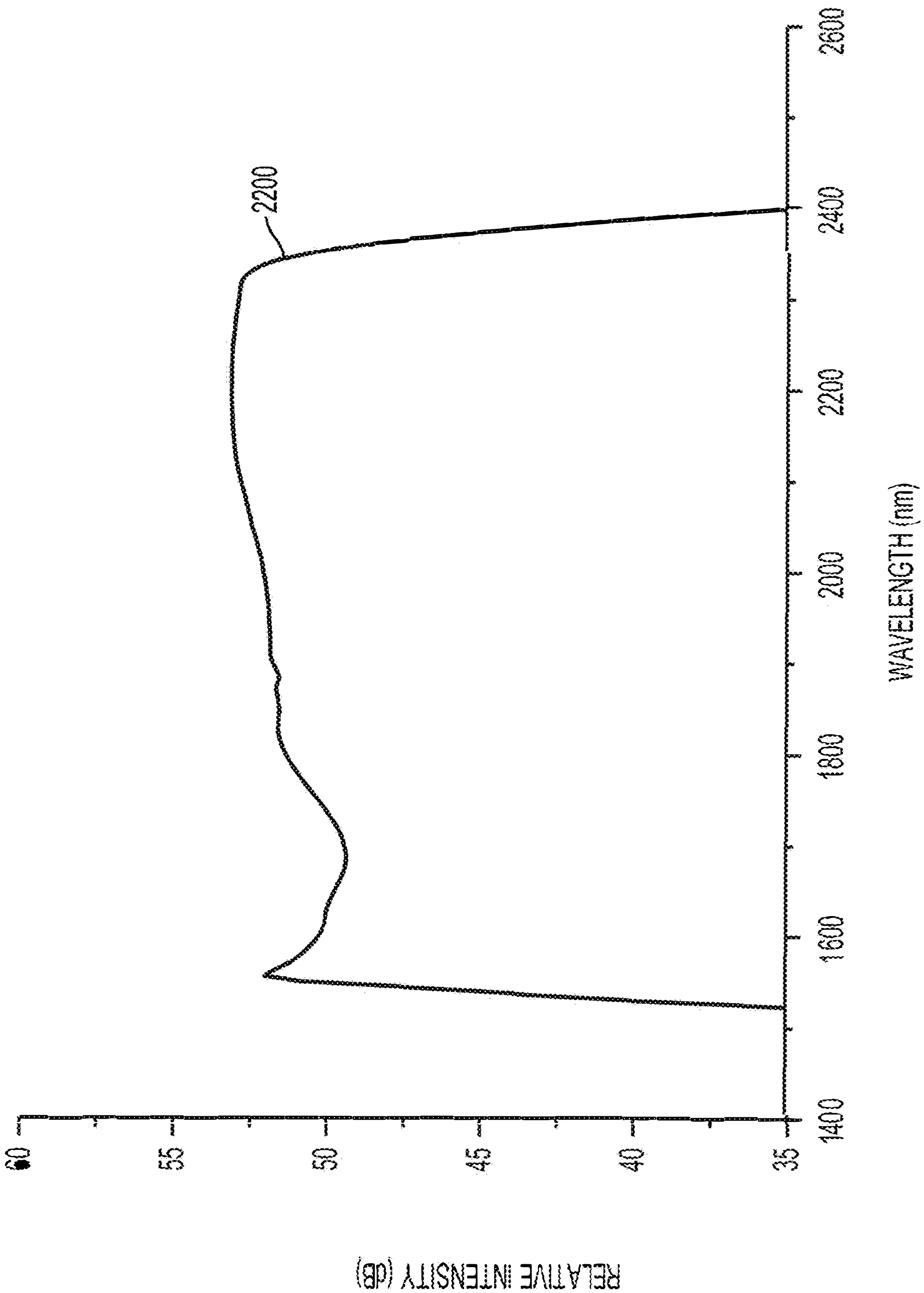
2200
RELATIVE INTENSITY (dB)
60
55
50
45
40
35
1400
1600
1800
2000
2200
2400
2600
WAVELENGTH (nm)

FIG. 22

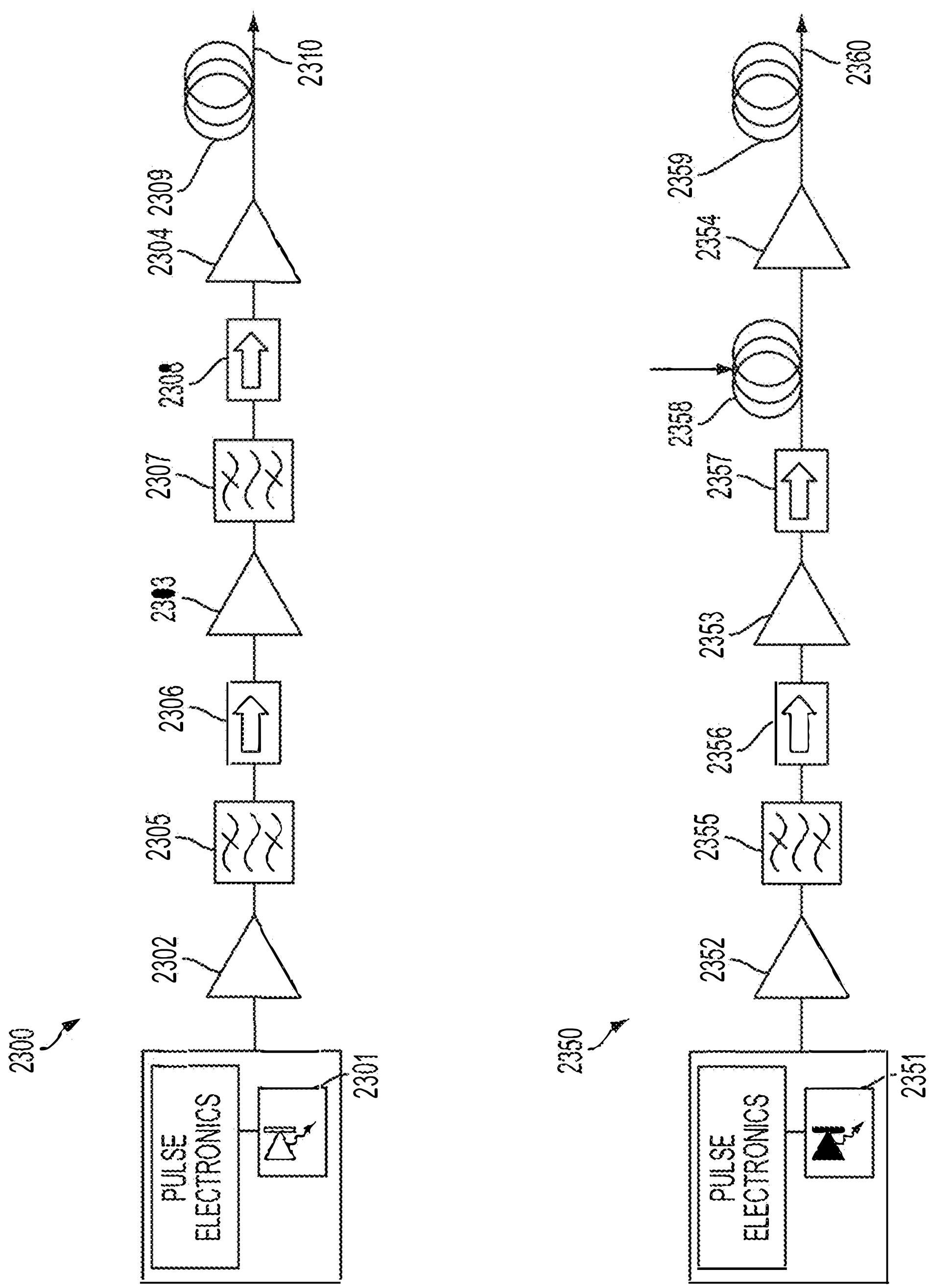
2300
PULSE ELECTRONICS
2301
2302
2305
2306
2303
2307
2308
2304
2309
2310
2350
PULSE ELECTRONICS
2351
2352
2355
2356
2353
2357
2358
2354
2359
2360

FIG. 23

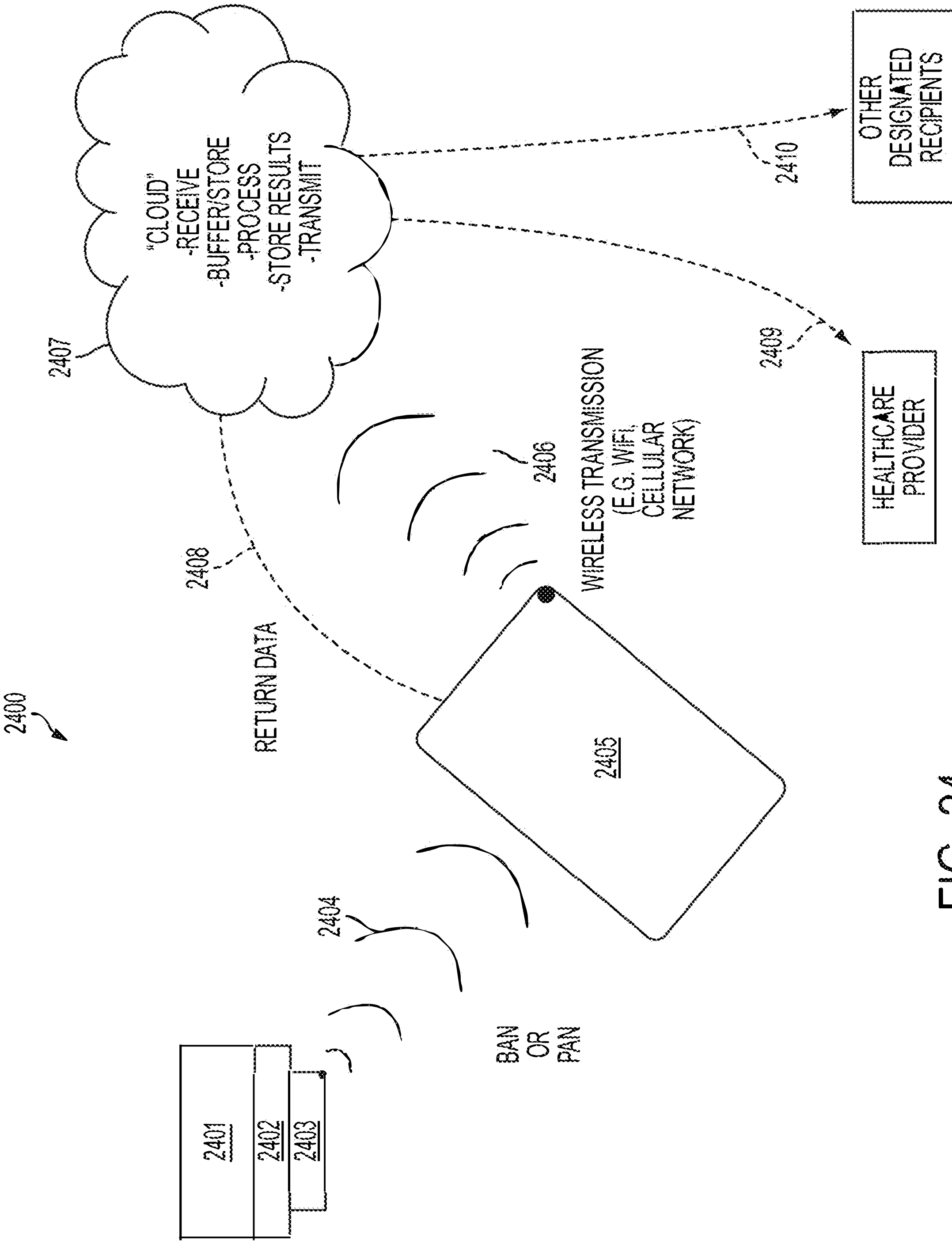
2400
2401
2402
2403
2404
BAN OR PAN
2405
RETURN DATA
2408
WIRELESS TRANSMISSION (E.G. WIFI, CELLULAR NETWORK)
2406
2407
"CLOUD"
-RECEIVE
-BUFFER/STORE
-PROCESS
-STORE RESULTS
-TRANSMIT
2409
HEALTHCARE PROVIDER
2410
OTHER DESIGNATED RECIPIENTS

FIG. 24

NEAR-INFRARED LASERS FOR NON-INVASIVE MONITORING OF GLUCOSE, KETONES, HBA1C, AND OTHER BLOOD CONSTITUENTS

CROSS-REFERENCE TO RELATED APPLICATIONS

This application is a continuation of U.S. application Ser. No. 14/650,897 filed Jun. 10, 2015, which is a U.S. National Phase of PCT/US2013/075700 filed Dec. 17, 2013, which claims the benefit of U.S. provisional application Ser. No. 61/747,472 filed Dec. 31, 2012, the disclosures of which are hereby incorporated in their entirety by reference herein.

This application is related to U.S. provisional application Ser. No. 61/747,477 filed Dec. 31, 2012; Ser. No. 61/747,481 filed Dec. 31, 2012; Ser. No. 61/747,485 filed Dec. 31, 2012; Ser. No. 61/747,487 filed Dec. 31, 2012; Ser. No. 61/747,492 filed Dec. 31, 2012; Ser. No. 61/747,553 filed Dec. 31, 2012; and Ser. No. 61/754,698 filed Jan. 21, 2013, the disclosures of which are hereby incorporated in their entirety by reference herein.

This application has a common priority date with International Application PCT/US2013/075736 entitled Short-Wave Infrared Super-Continuum Lasers For Early Detection Of Dental Caries; U.S. application Ser. No. 14/108,995 filed Dec. 17, 2013 entitled Focused Near-Infrared Lasers For Non-Invasive Vasectomy And Other Thermal Coagulation Or Occlusion Procedures; International Application PCT/US2013/075767 entitled Short-Wave Infrared Super-Continuum Lasers For Natural Gas Leak Detection, Exploration, And Other Active Remote Sensing Applications; U.S. application Ser. No. 14/108,986 filed Dec. 17, 2013 entitled Short-Wave Infrared Super-Continuum Lasers For Detecting Counterfeit Or Illicit Drugs And Pharmaceutical Process Control; U.S. application Ser. No. 14/108,974 filed Dec. 17, 2013 entitled Non-Invasive Treatment Of Varicose Veins; and U.S. application Ser. No. 14/109,007 filed Dec. 17, 2013 entitled Near-Infrared Super-Continuum Lasers For Early Detection Of Breast And Other Cancers, the disclosures of which are hereby incorporated in their entirety by reference herein.

TECHNICAL FIELD

This disclosure relates in general to lasers and light sources for healthcare, medical, or bio-technology applications including systems and methods for using near-infrared light sources for non-invasive monitoring of different blood constituents or blood analytes, such as glucose, ketones, and hemoglobin A1C (HbA1C).

BACKGROUND

With the growing obesity epidemic, the number of individuals with diabetes is also increasing dramatically. For example, there are over 200 million people who have diabetes. Diabetes control requires monitoring of the glucose level, and most glucose measuring systems available commercially require drawing of blood. Depending on the severity of the diabetes, a patient may have to draw blood and measure glucose four to six times a day. This may be extremely painful and inconvenient for many people. In addition, for some groups, such as soldiers in the battlefield, it may be dangerous to have to measure periodically their glucose level with finger pricks.

Thus, there is an unmet need for non-invasive glucose monitoring (e.g., monitoring glucose without drawing blood). The challenge has been that a non-invasive system requires adequate sensitivity and selectivity, along with repeatability of the results. Yet, this is a very large market, with an estimated annual market of over $10B in 2011 for self-monitoring of glucose levels.

One approach to non-invasive monitoring of blood constituents or blood analytes is to use near-infrared spectroscopy, such as absorption spectroscopy or near-infrared diffuse reflection or transmission spectroscopy. Some attempts have been made to use broadband light sources, such as tungsten lamps, to perform the spectroscopy. However, several challenges have arisen in these efforts. First, many other constituents in the blood also have signatures in the near-infrared, so spectroscopy and pattern matching, often called spectral fingerprinting, is required to distinguish the glucose with sufficient confidence. Second, the non-invasive procedures have often transmitted or reflected light through the skin, but skin has many spectral artifacts in the near-infrared that may mask the glucose signatures. Moreover, the skin may have significant water and blood content. These difficulties become particularly complicated when a weak light source is used, such as a lamp. More light intensity can help to increase the signal levels, and, hence, the signal-to-noise ratio.

As described in this disclosure, by using brighter light sources, such as fiber-based supercontinuum lasers, super-luminescent laser diodes, light-emitting diodes or a number of laser diodes, the near-infrared signal level from blood constituents may be increased. By shining light through the teeth, which have fewer spectral artifacts than skin in the near-infrared, the blood constituents may be measured with less interfering artifacts. Also, by using pattern matching in spectral fingerprinting and various software techniques, the signatures from different constituents in the blood may be identified. Moreover, value-add services may be provided by wirelessly communicating the monitored data to a handheld device such as a smart phone, and then wirelessly communicating the processed data to the cloud for storing, processing, and transmitting to several locations.

SUMMARY OF EXAMPLE EMBODIMENTS

In one embodiment, a wearable device for use with a smart phone or tablet comprises a measurement device including a light source comprising a plurality of light emitting diodes for measuring one or more physiological parameters, the measurement device configured to generate an input optical beam with one or more optical wavelengths, wherein at least a portion of the one or more optical wavelengths is a near-infrared wavelength between 700 nanometers and 2500 nanometers. The measurement device comprises one or more lenses configured to receive and to deliver a portion of the input optical beam to a sample comprising skin or tissue, wherein the sample reflects at least a portion of the input optical beam delivered to the sample. The measurement device further comprises a receiver to receive at least a portion of the input optical beam reflected from the sample. The light source is configured to increase the signal-to-noise ratio of the input optical beam reflected from the sample, wherein the increased signal-to-noise ratio results from an increase to the light intensity from at least one of the plurality of light emitting diodes and from a modulation of at least one of the plurality of light emitting diodes. The measurement device is configured to generate an output signal representing at least in part a non-invasive measurement on blood contained within the sample. The wearable device is configured to communicate with the smart phone or tablet, the smart phone or tablet comprising a wireless receiver, a wireless transmitter, a display, a voice input module, a speaker, and a touch screen, the smart phone or tablet configured to receive and to process at least a portion of the output signal, wherein the smart phone or tablet is configured to store and display the processed output signal, wherein at least a portion of the processed output signal is configured to be transmitted over a wireless transmission link.

In another embodiment, a wearable device for use with a smart phone or tablet comprises a measurement device including a light source comprising a plurality of light emitting diodes for measuring one or more physiological parameters. The measurement device is configured to generate an input optical beam with one or more optical wavelengths, wherein at least a portion of the one or more optical wavelengths is a near-infrared wavelength between 700 nanometers and 2500 nanometers. The measurement device comprises one or more lenses configured to receive and to deliver a portion of the input optical beam to a sample comprising skin or tissue, wherein the sample reflects at least a portion of the input optical beam delivered to the sample. The measurement device further comprises a receiver to receive at least a portion of the input optical beam reflected from the sample. The receiver is located a first distance from a first one of the plurality of light emitting diodes and a different distance from a second one of the plurality of light emitting diodes such that the receiver receives a first signal from the first light emitting diode and a second signal from the second light emitting diode. The measurement device is configured to generate an output signal representing at least in part a non-invasive measurement on blood contained within the sample. The wearable device is configured to communicate with the smart phone or tablet. The smart phone or tablet comprises a wireless receiver, a wireless transmitter, a display, a voice input module, a speaker, and a touch screen. The smart phone or tablet is configured to receive and to process at least a portion of the output signal, and to store and display the processed output signal, wherein at least a portion of the processed output signal is configured to be transmitted over a wireless transmission link.

Embodiments also include a method of measuring physiological information comprising providing a wearable device for use with a smart phone or tablet comprising a wireless receiver, a wireless transmitter, a display, a voice input module, a speaker, and a touch screen. The wearable device is capable of performing all of the steps comprising generating an input optical beam having one or more optical wavelengths using a light source comprising a plurality of light emitting diodes, wherein at least a portion of the one or more optical wavelengths is a near-infrared wavelength between 700 nanometers and 2500 nanometers, delivering a portion of the input optical beam to a sample comprising skin or tissue using one or more lenses, receiving a portion of the input optical beam reflected from the sample to generate an output signal representing at least in part a non-invasive measurement on blood contained within the sample, increasing the signal-to-noise ratio of the input optical beam reflected from the sample by increasing a light intensity from at least one of the plurality of light emitting diodes and by modulating at least one of the plurality of light emitting diodes, and transmitting at least a portion of the output signal to the smart phone or tablet for processing to generate a processed output signal and for transmitting from the smart phone or tablet at least a portion of the processed output signal over a wireless transmission link.

In one embodiment, a method of measuring physiological information comprises providing a wearable device for use with a smart phone or tablet comprising a wireless receiver, a wireless transmitter, a display, a voice input module, a speaker, and a touch screen. The wearable device is capable of performing all of the steps of generating a first and a second input optical beam each having one or more optical wavelengths using a light source comprising a plurality of light emitting diodes, wherein at least a portion of the one or more optical wavelengths is a near-infrared wavelength between 700 nanometers and 2500 nanometers, delivering a portion of the first input optical beam and a portion of the second input optical beam to a sample comprising skin or tissue using one or more lenses, receiving a portion of the first input optical beam reflected from the sample from a first one of the plurality of light emitting diodes located at a first distance and receiving a portion of the second input optical beam reflected from the sample from a different one of the plurality of light emitting diodes located at a distance different from the first distance to generate an output signal representing at least in part a non-invasive measurement on blood contained within the sample, transmitting at least a portion of the output signal to the smart phone or tablet for processing to generate a processed output signal and for transmitting from the smart phone or tablet at least a portion of the processed output signal over a wireless transmission link.

In one embodiment, a measurement system includes a light source generating an output optical beam comprising a plurality of semiconductor sources generating an input optical beam, a multiplexer configured to receive at least a portion of the input optical beam and to form an intermediate optical beam, one or more fibers configured to receive at least a portion of the intermediate optical beam and to form the output optical beam, wherein the output optical beam comprises one or more optical wavelengths. An interface device is configured to receive at least a portion of the output optical beam and to deliver the portion of the output optical beam to a sample comprising at least in part enamel, dentine and pulp, wherein the portion of the output optical beam is configured to generate a spectroscopy output beam from the sample. A receiver is configured to receive at least a portion of the spectroscopy output beam and to process the portion of the spectroscopy output beam to generate an output signal representing at least in part a property of blood contained within the pulp.

In another embodiment a diagnostic system includes a light source generating an output optical beam comprising a plurality of semiconductor sources generating an input optical beam, a multiplexer configured to receive at least a portion of the input optical beam and to form an intermediate optical beam, and one or more fibers configured to receive at least a portion of the intermediate optical beam and to form the output optical beam, wherein the output optical beam comprises one or more optical wavelengths, wherein at least a portion of the one or more optical wavelengths comprises a short-wave infrared wavelength between approximately 1400 nanometers and approximately 2500 nanometers, and wherein at least a portion of the one of more fibers is a fused silica fiber with a core diameter less than approximately 400 microns. An interface device is configured to receive at least a portion of the output optical beam and to deliver the portion of the output optical beam to a sample, wherein the portion of the output optical beam is configured to generate a spectroscopy output beam from the sample. A receiver is configured to receive at least a portion of the spectroscopy output beam having a bandwidth of at least 20 nanometers and to process the portion of the spectroscopy output beam to generate an output signal representing at least in part a property of hydro-carbon bonds.

In yet another embodiment, a method of measuring includes generating an output optical beam comprising generating an input optical beam from a plurality of semiconductor sources, multiplexing at least a portion of the input optical beam and forming an intermediate optical beam, guiding at least a portion of the intermediate optical beam and forming the output optical beam, wherein the output optical beam comprises one or more optical wavelengths. The method also may include receiving at least a portion of the output optical beam and delivering the portion of the output optical beam to a sample, wherein the sample comprises at least in part enamel, dentine and pulp. The method also includes generating a spectroscopy output beam from the sample, receiving at least a portion of the spectroscopy output beam, and processing the portion of the spectroscopy output beam and generating an output signal representing at least in part a property of blood contained within the pulp.

In one embodiment, a diagnostic system includes a light source configured to generate an output optical beam comprising one or more semiconductor sources configured to generate an input beam, one or more optical amplifiers configured to receive at least a portion of the input beam and to deliver an intermediate beam to an output end of the one or more optical amplifiers, and one or more optical fibers configured to receive at least a portion of the intermediate beam and to deliver at least the portion of the intermediate beam to a distal end of the one or more optical fibers to form a first optical beam. A nonlinear element is configured to receive at least a portion of the first optical beam and to broaden a spectrum associated with the at least a portion of the first optical beam to at least 10 nanometers through a nonlinear effect in the nonlinear element to form the output optical beam with an output beam broadened spectrum, wherein at least a portion of the output beam broadened spectrum comprises a short-wave infrared wavelength between approximately 1400 nanometers and approximately 2500 nanometers, and wherein at least a portion of the one of more fibers is a fused silica fiber with a core diameter less than approximately 400 microns. An interface device is configured to receive a received portion of the output optical beam and to deliver a delivered portion of the output optical beam to a sample, wherein the delivered portion of the output optical beam is configured to generate a spectroscopy output beam from the sample. A receiver is configured to receive at least a portion of the spectroscopy output beam having a bandwidth of at least 10 nanometers and to process the portion of the spectroscopy output beam to generate an output signal representing at least in part a property of hydro-carbon bonds.

In another embodiment, a measurement system includes a light source generating an output optical beam comprising a plurality of semiconductor sources generating an input optical beam, a multiplexer configured to receive at least a portion of the input optical beam and to form an intermediate optical beam, and one or more fibers configured to receive at least a portion of the intermediate optical beam and to form the output optical beam, wherein the output optical beam comprises one or more optical wavelengths. An interface device is configured to receive a received portion of the output optical beam and to deliver a delivered portion of the output optical beam to a sample comprising at least in part enamel, dentine and pulp, wherein the delivered portion of the output optical beam is configured to generate a spectroscopy output beam from the sample. A receiver is configured to receive at least a portion of the spectroscopy output beam and to process the portion of the spectroscopy output beam to generate an output signal representing at least in part a property of blood contained within the pulp.

In yet another embodiment, a method of measuring includes generating an output optical beam comprising generating an input optical beam from a plurality of semiconductor sources, multiplexing at least a portion of the input optical beam and forming an intermediate optical beam, and guiding at least a portion of the intermediate optical beam and forming the output optical beam, wherein the output optical beam comprises one or more optical wavelengths. The method may also include receiving a received portion of the output optical beam and delivering a delivered portion of the output optical beam to a sample, wherein the sample comprises at least in part enamel, dentine and pulp. The method further may include generating a spectroscopy output beam from the sample, receiving at least a portion of the spectroscopy output beam, and processing the portion of the spectroscopy output beam and generating an output signal representing at least in part a property of blood contained within the pulp.

BRIEF DESCRIPTION OF THE DRAWINGS

For a more complete understanding of the present disclosure, and for further features and advantages thereof, reference is now made to the following description taken in conjunction with the accompanying drawings, in which:

FIG. **1** plots the transmittance versus wavenumber for glucose in the mid-wave and long-wave infrared wavelengths between approximately 2.7 to 12 microns.

FIG. **2** illustrates measurements of the absorbance of different blood constituents, such as glucose, hemoglobin, and hemoglobin A1c. The measurements are done using an FTIR spectrometer in samples with a 1 mm path length.

FIG. **3**A shows the normalized absorbance of water and glucose (not drawn to scale). Water shows transmission windows between about 1500-1850 nm and 2050-2500 nm.

FIG. **3**B illustrates the absorbance of hemoglobin and oxygenated hemoglobin overlapped with water.

FIG. **4**A shows measured absorbance in different concentrations of glucose solution over the wavelength range of about 2000 to 2400 nm. This data is collected using a SWIR super-continuum laser with the sample path length of about 1.1 mm.

FIG. **4**B illustrates measured absorbance in different concentrations of glucose solution over the wavelength range of about 1550 to 1800 nm. The data is collected using a SWIR super-continuum laser with a sample path length of about 10 mm.

FIG. **5** illustrates the spectrum for different blood constituents in the wavelength range of about 2 to 2.45 microns (2000 to 2450 nm).

FIG. **6** shows the transmittance versus wavelength in microns for the ketone 3-hydroxybutyrate. The wavelength range is approximately 2 to 16 microns.

FIG. **7** illustrates the optical absorbance for ketones as well as some other blood constituents in the wavelength range of about 2100 to 2400 nm.

FIG. **8**A shows the first derivative spectra of ketone and protein at concentrations of 10 g/L (left). In addition, the first derivative spectra of urea, creatinine, and glucose are shown on the right at concentrations of 10 g/L.

FIG. **8**B illustrates the near infrared absorbance for triglyceride.

FIG. **8**C shows the near-infrared reflectance spectrum for cholesterol.

FIG. **8**D illustrates the near-infrared reflectance versus wavelength for various blood constituents, including cholesterol, glucose, albumin, uric acid, and urea.

FIG. **9** shows a schematic of the human skin. In particular, the dermis may comprise significant amounts of collagen, elastin, lipids, and water.

FIG. **10** illustrates the absorption coefficients for water (including scattering), adipose, collagen, and elastin.

FIG. **11** shows the dorsal of the hand, where a differential measurement may be made to at least partially compensate for or subtract out the skin interference.

FIG. **12** shows the dorsal of the foot, where a differential measurement may be made to at least partially compensate for or subtract out the skin interference.

FIG. **13** illustrates a typical human nail tissue structure and the capillary vessels below it.

FIG. **14** shows the attenuation coefficient for seven nail samples that are allowed to stand in an environment with a humidity level of 14%. These coefficients are measured using an FTIR spectrometer over the near-infrared wavelength range of approximately 1 to 2.5 microns. Below is also included the spectrum of glucose.

FIG. **15** illustrates the structure of a tooth.

FIG. **16**A shows the attenuation coefficient for dental enamel and water versus wavelength from approximately 600 nm to 2600 nm.

FIG. **16**B illustrates the absorption spectrum of intact enamel and dentine in the wavelength range of approximately 1.2 to 2.4 microns.

FIG. **17** shows the near infrared spectral reflectance over the wavelength range of approximately 800 nm to 2500 nm from an occlusal tooth surface. The black diamonds correspond to the reflectance from a sound, intact tooth section. The asterisks correspond to a tooth section with an enamel lesion. The circles correspond to a tooth section with a dentine lesion.

FIG. **18**A illustrates a clamp design of a human interface to cap over one or more teeth and perform a non-invasive measurement of blood constituents.

FIG. **18**B shows a mouth guard design of a human interface to perform a non-invasive measurement of blood constituents.

FIG. **19** illustrates a block diagram or building blocks for constructing high power laser diode assemblies.

FIG. **20** shows a platform architecture for different wavelength ranges for an all-fiber-integrated, high powered, super-continuum light source.

FIG. **21** illustrates one embodiment of a short-wave infrared (SWIR) super-continuum (SC) light source.

FIG. **22** shows the output spectrum from the SWIR SC laser of FIG. **21** when .about.10 m length of fiber for SC generation is used. This fiber is a single-mode, non-dispersion shifted fiber that is optimized for operation near 1550 nm.

FIG. **23** illustrates high power SWIR-SC lasers that may generate light between approximately 1.4-1.8 microns (top) or approximately 2-2.5 microns (bottom).

FIG. **24** schematically shows that the medical measurement device can be part of a personal or body area network that communicates with another device (e.g., smart phone or tablet) that communicates with the cloud. The cloud may in turn communicate information with the user, healthcare providers, or other designated recipients.

DETAILED DESCRIPTION

As required, detailed embodiments of the present disclosure are disclosed herein; however, it is to be understood that the disclosed embodiments are merely exemplary of the disclosure that may be embodied in various and alternative forms. The figures are not necessarily to scale; some features may be exaggerated or minimized to show details of particular components. Therefore, specific structural and functional details disclosed herein are not to be interpreted as limiting, but merely as a representative basis for teaching one skilled in the art to variously employ the present disclosure.

Various ailments or diseases may require measurement of the concentration of one or more blood constituents. For example, diabetes may require measurement of the blood glucose and HbA1c levels. On the other hand, diseases or disorders characterized by impaired glucose metabolism may require the measurement of ketone bodies in the blood. Examples of impaired glucose metabolism diseases include Alzheimer's, Parkinson's, Huntington's, and Lou Gehrig's or amyotrophic lateral sclerosis (ALS). Techniques related to near-infrared spectroscopy or hyper-spectral imaging may be particularly advantageous for non-invasive monitoring of some of these blood constituents.

As used throughout this document, the term "couple" and or "coupled" refers to any direct or indirect communication between two or more elements, whether or not those elements are physically connected to one another. As used throughout this disclosure, the term "spectroscopy" means that a tissue or sample is inspected by comparing different features, such as wavelength (or frequency), spatial location, transmission, absorption, reflectivity, scattering, refractive index, or opacity. In one embodiment, "spectroscopy" may mean that the wavelength of the light source is varied, and the transmission, absorption or reflectivity of the tissue or sample is measured as a function of wavelength. In another embodiment, "spectroscopy" may mean that the wavelength dependence of the transmission, absorption or reflectivity is compared between different spatial locations on a tissue or sample. As an illustration, the "spectroscopy" may be performed by varying the wavelength of the light source, or by using a broadband light source and analyzing the signal using a spectrometer, wavemeter, or optical spectrum analyzer.

As used throughout this document, the term "fiber laser" refers to a laser or oscillator that has as an output light or an optical beam, wherein at least a part of the laser comprises an optical fiber. For instance, the fiber in the "fiber laser" may comprise one of or a combination of a single mode fiber, a multi-mode fiber, a mid-infrared fiber, a photonic crystal fiber, a doped fiber, a gain fiber, or, more generally, an approximately cylindrically shaped waveguide or light-pipe. In one embodiment, the gain fiber may be doped with rare earth material, such as ytterbium, erbium, and/or thulium. In another embodiment, the mid-infrared fiber may comprise one or a combination of fluoride fiber, ZBLAN fiber, chalcogenide fiber, tellurite fiber, or germanium doped fiber. In yet another embodiment, the single mode fiber may include standard single-mode fiber, dispersion shifted fiber, non-zero dispersion shifted fiber, high-nonlinearity fiber, and small core size fibers.

As used throughout this disclosure, the term "pump laser" refers to a laser or oscillator that has as an output light or an optical beam, wherein the output light or optical beam is coupled to a gain medium to excite the gain medium, which in turn may amplify another input optical signal or beam. In one particular example, the gain medium may be a doped fiber, such as a fiber doped with ytterbium, erbium or thulium. In one embodiment, the "pump laser" may be a fiber laser, a solid state laser, a laser involving a nonlinear crystal, an optical parametric oscillator, a semiconductor laser, or a plurality of semiconductor lasers that may be multiplexed together. In another embodiment, the "pump laser" may be coupled to the gain medium by using a fiber coupler, a dichroic mirror, a multiplexer, a wavelength division multiplexer, a grating, or a fused fiber coupler.

As used throughout this document, the term "super-continuum" and or "supercontinuum" and or "SC" refers to a broadband light beam or output that comprises a plurality of wavelengths. In a particular example, the plurality of wavelengths may be adjacent to one-another, so that the spectrum of the light beam or output appears as a continuous band when measured with a spectrometer. In one embodiment, the broadband light beam may have a bandwidth of at least 10 nm. In another embodiment, the "super-continuum" may be generated through nonlinear optical interactions in a medium, such as an optical fiber or nonlinear crystal. For example, the "super-continuum" may be generated through one or a combination of nonlinear activities such as four-wave mixing, the Raman effect, modulational instability, and self-phase modulation.

As used throughout this disclosure, the terms "optical light" and or "optical beam" and or "light beam" refer to photons or light transmitted to a particular location in space. The "optical light" and or "optical beam" and or "light beam" may be modulated or unmodulated, which also means that they may or may not contain information. In one embodiment, the "optical light" and or "optical beam" and or "light beam" may originate from a fiber, a fiber laser, a laser, a light emitting diode, a lamp, a pump laser, or a light source. In general, the "near-infrared (NIR)" region of the electromagnetic spectrum covers between approximately 0.7 microns (700nm) to about 2.5 microns (2500 nm). However, it may also be advantageous to use just the short-wave infrared between approximately 1.4 microns (1400 nm) and about 2.5 microns (2500 nm). One reason for preferring the SWIR over the entire NIR may be to operate in the so-called "eye-safe" window, which corresponds to wavelengths longer than about 1400 nm. Therefore, for the remainder of the disclosure the SWIR will be used for illustrative purposes. However, it should be clear that the discussion that follows could also apply to using the NIR wavelength range, or other wavelength bands.

Spectrum for Glucose

One molecule of interest is glucose. The glucose molecule has the chemical formula C.sub.6H.sub.12O.sub.6, so it has a number of hydro-carbon bonds. An example of the infrared transmittance of glucose **100** is illustrated in FIG. **1**. The vibrational spectroscopy shows that the strongest lines for bending and stretching modes of C—H and O—H bonds lie in the wavelength range of approximately 6-12 microns. However, light sources and detectors are more difficult in the mid-wave infrared and long-wave infrared, and there is also strongly increasing water absorption in the human body beyond about 2.5 microns. Although weaker, there are also non-linear combinations of stretching and bending modes between about 2 to 2.5 microns, and first overtone of C—H stretching modes between approximately 1.5-1.8 microns. These signatures may fall in valleys of water absorption, permitting non-invasive detection through the body. In addition, there are yet weaker features from the second overtones and higher-order combinations between about 0.8-1.2 microns; in addition to being weaker, these features may also be masked by absorption in the hemoglobin. Hence, the short-wave infrared (SWIR) wavelength range of approximately 1.4 to 2.5 microns may be an attractive window for near-infrared spectroscopy of blood constituents.

As an example, measurements of the optical absorbance **200** of hemoglobin, glucose and HbA1c have been performed using a Fourier-Transform Infrared Spectrometer—FTIR. As FIG. **2** shows, in the SWIR wavelength range hemoglobin is nearly flat in spectrum **201** (the noise at the edges is due to the weaker light signal in the measurements). On the other hand, the glucose absorbance **202** has at least five distinct peaks near 1587 nm, 1750 nm, 2120 nm, 2270 nm and 2320 nm.

FIG. **3**A overlaps **300** the normalized absorbance of glucose **301** with the absorbance of water **302** (not drawn to scale). It may be seen that water has an absorbance feature between approximately 1850 nm and 2050 nm, but water **302** also has a nice transmission window between approximately 1500-1850 nm and 2050 to 2500 nm. For wavelengths less than about 1100 nm, the absorption of hemoglobin **351** and oxygenated hemoglobin **352** in FIG. **3**B has a number of features **350**, which may make it more difficult to measure blood constituents. Also, beyond 2500 nm the water absorption becomes considerably stronger over a wide wavelength range. Therefore, an advantageous window for measuring glucose and other blood constituents may be in the SWIR between 1500 and 1850 nm and 2050 to 2500 nm. These are exemplary wavelength ranges, and other ranges can be used that would still fall within the scope of this disclosure.

One further consideration in choosing the laser wavelength is known as the "eye safe" window for wavelengths longer than about 1400 nm. In particular, wavelengths in the eye safe window may not transmit down to the retina of the eye, and therefore, these wavelengths may be less likely to create permanent eye damage. The near-infrared wavelengths have the potential to be dangerous, because the eye cannot see the wavelengths (as it can in the visible), yet they can penetrate and cause damage to the eye. Even if a practitioner is not looking directly at the laser beam, the practitioner's eyes may receive stray light from a reflection or scattering from some surface. Hence, it can always be a good practice to use eye protection when working around lasers. Since wavelengths longer than about 1400 nm are substantially not transmitted to the retina or substantially absorbed in the retina, this wavelength range is known as the eye safe window. For wavelengths longer than 1400 nm, in general only the cornea of the eye may receive or absorb the light radiation.

Beyond measuring blood constituents such as glucose using FTIR spectrometers, measurements have also been conducted in another embodiment using super-continuum lasers, which will be described later in this disclosure. In this particular embodiment, some of the exemplary preliminary data for glucose absorbance are illustrated in FIGS. **4**A and **4**B. The optical spectra **401** in FIG. **4**A for different levels of glucose concentration in the wavelength range between 2000 and 2400 nm show the three absorption peaks near 2120 nm (2.12.mu.m), 2270 nm (2.27.mu.m) and 2320 nm (2.32.mu.m). Moreover, the optical spectra **402** in FIG. **4**B for different levels of glucose concentration in the wavelength range between 1500 and 1800 nm show the two broader absorption peaks near 1587 nm and 1750 nm. It should be appreciated that although data measured with

FTIR spectrometers or super-continuum lasers have been illustrated, other light sources can also be used to obtain the data, such as super-luminescent laser diodes, light emitting diodes, a plurality of laser diodes, or even bright lamp sources that generate adequate light in the SWIR.

Although glucose has a distinctive signature in the SWIR wavelength range, one problem of non-invasive glucose monitoring is that many other blood constituents also have hydro-carbon bonds. Consequently, there can be interfering signals from other constituents in the blood. As an example, FIG. **5** illustrates the spectrum **500** for different blood constituents in the wavelength range of 2 to 2.45 microns. The glucose absorption spectrum **501** can be unique with its three peaks in this wavelength range. However, other blood constituents such as triacetin **502**, ascorbate **503**, lactate **504**, alanine **505**, urea **506**, and BSA **507** also have spectral features in this wavelength range. To distinguish the glucose **501** from these overlapping spectra, it may be advantageous to have information at multiple wavelengths. In addition, it may be advantageous to use pattern matching algorithms and other software and mathematical methods to identify the blood constituents of interest. In one embodiment, the spectrum may be correlated with a library of known spectra to determine the overlap integrals, and a threshold function may be used to quantify the concentration of different constituents. This is just one way to perform the signal processing, and many other techniques, algorithms, and software may be used and would fall within the scope of this disclosure.

Ketone Bodies Monitoring

Beyond glucose, there are many other blood constituents that may also be of interest for health or disease monitoring. In another embodiment, it may be desirous to monitor the level of ketone bodies in the blood stream. Ketone bodies are three water-soluble compounds that are produced as by-products when fatty acids are broken down for energy in the liver. Two of the three are used as a source of energy in the heart and brain, while the third is a waste product excreted from the body. In particular, the three endogenous ketone bodies are acetone, acetoacetic acid, and beta-hydroxybutyrate or 3-hydroxybutyrate, and the waste product ketone body is acetone.

Ketone bodies may be used for energy, where they are transported from the liver to other tissues. The brain may utilize ketone bodies when sufficient glucose is not available for energy. For instance, this may occur during fasting, strenuous exercise, low carbohydrate, ketogenic diet and in neonates. Unlike most other tissues that have additional energy sources such as fatty acids during periods of low blood glucose, the brain cannot break down fatty acids and relies instead on ketones. In one embodiment, these ketone bodies are detected.

Ketone bodies may also be used for reducing or eliminating symptoms of diseases or disorders characterized by impaired glucose metabolism. For example, diseases associated with reduced neuronal metabolism of glucose include Parkinson's disease, Alzheimer's disease, amyotrophic lateral sclerosis (ALS, also called Lou Gehrig's disease), Huntington's disease and epilepsy. In one embodiment, monitoring of alternate sources of ketone bodies that may be administered orally as a dietary supplement or in a nutritional composition to counteract some of the glucose metabolism impairments is performed. However, if ketone bodies supplements are provided, there is also a need to monitor the ketone level in the blood stream. For instance, if elevated levels of ketone bodies are present in the body, this may lead to ketosis; hyperketonemia is also an elevated level of ketone bodies in the blood. In addition, both acetoacetic acid and beta-hydroxybutyric acid are acidic, and, if levels of these ketone bodies are too high, the pH of the blood may drop, resulting in ketoacidosis.

The general formula for ketones is C.sub.nH.sub.2n0. In organic chemistry, a ketone is an organic compound with the structure RC(.dbd.O)R', where R and R' can be a variety of carbon-containing substituents. It features a carbonyl group (C.dbd.O) bonded to two other carbon atoms. Because the ketones contain the hydrocarbon bonds, there might be expected to be features in the SWIR, similar in structure to those found for glucose.

The infrared spectrum **600** for the ketone 3-hydroxybutyrate is illustrated in FIG. **6**. Just as in glucose, there are significant features in the mid- and long-wave infrared between 6 to 12 microns, but these may be difficult to observe non-invasively. On the other hand, there are some features in the SWIR that may be weaker, but they could potentially be observed non-invasively, perhaps through blood and water.

The optical spectra **700** for ketones as well as some other blood constituents are exemplified in FIG. **7** in the wavelength range of 2100 nm to 2400 nm. In this embodiment, the absorbance for ketones is 701, while the absorbance for glucose is 702. However, there are also features in this wavelength range for other blood constituents, such as urea **703**, albumin or blood protein **704**, creatinine **705**, and nitrite **706**. In this wavelength range of 2100 to 2400 nm, the features for ketone **701** seem more spectrally pronounced than even glucose.

Different signal processing techniques can be used to enhance the spectral differences between different constituents. In one embodiment, the first or second derivatives of the spectra may enable better discrimination between substances. The first derivative may help remove any flat offset or background, while the second derivative may help to remove any sloped offset or background. In some instances, the first or second derivative may be applied after curve fitting or smoothing the reflectance, transmittance, or absorbance. For example, FIG. **8**A illustrates the derivative spectra for ketone **801** and glucose **802**, which can be distinguished from the derivative spectra for protein **803**, urea **804** and creatinine **805**. Based on FIG. **8**A, it appears that ketones **801** may have a more pronounced difference than even glucose **802** in the wavelength range between 2100 and 2400 nm. Therefore, ketone bodies should also be capable of being monitored using a non-invasive optical technique in the SWIR, and a different pattern matching library could be used for glucose and ketones.

Hemoglobin A1c Monitoring

Another blood constituent that may be of interest for monitoring of health or diseases is hemoglobin A1c, also known as HbA1c or glycated hemoglobin (glycol-hemoglobin or glycosylated hemoglobin). HbA1c is a form of hemoglobin that is measured primarily to identify the average plasma glucose concentration over prolonged periods of time. Thus, HbA1c may serve as a marker for average blood glucose levels over the previous months prior to the measurements.

In one embodiment, when a physician suspects that a patient may be diabetic, the measurement of HbA1c may be one of the first tests that are conducted. An HbA1c level less than approximately 6% may be considered normal. On the other hand, an HbA1c level greater than approximately 6.5% may be considered to be diabetic. In diabetes mellitus, higher amounts of HbA1c indicate poorer control of blood glucose levels. Thus, monitoring the HbA1c in diabetic patients may improve treatment. Current techniques for measuring HbA1c require drawing blood, which may be inconvenient and painful. The point-of-care devices use immunoassay or boronate affinity chromatography, as an example. Thus, there is also an unmet need for non-invasive monitoring of HbA1c.

FIG. **2** illustrates the FTIR measurements of HbA1c absorbance **203** over the wavelength range between 1500 and 2400 nm for a concentration of approximately 1 mg/ml. Whereas the absorbance of hemoglobin **201** over this wavelength range is approximately flat, the HbA1c absorbance **203** shows broad features and distinct curvature. Although the HbA1c absorbance **203** does not appear to exhibit as pronounced features as glucose **202**, the non-invasive SWIR measurement should be able to detect HbA1c with appropriate pattern matching algorithms. Moreover, the spectrum for HbA1c may be further enhanced by using first or second derivative data, as seen for ketones in FIG. **8**A. Beyond absorption, reflectance, or transmission spectroscopy, it may also be possible to detect blood constituents such as HbA1c using Raman spectroscopy or surface-enhanced Raman spectroscopy. In general, Raman spectroscopy may require higher optical power levels.

As an illustration, non-invasive measurement of blood constituents such as glucose, ketone bodies, and HbA1c has been discussed thus far. However, other blood constituents can also be measured using similar techniques, and these are also intended to be covered by this disclosure. In other embodiments, blood constituents such as proteins, albumin, urea, creatinine or nitrites could also be measured. For instance, the same type of SWIR optical techniques might be used, but the pattern matching algorithms and software could use different library features or functions for the different constituents.

In yet another embodiment, the optical techniques described in this disclosure could also be used to measure levels of triglycerides. Triglycerides are bundles of fats that may be found in the blood stream, particularly after ingesting meals. The body manufactures triglycerides from carbohydrates and fatty foods that are eaten. In other words, triglycerides are the body's storage form of fat. Triglycerides are comprised of three fatty acids attached to a glycerol molecule, and measuring the level of triglycerides may be important for diabetics. The triglyceride levels or concentrations in blood may be rated as follows: desirable or normal may be less than 150 mg/dl; borderline high may be 150-199 mg/dl; high may be 200-499 mg/dl; and very high may be 500 mg/dl or greater. FIG. **8**B illustrates one example of the near-infrared absorbance **825** for triglycerides. There are distinct absorbance peaks in the spectrum that should be measurable. The characteristic absorption bands may be assigned as follows: (a) the first overtones of C—H stretching vibrations (1600-1900 nm); (b) the region of second overtones of C—H stretching vibrations (1100-1250 nm); and, (c) two regions (2000-2200 nm and 1350-1500 nm) that comprise bands due to combinations of C—H stretching vibrations and other vibrational modes.

A further example of blood compositions that can be detected or measured using near-infrared light includes cholesterol monitoring. For example, FIG. **8**C shows the near-infrared reflectance spectrum for cholesterol **850** with wavelength in microns (.mu.m). Distinct absorption peaks are observable near 1210 nm (1.21.mu.m), 1720 nm (1.72.mu.m), and between 2300-2500 nm (2.3-2.5.mu.m). Also, there are other features near 1450 nm (1.45.mu.m) and 2050 nm (2.05.mu.m). In FIG. **8**D the near-infrared reflectances **875** are displayed versus wavelength (nm) for various

blood constituents. The spectrum for cholesterol **876** is overlaid with glucose **877**, albumin **878**, uric acid **879**, and urea **880**. As may be noted from FIG. **8**D, at about 1720 nm and 2300 nm, cholesterol **876** reaches approximate reflectance peaks, while some of the other analytes are in a more gradual mode. Various signal processing methods may be used to identify and quantify the concentration of cholesterol **876** and/or glucose **877**, or some of the other blood constituents.

As illustrated by FIGS. **5** and **7**, one of the issues in measuring a particular blood constituent is the interfering and overlapping signal from other blood constituents. The selection of the constituent of interest may be improved using a number of techniques. For example, a higher light level or intensity may improve the signal-to-noise ratio for the measurement. Second, mathematical modeling and signal processing methodologies may help to reduce the interference, such as multivariate techniques, multiple linear regression, and factor-based algorithms, for example. For instance, a number of mathematical approaches include multiple linear regression, partial least squares, and principal component regression (PCR). Also, as illustrated in FIG. **8**A, various mathematical derivatives, including the first and second derivatives, may help to accentuate differences between spectra. In addition, by using a wider wavelength range and using more sampling wavelengths may improve the ability to discriminate one signal from another. These are just examples of some of the methods of improving the ability to discriminate between different constituents, but other techniques may also be used and are intended to be covered by this disclosure.

By use of an active illuminator, a number of advantages may be achieved. First, the variations due to sunlight and time-of-day may be factored out. The effects of the weather, such as clouds and rain, might also be reduced. Also, higher signal-to-noise ratios may be achieved. For example, one way to improve the signal-to-noise ratio would be to use modulation and lock-in techniques. In one embodiment, the light source may be modulated, and then the detection system would be synchronized with the light source. In a particular embodiment, the techniques from lock-in detection may be used, where narrow band filtering around the modulation frequency may be used to reject noise outside the modulation frequency. In an alternate embodiment, change detection schemes may be used, where the detection system captures the signal with the light source on and with the light source off. Again, for this system the light source may be modulated. Then, the signal with and without the light source is differenced. This may enable the sun light changes to be subtracted out. In addition, change detection may help to identify objects that change in the field of view. In the following some exemplary detection systems are described.

Interference from Skin

Several proposed non-invasive glucose monitoring techniques rely on transmission, absorption, and/or diffuse reflection through the skin to measure blood constituents or blood analytes in veins, arteries, capillaries or in the tissue itself. However, on top of the interference from other blood constituents or analytes, the skin also introduces significant interference. For example, chemical, structural, and physiological variations occur that may produce relatively large and nonlinear changes in the optical properties of the tissue sample. In one embodiment, the near-infrared reflectance or absorbance spectrum may be a complex combination of the tissue scattering properties that result from the concentration and characteristics of a multiplicity of tissue components including water, fat, protein, collagen, elastin, and/or glucose. Moreover, the optical properties of the skin may also change with environmental factors such as humidity, temperature and pressure. Physiological variation may also cause changes in the tissue measurement over time and may vary based on lifestyle, health, aging, etc. The structure and composition of skin may also vary widely among individuals, between different sites within an individual, and over time on the same individual. Thus, the skin introduces a dynamic interference signal that may have a wide variation due to a number of parameters.

FIG. **9** shows a schematic cross-section of human skin **900**, **901**. The top layer of the skin is epidermis **902**, followed by a layer of dermis **903** and then subcutaneous fat **904** below the dermis. The epidermis **902**, with a thickness of approximately 10-150 microns, may provide a barrier to infection and loss of moisture and other body constituents. The dermis **903** ranges in thickness from approximately 0.5 mm to 4 mm (averages approximately 1.2 mm over most of the body) and may provide the mechanical strength and elasticity of skin.

In the dermis **903**, water may account for approximately 70% of the volume. The next most abundant constituent in the dermis **903** may be collagen **905**, a fibrous protein comprising 70-75% of the dry weight of the dermis **903**. Elastin fibers **906**, also a protein, may also be plentiful in the dermis **903**, although they constitute a smaller portion of the bulk. In addition, the dermis **903** may contain a variety of structures (e.g., sweat glands, hair follicles with adipose rich sebaceous glands **907** near their roots, and blood vessels) and other cellular constituents.

Below the dermis **903** lies the subcutaneous layer **904** comprising mostly adipose tissue. The subcutaneous layer **904** may be by volume approximately 10% water and may be comprised primarily of cells rich in triglycerides or fat. With this complicated structure of the skin **900**, **901**, the concentration of glucose may vary in each layer according to a variety of factors including the water content, the relative sizes of the fluid compartments, the distribution of capillaries, the perfusion of blood, the glucose uptake of cells, the concentration of glucose in blood, and the driving forces (e.g., osmotic pressure) behind diffusion.

To better understand the interference that the skin introduces when attempting to measure glucose, the absorption coefficient for the various skin constituents should be examined. For example, FIG. **10** illustrates **1000** the absorption coefficients for water (including scattering) **1001**, adipose **1002**, collagen **1003** and elastin **1004**. Note that the absorption curves for water **1001** and adipose **1002** are calibrated, whereas the absorption curves for collagen **1003** and elastin **1004** are in arbitrary units. Also shown are vertical lines demarcating the wavelengths near 1210 nm **1005** and 1720 nm **1006**. In general, the water absorption increases with increasing wavelength. With the increasing absorption beyond about 2000 nm, it may be difficult to achieve deeper penetration into biological tissue in the infrared wavelengths beyond approximately 2500 nm.

Although the absorption coefficient may be useful for determining the material in which light of a certain infrared wavelength will be absorbed, to determine the penetration depth of the light of a certain wavelength may also require the addition of scattering loss to the curves. For example, the water curve **1001** includes the scattering loss curve in addition to the water absorption. In particular, the scattering loss can be significantly higher at shorter wavelengths. In one embodiment, near the wavelength of 1720 nm (vertical line **1006** shown in FIG. **10**), the adipose absorption **1002** can still be higher than the water plus scattering loss **1001**. For tissue that contains adipose, collagen and elastin, such as the dermis of the skin, the total absorption can exceed the light energy lost to water absorption and light scattering at 1720 nm. On the other hand, at 1210 nm the adipose absorption **1002** can be considerably lower than the water plus scattering loss **1001**, particularly since the scattering loss can be dominant at these shorter wavelengths.

The interference for glucose lines observed through skin may be illustrated by overlaying the glucose lines over the absorption curves **1000** for the skin constituents. For example, FIG. **2** illustrated that the glucose absorption **202** included features centered around 1587 nm, 1750 nm, 2120 nm, 2270 nm and 2320 nm. On FIG. **10** vertical lines have been drawn at the glucose line wavelengths of 1587 nm **1007**, **1750** nm **1008**, **2120** nm **1009**, **2270** nm **1010** and 2320 nm **1011**. In one embodiment, it may be difficult to detect the glucose lines near 1750 nm **1008**, **2270** nm **1010** and 2320 nm **1011** due to significant spectral interference from other skin constituents. On the other hand, the glucose line near 1587 m **1007** may be more easily detected because it peaks while most of the other skin constituents are sloped downward toward an absorption valley. Moreover, the glucose line near 2120 nm **1009** may also be detectable for similar reasons, although adipose may have conflicting behavior due to local absorption minimum and maximum nearby in wavelength.

Thus, beyond the problem of other blood constituents or analytes having overlapping spectral features (e.g., FIG. **5**), it may be difficult to observe glucose spectral signatures through the skin and its constituents of water, adipose, collagen and elastin. One approach to overcoming this difficulty may be to try to measure the blood constituents in veins that are located at relatively shallow distances below the skin. Veins may be more beneficial for the measurement than arteries, since arteries tend to be located at deeper levels below the skin. Also, in one embodiment it may be advantageous to use a differential measurement to subtract out some of the interfering absorption lines from the skin. For example, an instrument head may be designed to place one probe above a region of skin over a blood vein, while a second probe may be placed at a region of the skin without a noticeable blood vein below it. Then, by differencing the signals from the two probes, at least part of the skin interference may be cancelled out.

Two representative embodiments for performing such a differential measurement are illustrated in FIG. **11** and FIG. **12**. In one embodiment shown in FIG. **11**, the dorsal of the hand **1100** may be used for measuring blood constituents or analytes. The dorsal of the hand **1100** may have regions that have distinct veins **1101** as well as regions where the veins are not as shallow or pronounced **1102**. By stretching the hand and leaning it backwards, the veins **1101** may be accentuated in some cases. A near-infrared diffuse reflectance measurement may be performed by placing one probe **1103** above the vein-rich region **1101**. To turn this into a differential measurement, a second probe **1104** may be placed above a region without distinct veins **1102**. Then, the outputs from the two probes may be subtracted **1105** to at least partially cancel out the features from the skin. The subtraction may be done preferably in the electrical domain, although it can also be performed in the optical domain or digitally/mathematically using sampled data based on the electrical and/or optical signals. Although one example of using the dorsal of the hand **1100** is shown, many other parts of the hand can be used within the scope of this disclosure. For example, alternate methods may use transmission through the webbing between the thumb and the fingers **1106**, or transmission or diffuse reflection through the tips of the fingers **1107**.

In another embodiment, the dorsal of the foot **1200** may be used instead of the hand. One advantage of such a configuration may be that for self-testing by a user, the foot may be easier to position the instrument using both hands. One probe **1203** may be placed over regions where there are more distinct veins **1201**, and a near-infrared diffuse reflectance measurement may be made. For a differential measurement, a second probe **1204** may be placed over a region with less prominent veins **1202**, and then the two probe signals may be subtracted, either electronically or optically, or may be digitized/sampled and processed mathematically depending on the particular application and implementation. As with the hand, the differential measurements may be intended to compensate for or subtract out (at least in part) the interference from the skin. Since two regions are used in close proximity on the same body part, this may also aid in removing some variability in the skin from environmental effects such as temperature, humidity, or pressure. In addition, it may be advantageous to first treat the skin before the measurement, by perhaps wiping with a cloth or treated cotton ball, applying some sort of cream, or placing an ice cube or chilled bag over the region of interest.

Although two embodiments have been described, many other locations on the body may be used using a single or differential probe within the scope of this disclosure. In yet another embodiment, the wrist may be advantageously used, particularly where a pulse rate is typically monitored. Since the pulse may be easily felt on the wrist, there is underlying the region a distinct blood flow. Other embodiments may use other parts of the body, such as the ear lobes, the tongue, the inner lip, the nails, the eye, or the teeth. Some of these embodiments will be further described below. The ear lobes or the tip of the tongue may be advantageous because they are thinner skin regions, thus permitting transmission rather than diffuse reflection. However, the interference from the skin is still a problem in these embodiments. Other regions such as the inner lip or the bottom of the tongue may be contemplated because distinct veins are observable, but still the interference from the skin may be problematic in these embodiments. The eye may seem as a viable alternative because it is more transparent than skin. However, there are still issues with scattering in the eye. For example, the anterior chamber of the eye (the space between the cornea and the iris) comprises a fluid known as aqueous humor. However, the glucose level in the eye chamber may have a significant temporal lag on changes in the glucose level compared to the blood glucose level.

Because of the complexity of the interference from skin in non-invasive glucose monitoring (e.g., FIG. **10**), other parts of the body without skin above blood vessels or capillaries may be alternative candidates for measuring blood constituents. One embodiment may involve transmission or reflection through human nails. As an example, FIG. **13** illustrates a typical human nail tissue structure **1300** and the capillary vessels below it. The fingernail **1301** is approximately 1 mm thick, and below this resides a layer of epidermis **1302** with a thickness of approximately 1 mm. The dermis **1304** is also shown, and within particularly the top about 0.5 mm of dermis are a significant number of capillary vessels. To measure the blood constituents, the light exposed on the top of the fingernail must penetrate about 2-2.5 mm or more, and the reflected light (round trip passage) should be sufficiently

strong to measure. In one embodiment, the distance required to penetrate could be reduced by drilling a hole in the fingernail **1301**.

In this alternative embodiment using the fingernail, there may still be interference from the nail's spectral features. For example, FIG. **14** illustrates the attenuation coefficient **1400** for seven nail samples that are allowed to stand in an environment with a humidity level of 14%. These coefficients are measured using an FTIR spectrometer over the near-infrared wavelength range of approximately 1 to 2.5 microns. These spectra are believed to correspond to the spectra of keratin contained in the nail plate. The base lines for the different samples are believed to differ because of the influence of scattering. Several of the absorption peaks observed correspond to peaks of keratin absorption, while other features may appear from the underlying epidermis and dermis. It should also be noted that the attenuation coefficients **1400** also vary considerably depending on humidity level or water content as well as temperature and other environmental factors. Moreover, the attenuation coefficient may also change in the presence of nail polish of various sorts.

Similar to skin, the large variations in attenuation coefficient for fingernails also may interfere with the absorption peaks of glucose. As an example, in FIG. **14** below the fingernail spectrum is also shown the glucose spectrum **1401** for two different glucose concentrations. The vertical lines **1402**, **1403**, **1404**, **1405** and **1406** are drawn to illustrate the glucose absorption peaks and where they lie on the fingernail spectra **1400**. As is apparent, the nail has interfering features that may be similar to skin, particularly since both have spectra that vary not only in wavelength but also with environmental factors. In one embodiment, it may be possible to see the glucose peaks **1402** and **1404** through the fingernail, but it may be much more difficult to observe the glucose peaks near **1403**, **1405** and **1406**.

Transmission or Reflection Through Teeth

Yet another embodiment may observe the transmittance or reflectance through teeth to measure blood constituents or analytes. FIG. **15** illustrates an exemplary structure of a tooth **1500**. The tooth **1500** has a top layer called the crown **1501** and below that a root **1502** that reaches well into the gum **1506** and bone **1508** of the mouth. The exterior of the crown **1501** is an enamel layer **1503**, and below the enamel is a layer of dentine **1504** that sits atop a layer of cementum **1507**. Below the dentine **1504** is a pulp region **1505**, which comprises within it blood vessels **1509** and nerves **1510**. If the light can penetrate the enamel **1503** and dentine **1504**, then the blood flow and blood constituents can be measured through the blood vessels in the dental pulp **1505**. While it may be true that the amount of blood flow in the dental pulp **1505** may be less since it comprises capillaries, the smaller blood flow could still be advantageous if there is less interfering spectral features from the tooth.

The transmission, absorption and reflection from teeth has been studied in the near infrared, and, although there are some features, the enamel and dentine appear to be fairly transparent in the near infrared (particularly wavelengths between 1500 and 2500 nm). For example, the absorption or extinction ratio for light transmission has been studied. FIG. **16**A illustrates the attenuation coefficient **1600** for dental enamel **1601** (filled circles) and the absorption coefficient of water **1602** (open circles) versus wavelength. Near-infrared light may penetrate much further without scattering through all the tooth enamel, due to the reduced scattering coefficient in normal enamel. Scattering in enamel may be fairly strong in the visible, but decreases as approximately $1/\text{wavelength}^3$

(i.e., inverse of the wavelength cubed) with increasing wavelength to a value of only 2-3 cm-1 at 1310 nm and 1550 nm in the near infrared. Therefore, enamel may be virtually transparent in the near infrared with optical attenuation 1-2 orders of magnitude less than in the visible range.

As another example, FIG. **16**B illustrates the absorption spectrum **1650** of intact enamel **1651** (dashed line) and dentine **1652** (solid line) in the wavelength range of approximately 1.2 to 2.4 microns. In the near infrared there are two absorption bands around 1.5 and 2 microns. The band with a peak around 1.57 microns may be attributed to the overtone of valent vibration of water present in both enamel and dentine. In this band, the absorption is greater for dentine than for enamel, which may be related to the large water content in this tissue. In the region of 2 microns, dentine may have two absorption bands, and enamel one. The band with a maximum near 2.1 microns may belong to the overtone of vibration of PO hydroxyapatite groups, which is the main substance of both enamel and dentine. Moreover, the band with a peak near 1.96 microns in dentine may correspond to water absorption (dentine may contain substantially higher water than enamel).

In addition to the absorption coefficient, the reflectance from intact teeth and teeth with dental caries (e.g., cavities) has been studied. In one embodiment, FIG. **17** shows the near infrared spectral reflectance **1700** over the wavelength range of approximately 800 nm to 2500 nm from an occlusal (e.g., top/bottom) tooth surface **1704**. The curve with black diamonds **1701** corresponds to the reflectance from a sound, intact tooth section. The curve with asterisks * **1702** corresponds to a tooth section with an enamel lesion. The curve with circles **1703** corresponds to a tooth section with a dentine lesion. Thus, when there is a lesion, more scattering occurs and there may be an increase in the reflected light.

For wavelengths shorter than approximately 1400 nm, the shapes of the spectra remain similar, but the amplitude of the reflection changes with lesions. Between approximately 1400 nm and 2500 nm, an intact tooth **1701** has low reflectance (e.g., high transmission), and the reflectance appears to be more or less independent of wavelength. On the other hand, in the presence of lesions **1702** and **1703**, there is increased scattering, and the scattering loss may be wavelength dependent. For example, the scattering loss may decrease as 1/(wavelength).sup.3—so, the scattering loss decreases with longer wavelengths. When there is a lesion in the dentine **1703**, more water can accumulate in the area, so there is also increased water absorption. For example, the dips near 1450 nm and 1900 nm correspond to water absorption, and the reflectance dips are particularly pronounced in the dentine lesion **1703**. One other benefit of the absorption, transmission or reflectance in the near infrared may be that stains and non-calcified plaque are not visible in this wavelength range, enabling better discrimination of defects, cracks, and demineralized areas.

Compared with the interference from skin **1000** in FIG. **10** or fingernails **1400** in FIG. **14**, the teeth appear to introduce much less interference for non-invasive monitoring of blood constituents. The few features in FIG. **16**B or **17** may be calibrated out of the measurement. Also, using an intact tooth **1701** may further minimize any interfering signals. Furthermore, since the tooth comprises relatively hard tissue, higher power from the light sources in the near infrared may be used without damaging the tissue, such as with skin.

Human Interface for Measurement System

A number of different types of measurements may be used to sample the blood in the dental pulp. The basic feature of the measurements should be that the optical properties are

measured as a function of wavelength at a plurality of wavelengths. As further described below, the light source may output a plurality of wavelengths, or a continuous spectrum over a range of wavelengths. In a preferred embodiment, the light source may cover some or all of the wavelength range between approximately 1400 nm and 2500 nm. The signal may be received at a receiver, which may also comprise a spectrometer or filters to discriminate between different wavelengths. The signal may also be received at a camera, which may also comprise filters or a spectrometer. In an alternate embodiment, the spectral discrimination using filters or a spectrometer may be placed after the light source rather than at the receiver. The receiver usually comprises one or more detectors (optical-to-electrical conversion element) and electrical circuitry. The receiver may also be coupled to analog to digital converters, particularly if the signal is to be fed to a digital device.

Referring to FIG. **15**, one or more light sources **1511** may be used for illumination. In one embodiment, a transmission measurement may be performed by directing the light source output **1511** to the region near the interface between the gum **1506** and dentine **1504**. In one embodiment, the light may be directed using a light guide or a fiber optic. The light may then propagate through the dental pulp **1505** to the other side, where the light may be incident on one or more detectors or another light guide to transport the signal to a spectrometer, receiver or camera **1512**. In another embodiment, the light source may be directed to one or more locations near the interface between the gum **1506** and dentine **1504** (in one example, could be from the two sides of the tooth). The transmitted light may then be detected in the occlusal surface above the tooth using a spectrometer, receiver, or camera **1512**. In yet another embodiment, a reflectance measurement may be conducted by directing the light source output **1511** to, for example, the occlusal surface of the tooth, and then detecting the reflectance at a spectrometer, receiver or camera **1513**. Although a few embodiments for measuring the blood constituents through a tooth are described, other embodiments and techniques may also be used and are intended to be covered by this disclosure.

The human interface for the non-invasive measurement of blood constituents may be of various forms. In one embodiment, a "clamp" design **1800** may be used cap over one or more teeth, as illustrated in FIG. **18**A. The clamp design may be different for different types of teeth, or it may be flexible enough to fit over different types of teeth. For example, different types of teeth include the molars (toward the back of the mouth), the premolars, the canine, and the incisors (toward the front of the mouth). One embodiment of the clamp-type design is illustrated in FIG. **18**A for a molar tooth **1808**. The C-clamp **1801** may be made of a plastic or rubber material, and it may comprise a light source input **1802** and a detector output **1803** on the front or back of the tooth.

The light source input **1802** may comprise a light source directly, or it may have light guided to it from an external light source. Also, the light source input **1802** may comprise a lens system to collimate or focus the light across the tooth. The detector output **1803** may comprise a detector directly, or it may have a light guide to transport the signal to an external detector element. The light source input **1802** may be coupled electrically or optically through **1804** to a light input **1806**. For example, if the light source is external in **1806**, then the coupling element **1804** may be a light guide, such as a fiber optic. Alternately, if the light source is contained in **1802**, then the coupling element **1804** may be electrical wires connecting to a power supply in **1806**.

Similarly, the detector output **1803** may be coupled to a detector output unit **1807** with a coupling element **1805**, which may be one or more electrical wires or a light guide, such as a fiber optic. This is just one example of a clamp over one or more teeth, but other embodiments may also be used and are intended to be covered by this disclosure.

In yet another embodiment, one or more light source ports and sensor ports may be used in a mouth-guard type design. For example, one embodiment of a dental mouth guard **1850** is illustrated in FIG. **18**B. The structure of the mouth guard **1851** may be similar to mouth guards used in sports (e.g., when playing football or boxing) or in dental trays used for applying fluoride treatment, and the mouth guard may be made from plastic or rubber materials, for example. As an example, the mouth guard may have one or more light source input ports **1852**, **1853** and one or more detector output ports **1854**, **1855**. Although six input and output ports are illustrated, any number of ports may be used.

Similar to the clamp design described above, the light source inputs **1852**, **1853** may comprise one or more light sources directly, or they may have light guided to them from an external light source. Also, the light source inputs **1852**, **1853** may comprise lens systems to collimate or focus the light across the teeth. The detector outputs **1854**, **1855** may comprise one or more detectors directly, or they may have one or more light guides to transport the signals to an external detector element. The light source inputs **1852**, **1853** may be coupled electrically or optically through **1856** to a light input **1857**. For example, if the light source is external in **1857**, then the one or more coupling elements **1856** may be one or more light guides, such as a fiber optic. Alternately, if the light sources are contained in **1852**, **1853**, then the coupling element **1856** may be one or more electrical wires connecting to a power supply in **1857**. Similarly, the detector outputs **1854**, **1855** may be coupled to a detector output unit **1859** with one or more coupling elements **1858**, which may be one or more electrical wires or one or more light guides, such as a fiber optic. This is just one example of a mouth guard design covering a plurality of teeth, but other embodiments may also be used and are intended to be covered by this disclosure. For instance, the position of the light source inputs and detector output ports could be exchanged, or some mixture of locations of light source inputs and detector output ports could be used.

Also, if reflectance from the teeth is to be measured, then the light sources and detectors may be on the same side of the tooth. Moreover, it may be advantageous to pulse the light source with a particular pulse width and pulse repetition rate, and then the detection system can measure the pulsed light returned from or transmitted through the tooth. Using a lock-in type technique (e.g., detecting at the same frequency as the pulsed light source and also possibly phase locked to the same signal), the detection system may be able to reject background or spurious signals and increase the signal-to-noise ratio of the measurement.

Other elements may be added to the human interface designs of FIG. **18** and are also intended to be covered by this disclosure. For instance, in one embodiment it may be desirable to have replaceable inserts that may be disposable. Particularly in a doctor's office or hospital setting, the same instrument may be used with a plurality of patients. Rather than disinfecting the human interface after each use, it may be preferable to have disposable inserts that can be thrown away after each use. In one embodiment, a thin plastic coating material may enclose the clamp design of FIG. **18**A or mouth guard design of FIG. **18**B. The coating material may be inserted before each use, and then after the measurement is exercised the coating material may be peeled off and replaced. Such a design may save the physician or user considerable time, while at the same time provide the business venture with a recurring cost revenue source. Any coating material or other disposable device may be constructed of a material having suitable optical properties that may be considered during processing of the signals used to detect any anomalies in the teeth.

Light Sources for Near Infrared

In general, the near-infrared (NIR) region of the electromagnetic spectrum covers between approximately 0.7 microns (700 nm) to about 2.5 microns (2500 nm). However, it may also be advantageous to use just the short-wave infrared between approximately 1.4 microns (1400 nm) and about 2.5 microns (2500 nm). One reason for preferring the SWIR over the entire NIR may be to operate in the so-called "eye-safe" window, which corresponds to wavelengths longer than about 1400 nm. While the SWIR is used for illustrative purposes, it should be clear that the discussion that follows could also apply to using the NIR wavelength range, or other wavelength bands. There are a number of light sources that may be used in the near infrared. To be more specific, the discussion below will consider light sources operating in the so-called short wave infrared (SWIR), which may cover the wavelength range of approximately 1400 nm to 2500 nm. Other wavelength ranges may also be used for the applications described in this disclosure, so the discussion below is merely provided for exemplary types of light sources. The SWIR wavelength range may be valuable for a number of reasons. First, the SWIR corresponds to a transmission window through water and the atmosphere. For example, **302** in FIG. **3**A and **1602** in FIG. **16**A illustrate the water transmission windows. Also, through the atmosphere, wavelengths in the SWIR have similar transmission windows due to water vapor in the atmosphere. Second, the so-called "eye-safe" wavelengths are wavelengths longer than approximately 1400 nm. Third, the SWIR covers the wavelength range for nonlinear combinations of stretching and bending modes as well as the first overtone of C—H stretching modes. Thus, for example, glucose and ketones among other substances may have unique signatures in the SWIR. Moreover, many solids have distinct spectral signatures in the SWIR, so particular solids may be identified using stand-off detection or remote sensing. For instance, many explosives have unique signatures in the SWIR.

Different light sources may be selected for the SWIR based on the needs of the application. Some of the features for selecting a particular light source include power or intensity, wavelength range or bandwidth, spatial or temporal coherence, spatial beam quality for focusing or transmission over long distance, and pulse width or pulse repetition rate. Depending on the application, lamps, light emitting diodes (LEDs), laser diodes (LD's), tunable LD's, super-luminescent laser diodes (SLDs), fiber lasers or super-continuum sources (SC) may be advantageously used. Also, different fibers may be used for transporting the light, such as fused silica fibers, plastic fibers, mid-infrared fibers (e.g., tellurite, chalcogenides, fluorides, ZBLAN, etc), or a hybrid of these fibers.

Lamps may be used if low power or intensity of light is required in the SWIR, and if an incoherent beam is suitable. In one embodiment, in the SWIR an incandescent lamp that can be used is based on tungsten and halogen, which have an emission wavelength between approximately 500 nm to 2500 nm. For low intensity applications, it may also be possible to use thermal sources, where the SWIR radiation is based on the black body radiation from the hot object. Although the thermal and lamp based sources are broadband and have low intensity fluctuations, it may be difficult to achieve a high signal-to-noise ratio in a non-invasive blood constituent measurement due to the low power levels. Also, the lamp based sources tend to be energy inefficient.

In another embodiment, LED's can be used that have a higher power level in the SWIR wavelength range. LED's also produce an incoherent beam, but the power level can be higher than a lamp and with higher energy efficiency. Also, the LED output may more easily be modulated, and the LED provides the option of continuous wave or pulsed mode of operation. LED's are solid state components that emit a wavelength band that is of moderate width, typically between about 20 nm to 40 nm. There are also so-called super-luminescent LEDs that may even emit over a much wider wavelength range. In another embodiment, a wide band light source may be constructed by combining different LEDs that emit in different wavelength bands, some of which could preferably overlap in spectrum. One advantage of LEDs as well as other solid state components is the compact size that they may be packaged into.

In yet another embodiment, various types of laser diodes may be used in the SWIR wavelength range. Just as LEDs may be higher in power but narrower in wavelength emission than lamps and thermal sources, the LDs may be yet higher in power but yet narrower in wavelength emission than LEDs. Different kinds of LDs may be used, including Fabry-Perot LDs, distributed feedback (DFB) LDs, distributed Bragg reflector (DBR) LDs. Since the LDs have relatively narrow wavelength range (typically under 10 nm), in one embodiment a plurality of LDs may be used that are at different wavelengths in the SWIR. For example, in a preferred embodiment for non-invasive glucose monitoring, it may be advantageous to use LDs having emission spectra near some or all of the glucose spectral peaks (e.g., near 1587 nm, 1750 nm, 2120 nm, 2270 nm, and 2320 nm). The various LDs may be spatially multiplexed, polarization multiplexed, wavelength multiplexed, or a combination of these multiplexing methods. Also, the LDs may be fiber pig-tailed or have one or more lenses on the output to collimate or focus the light. Another advantage of LDs is that they may be packaged compactly and may have a spatially coherent beam output. Moreover, tunable LDs that can tune over a range of wavelengths are also available. The tuning may be done by varying the temperature, or electrical current may be used in particular structures, such as distributed Bragg reflector LDs. In another embodiment, external cavity LDs may be used that have a tuning element, such as a fiber grating or a bulk grating, in the external cavity.

In another embodiment, super-luminescent laser diodes may provide higher power as well as broad bandwidth. An SLD is typically an edge emitting semiconductor light source based on super-luminescence (e.g., this could be amplified spontaneous emission). SLDs combine the higher power and brightness of LDs with the low coherence of conventional LEDs, and the emission band for SLD's may be 5 to 100 nm wide, preferably in the 60 to 100 nm range. Although currently SLDs are commercially available in the wavelength range of approximately 400 nm to 1700 nm, SLDs could and may in the future be made to cover a broader region of the SWIR.

In yet another embodiment, high power LDs for either direct excitation or to pump fiber lasers and SC light sources may be constructed using one or more laser diode bar stacks. As an example, FIG. **19** shows an example of the block diagram **1900** or building blocks for constructing the high power LDs. In this embodiment, one or more diode bar stacks **1901** may be used, where the diode bar stack may be an array of several single emitter LDs. Since the fast axis (e.g., vertical direction) may be nearly diffraction limited while the slow-axis (e.g., horizontal axis) may be far from diffraction limited, different collimators **1902** may be used for the two axes.

Then, the brightness may be increased by spatially combining the beams from multiple stacks **1903**. The combiner may include spatial interleaving, it may include wavelength multiplexing, or it may involve a combination of the two. Different spatial interleaving schemes may be used, such as using an array of prisms or mirrors with spacers to bend one array of beams into the beam path of the other. In another embodiment, segmented mirrors with alternate high-reflection and anti-reflection coatings may be used. Moreover, the brightness may be increased by polarization beam combining **1904** the two orthogonal polarizations, such as by using a polarization beam splitter. In one embodiment, the output may then be focused or coupled into a large diameter core fiber. As an example, typical dimensions for the large diameter core fiber range from approximately 100 microns in diameter to 400 microns or more. Alternatively or in addition, a custom beam shaping module **1905** may be used, depending on the particular application. For example, the output of the high power LD may be used directly **1906**, or it may be fiber coupled **1907** to combine, integrate, or transport the high power LD energy. These high power LDs may grow in importance because the LD powers can rapidly scale up. For example, instead of the power being limited by the power available from a single emitter, the power may increase in multiples depending on the number of diodes multiplexed and the size of the large diameter fiber. Although FIG. **19** is shown as one embodiment, some or all of the elements may be used in a high power LD, or additional elements may also be used.

SWIR Super-Continuum Lasers

Each of the light sources described above have particular strengths, but they also may have limitations. For example, there is typically a trade-off between wavelength range and power output. Also, sources such as lamps, thermal sources, and LEDs produce incoherent beams that may be difficult to focus to a small area and may have difficulty propagating for long distances. An alternative source that may overcome some of these limitations is an SC light source. Some of the advantages of the SC source may include high power and intensity, wide bandwidth, spatially coherent beam that can propagate nearly transform limited over long distances, and easy compatibility with fiber delivery.

Supercontinuum lasers may combine the broadband attributes of lamps with the spatial coherence and high brightness of lasers. By exploiting a modulational instability initiated supercontinuum (SC) mechanism, an all-fiber-integrated SC laser with no moving parts may be built using commercial-off-the-shelf (COTS) components. Moreover, the fiber laser architecture may be a platform where SC in the visible, near-infrared/SWIR, or mid-IR can be generated by appropriate selection of the amplifier technology and the SC generation fiber. But until now, SC lasers were used primarily in laboratory settings since typically large, table-top, mode-locked lasers were used to pump nonlinear media such as optical fibers to generate SC light. However, those large pump lasers may now be replaced with diode lasers and fiber amplifiers that gained maturity in the telecommunications industry.

In one embodiment, an all-fiber-integrated, high-powered SC light source **2000** may be elegant for its simplicity (FIG.

20). The light may be first generated from a seed laser diode **2001**. For example, the seed LD **2001** may be a distributed feedback laser diode with a wavelength near 1542 or 1550 nm, with approximately 0.5-2.0 ns pulsed output, and with a pulse repetition rate between a kilohertz to about 100 MHz or more. The output from the seed laser diode may then be amplified in a multiple-stage fiber amplifier **2002** comprising one or more gain fiber segments. In one embodiment, the first stage pre-amplifier **2003** may be designed for optimal noise performance. For example, the pre-amplifier **2003** may be a standard erbium-doped fiber amplifier or an erbium/ytterbium doped cladding pumped fiber amplifier. Between amplifier stages **2003** and **2006**, it may be advantageous to use band-pass filters **2004** to block amplified spontaneous emission and isolators **2005** to prevent spurious reflections. Then, the power amplifier stage **2006** may use a cladding-pumped fiber amplifier that may be optimized to minimize nonlinear distortion. The power amplifier fiber **2006** may also be an erbium-doped fiber amplifier, if only low or moderate power levels are to be generated.

The SC generation **2007** may occur in the relatively short lengths of fiber that follow the pump laser. In one exemplary embodiment, the SC fiber length may range from a few millimeters to 100 m or more. In one embodiment, the SC generation may occur in a first fiber **2008** where the modulational-instability initiated pulse break-up primarily occurs, followed by a second fiber **2009** where the SC generation and spectral broadening primarily occurs.

In one embodiment, one or two meters of standard single-mode fiber (SMF) after the power amplifier stage may be followed by several meters of SC generation fiber. For this example, in the SMF the peak power may be several kilowatts and the pump light may fall in the anomalous group-velocity dispersion regime---often called the soliton regime. For high peak powers in the dispersion regime, the nanosecond pulses may be unstable due to a phenomenon known as modulational instability, which is basically parametric amplification in which the fiber nonlinearity helps to phase match the pulses. As a consequence, the nanosecond pump pulses may be broken into many shorter pulses as the modulational instability tries to form soliton pulses from the quasi-continuous-wave background. Although the laser diode and amplification process starts with approximately nanosecond-long pulses, modulational instability in the short length of SMF fiber may form approximately 0.5 ps to several-picosecond-long pulses with high intensity. Thus, the few meters of SMF fiber may result in an output similar to that produced by mode-locked lasers, except in a much simpler and cost-effective manner.

The short pulses created through modulational instability may then be coupled into a nonlinear fiber for SC generation. The nonlinear mechanisms leading to broadband SC may include four-wave mixing or self-phase modulation along with the optical Raman effect. Since the Raman effect is self-phase-matched and shifts light to longer wavelengths by emission of optical photons, the SC may spread to longer wavelengths very efficiently. The short-wavelength edge may arise from four-wave mixing, and often times the short wavelength edge may be limited by increasing group-velocity dispersion in the fiber. In many instances, if the particular fiber used has sufficient peak power and SC fiber length, the SC generation process may fill the long-wavelength edge up to the transmission window.

Mature fiber amplifiers for the power amplifier stage **2006** include ytterbium-doped fibers (near 1060 nm), erbium-doped fibers (near 1550 nm), erbium/ytterbium-doped fibers (near 1550 nm), or thulium-doped fibers (near 2000 nm). In various embodiments, candidates for SC fiber **2009** include fused silica fibers (for generating SC between 0.8-2.7.mu.m), mid-IR fibers such as fluorides, chalcogenides, or tellurites (for generating SC out to 4.5.mu.m or longer), photonic crystal fibers (for generating SC between 0.4 and 1.7.mu.m), or combinations of these fibers. Therefore, by selecting the appropriate fiber-amplifier doping for **2006** and nonlinear fiber **2009**, SC may be generated in the visible, near-IR/SWIR, or mid-IR wavelength region.

The configuration **2000** of FIG. **20** is just one particular example, and other configurations can be used and are intended to be covered by this disclosure. For example, further gain stages may be used, and different types of lossy elements or fiber taps may be used between the amplifier stages. In another embodiment, the SC generation may occur partially in the amplifier fiber and in the pig-tails from the pump combiner or other elements. In yet another embodiment, polarization maintaining fibers may be used, and a polarizer may also be used to enhance the polarization contrast between amplifier stages. Also, not discussed in detail are many accessories that may accompany this set-up, such as driver electronics, pump laser diodes, safety shut-offs, and thermal management and packaging.

One example of an SC laser that operates in the SWIR used in one embodiment is illustrated in FIG. **21**. This SWIR SC source **2100** produces an output of up to approximately 5 W over a spectral range of about 1.5 to 2.4 microns, and this particular laser is made out of polarization maintaining components. The seed laser **2101** is a distributed feedback (DFB) laser operating near 1542 nm producing approximately 0.5 nanosecond (ns) pulses at an about 8 MHz repetition rate. The pre-amplifier **2102** is forward pumped and uses about 2 m length of erbium/ytterbium cladding pumped fiber **2103** (often also called dual-core fiber) with an inner core diameter of 12 microns and outer core diameter of 130 microns. The pre-amplifier gain fiber **2103** is pumped using a 10 W 940 nm laser diode **2105** that is coupled in using a fiber combiner **2104**.

In this particular 5 W unit, the mid-stage between amplifier stages **2102** and **2106** comprises an isolator **2107**, a band-pass filter **2108**, a polarizer **2109** and a fiber tap **2110**. The power amplifier **2106** uses a 4 m length of the 12/130 micron erbium/ytterbium doped fiber **2111** that is counter-propagating pumped using one or more 30 W 940 nm laser diodes **2112** coupled in through a combiner **2113**. An approximately 1-2 meter length of the combiner pig-tail helps to initiate the SC process, and then a length of PM-1550 fiber **2115** (polarization maintaining, single-mode, fused silica fiber optimized for 1550 nm) is spliced **2114** to the combiner output.

If an output fiber of about 10 m in length is used, then the resulting output spectrum **2200** is shown in FIG. **22**. The details of the output spectrum **2200** depend on the peak power into the fiber, the fiber length, and properties of the fiber such as length and core size, as well as the zero dispersion wavelength and the dispersion properties. For example, if a shorter length of fiber is used, then the spectrum actually reaches to longer wavelengths (e.g., a 2 m length of SC fiber broadens the spectrum to −2500 nm). Also, if extra-dry fibers are used with less O—H content, then the wavelength edge may also reach to a longer wavelength. To generate more spectrum toward the shorter wavelengths, the pump wavelength (in this case .about.1542 nm) should be close to the zero dispersion wavelength in the fiber. For example, by using a dispersion shifted fiber or so-called non-zero dispersion shifted fiber, the short wavelength edge may shift to shorter wavelengths.

Although one particular example of a 5 W SWIR-SC has been described, different components, different fibers, and different configurations may also be used consistent with this disclosure. For instance, another embodiment of the similar configuration **2100** in FIG. **21** may be used to generate high powered SC between approximately 1060 and 1800 nm. For this embodiment, the seed laser **2101** may be a 1064 nm distributed feedback (DFB) laser diode, the pre-amplifier gain fiber **2103** may be a ytterbium-doped fiber amplifier with 10/125 microns dimensions, and the pump laser **2105** may be a 10 W 915 nm laser diode. In the mid-stage, a mode field adapter may be included in addition to the isolator **2107**, band pass filter **2108**, polarizer **2109** and tap **2110**. The gain fiber **2111** in the power amplifier may be a 20 m length of ytterbium-doped fiber with 25/400 microns dimension for example. The pump **2112** for the power amplifier may be up to six pump diodes providing 30 W each near 915 nm, for example. For this much pump power, the output power in the SC may be as high as 50 W or more.

In another embodiment, it may be desirous to generate high power SWIR SC over 1.4-1.8 microns and separately 2-2.5 microns (the window between 1.8 and 2 microns may be less important due to the strong water and atmospheric absorption). For example, the top SC source of FIG. **23** can lead to bandwidths ranging from about 1400 nm to 1800 nm or broader, while the lower SC source of FIG. **23** can lead to bandwidths ranging from about 1900 nm to 2500 nm or broader. Since these wavelength ranges are shorter than about 2500 nm, the SC fiber can be based on fused silica fiber. Exemplary SC fibers include standard single-mode fiber SMF, high-nonlinearity fiber, high-NA fiber, dispersion shifted fiber, dispersion compensating fiber, and photonic crystal fibers. Non-fused-silica fibers can also be used for SC generation, including chalcogenides, fluorides, ZBLAN, tellurites, and germanium oxide fibers.

In one embodiment, the top of FIG. **23** illustrates a block diagram for an SC source **2300** capable of generating light between approximately 1400 and 1800 nm or broader. As an example, a pump fiber laser similar to FIG. **21** can be used as the input to a SC fiber **2309**. The seed laser diode **2301** can comprise a DFB laser that generates, for example, several milliwatts of power around 1542 or 1553 nm. The fiber pre-amplifier **2302** can comprise an erbium-doped fiber amplifier or an erbium/ytterbium doped double clad fiber. In this example a mid-stage amplifier **2303** can be used, which can comprise an erbium/ytterbium doped double-clad fiber. A bandpass filter **2305** and isolator **2306** may be used between the pre-amplifier **2302** and mid-stage amplifier **2303**. The power amplifier stage **2304** can comprise a larger core size erbium/ytterbium doped double-clad fiber, and another bandpass filter **2307** and isolator **2308** can be used before the power amplifier **2304**. The output of the power amplifier can be coupled to the SC fiber **2309** to generate the SC output **2310**. This is just one exemplary configuration for an SC source, and other configurations or elements may be used consistent with this disclosure.

In yet another embodiment, the bottom of FIG. **23** illustrates a block diagram for an SC source **2350** capable of generating light between approximately 1900 and 2500 nm or broader. As an example, the seed laser diode **2351** can comprise a DFB or DBR laser that generates, for example, several milliwatts of power around 1542 or 1553 nm. The fiber pre-amplifier **2352** can comprise an erbium-doped fiber amplifier or an erbium/ytterbium doped double-clad fiber. In this example a mid-stage amplifier **2353** can be used, which can comprise an erbium/ytterbium doped double-clad fiber. A bandpass filter **2355** and isolator **2356** may be used between the pre-amplifier **2352** and mid-stage amplifier **2353**. The power amplifier stage **2354** can comprise a thulium doped double-clad fiber, and another isolator **2357** can be used before the power amplifier **2354**. Note that the output of the mid-stage amplifier **2353** can be approximately near 1550 nm, while the thulium-doped fiber amplifier **2354** can amplify wavelengths longer than approximately 1900 nm and out to about 2100 nm. Therefore, for this configuration wavelength shifting may be required between **2353** and **2354**. In one embodiment, the wavelength shifting can be accomplished using a length of standard single-mode fiber **2358**, which can have a length between approximately 5 and 50 meters, for example. The output of the power amplifier **2354** can be coupled to the SC fiber **2359** to generate the SC output **2360**. This is just one exemplary configuration for an SC source, and other configurations or elements can be used consistent with this disclosure. For example, the various amplifier stages can comprise different amplifier types, such as erbium doped fibers, ytterbium doped fibers, erbium/ytterbium co-doped fibers and thulium doped fibers. One advantage of the SC lasers illustrated in FIGS. **20-23** are that they may use all-fiber components, so that the SC laser can be all-fiber, monolithically integrated with no moving parts. The all-integrated configuration can consequently be robust and reliable.

FIGS. **20-23** are examples of SC light sources that may be advantageously used for SWIR light generation in various medical diagnostic and therapeutic applications. However, many other versions of the SC light sources may also be made that are intended to also be covered by this disclosure. For example, the SC generation fiber could be pumped by a mode-locked laser, a gain-switched semiconductor laser, an optically pumped semiconductor laser, a solid state laser, other fiber lasers, or a combination of these types of lasers. Also, rather than using a fiber for SC generation, either a liquid or a gas cell might be used as the nonlinear medium in which the spectrum is to be broadened.

Even within the all-fiber versions illustrated such as in FIG. **21**, different configurations could be used consistent with the disclosure. In an alternate embodiment, it may be desirous to have a lower cost version of the SWIR SC laser of FIG. **21**. One way to lower the cost could be to use a single stage of optical amplification, rather than two stages, which may be feasible if lower output power is required or the gain fiber is optimized. For example, the pre-amplifier stage **2102** might be removed, along with at least some of the mid-stage elements. In yet another embodiment, the gain fiber could be double passed to emulate a two stage amplifier. In this example, the pre-amplifier stage **2102** might be removed, and perhaps also some of the mid-stage elements. A mirror or fiber grating reflector could be placed after the power amplifier stage **2106** that may preferentially reflect light near the wavelength of the seed laser **2101**. If the mirror or fiber grating reflector can transmit the pump light near 940 nm, then this could also be used instead of the pump combiner **2113** to bring in the pump light **2112**. The SC fiber **2115** could be placed between the seed laser **2101** and the power amplifier stage **2106** (SC is only generated after the second pass through the amplifier, since the power level may be sufficiently high at that time). In addition, an output coupler may be placed between the seed laser diode **2101** and the SC fiber, which now may be in front of the power amplifier **2106**. In a particular embodiment, the output coupler could be a power coupler or divider, a dichroic coupler (e.g., passing seed laser wavelength but outputting the SC wavelengths), or a wavelength division multiplexer coupler. This is just one further example, but a myriad of other combinations of components and architectures could also be used for SC light sources to generate SWIR light that are intended to be covered by this disclosure.

Wireless Link to the Cloud

The non-invasive blood constituent or analytes measurement device may also benefit from communicating the data output to the "cloud" (e.g., data servers and processors in the web remotely connected) via wired and/or wireless communication strategies. The non-invasive devices may be part of a series of biosensors applied to the patient, and collectively these devices form what might be called a body area network or a personal area network. The biosensors and non-invasive devices may communicate to a smart phone, tablet, personal data assistant, computer, and/or other microprocessor-based device, which may in turn wirelessly or over wire and/or fiber optically transmit some or all of the signal or processed data to the internet or cloud. The cloud or internet may in turn send the data to doctors or health care providers as well as the patients themselves. Thus, it may be possible to have a panoramic, high-definition, relatively comprehensive view of a patient that doctors can use to assess and manage disease, and that patients can use to help maintain their health and direct their own care.

In a particular embodiment **2400**, the physiological measurement device or non-invasive blood constituent measurement device **2401** may comprise a transmitter **2403** to communicate over a first communication link **2404** in the body area network or personal area network to a receiver in a smart phone, tablet cell phone, PDA, or computer **2405**. For the measurement device **2401**, it may also be advantageous to have a processor **2402** to process some of the physiological data, since with processing the amount of data to transmit may be less (hence, more energy efficient). The first communication link **2404** may operate through the use of one of many wireless technologies such as Bluetooth, Zigbee, WiFi, IrDA (infrared data association), wireless USB, or Z-wave, to name a few. Alternatively, the communication link **2404** may occur in the wireless medical band between 2360 and 2390 MHz, which the FCC allocated for medical body area network devices, or in other designated medical device or WMTS bands. These are examples of devices that can be used in the body area network and surroundings, but other devices could also be used and are included in the scope of this disclosure.

The personal device **2405** may store, process, display, and transmit some of the data from the measurement device **2401**. The device **2405** may comprise a receiver, transmitter, display, voice control and speakers, and one or more control buttons or knobs and a touch screen. Examples of the device **2405** include smart phones such as the Apple iPhones® or phones operating on the Android or Microsoft systems. In one embodiment, the device **2405** may have an application, software program, or firmware to receive and process the data from the measurement device **2401**. The device **2405** may then transmit some or all of the data or the processed data over a second communication link **2406** to the internet or "cloud" **2407**. The second communication link **2406** may advantageously comprise at least one segment of a wireless transmission link, which may operate using WiFi or the cellular network. The second communication link **2406** may additionally comprise lengths of fiber optic and/or communication over copper wires or cables.

The internet or cloud **2407** may add value to the measurement device **2401** by providing services that augment the physiological data collected. In a particular embodiment, some of the functions performed by the cloud include: (a) receive at least a fraction of the data from the device **2405**; (b) buffer or store the data received; (c) process the data using software stored on the cloud; (d) store the resulting processed data; and (e) transmit some or all of the data either upon request or based on an alarm. As an example, the data or processed data may be transmitted **2408** back to the originator (e.g., patient or user), it may be transmitted **2409** to a health care provider or doctor, or it may be transmitted **2410** to other designated recipients.

The cloud **2407** may provide a number of value-add services. For example, the cloud application may store and process the physiological data for future reference or during a visit with the healthcare provider. If a patient has some sort of medical mishap or emergency, the physician can obtain the history of the physiological parameters over a specified period of time. In another embodiment, if the physiological parameters fall out of acceptable range, alarms may be delivered to the user **2408**, the healthcare provider **2409**, or other designated recipients **2410**. These are just some of the features that may be offered, but many others may be possible and are intended to be covered by this disclosure. As an example, the device **2405** may also have a GPS sensor, so the cloud **2407** may be able to provide time, data and position along with the physiological parameters. Thus, if there is a medical emergency, the cloud **2407** could provide the location of the patient to the healthcare provider **2409** or other designated recipients **2410**. Moreover, the digitized data in the cloud **2407** may help to move toward what is often called "personalized medicine." Based on the physiological parameter data history, medication or medical therapies may be prescribed that are customized to the particular patient.

Beyond the above benefits, the cloud application **2407** and application on the device **2405** may also have financial value for companies developing measurement devices **2401** such as a non-invasive blood constituent monitor. In the case of glucose monitors, the companies make the majority of their revenue on the measurement strips. However, with a non-invasive monitor, there is no need for strips, so there is less of an opportunity for recurring costs (e.g., the razor/razor blade model does not work for non-invasive devices). On the other hand, people may be willing to pay a periodic fee for the value-add services provided on the cloud **2407**. Diabetic patients, for example, would probably be willing to pay a periodic fee for monitoring their glucose levels, storing the history of the glucose levels, and having alarm warnings when the glucose level falls out of range. Similarly, patients taking ketone bodies supplement for treatment of disorders characterized by impaired glucose metabolism (e.g., Alzheimer's, Parkinson's, Huntington's or ALS) may need to monitor their ketone bodies level. These patients would also probably be willing to pay a periodic fee for the value-add services provided on the cloud **2407**. Thus, by leveraging the advances in wireless connectivity and the widespread use of handheld devices such as smart phones that can wirelessly connect to the cloud, businesses can build a recurring cost business model even using non-invasive measurement devices.

Described herein are just some examples of the beneficial use of near-infrared or SWIR lasers for non-invasive monitoring of glucose, ketones, HbA1c and other blood constituents. However, many other medical procedures can use the near-infrared or SWIR light consistent with this disclosure and are intended to be covered by the disclosure.

Although the present disclosure has been described in several embodiments, a myriad of changes, variations, alterations, transformations, and modifications may be suggested to one skilled in the art, and it is intended that the present disclosure encompass such changes, variations, alterations, transformations, and modifications as falling within the spirit and scope of the appended claims.

While exemplary embodiments are described above, it is not intended that these embodiments describe all possible forms of the disclosure. Rather, the words used in the specification are words of description rather than limitation, and it is understood that various changes may be made without departing from the spirit and scope of the disclosure. Additionally, the features of various implementing embodiments may be combined to form further embodiments of the disclosure. While various embodiments may have been described as providing advantages or being preferred over other embodiments with respect to one or more desired characteristics, as one skilled in the art is aware, one or more characteristics may be compromised to achieve desired system attributes, which depend on the specific application and implementation. These attributes include, but are not limited to: cost, strength, durability, life cycle cost, marketability, appearance, packaging, size, serviceability, weight, manufacturability, ease of assembly, etc. The embodiments described herein that are described as less desirable than other embodiments or prior art implementations with respect to one or more characteristics are not outside the scope of the disclosure and may be desirable for particular applications.

What is claimed is:

1. A wearable device, comprising:

a measurement device including a light source comprising a plurality of light emitting diodes (LEDs) for measuring one or more physiological parameters, the measurement device configured to generate, by modulating at least one of the LEDs having an initial light intensity, an input optical beam having one or more optical wavelengths, wherein at least a portion of the one or more optical wavelengths is a near-infrared wavelength between 700 nanometers and 2500 nanometers;

the measurement device comprising one or more lenses configured to receive and to deliver a portion of the input optical beam to tissue, wherein the tissue reflects at least a portion of the input optical beam delivered to the tissue;

the measurement device further comprising a receiver, wherein the receiver includes a plurality of spatially separated detectors, the detectors configured to:

capture light while the LEDs are off and convert the captured light into a first signal; and

capture light while at least one of the LEDs is on and convert the captured light into a second signal, the captured light including at least a portion of the input optical beam reflected from the tissue;

wherein at least one analog to digital converter is coupled to the spatially separated detectors and is configured to generate at least a first data signal from the first signal and at least a second data signal from the second signal;

the measurement device configured to improve a signal-to-noise ratio of the input optical beam reflected from the tissue by differencing the first data signal and the second data signal to generate an output signal representing at least in part a non-invasive measurement on blood contained within the tissue; and

wherein the modulating at least one of the LEDs has a modulation frequency, and wherein the receiver is configured to use a lock-in technique that detects the modulation frequency.

2. The wearable device of claim 1, wherein the plurality of LEDs and the plurality of spatially separated detectors are mounted on a common structure, and wherein the plurality of LEDs are coupled electrically to a power supply.

3. The wearable device of claim 1, wherein the light source is configured to further improve the signal-to-noise ratio of the input beam reflected from the tissue by increasing the light intensity relative to the initial light intensity from at least one of the LEDs, and wherein the receiver is configured to be synchronized to at least one of the LEDs.

4. The wearable device of claim 1, wherein the receiver further comprises one or more filters in front of one or more detectors to select a fraction of the one or more optical wavelengths.

5. The wearable device of claim 1, wherein the wearable device is configured to communicate with a smart phone or tablet, the smart phone or tablet comprising a wireless receiver, a wireless transmitter, a display, a voice input module, a speaker, and a touch screen, the smart phone or tablet configured to receive and to process at least a portion of the output signal, wherein the smart phone or tablet is configured to store and display the processed output signal, wherein at least a portion of the processed output signal is configured to be transmitted over a wireless transmission link.

6. The wearable device of claim 5, further comprising a remote device configured to receive over the wireless transmission link an output status comprising the at least a portion of the processed output signal, to process the output status to generate processed data and to store the processed data, and wherein the remote device is capable of storing a history of at least a portion of the output status over a specified period of time, and

wherein the remote device is further configured to transmit at least a portion of the processed data to one or more other locations, wherein the one or more other locations is selected from the group consisting of the smart phone or tablet, a doctor, a healthcare provider, a cloud-based server and one or more designated recipients.

7. The wearable device of claim 1, wherein the measurement device further comprises a signal processor configured to process a portion of the output signal to reduce an amount of data to be transmitted.

8. The wearable device of claim 1, wherein the receiver is configured to perform narrow band filtering at the modulation frequency.

9. The wearable device of claim 1, wherein the modulation frequency has a phase, and wherein the receiver is configured to lock onto the phase.

10. A method of measuring physiological information, the method comprising providing a wearable device, the wearable device being capable of performing all of the steps comprising:

generating a first and a second input optical beam each having one or more optical wavelengths using a light source comprising a plurality of light emitting diodes (LEDs) by modulating at least one of the LEDs, wherein at least a portion of the one or more optical wavelengths is a near-infrared wavelength between 700 nanometers and 2500 nanometers;

delivering a portion of the first input optical beam and a portion of the second input optical beam to tissue using one or more lenses;

capturing light using at least one of a plurality of spatially separated detectors of a receiver while the LEDs are off and converting the light into a first data signal using at least one analog to digital converter coupled to the spatially separated detectors;

capturing light using at least one of the plurality of spatially separated detectors of the receiver while the at least one of the LEDs is on and converting the captured light into a second data signal using the at least one analog to digital converter, the captured light including at least a portion of the first input optical beam reflected from the tissue and at least a portion of the second input optical beam reflected from the tissue;

increasing a signal-to-noise ratio of the first and second input optical beams reflected from the tissue by differencing the first data signal and the second data signal; and

generating an output signal representing at least in part a non-invasive measurement on blood contained within the tissue based at least in part on the first data signal and the second data signal;

wherein the modulating at least one of the LEDs has a modulation frequency, and wherein the receiver is configured to use a lock-in technique that detects the modulation frequency.

11. The method of claim **10**, wherein the plurality of LEDs and the plurality of spatially separated detectors are mounted on a common structure, and wherein the plurality of LEDs are coupled electrically to a power supply.

12. The method of claim **10** further comprising transmitting at least a portion of the output signal to a smart phone or tablet for processing to generate a processed output signal, and for transmitting from the smart phone or tablet at least a portion of the processed output signal over a wireless transmission link.

13. The method of claim **12**, further comprising the steps of:

receiving at a remote device an output status comprising the at least a portion of the processed output signal transmitted over the wireless transmission link;

storing at the remote device a history of at least a portion of the output status over a period of time;

processing the output status at the remote device to generate processed data;

storing the processed data at the remote device; and

transmitting from the remote device at least a portion of the processed data to one or more other locations, wherein the one or more other locations is selected from the group consisting of the smart phone or tablet, a doctor, a healthcare provider, a cloud-based server and one or more designated recipients.

14. The method of claim **10**, further comprising the steps of:

increasing the signal-to-noise ratio of the first and second portions of the input optical beam reflected from the tissue by increasing a light intensity from at least one of the LEDs; and

wherein the capturing steps are synchronized to of the at least one of the LEDs.

15. The method of claim **10**, wherein the capturing step that captures light while at least one of the LEDs is on further comprises filtering to select a fraction of the one or more optical wavelengths.

16. The method of claim **10**, further comprising processing a portion of the output signal to reduce an amount of data for transmitting to the smart phone or tablet.

17. The method of claim **10**, wherein the steps of capturing light comprise narrow-band filtering at the modulation frequency.

18. The method of claim **10**, wherein the modulation frequency has a phase, the method further comprising locking onto the phase.

* * * * *

EXHIBIT D

UNITED STATES PATENT AND TRADEMARK OFFICE

UNITED STATES DEPARTMENT OF COMMERCE
United States Patent and Trademark Office
Address: COMMISSIONER FOR PATENTS
P.O. Box 1450
Alexandria, Virginia 22313-1450
www.uspto.gov

APPLICATION NO.	ISSUE DATE	PATENT NO.	ATTORNEY DOCKET NO.	CONFIRMATION NO.
15/594,053	01/29/2019	10188299	OMNI 0105 PUSP2	1876

109543 7590 01/09/2019

Brooks, Kushman P.C./Cheetah Omni MedSci
1000 Town Center
Twenty Second Floor
Southfield, MI 48075

ISSUE NOTIFICATION

The projected patent number and issue date are specified above.

Determination of Patent Term Adjustment under 35 U.S.C. 154 (b)
(application filed on or after May 29, 2000)

The Patent Term Adjustment is 0 day(s). Any patent to issue from the above-identified application will include an indication of the adjustment on the front page.

If a Continued Prosecution Application (CPA) was filed in the above-identified application, the filing date that determines Patent Term Adjustment is the filing date of the most recent CPA.

Applicant will be able to obtain more detailed information by accessing the Patent Application Information Retrieval (PAIR) WEB site (http://pair.uspto.gov).

Any questions regarding the Patent Term Extension or Adjustment determination should be directed to the Office of Patent Legal Administration at (571)-272-7702. Questions relating to issue and publication fee payments should be directed to the Application Assistance Unit (AAU) of the Office of Data Management (ODM) at (571)-272-4200.

APPLICANT(s) (Please see PAIR WEB site http://pair.uspto.gov for additional applicants):

Mohammed N. ISLAM, Ann Arbor, MI;
OMNI MEDSCI, INC., Ann Arbor, MI;